DIFFRACTION PRODUCTION OF BOSONS[*]

T. Ferbel[†]

Department of Physics and Astronomy[††]

University of Rochester

Rochester, New York

March 29, 1971

We summarize recent results obtained in the analysis of diffractively produced multimeson systems and speculate on the mechanism responsible for these production processes.

Since the initial discovery of the A_1-A_2 enhancement[1] reactions of the type $X + T \rightarrow (X\pi\pi) + T$, where X refers to a projectile meson and T refers to a nucleon or nuclear target, have been studied quite extensively.[2] The most outstanding feature found in these final states, particularly at the higher beam energies, is the large cross section which is observed for small invariant mass values of the $(X\pi\pi)$ system. The $X\pi\pi$ system for masses below 2 GeV consists almost entirely of resonant two-body sub-systems. A plot of the cross section as a function of $M_{X\pi\pi}$ shows a dramatic rise near the πX^* threshold (where the vector meson X^* subsequently decays into $X + \pi$). The maximum in the $X\pi\pi$ mass distribution occurs roughly 230 MeV ($\pm$ 20MeV) above the sum of the pion mass (M_π) and the central mass value of the X^* (M_{X^*}).

When X is a π-meson the observed $\pi\rho$ low-mass enhancement is referred to as the A_1 region, while when X is a K-meson the low-mass $\pi K^*(890)$ enhancement is referred to as the Q region. (The Q region contains a sizeable $K\rho$ contribution in addition to the $\pi K^*(890)$ element. The $K\rho$ component appears to be particularly strong near the peak value of the Q, i.e., when $M_Q = M_K + M_\rho = 1260$ MeV $= M_\pi + M_{K^*} + 230$ MeV.) After the initial maximum in the $M_{X\pi\pi}$ distribution there appears to be a secondary peak in $M_{X\pi\pi}$ which is shifted by about 160 MeV in mass relative to the first maximum. These secondary peaks occur in the A_2 and in the $K^{**}(1420)$ mass regions for incident π-mesons and K-mesons respectively.

Another sharp peak in the $M_{X\pi\pi}$ distribution occurs, again, approximately 230 MeV ($\pm$ 20 MeV) above another threshold, this time it is the πX^{**} threshold, where X^{**} refers to the $J^P = 2^+$ mesons: $f^0 \to \pi\pi$ and $K^{**}(1420) \to K\pi$. These effects in the $M_{X\pi\pi}$ are commonly referred to as the $\pi(1630)$ and the L. (Here again it is interesting to note that $M_L \simeq M_K + M_{f^0} \simeq 1780 = M_\pi + M_{K^{**}} + 230$ MeV. Although the Kf^0 component of the L effect has not yet been definitely established, several experiments are in fact consistent with a substantial Kf^0 subset in the L-region.)[3]

Although the rest of my discussion will often be pertinent to the L and its $\pi(1630)$ analog (and for that matter also pertinent to the low-mass $N\pi\pi$ enhancements), in what follows I will concentrate my attention on the A_1 and the Q.

Figure 1 shows a "typical" $\pi^\pm \pi^+ \pi$ mass distribution (as compiled by Chien[2]) using the SLAC 16 GeV/c $\pi^\pm p$ and the Notre Dame 18.5 GeV/c $\pi^\pm p$ data. A relatively narrow A_2 shoulder is observed to the right of the broad A_1 peak ($M_{A_1} \simeq 1150$ MeV, $\Gamma_{A_1} \simeq 300$ MeV after correction for A_2), and another small peak is observed in the $\pi(1630)$ mass region (see Chien's paper for higher statistics results at lower $\pi^\pm$ energies). Figure 2 shows the analogous bumps as observed in the $K\pi\pi$ system (for details see Firestone's and Chien's papers and Slattery's discussion).[1] The data shown in the two graphs of Fig. 2 are essentially the same, the different appearance stemming mainly from the different bin widths used by the two authors.

$$\pi^{\pm}p \longrightarrow \pi^{\pm}p\pi^{+}\pi^{-} \qquad \Delta^{++} \text{ REMOVED}$$

SLAC 16 GeV/c $\pi^{\pm}p$ 3600 EVENTS
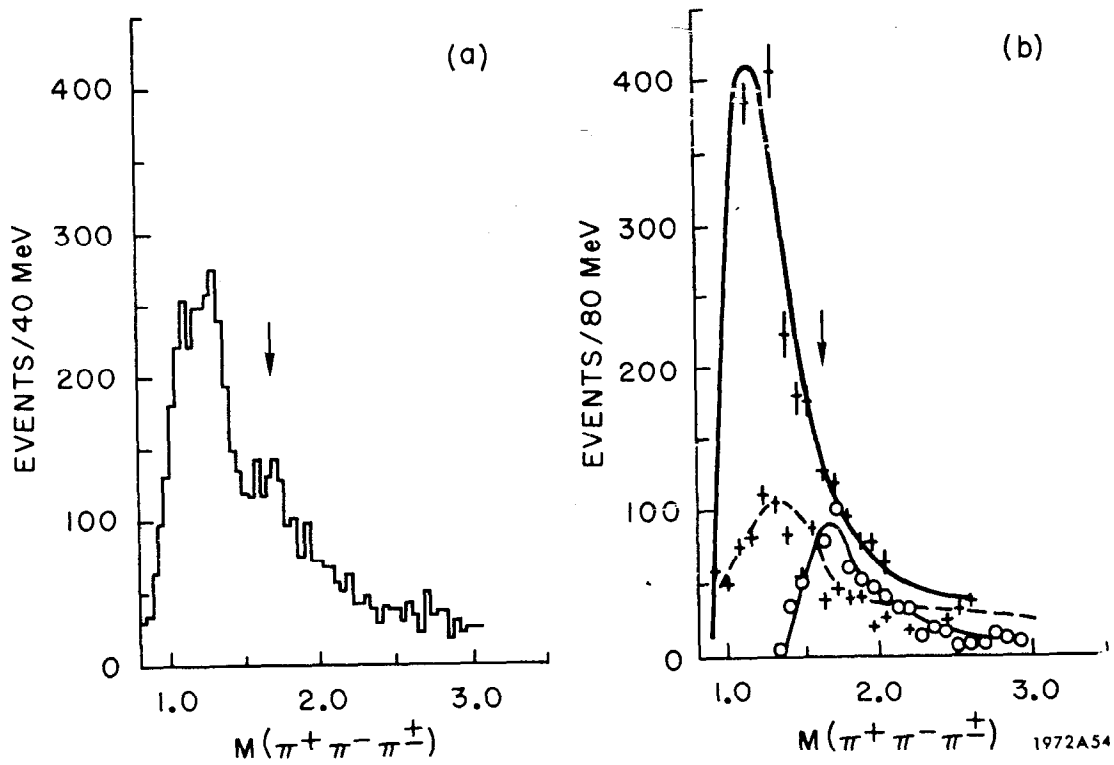
Notre Dame 18 GeV/c $\pi^{\pm}p$ 4800 EVENTS

FIG. 1--Reaction $\pi^{\pm}p \rightarrow \pi^{\pm}p\pi^{+}\pi^{-}$ at 16 and 18.5 GeV/c. (a) $M(\pi^{+}\pi^{+}\pi^{\pm})$ distribution. (b) Amount of $\rho\pi$ (top curve), $\pi^{+}\pi^{-}\pi^{\pm}$ (dashed curve) and $f^{0}\pi$ (bottom curve) in each 3π mass band (from compilation of C. Chien). The arrow is at mass 1630 MeV.
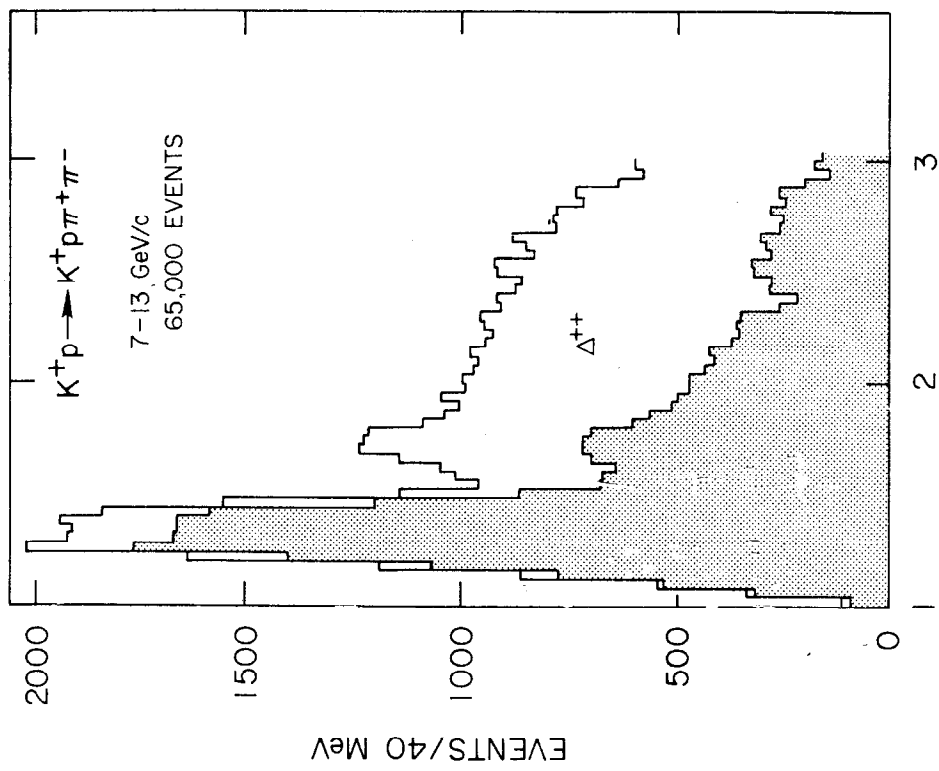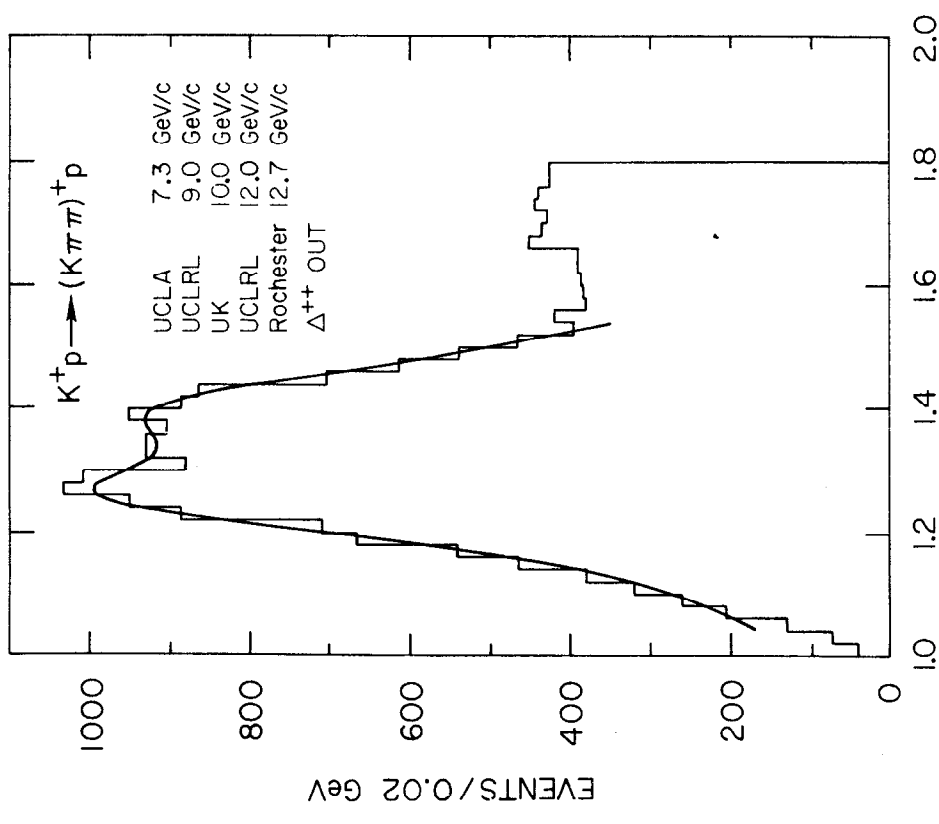
FIG. 2--Reaction $K^+ p \rightarrow (K\pi\pi)^+ p$: $M(K\pi\pi)^+$ taken from the compilation of A. Firestone and C. Chien.

Many analyses have been performed in order to ascertain the nature of the A_1 and the Q effects. In the more common approaches experimentalists have endeavored to answer the following three questions: (1) Can these low-mass effects be regarded, in the main, as resonances? (2) Can these effects be regarded as non-resonant kinematic reflections of specific production mechanisms? (3) Can these effects be understood from a dual point of view, i.e., using a Regge formulation in the region of small $M_{\pi X}*$? I will try to briefly answer these questions using the Rochester 12.7 CeV/c K^+p results as ex-ample.[4]

Using D. Griffiths' model[5] to describe the line shape of the Q as well as its decay into πK^* and into $K\rho$, we were able to show that the only acceptable J^P for the Q was 1^+ (assuming that the main background was slowly varying and iso-tropic on the Dalitz plot). The interference in the overlap of the ρ and K^* bands on the Dalitz Plot provided us with in-formation pertaining to the R-symmetry of the Q. We observed that if the Q belonged to an SU_3 octet, then it would belong to the same octet as the A_1 (i.e., if the A_1 were a resonance); namely, we established that $J_Q^{PC} = 1^{++}$. The results of the fit to the $K\pi\pi$ Dalitz plot using the resonance hypothesis for the Q are shown in Fig. 3. Data from the $K^+\pi^+\pi^-p$ and the $K^o\pi^+\pi^op$ final states are presented. Figure 4 shows the resonance fit to the mass spectrum.

Figures 5, 6 and 7 attempt to answer the two other
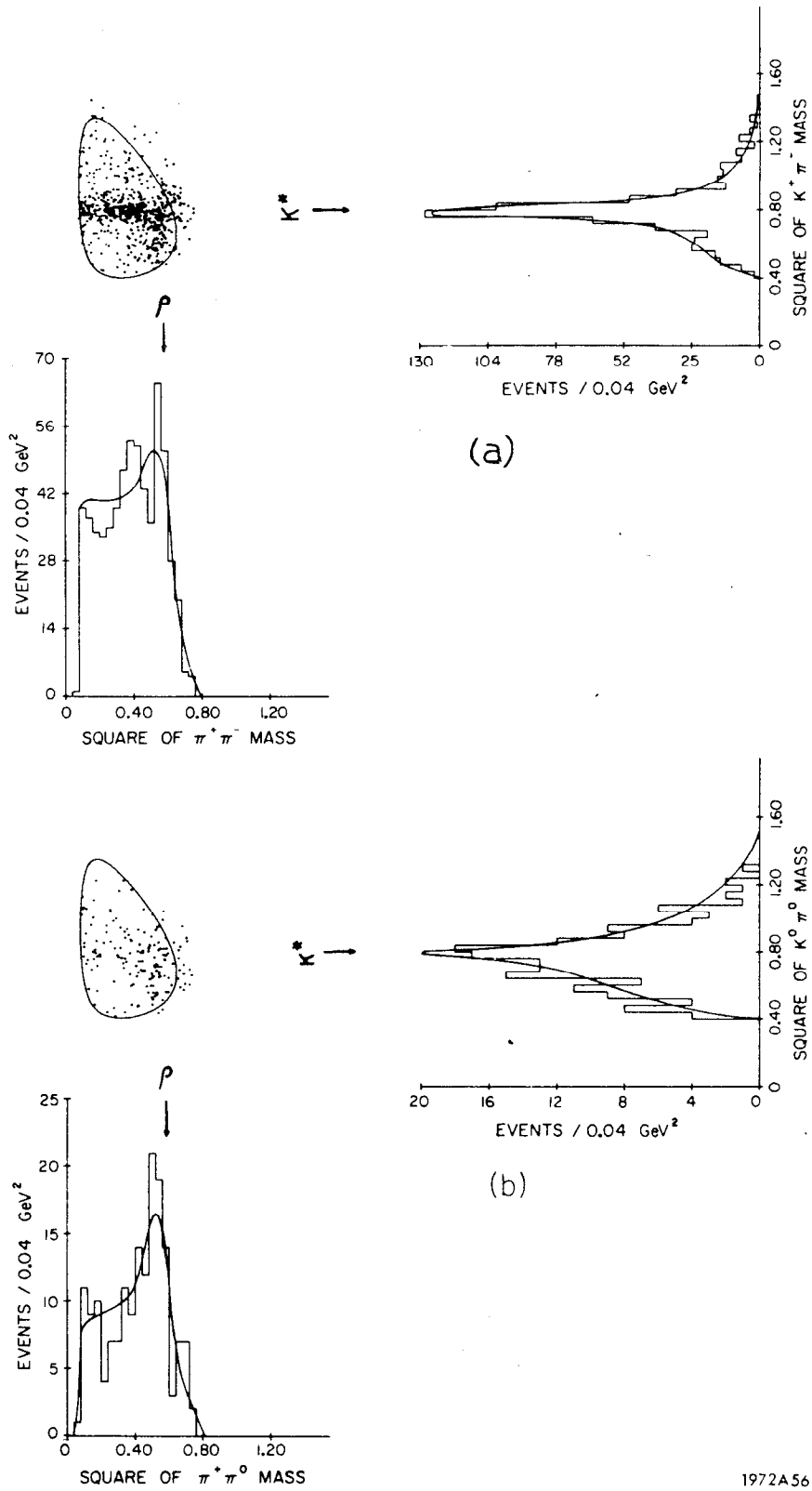
FIG. 3--Fit to the K$\pi\pi$ Dalitz plot (Ref. 4).
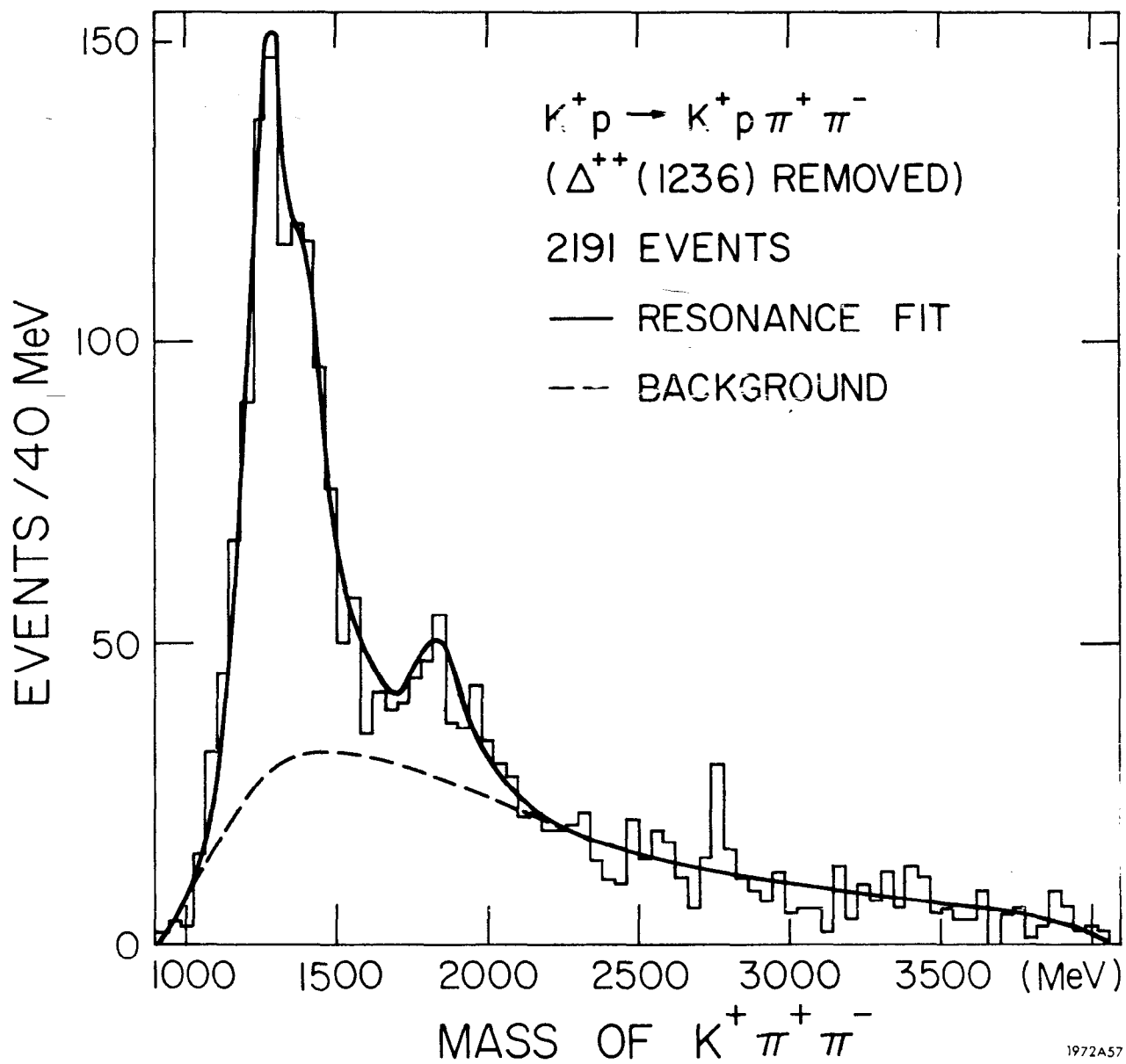
FIG. 4--Reaction $K^+p \rightarrow K^+p\pi^+\pi^-$: fit to the $K\pi\pi$ mass spectrum assuming resonances at the Q and L masses (Rochester data, Ref. 4).
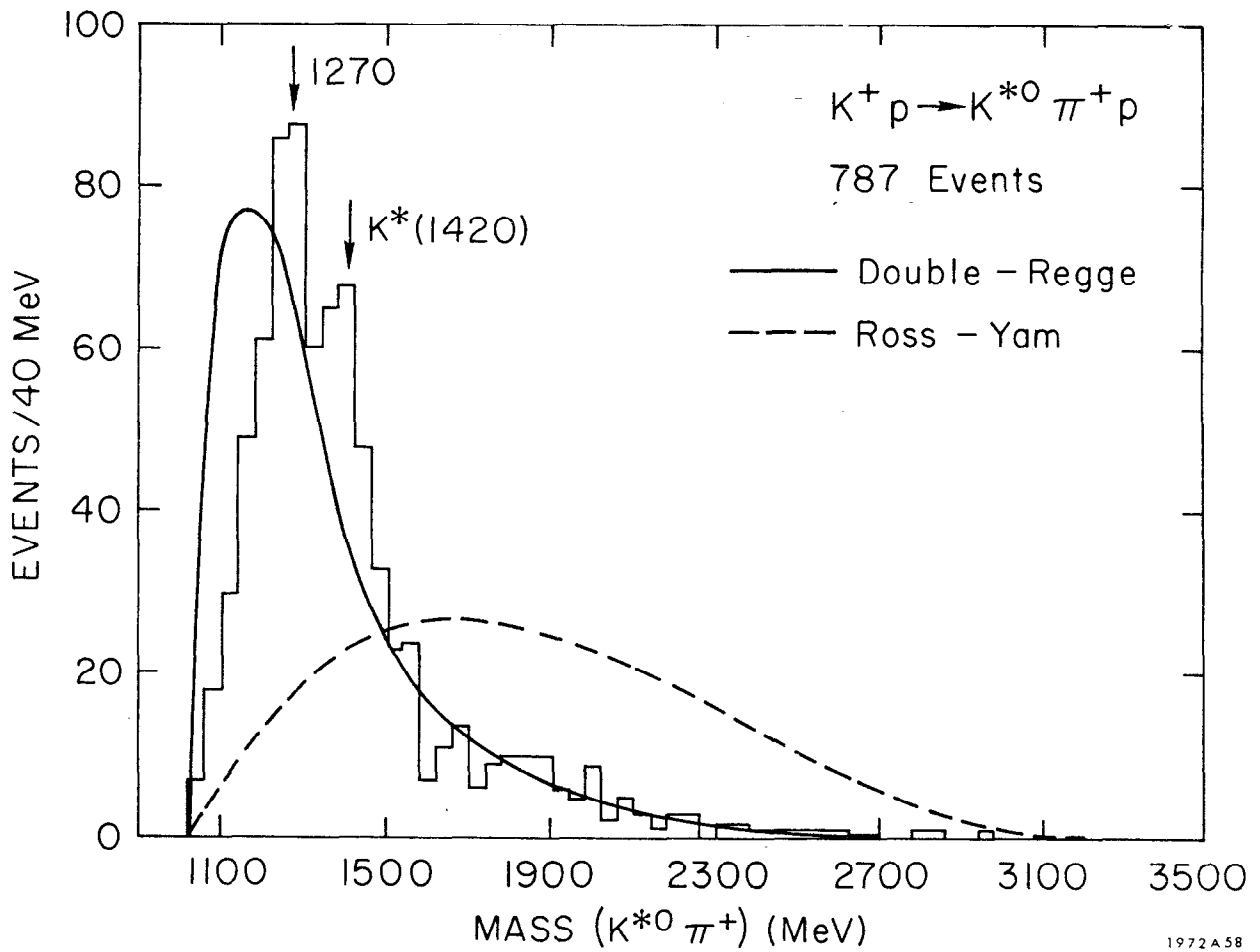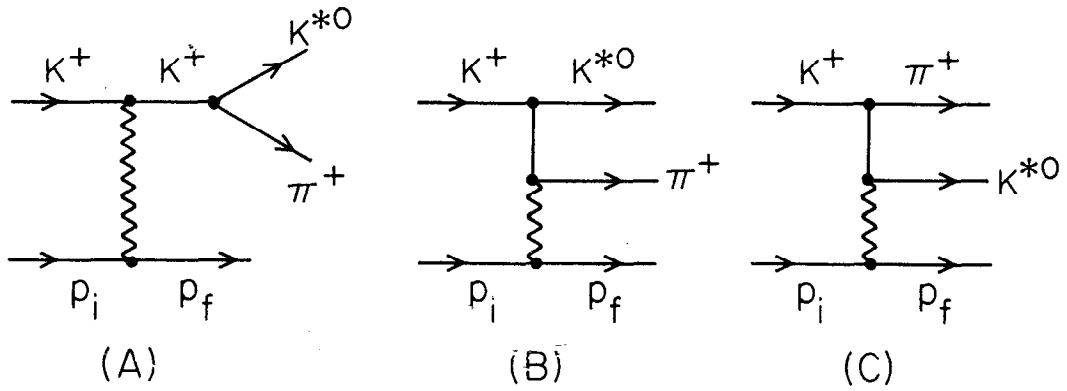
FIG. 5--Prediction of the $K\pi\pi$ mass spectrum by the double Regge
model (Ref. 6) and the Ross-Yam model (Ref. 6).
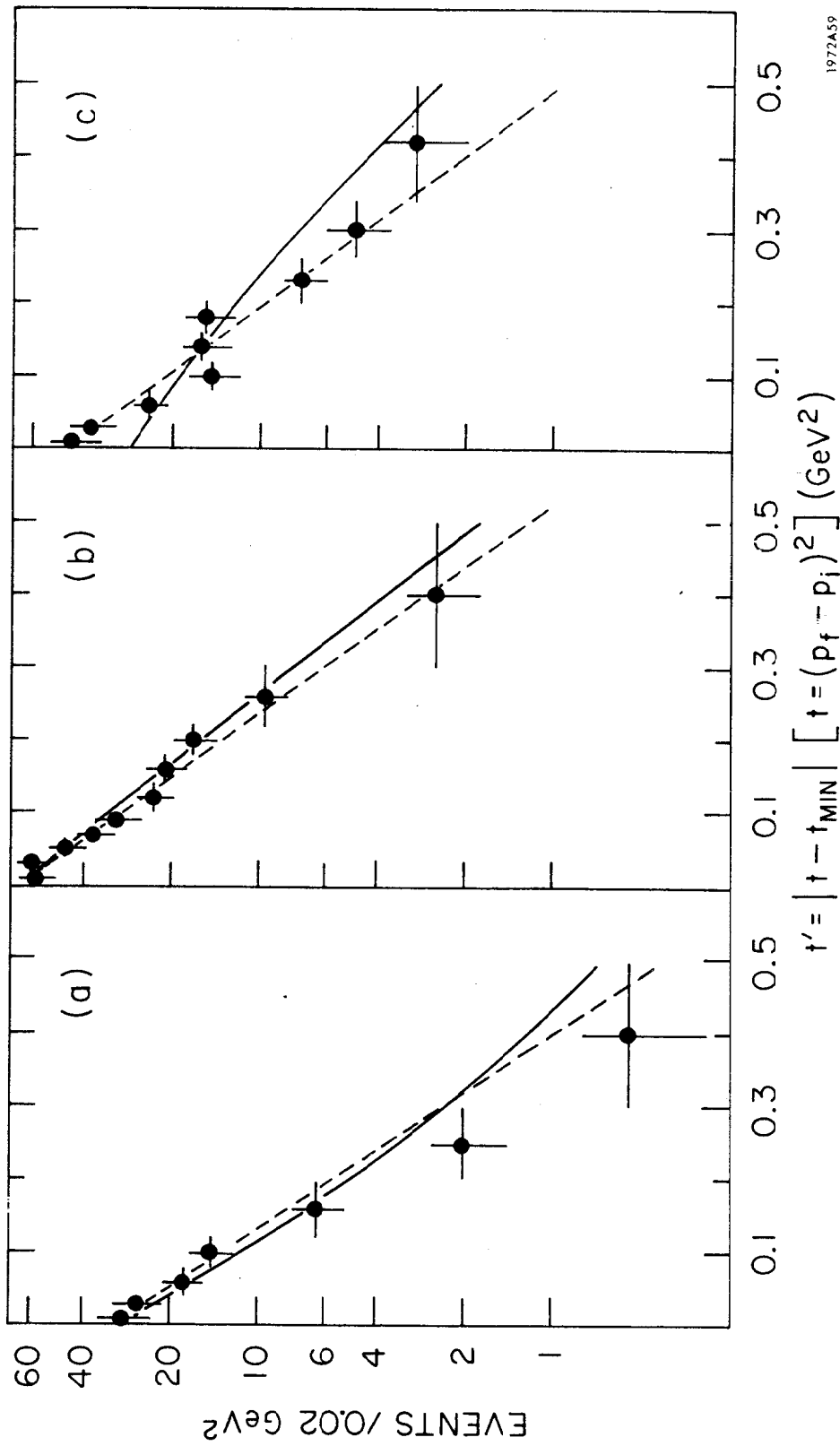
FIG. 6--Comparison of t distribution with the double Regge and Ross-Yam models.

"JACKSON" ANGLES OF K* IN Q FRAME
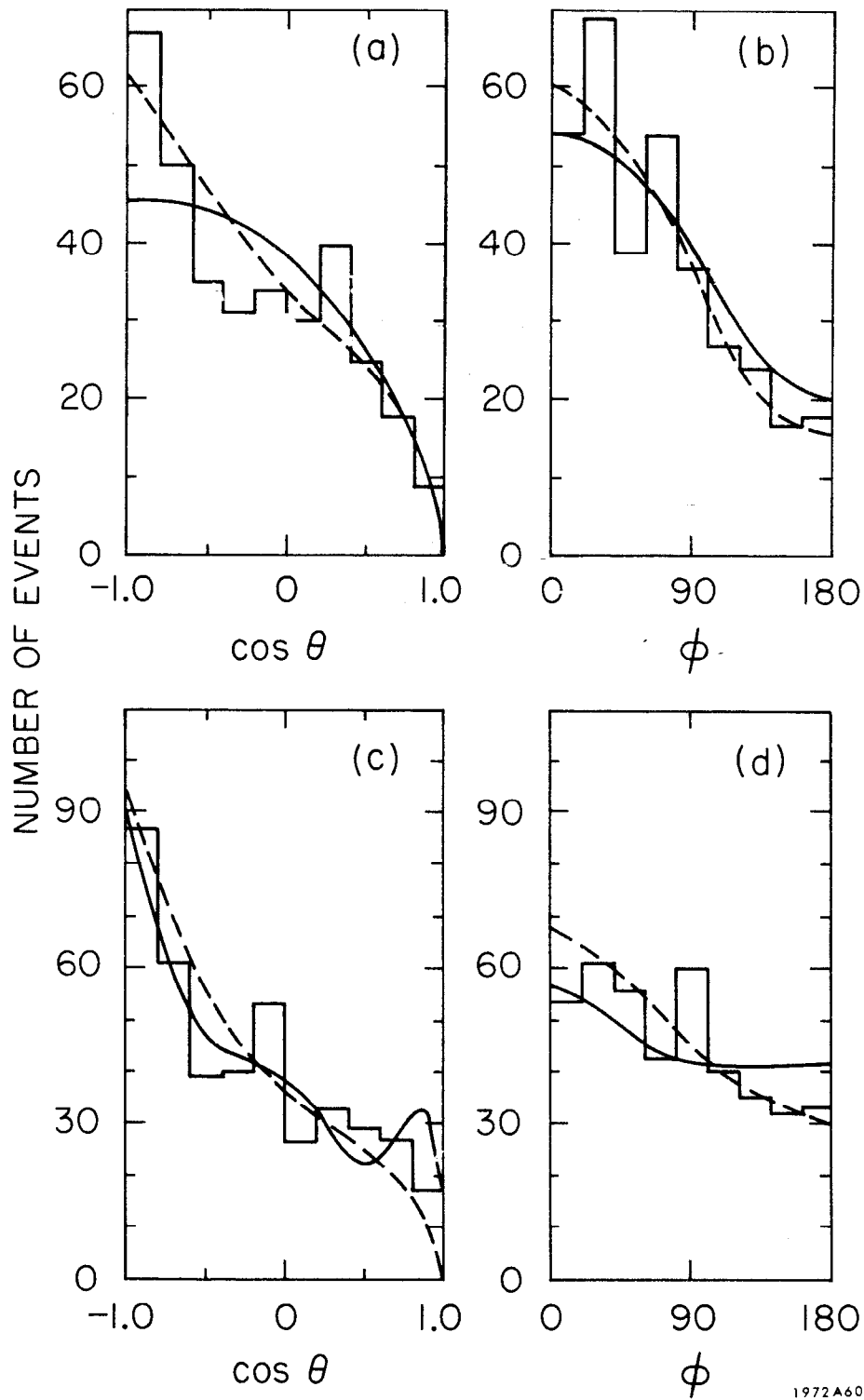
FIG. 7--Comparison of angular distributions with the double Regge and Ross-Yam models.

questions raised previously regarding the nature of the Q.

We compared our data for the $K^*\pi p$ final state to the Ross-Yam model (generalized Deck-model) and to a double Regge-pole exchange model (generalization of Berger's model).[6] The Ross-Yam model can be thought of as an attempt at a non-resonant interpretation of the Q. Our Ross-Yam calculation involved the coherent addition of the three particle-exchange diagrams A, B and C shown in Fig. 5 (we ignored all form factors). For the Regge-pole model we minimized double counting by not considering diagram A. We further assumed that the vertex functions for the Regge-pole versions of diagrams B and C are independent of t. The essential results of the analysis (ignoring the overall normalization difficulties) are that, except for the $M_{\pi K^*}$ distribution, the Ross-Yam model gives a superior description of the data than the double Regge model. Recall that, aside from the normalization, the Ross-Yam model has no free parameters. The Regge model has one additional free parameter, this being the ratio of diagram B to diagram C. Both models provide the interesting variation of the slope of the t-distribution with $M_{\pi K^*}$ (this is due to the contribution of diagram B, as has been noted independently by W. D. Walker).

Because we have not availed ourselves of the extra flexibility which is possible in the Regge parameterization, namely the freedom due to the t-dependence of the coupling at each vertex, our results therefore would suggest that although the

resonance interpretation seems valid for the Q, we cannot exclude the Berger type of Regge parameterization.

The relative success of the Regge model in describing the Q effect has led us to a further probing of its "predictive" powers. Figure 8 displays a possible Regge pole exchange diagram which is very similar to the diffraction dissociation diagram B which was shown previously in Fig. 5. The only apparent difference between these two diagrams lies in the coupling at the nucleon vertex. The diffraction diagram contains the elastic scattering of a virtual particle, while the charge-exchange diagram contains the charge exchange scattering of the same virtual particle. Since the differential charge exchange cross section is known quite accurately as a function of the πN mass, it should then be possible to calculate the relative cross sections for the usual diffractively produced Q and for the analogous charge-exchange produced Q (Q_{CE}). The results of these relative calculations are displayed in Fig. 9.[7] We see that if the only relevant diagrams were the ones displayed in Fig. 8, we would predict that the $M_{\pi K^*}$ distributions in the reactions:

$$K^+ p \to Q^{++} n$$
$$\phantom{K^+ p \to Q^{++}} \big|_{\to \pi^+ K^{*+}} \qquad\qquad (1)$$

$$K^+ p \to Q^+ p$$
$$ \big|_{\to \pi^+ K^{*o}} \qquad\qquad (2)$$

$$K^- p \to Q^o n$$
$$ \big|_{\to \pi^+ K^{*-}} \qquad\qquad (3)$$

$$\sum |M|^2 \approx \frac{q^2}{1-\cos \pi \alpha_\pi} \left(\frac{S_2}{S_0}\right)^{z\alpha_\pi} S_1 q_1^2 \left.\frac{d\sigma}{dt}\right|_{exp}$$

DIFFRACTION   CHARGE EXCHANGE

$$\left.\frac{d\sigma}{dt}\right|_{exp} = \left.\frac{d\sigma}{dt}\right|_{elastic} \qquad \left.\frac{d\sigma}{dt}\right|_{exp} = \left.\frac{d\sigma}{dt}\right|_{charge-exchange}$$
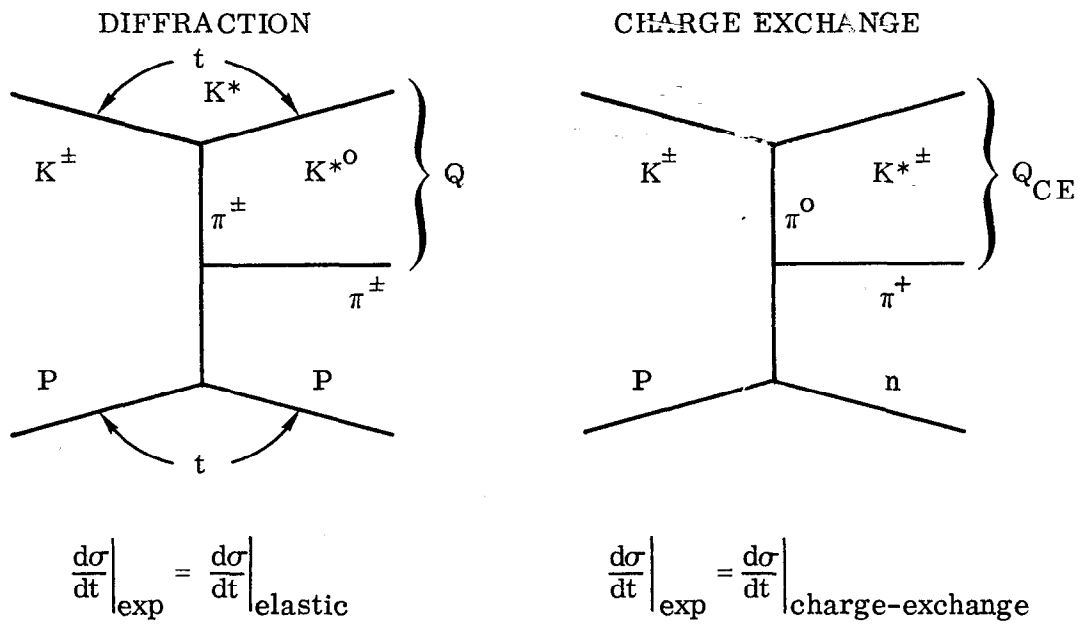
1972A61

FIG. 8--Diffractive and charge exchange double Regge diagrams.

CALCULATED Kππ MASS DISTRIBUTION
12.7 GeV/c
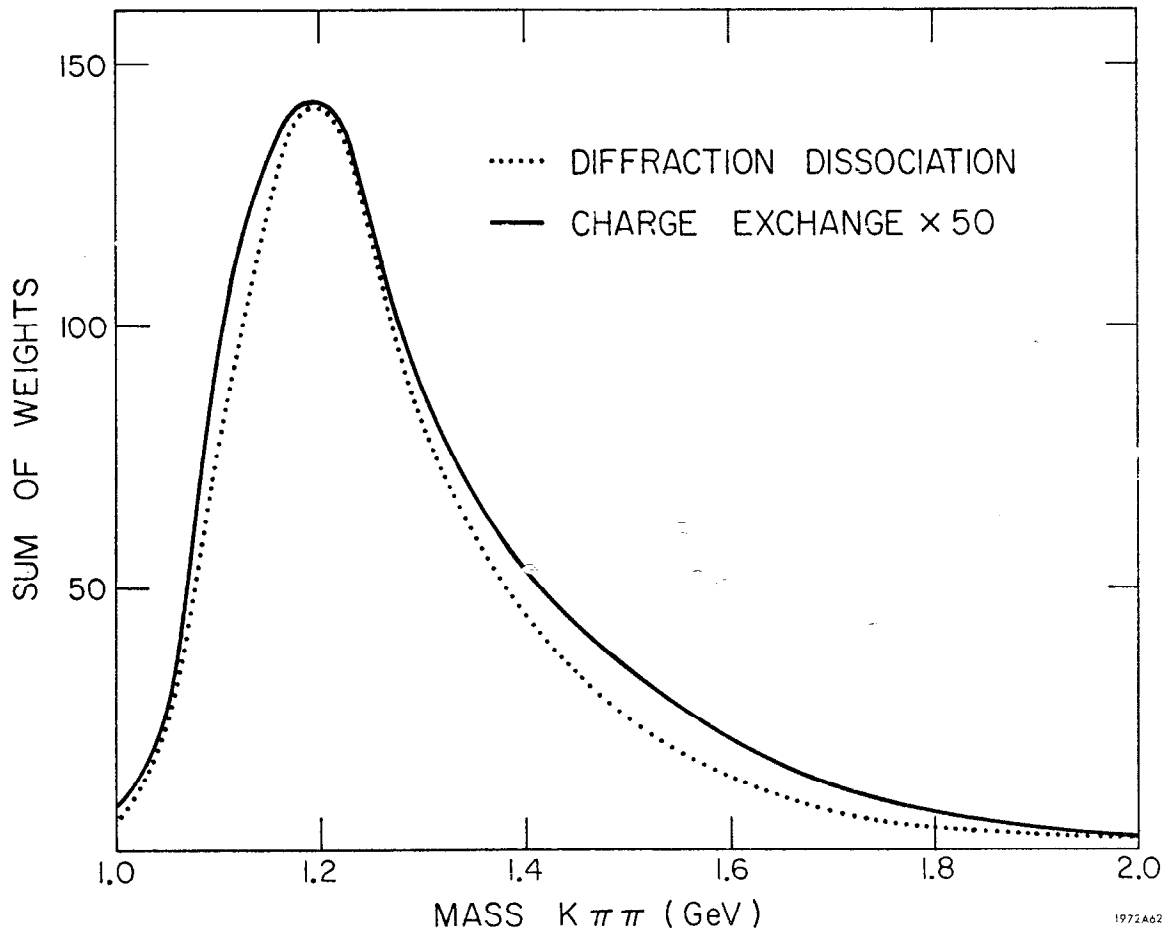
FIG. 9--Predicted Kππ mass spectra for the reaction Kp → Kππp: ---- $K^{\pm}p \rightarrow K^{\pm}\pi^{+}\pi^{-}p$, —— $K^{+}p \rightarrow K^{\pm}\pi^{+}\pi^{0}n$, scaled up a factor 50.

$$K^- p \rightarrow Q^- p$$
$$\hspace{2cm} \big\downarrow_{\rightarrow \pi^- K^{*o}} \hspace{4cm} (4)$$

would have the following relative cross sections:

$$\sigma_{Q^o}/\sigma_{Q^-} \approx \sigma_{Q^{++}}/\sigma_{Q^+} \approx \frac{1}{50} \quad .$$

It is well known that the Q is predominantly $I=\frac{1}{2}$. If the Q were an $I=\frac{1}{2}$ resonance then it would be quite natural to observe the Q^o at $\approx \frac{1}{50}$ of the Q^- rate. (The 0^{++} enhancement would clearly not be expected to be observed; and, in fact, a cancellation of the cross section for the exotic Q^{++} channel would be hypothesized on the basis of duality arguments involving the exchange degeneracy of Regge trajectories contributing to reaction (1).) If the Q were a kinematic effect (as distinguished from a "dual" object) we might expect to see a Q^{++}, as well as a Q^o signal, at $\approx \frac{1}{50}$ of the cross section observed for the diffractively produced $Q^{\pm}$.

Folding in the K^o detection efficiency with other correction factors we calculated that only ≈ 5 Q^{++} events would be expected for reaction (1) in our 10 event/μb exposure. To test the validity of these ideas we therefore compiled the existing world data on reactions (1), (3), and their counterparts as studied in Kd interactions. Figure 10 shows a list of the contributors to the data compilation. Figures 11 and 12 show the $M_{\pi X^*}$ distributions for the charge-exchange reactions. No Q-type of enhancement is observed in the data (about 60 events were "expected" in Fig. 11 and about 40

K ππ Charge Exchange Compilation (~ July 1970)

Contributor	Reaction	Momentum	of Events	
LRL	$K^+ p \to K^0 \pi^+ \pi^+ n$	4.6	170	World K^+ data tape
CERN Brussels	$K^+ p \to K^0 \pi^+ \pi^+ n$	5.0	662	World K^+ data tape
Johns Hopkins	$K^+ p \to K^0 \pi^+ \pi^+ n$	5.5	206	World K^+ data tape
UCLA	$K^+ p \to K^0 \pi^+ \pi^+ n$	7.3	198	Phys. Letters 28B, 143 (1968)
LRL	$K^+ p \to K^0 \pi^+ \pi^+ n$	9.0	445	World K^+ data tape
Birmingham Oxford Glasgow	$K^+ p \to K^0 \pi^+ \pi^+ n$	10.0	976	Private communication
Rochester	$K^+ p \to K^0 \pi^+ \pi^+ n$	12.7	504	This experiment
Purdue	$K^- d \to \bar{K}^0 \pi^- \pi^- pp$	4.5	642	Private communication
ANL-NU	$K^- p \to \bar{K}^0 \pi^- \pi^+ n$	5.5	2055	Phys. Rev. 166, 1317 (1968)
CERN Aachen Berlin Imperial College Vienna	$K^- p \to \bar{K}^0 \pi^- \pi^+ n$	10.0	492	Private communication
Yale	$K^- p \to \bar{K}^0 \pi^- \pi^+ n$	12.6	249	Private communication
			6599	

FIG. 10--List of contributors to data compilation of Kππ charge exchange reactions.

1972A149

(From Reactions In Fig. IO)

K**(1420)

Q

EVENTS / 40 MeV

MASS K*PI   (ALL EVENTS)
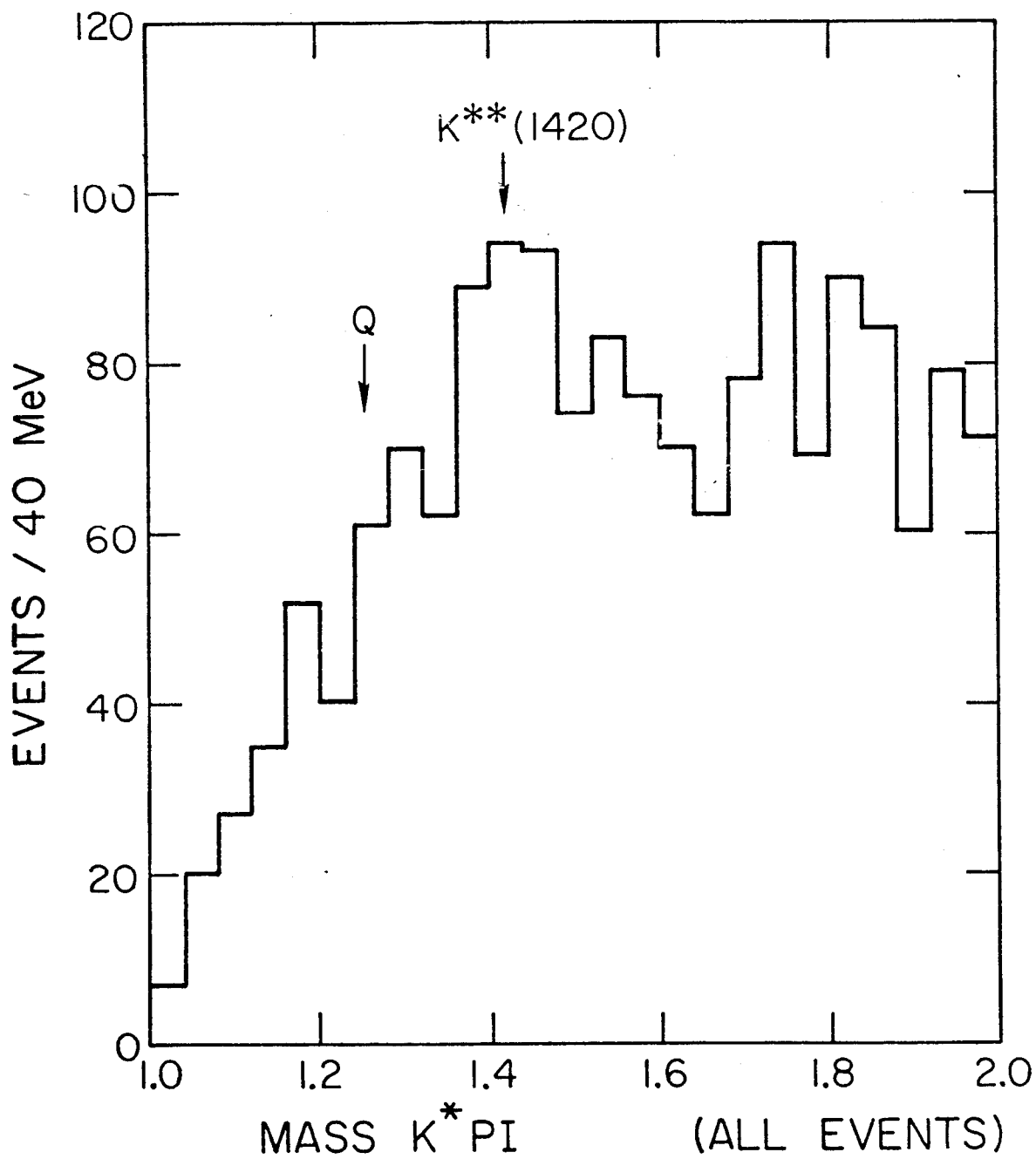
1972A63

FIG. 11--Mass of K*(890)π for all reactions of Fig. 10.

FIG. 12--Mass of K*(890)π for $K^+p \rightarrow K^{*+}(890)\pi^+n$ with $p_{inc} > 9$ GeV/c.

events were expected in Fig. 12). This result is somewhat
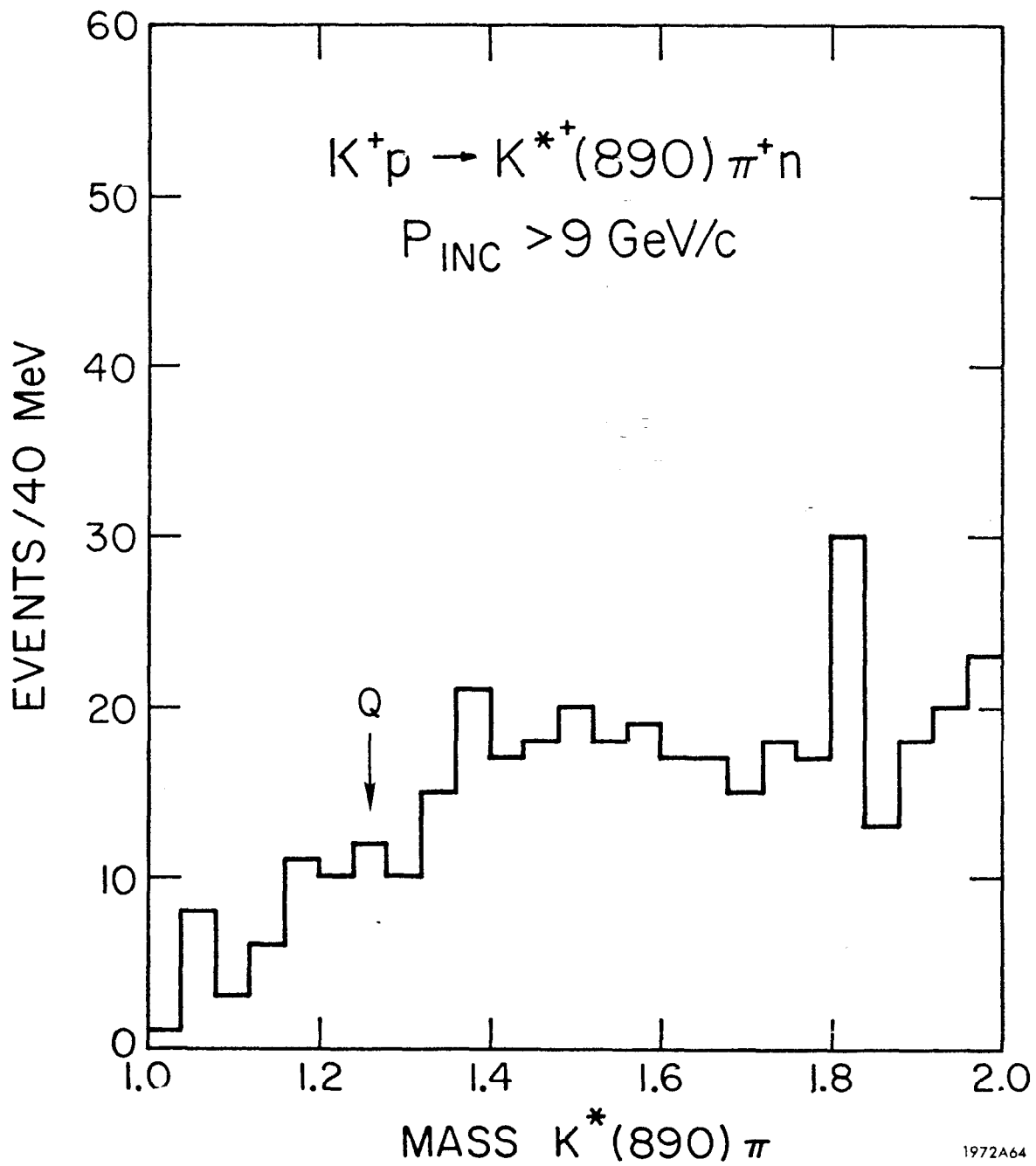
surprising since we would expect that at the very least, the

$I_z=\frac{1}{2}$ charge-exchange Q would appear in the mass spectrum. It

will be very interesting to see what happens when more data

are added to these distributions!

Now I would like to turn to several new results which

have stimulated my speculations concerning the A_1/A_2 and

$Q/K^*(1420)$ problems.

Figure 13 is taken from D. Brockway's thesis (Illinois);

the graph presents the result of a spin-parity analysis of the

$\pi^-\pi^+\pi^-$ mass system in the A_1-A_2 region for the reaction

$\pi^-p\to\pi^-\pi^+\pi^-p$ at 5.0 GeV/c and 7.5 GeV/c incident π^- momentum.

The figure clearly shows the inherent complexity of the $\pi\pi\pi$

low mass region, and indicates that only to a very rough approx-

imation can the A_1 region be considered as consisting of a

superposition of a broad $J^P=1^+$ resonance and a simple, slowly-

varying, background. The Illinois Group and Collaborators have

examined the energy dependence of the $J^P=1^+$ component of the

A_1 region, and the results of this 1^+ projection of the data

are given in Fig. 14. It is observed that the "A_1^-" cross

section falls considerably with energy. The fall off is clearly

faster than that expected on the basis of a fixed Pomeranchukon

pole exchange ($\sim\ell n$ s dependence); the fall is even steeper than

(although probably consistent with) that expected for a

Pomeranchukon trajectory with a slope of ~ 1 GeV^{-2} (i.e. the

effective value for $\alpha(t) \sim 0.9$ and $s^{2(\alpha(t)-1)} \sim s^{-0.2}$).

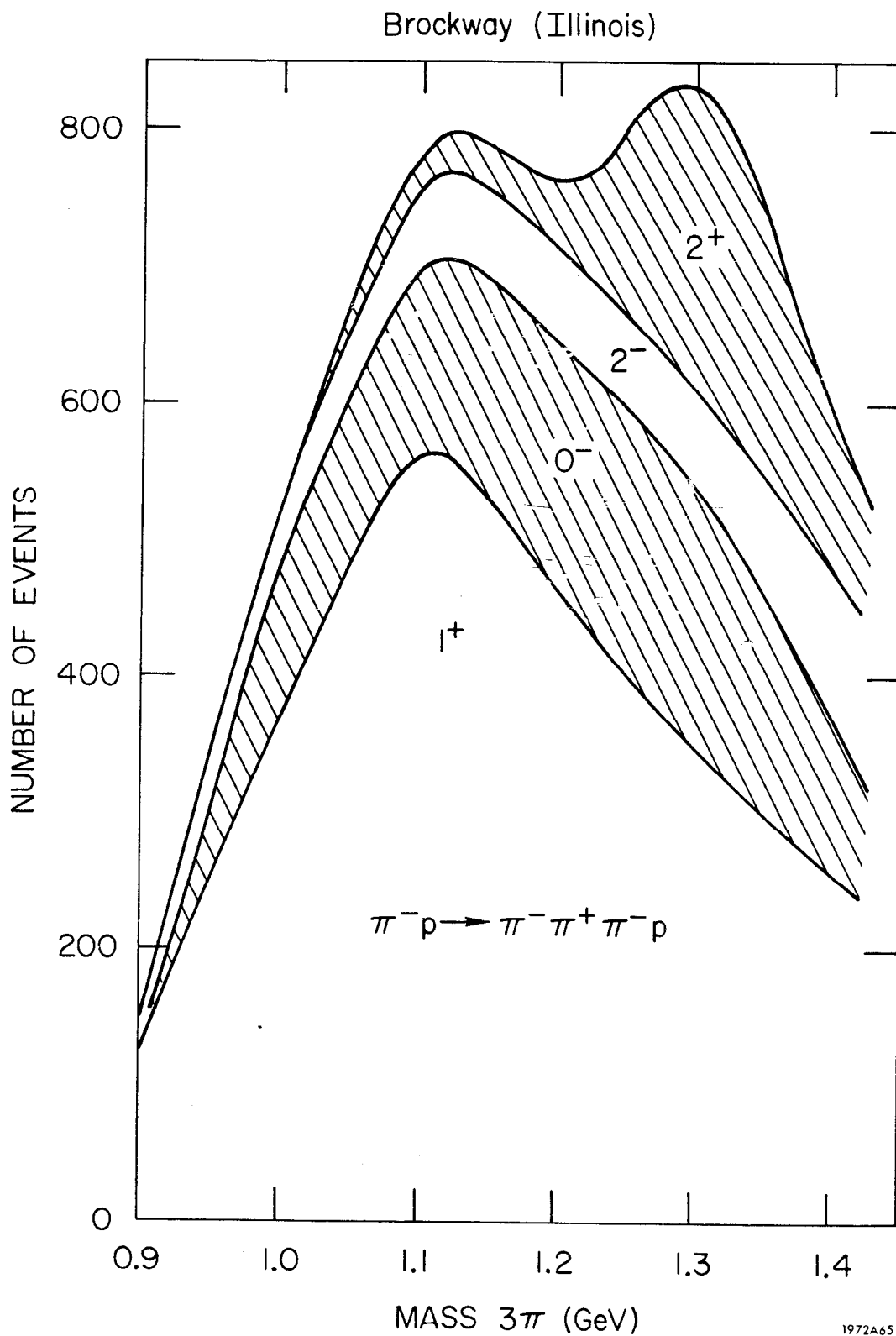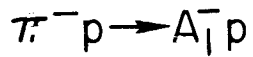FIG. 13--Results of a spin-parity analysis of the A_1 region (D. Brockway, Ref. 11).

$\pi^- p \rightarrow A_1^- p$
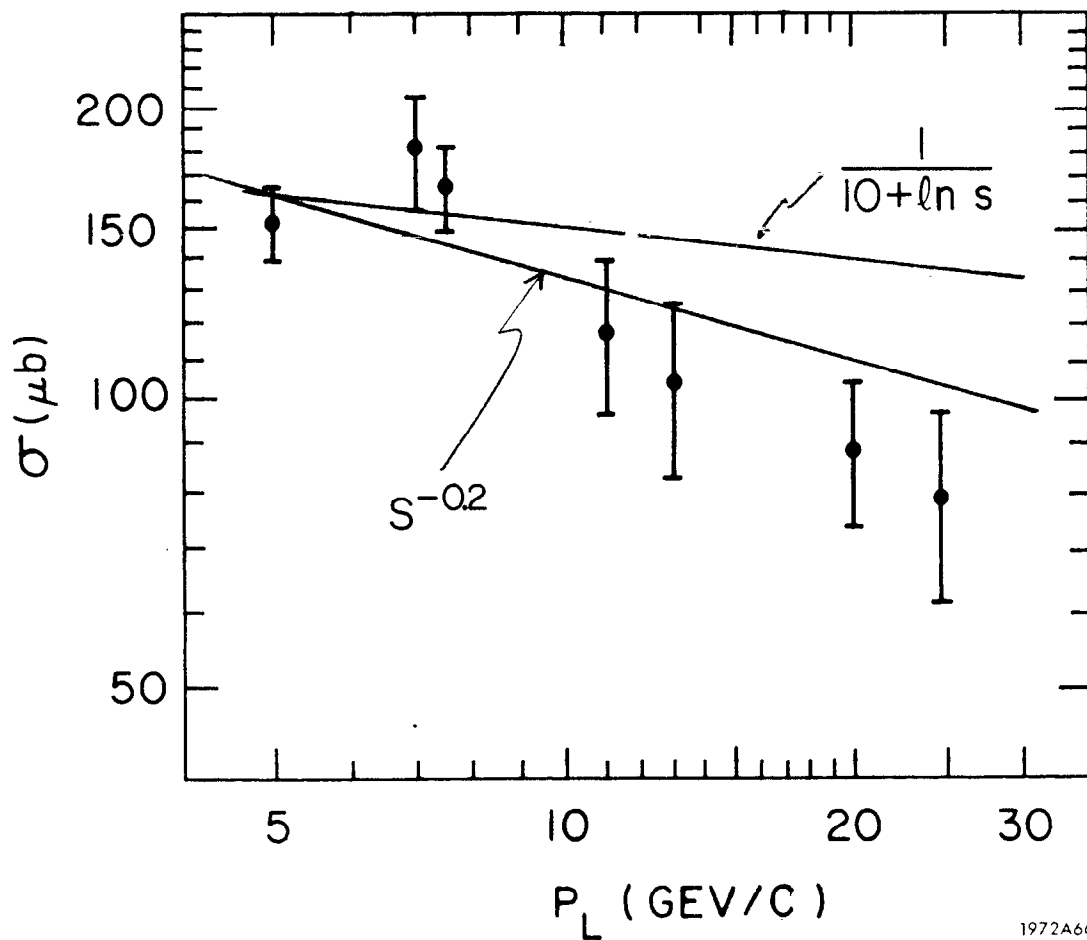
Illinois et al. (Ref 10)

FIG. 14--A_1 cross section (Ascoli et al., Ref. 10) as a function of lab momentum.

13-22

Figure 15 shows the results of a compilation by K.Paler[8]
of cross sections versus incident π^- energy for various re-
gions of $\pi^-\pi^+\pi^-$ mass. I have added several check points and
several π^+p measurements from the literature. The trend of
the π^- data in the A_1 region is similar to that observed in
the Illinois $J^P=1^+$ wave projections. It is also observed
that the π^+p points lie considerably above the π^-p data.
Since $\Delta^{++}(1236)$ background is somewhat larger in the π^+p in-
cident channels than in the π^-p experiments the difference
between "A_1^+" and "A_1^-" production may not be as large as ob-
served on the graph. (M. Ross has previously noted this dis-
crepancy in cross sections.)

In Fig. 16 I present ratios observed for Q^+/Q^- and A_1^+/A_1^-
production (i.e., for K^+p/K^-p and π^+p/π^-p incident channels)
at several prejudicially (?) chosen energies. We see that
there is considerable evidence that Q^+ production is larger
than Q^- production (whereas the opposite would be expected on
the basis of the previously discussed diffraction models!).
These ratios are essentially independent of the manner in which
one defines the A_1 or Q events, i.e., whether Δ^{++} background
is removed or not, whether there is a smooth background sub-
traction, or whether one just simply counts events below a
certain mass value. Although the three results indicated in
Fig. 16 appear to be significant it is important that they be
confirmed at other $K^\pm$ and $\pi^\pm$ beam energies.

The past few graphs have been aimed at dispelling certain
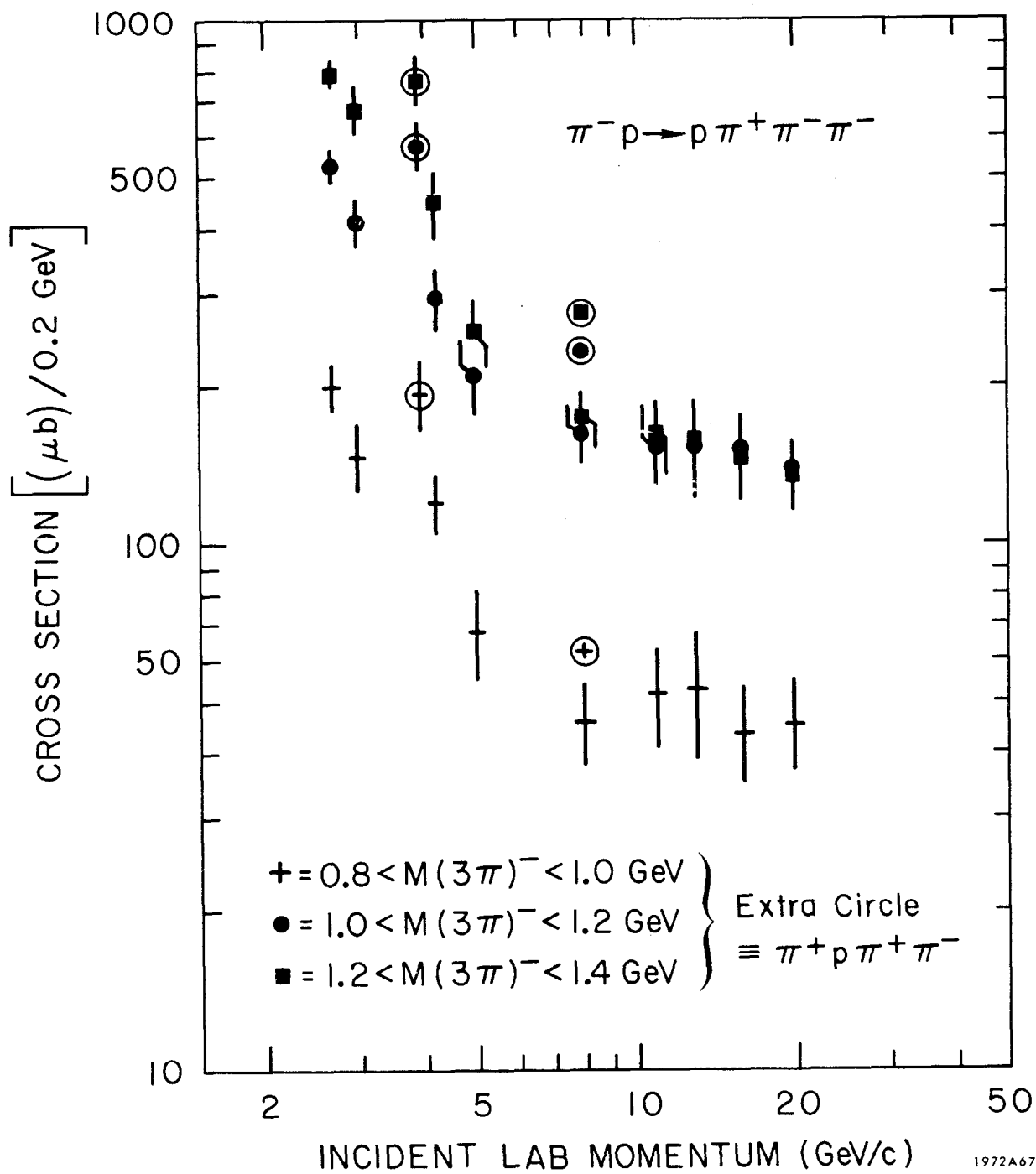
FIG. 15--Compilation by K. Paler (Ref. 8) of cross sections versus incident π^- energy for various regions of 3π mass.

7 GeV/c K^+/K^-	$\geq 1.4 \pm 0.3*$ (UCLA/BNL)
12.7 GeV/c K^+/K^-	$1.5 \pm 0.2**$ (UR/YALE)
18.5 GeV/c π^+/π^-	$1.5 \pm 0.2\dagger$ (ND/ND)

---

*Using published data (C. Y. Chien et al., Phys. Letters 29B, 433 (1969) and S. U. Chung et al., Phys. Rev. 182, 1443 (1969)) this ratio is 2.2 ± 0.4. There appears to be an error, however, in the published K^+ data (private communication from C. Y. Chien).

**The K^-p result is from T. Ludlam's thesis and private communication.

†Private communication from Neal Cason at Notre Dame.

1972A150

FIG. 16--Q^+/Q^-, A_1^+/A_1^- cross section ratios.

myths that we all have been fed (or fed to others) regarding

the A_1 and Q. The constancy of the cross section with energy

is at best only approximate, and the ratio of Q^+/Q^- and A_1^+/A_1^-

production does not appear to be what intuition would lead

some of us to expect.

An interesting hypothesis was put forth recently by

Gilman, Pumplin, Schwimmer and Stodolsky (PL 31B,387) suggest-

ing that, just as in the case of the diffractive ρ-photopro-

duction process, the diffractively produced A_1 and Q should

also be produced conserving helicity in the s-channel rather

than in the t-channel. Examining all the available data on

A_1 and Q production leads me to conclude that, if anything,

the beam direction is the quantization axis which leads to a

simpler description of the decay characteristics in the A_1 and

Q mass regions. That is, in the t-channel (or Gottfried-

Jackson frame) the density matrix elements appear to have less

momentum transfer dependence than in the s-channel (wherein

the z-axis is defined by the line of flight of the object in

the collision center of mass).

In Figs. 17 and 18 I present results pertinent to A_1^+ and

Q^+ decay. The distributions, as a function of t and three-

body invariant mass, are in the angle of the normal to the

three-body decay plane relative to the chosen quantization

axis (θ_t=Gottfried Jackson, θ_H=Helicity). The events which

overlap with Δ^{++}(1236) production are shown shaded on the

figures. (Although this overlap is substantial in the $\pi^+ p$

$$\pi^+ p \longrightarrow \pi^+ p \pi^+ \pi^-$$

(Columbia – Rochester – Rutgers – Yale)

$$0.8 < M_{3\pi} < 1.0$$
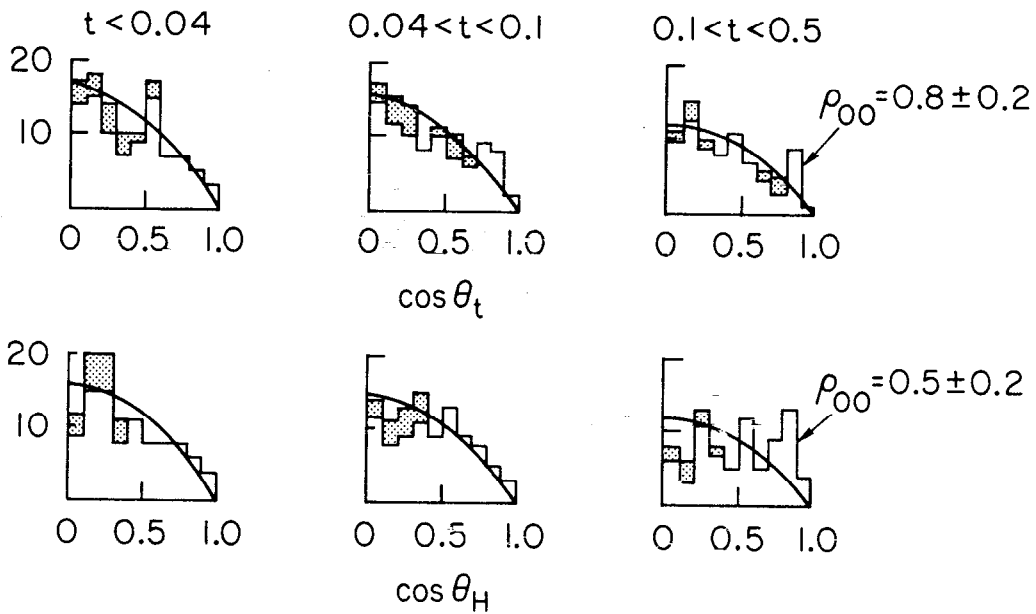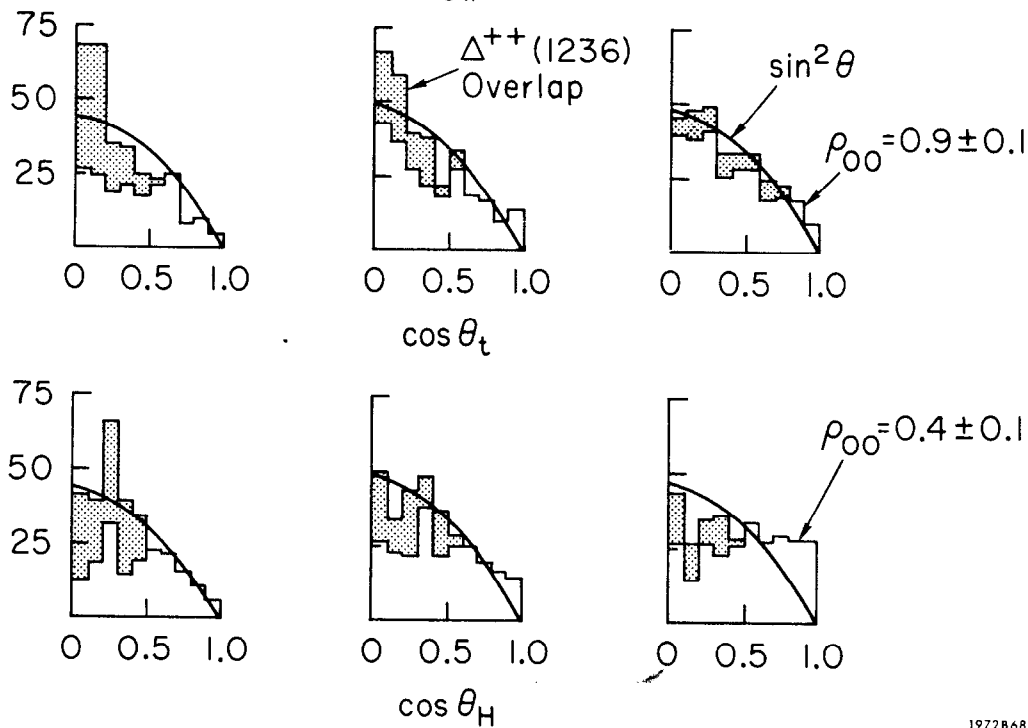
FIG. 17--A_1^+ region angular distributions: θ_t in Gottfried-Jackson frame, θ_H in helicity frame.

$K^+ p \longrightarrow (K\pi\pi)^+ p$ (Rochester)

$1.0 < M_{K\pi\pi} < 1.2$

cos θ_H

cos θ_t

$1.2 < M_{K\pi\pi} < 1.4$

cos θ_H

cos θ_t

1972869
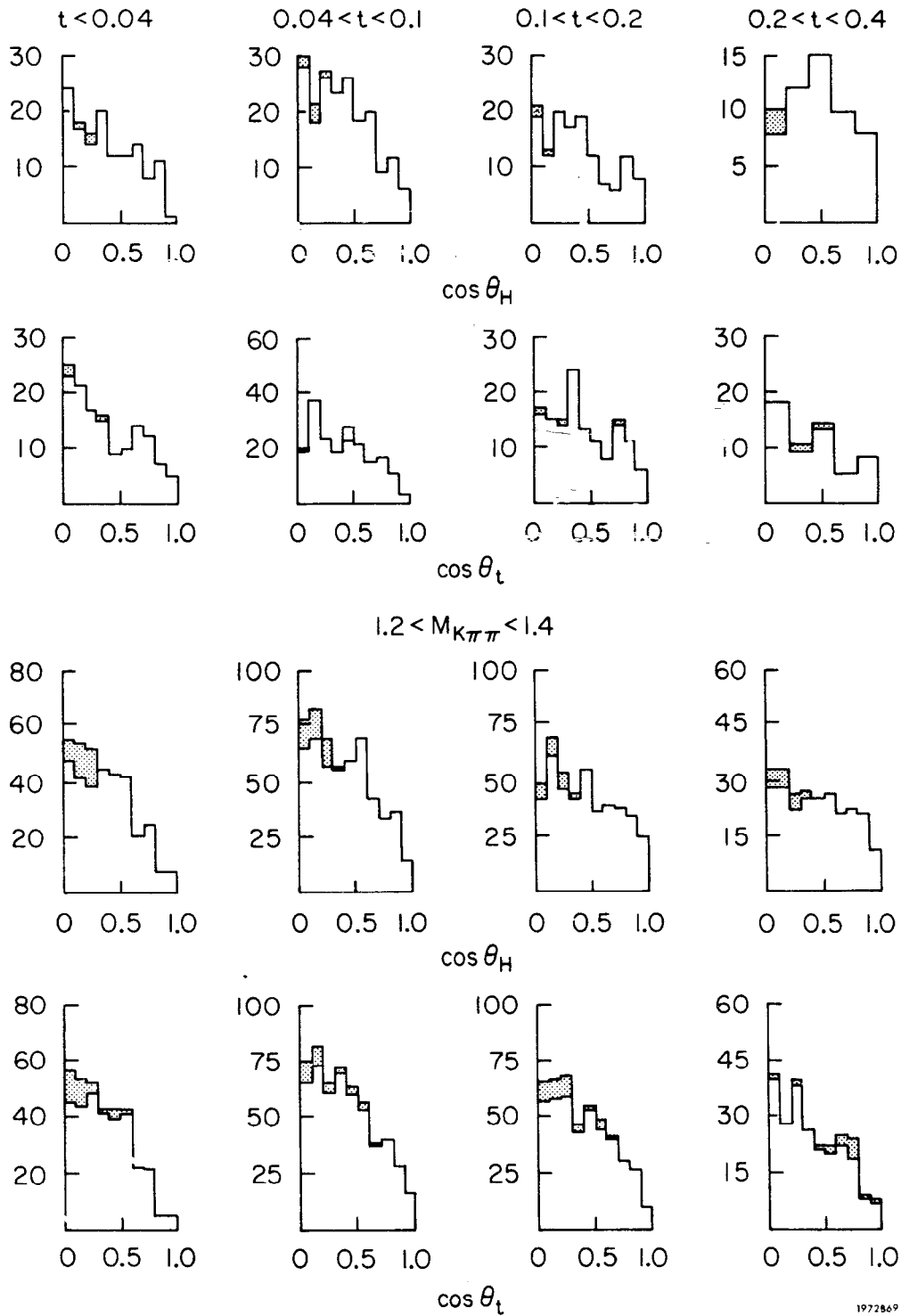
FIG. 18--Q$^+$ region angular distribution: θ_t in Gottfried-Jackson frame, θ_H in helicity frame.

data it does not change the essential conclusions which can be deduced from these figures.) Assuming the Q is a $J^P=1^+$ object we have calculated the density matrix elements $\rho_{0,0}$, $Re\rho_{1,0}$ and $\rho_{1,-1}$ for the Q^+ in the "t-channel", as well as in the "s-channel". All matrix elements, except for the diagonal $\rho_{0,0}$ (and $\rho_{1,1}$), are consistent with being zero for $t \lesssim 0.4$ GeV^2. The value of ρ_{00} as a function of t for the two quantization axes (t and H) are shown in Fig. 19. (There is some evidence for a variation of $\rho_{0,0}$ with the mass of the Q object; see, for example, Table III in P.R. $\underline{D1}$, 78 of Farber et al).. Similar results for the $A_1^{\pm}$ and Q^- from a European Collaboration are shown in Fig. 20 (Δ^{++}(1236) has not been removed).[9]

The Illinois group and Collaborators (Illinois, Genova, Hamburg, Milano, Saclay, Harvard, Toronto, Wisconsin)[10] have calculated the decay density matrix elements only for the $J^P=1^+$ projection in the A_1^- mass region (also correcting for Δ^{++}(1236) in the $A_1-\Delta$ overlap). Their results again clearly indicate that in the t-channel the density matrix elements assume a far simpler form than they do in the s-channel. The results from the Illinois $\underline{et}$ $\underline{al}$ Collaboration also indicate that the beam energy does not have an important effect on the question of t-channel as opposed to s-channel helicity conservation. The value of $\rho_{0,0}(t)$ is essentially equal to unity for all energies and t-values $\lesssim 0.4$ GeV^2, while $\rho_{0,0}(H)$ is strongly t-dependent. (The off-diagonal density matrix

$$K^+ p \longrightarrow Q^+ (1.2-1.4)\, p$$
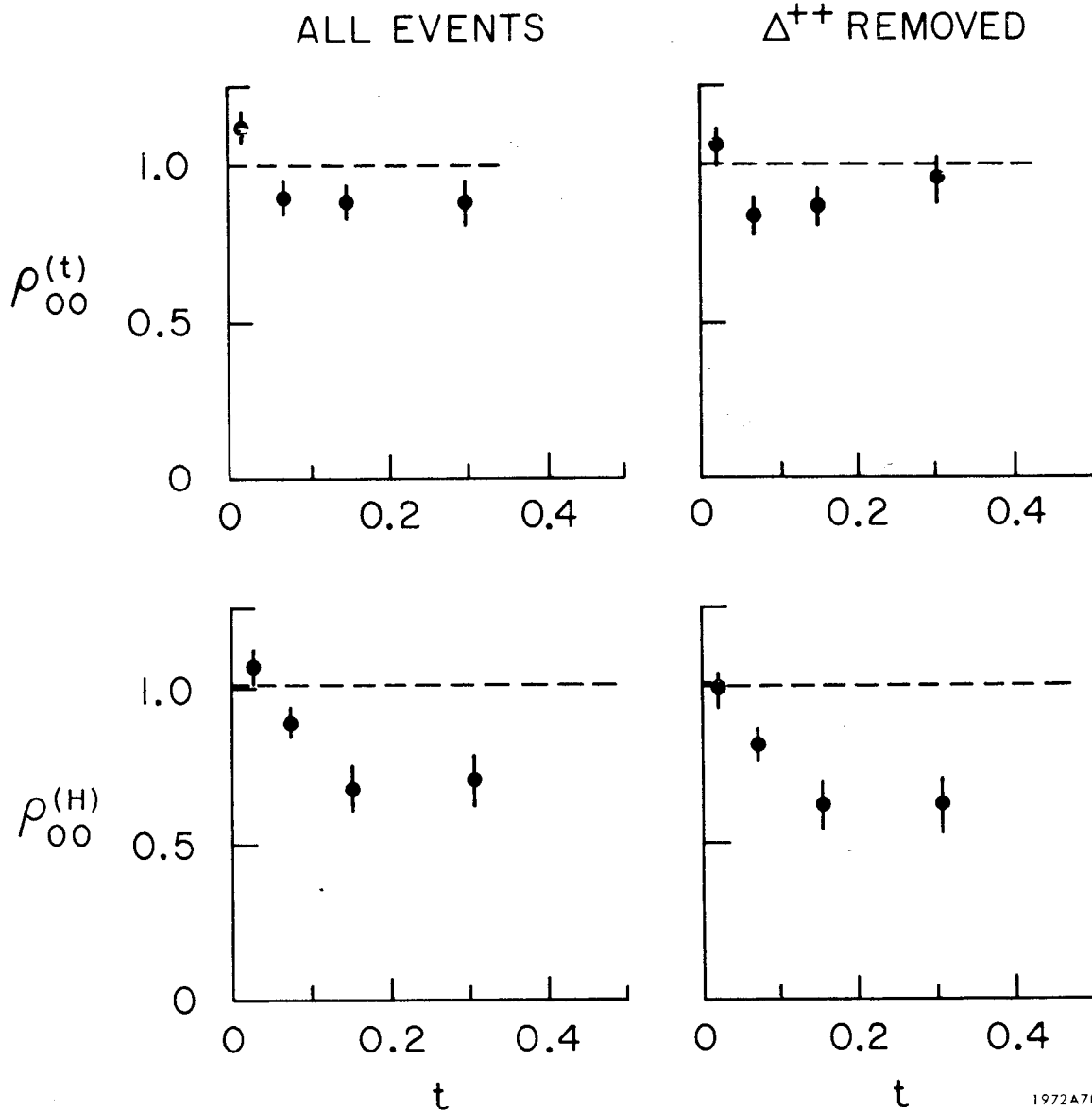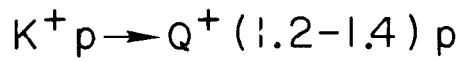
FIG. 19--ρ_{00} in Gottfried-Jackson (t) and helicity (H) frames as a function of t for the Q region.
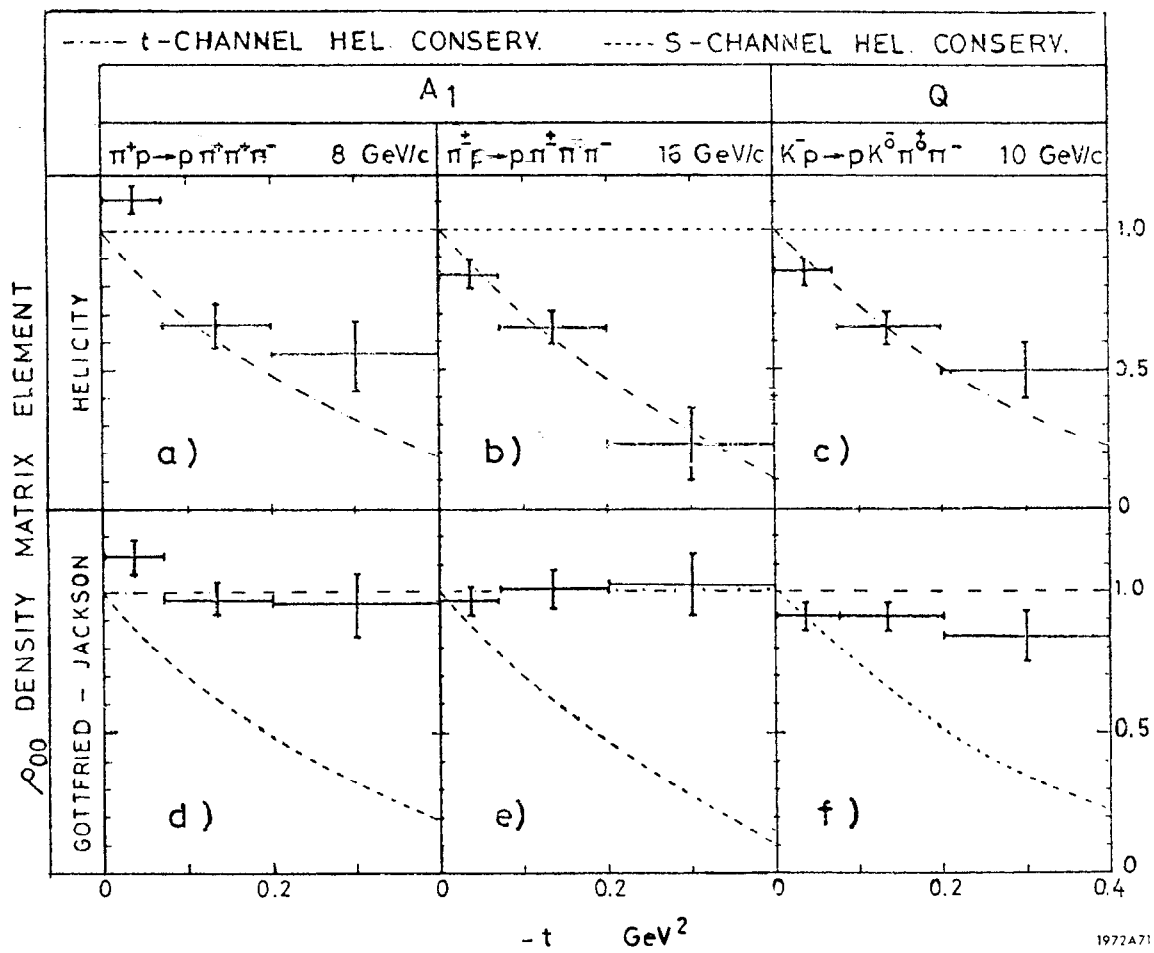
FIG. 20--ρ_{00} as a function of t for A_1 and Q regions (Ref. 9).

element $\text{Re}\rho_{1,0}$ is particularly large in the helicity frame while it is small, although significantly different from zero, in the Jackson frame.) A safe conclusion from all the preceding material is that the frame in which the decay density matrix elements are simplest is the Jackson rather than the helicity frame of the A_1 and/or the Q.

Now I would like to discuss the speculations I have regarding the production mechanism in the A_1/A_2 and in the Q/K^{**} mass regions. Several of the previously discussed results and some old prejudices have gone into these speculations. The most important of these prejudices are:

(1) The Q and the A_1 are smooth, resonant-like peaks.

(2) The bumps which appear in the mass region above the A_1 and Q are "simply" the $J^P = 2^+$ A_2 and $K^*(1420)$ mesons. (I am ignoring A_2 splitting, if any, as well as the suggestions of Gerson Goldhaber, Alex Firestone and others concerning the existence of a $J^{PC} = 1^{+-}$ $K\pi\pi$ object below 1400 MeV in mass.)

The new results of interest (some of these have already been discussed) are:

(1) Another Illinois et al Collaboration (Aachen, Berlin, CERN, Columbia, Rutgers, Illinois, Rochester, Yale)[11] and the Wisconsin-Toronto Groups (Paper presented at Austin) have confirmed the fact that the cross section for A_2 production in the reaction $\pi^{\pm} p \to A_2^{\pm} p$ falls far less rapidly with energy $(\approx \frac{1}{p})$ than for the charge exchange reactions $\pi^+ n \to p A_2^0$ or $\pi^- p \to n A_2^0$ $(\approx \frac{1}{p^2})$,

(This has been suspected for some time. See, for example, K.

Lai in 1968 Philadelphia Conference Proceedings.)

(2)   The Second Illinois et al Group[11] observes a large I=0

exchange term for A_2 production in addition to the usual I=1

ρ-exchange contribution. (The relative importance of I=0 ex-

change may grow with energy). The natural assumption would

be that the I=0 term must be due to f^o exchange. I do not see,

however, why f^o-exchange should have a different energy depen-

dence than that observed for reactions involving A_2 exchange

(e.g., $\pi p \rightarrow \eta \Delta$), which appear to have the standard $\approx \frac{1}{p^2}$ energy

behavior observed for nearly all quasi two-body reactions.

Thus I would conclude that the I=0 exchange contribution to

$A_2^{\pm}$ production may stem from a different mechanism - possibly

Pomeranchukon exchange.

(3)   The fact that the Q^+/Q^- and A_1^+/A_1^- production ratios are

greater than unity suggests to me that the Q and A_1 effects

may contain large resonant contributions. Other explanations

involving interference between I=0 and I=1 exchange are also

possible; I will ignore these, however, since there is no

evidence at present for this sort of interference. (I must

also ignore the result reported by Illinois et al that the

I=0 and I=1 exchanges do not seem to interfere in the produc-

tion of the $J^P = 2^+$ wave in the A_2 region. This result, if con-

firmed, may be difficult to fit into my picture of the low-

mass $X\pi\pi$ enhancements.)

(4) The final bit of new evidence is related to a recent re-examination, by Paul Slattery, of the branching ratio of $K^*(1420)$ $\to K\pi\pi/K\pi \equiv R$. Slattery finds[2] that, ignoring the Q-type of channels (i.e., using only reactions of the type $K^-p \to nK^*(1420)$ or $K^+p \to \Delta^{++}(1236)+K^*(1420)$), the value for R is 0.65 ± 0.09. Figure 21 is taken from Slattery's review (original $K\pi\pi$ mass compilation is from Firestone). I have drawn a Ross-Yam type of background under the mass spectrum (my arguments do not depend very strongly on the detailed shape of this curve). In Fig. 22 I have shown the subtracted difference between the $K\pi\pi$ mass spectrum and the dashed curve in Fig. 21 (ignoring the $K^*(1420)$ signal expected on the basis of known $K^*(1420)$ production in the $pK\pi$ final state and the new value for R). Now, using my prejudice about the Q, I have shown on Fig.22 what a Breit-Wigner shape would look like compared to the data (normalized approximately at the highest bit). To the right of this "difference" mass spectrum is a "second difference" mass distribution which corresponds to the cross-hatched area shown on the "first difference" spectrum. A simple Breit-Wigner has been drawn on the "second difference" spectrum to guide the eye. The parameters of this simple Breit-Wigner should be reminiscent of the $K^*(1420)$. This large apparent $K^*(1420)$ excess is not obtained simply through the judicious choice of a background. The type of background which is used is not important (although I maintain that the one drawn in Fig. 21 looks quite reasonable). In Fig. 23 I show the result
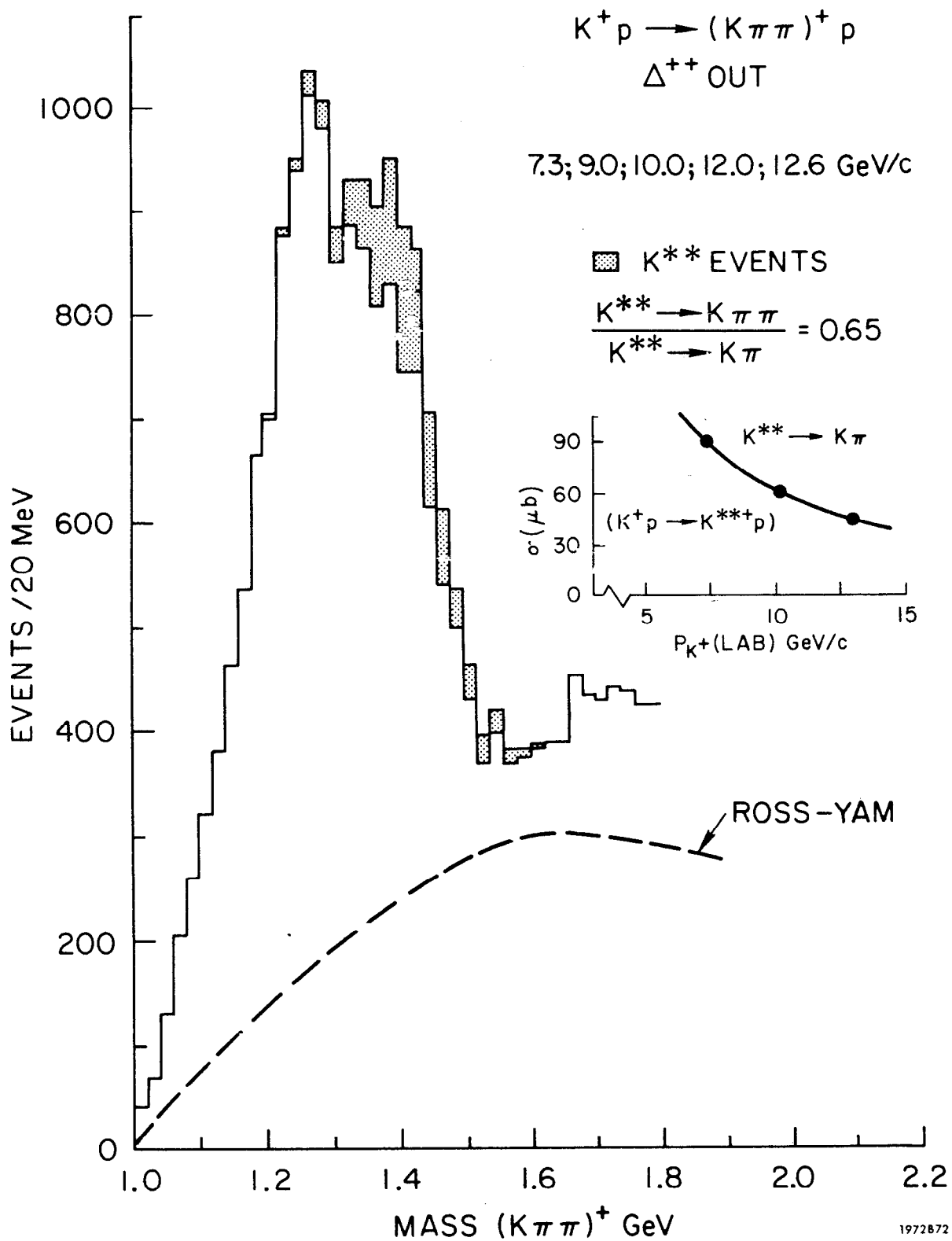
FIG. 21--$K^+p \rightarrow (K\pi\pi)^+p$: $(K\pi\pi)^+$ mass spectrum; ---- Ross-Yam background.
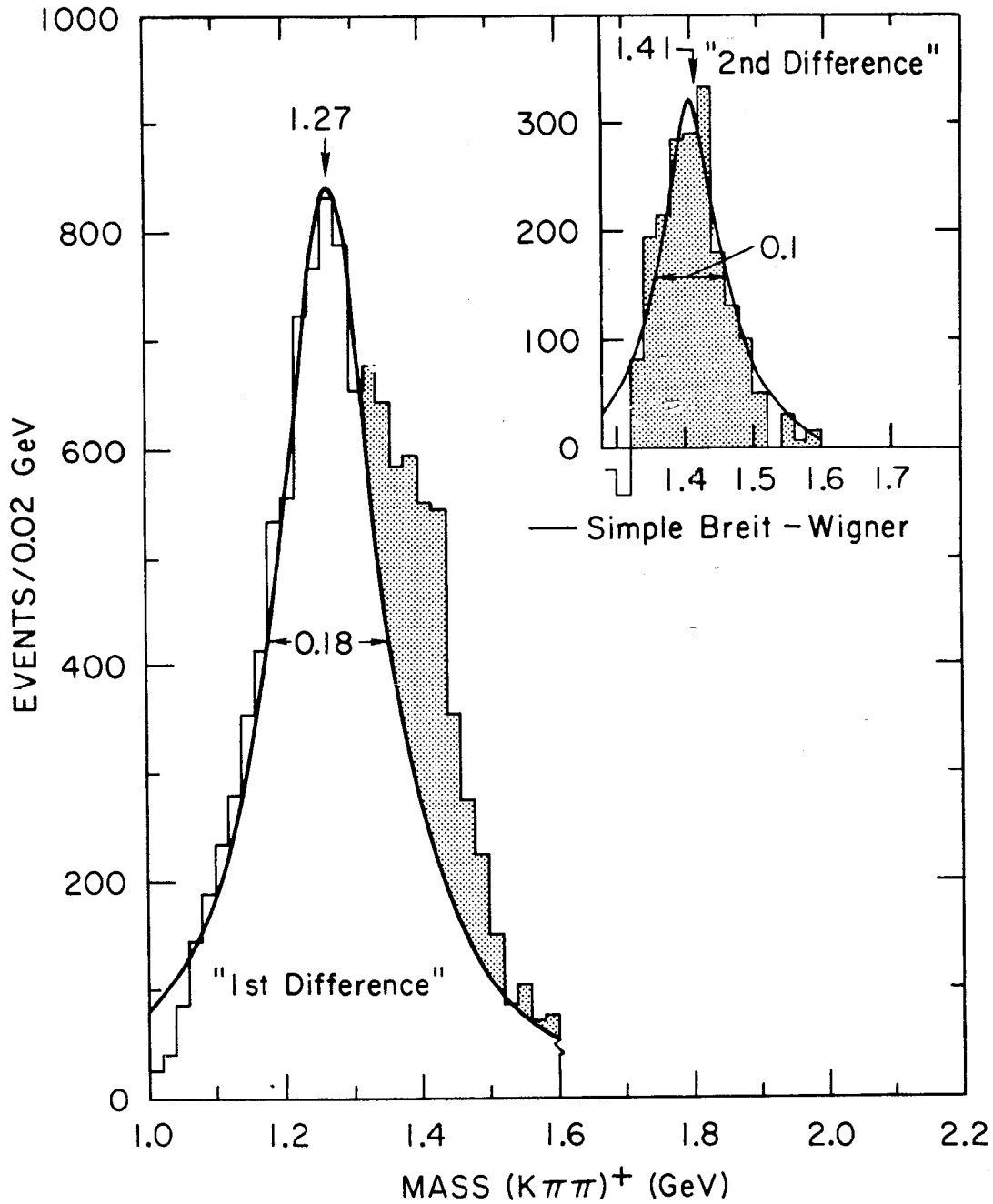
FIG. 22--K$^+$p → (Kππ)$^+$p: (Kππ)$^+$ mass spectrum after subtracting Ross-Yam background. Shaded area shows the events remaining after subtraction of the Q represented by a Breit-Wigner of mass 1.27 GeV and width 0.18 GeV.
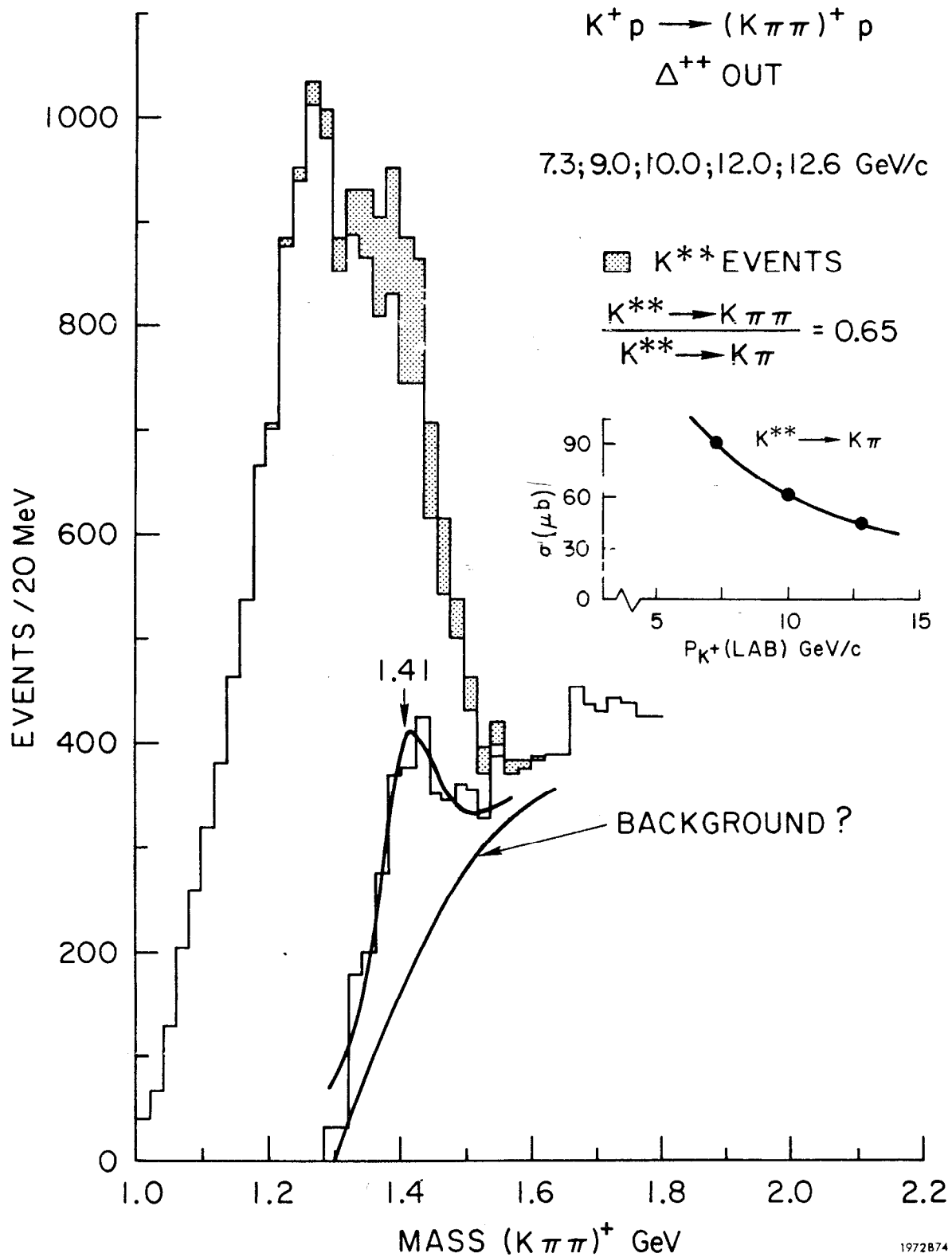
FIG. 23--$K^+p \rightarrow (K\pi\pi)^+p$: $(K\pi\pi)^+$ mass spectrum. Shaded area shows events remaining after subtraction of a Breit-Wigner distribution for Q^+.

of a similar set of subtraction steps wherein no background was assumed to be present in the $M_{K\pi\pi}$ plot of Fig. 21. It is clear that even under this severe assumption there is a substantial excess at the $K^*(1420)$ mass. (Goldhaber, Firestone et al, have been arguing for a long time about the existence of an energy dependent excess below 1400 MeV. I only maintain that this excess is always centered at the $K^*(1420)$ mass and not below.) My conclusion from all the trickery of the past few graphs is that there is an extra amount ($\gtrsim$ a factor of two) of what appears to be $K^*(1420) \to K\pi\pi$ in the reaction $K^+ p \to (K\pi\pi)^+ p$.

Now I come to my speculation (although some may argue that I have been speculating for the past few pages) which "explains" the slow variation of the A_2 cross section with energy as well as the <u>apparent</u> violation of probability conservation due to the observed variation in the $K^*(1420)$ partial branching rates. Since the Pomeranchuk (P) trajectory appears to have a finite slope, this, naively, suggests that the higher moments ($2^{++}, 4^{++} \ldots$) may be important to consider in the P-exchange processes. Thus the rule (Morrison) that the parity change of the meson system in the dissociation $X \to (X\pi\pi)$ changes such that $\Delta(\text{parity}) = (-1)^J$, may not be adequate to describe the general dissociation problem.

In Fig. 24 I have indicated the sort of J^{PC} quantum numbers of meson systems one can get in the more general dissociation case. (My arguments are extremely simplistic in

$$0^{-+}, 1^{++}, 2^{-+}, \ldots$$
$$2^{-+}, 1^{++}, 2^{++}, 3^{++}, \ldots$$
$$4^{-+}, 3^{++}, 4^{++}, 5^{++}, \ldots$$

0^{-+}

P

$0^{++}, 2^{++}, 4^{++}, \ldots$

N   N
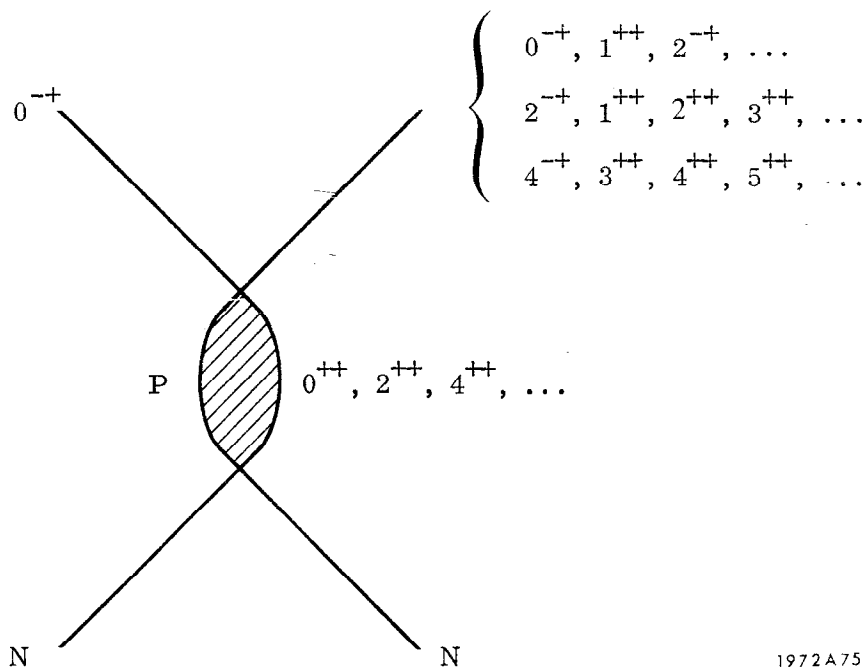
1972A75

FIG. 24--Exchanges possible in diffraction excitation.

that I am treating the P trajectory as a series of particles.) Note that a $J^{PC}=2^{++}$ meson system can be produced via a p-wave interaction between the incident meson ($J^{PC}=0^{-+}$) and the second moment of the P-trajectory (2^{++}). This would suggest that a 2^+ background, due to the sort of mechanisms shown previously in Fig. 5, may be present in the A_2 and $K^*(1420)$ mass regions for the reactions $Xp \rightarrow (X\pi\pi)p$. I must stress, however, that a considerably different background would be expected to be present in the A_2 and $K^*(1420)$ mass regions when these tensor mesons decay into two pseudoscalar mesons (that is, in the final states $K\bar{K}p$, $\pi\eta p$ for the A_2, and $K\pi p$ for the $K^*(1420)$). There is in fact no reason to suspect that a 2^+ background will be present in these simpler final states. Thus it is conceivable that interference between the "resonant" 2^+ contribution (A_2 and K^{**}) and the background 2^+ wave in the $X\pi\pi p$ final state would alter the apparent tensor cross sections as a function of energy. This, however, would occur only in the $X\pi\pi p$ final state and would not effect the cross sections involving two-body decays of the tensor mesons.

The conclusions which we now obtain using the assumption of $J^{PC}=2^{++}$ meson production via P-exchange are that: (1) The tensor meson production cross section will change more slowly with energy in the $X\pi\pi p$ final state than in the $X\pi p$ or $X\pi\pi n$ final states due to the possibility of interference with the background in the $X\pi\pi p$ channel (this is in fact observed to be the case for A_2 production).

(2) A consequence of (1) is that the <u>apparent</u> branching rate of the $A_2 \to K\bar{K}/\pi\pi\pi$ or $K^{**} \to K\pi/K\pi\pi$ will not be constant (except when measured in the non-diffractive channels).

(3) The Q and A_1 can now have nice resonance shapes (as my prejudices require), with the upper mass regions being artificially distorted due to interference (and thus a possible unexpected excess) between the $2^+ A_2$ resonant contribution and the 2^+ background wave near the A_2. (Ed Berger is examining the possibility of a large 2^+ wave in the πX^* system for diagram B in Fig. 5).

(4) Finally, I expect that even in coherent production off nuclei similar effects should be present. That is, there should be an A_2 (K^{**}) shoulder next to the $A_1(Q)$ peak (although this may be difficult to prove because it is hard to separate the coherent from incoherent data, even at small t). Interestingly enough, there is a substantial amount of A_2^+ production reported by the Toronto-Wisconsin Group in coherent interactions off deuterium (Bull. Am. Phys. Soc., Feb. 1971).

The last figure, Fig. 25, shows some more graphing trickery I have performed. I have folded the experimental mass spectrum (above the "Ross-Yam" dashed curve) about the central peak value of 1.11 GeV, and subtracted bin by bin the data on the left of the peak from the data on the right. The difference is shown cross hatched, with a Breit-Wigner drawn on the "second difference" graph in order to guide the eye. The A_2-like peak is certainly suggestive (although far from conclusive).
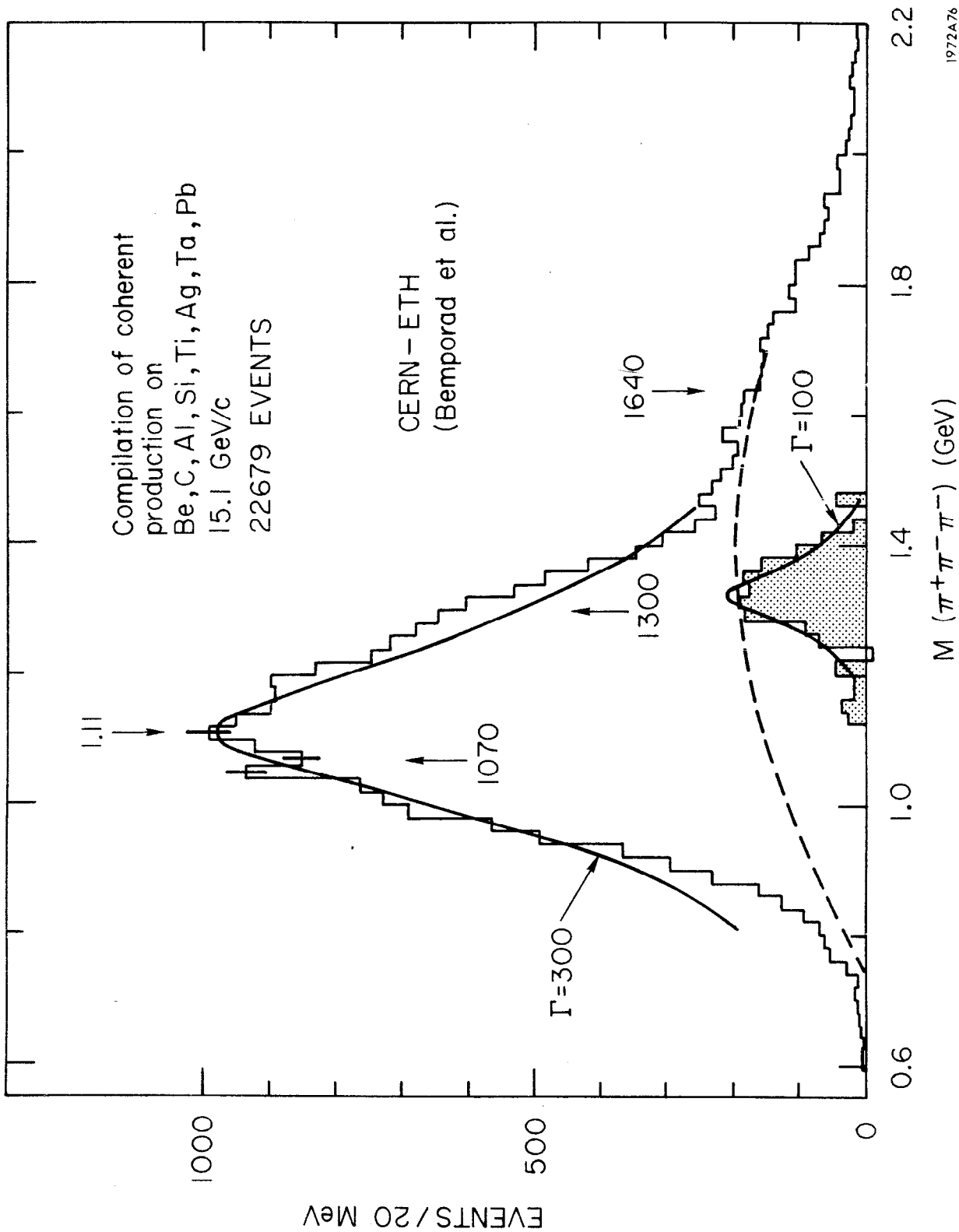
FIG. 25--$\pi^+\pi^+\pi^-$ spectrum: shaded area shows the events remaining after subtraction of a Q^+ Breit-Wigner, and background.

Professor Takeda in his summary talk at the Joint Japanese-U.S. Seminar pointed out how the prejudices and interests of the experimentalists often color the conclusions regarding their data. Although most experimentalists consider themselves free of personal biases, it is safe to assume that at least, to some extent, the experimentalist's view of nature will affect his thinking and his vision. I must admit that I too am guilty of having a particular liking for my own ideas! With this apology I end my version of the summary of experimental facts and their implications.

References

1. G. Bellini et al, Nuovo Cimento 29, 896 (1963); F. R.
    Huson and W. B. Fretter, Bull. Am. Phys. Soc. 8, 325 (1963);
    and particularly G. Goldhaber et al, Phys. Rev.Letts. 12, 336
    (1964), and S.U.Chung et al,Phys.Rev. Letts. 12, 621 (1964).

2. For most recent summaries see the articles of C. Y. Chien
    and of A. Firestone in Experimental Meson Spectroscopy,
    Columbia University Press, C. Baltay and A. Rosenfeld, eds.
    (1970). Also see the review of P. Slattery, University of
    Rochester Report UR-875-332 (1971). For coherent processes
    see the CERN report by H. Bingham,CERN/C.Ph.II/Phys.70-60.

3. See Slattery's paper for a further discussion of threshold
    characteristics. Also see Chien's comments pertaining to
    threshold enhancements.

4. For details see M. S .Farber et al, Phys.Rev. D1, 78 (1970)
    for a discussion of the resonance properties of the Q; see
    M. S. Farber et al, Phys.Rev. Letts. 22, 1394 (1969) for a
    discussion of the non-resonant formulation.

5. D. Griffiths, Nuclear Physics B18, 24 (1970).

6. For details of the calculations see H. Yuta, University of
    Rochester Report UR-875-271 (1969); M. Ross and Y. Yam,
    Phys. Rev. Letts. 19, 546 (1967); E. L. Berger, Phys. Rev.
    Letts. 21, 701 (1968).

7. For more details see B. Werner et al, University of
    Rochester Report UR-875-312 (1970).

8. K. Paler, Nuclear Physics $\underline{B18}$, 211 (1970).

9. Aachen, Berlin, Bonn, CERN, Cracow, Heidelberg, London-Vienna Collaboration, Physics Letters $\underline{34B}$, 160 (1971).

10. G. Ascoli et al, University of Illinois Report COO-1195-204 (1971).

11. D. Brockway et al, University of Illinois Report COO-1195-202 (1970).

p̄p → N̄N INTERACTION AT LOW ENERGY

T. Hirose

Institute for Nuclear Study, University of Tokyo
Tokyo, Japan

T. Yamagata

Tokyo Metropolitan University
Tokyo, Japan

M. Fukawa

Sofia University
Sofia, Bulgaria

T. Emura, K. Takahashi and I. Kita

Tokyo University of Agriculture and Technology
Tokyo, Japan

H. Kohno, T. Ohsugi, R. Hamatsu, Y. Murata and S. Kaneko

Hiroshima University
Hiroshima, Japan

M. Rikihisa

Waseda University
Tokyo, Japan

Introduction

The angular distributions of charge exchange (p̄p → n̄n) and elastic scattering (p̄p → p̄p) have been measured at an incident antiproton kinetic energy of 232 MeV. Since various annihilation channels are open even at zero energy in the N̄-N case, the behavior of the N̄-N interactions in the nonrelativistic energy range is very complicated compared with the N-N interactions. In order to understand the N̄-N interactions together with the N-N interactions, more experimental data on the N̄-N interactions should be accumulated at various energies.

Charge exchange and elastic scattering are complementary to each other because the interference term between the scattering amplitudes of isospin 0 and 1 contributes constructively in one and destructively in the other. This is a preliminary report based on 4×10^4 frames for p̄p → n̄n and 1.5×10^3 frames for p̄p → p̄p. We expect to double our event statistics in the future.

Experimental Procedure

The pictures used were obtained in an exposure of the 80 cm Saclay chamber. In order to identify the reaction $\bar{p}p \rightarrow \bar{n}n$, the emitted $\bar{n}$'s were observed inside the fiducial volume as characteristic annihilation stars with an odd number of prongs with a positive net charge. This is schematically shown in Fig. 1. The one-prong events were very ambiguous and were excluded from the analysis. For $\bar{p}p \rightarrow \bar{n}n$, 42,018 pictures were scanned twice for 3, 5 and 7 prong stars associated with 0-prong stars, and 282 events were obtained. 664 events of $\bar{p}p \rightarrow \bar{p}p$ were obtained from the scan of 1540 pictures. The scanning efficiency was 95.6% for $\bar{p}p \rightarrow \bar{n}n$ and 98.0% for $\bar{p}p \rightarrow \bar{p}p$. The contamination of π^- or μ^- in the $\bar{p}$ beam was about 13%, but these could easily be identified on account of the high bubble density of the $\bar{p}$. For a track to be considered as an incident antiproton, we applied some criteria involving its momentum, fiducial volume, and angle with respect to the average direction of the beam tracks. Thirteen pictures containing two 0-prongs or two odd-prongs were excluded for the analysis of the angular distribution.

Odd-prong stars, 3-prong stars in particular, were excluded as spurious events if they were considered to be the elastic scattering of pions coming from the side wall of the bubble chamber.

The total energy of $\bar{p}p$ is not enough to produce π^0 together with $\bar{n}$ and n in the final state. Multivertex fitting is therefore possible, if the point measurements on the primary and secondary vertices are made with enough accuracy. 4C fits were obtained for the $\bar{n}$ stars without neutral particles, and 1C fits for those with one neutral meson.

The bubble density of each track predicted by GRIND was checked carefully on the scan table. The constrainable pionic final states and their numbers are

$$\bar{n}p \rightarrow \pi\pi\pi \qquad \text{7 events,}$$
$$\rightarrow \pi\pi\pi\pi^0 \qquad \text{46 events,}$$
$$\rightarrow \pi\pi\pi\pi\pi \qquad \text{6 events,}$$
$$\rightarrow \pi\pi\pi\pi\pi\pi^0 \qquad \text{20 events.}$$

This result is consistent with the available data from $\bar{p}d$. The ratio of 5 prongs to 3 prongs was found to be 31%.

In addition to these 79 events, another 190 events with multineutral mesons were used for the analysis of the angular distribution. If the incident antiproton
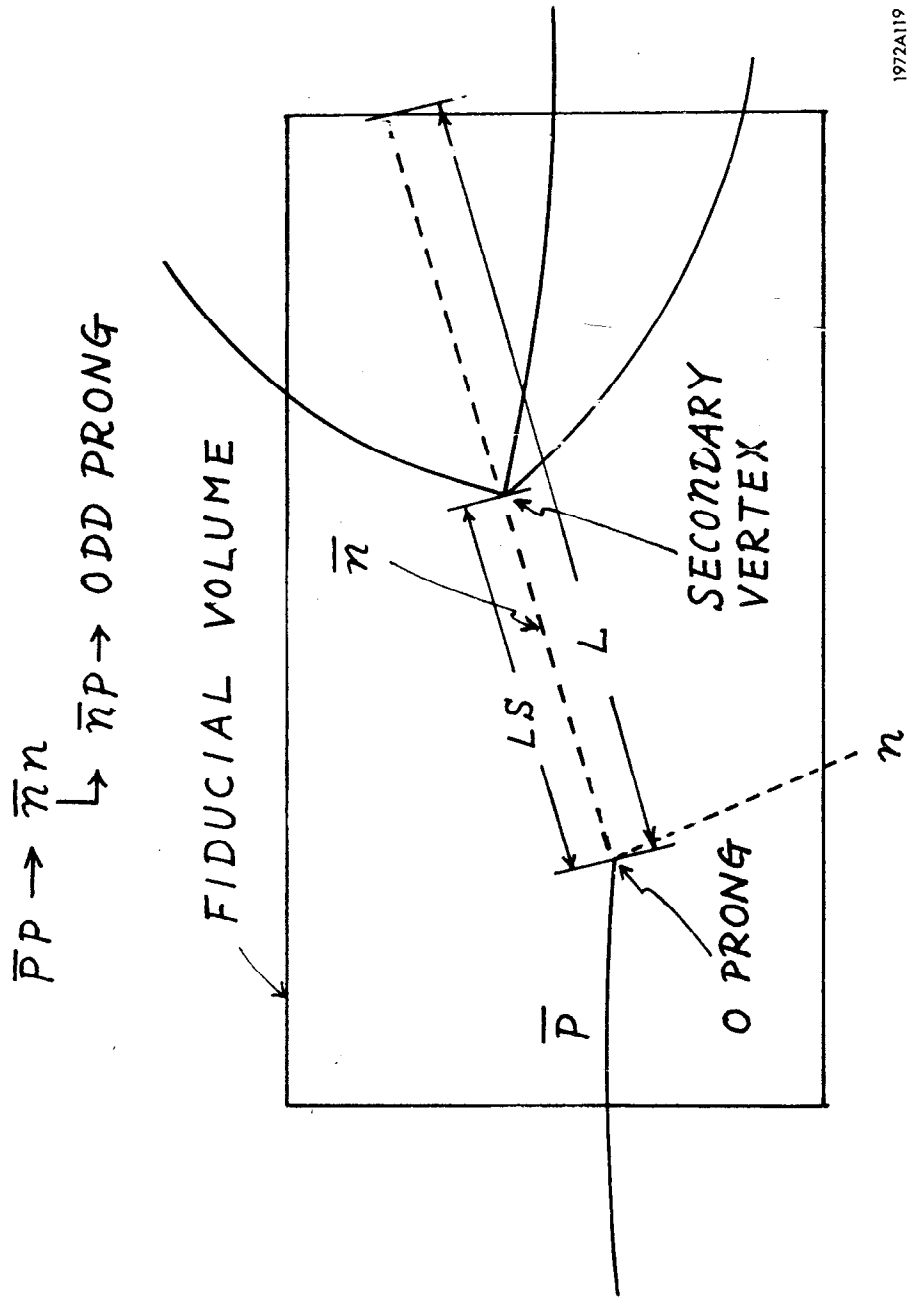
FIG. 1--Schematic view of the charge-exchange scattering with a 3-prong annihilation star of n̄. L is the potential path length of n̄ before leaving the fiducial volume. LS is the distance between the primary (0 prong) and the secondary vertex (odd prong).

is not polarized, the scattered $\bar{p}$ and the odd-prong stars should distribute uniformly in the azimuthal angle measured around the beam direction. Figure 2 shows the flatness of the distribution within statistical errors for $\bar{p}p \to \bar{p}p$ and $\bar{p}p \to \bar{n}n$. The quantity LS/L is also given in Fig. 3 where LS is the distance between a primary and a secondary vertices, and L the potential length of $\bar{n}$ before leaving the fiducial volume. This figure shows that the mean free path of $\bar{n}$ is longer than the path length within the fiducial volume.

Angular Distributions

For the analysis of $\bar{p}p \to \bar{n}n$, each event must be weighted by the detection probability $P(T)$ of annihilation stars of $\bar{n}$,

$$P(T) = \left\{ 1 - \exp\left[-NL\,\sigma(T) \right] \right\}$$

where N represents the density of liquid hydrogen, L the potential length calculated for each event, and $\sigma(T)$ the energy-dependent annihilation cross section of $\bar{n}$ where T is the $\bar{n}$ kinetic energy. Since the energy of $\bar{n}$ is distributed between 0 and 232 MeV, it is necessary to know the energy dependence of the $\bar{n}p$ annihilation cross section. By charge symmetry, the $\bar{n}p$ annihilation cross section is equal to the $\bar{p}n$ cross section. Since the relative rates into various charged prongs may be independent of $\bar{p}$ momentum below 1 GeV/c, the contribution of 1 prongs is estimated to be 17% from $\bar{p}n$ annihilation at rest. The ratio of $\bar{p}n$ annihilation to that for $\bar{p}p$ is nearly 0.75 in $\bar{p}d$ at rest. The energy dependence of the $\bar{p}p$ annihilation cross section is well represented by $1160/\sqrt{T}$ mb up to $T \approx 300$ MeV. Therefore, we obtain

$$\sigma(\bar{n}p \to \text{3 and 5 prongs}) = \frac{1160}{\sqrt{T}} \times 0.83 \times 0.75 = \frac{722}{\sqrt{T}} \text{ mb}.$$

It is not serious to neglect the elastic scattering ($\bar{n}p \to \bar{n}p$), because the energy dependence of σ_{el} is almost the same as that of σ_{an}. In $\bar{p}p \to \bar{p}p$, the scattered $\bar{p}$'s in the extreme forward direction were carefully scanned but only those with a laboratory scattering angle larger than $9°$ ($\cos\theta \leq 0.95$) were used for the analysis of the angular distribution. Due to the mass difference between $\bar{p}(p)$ and $\bar{n}(n)$, the center-of-mass angle θ^* cannot be uniquely determined from the laboratory angle. This kinematical ambiguity could be resolved by referring to the results of the constrained kinematic fits. Taking into account the scanning efficiency, the cross sections of $\bar{p}p \to \bar{n}n$ and $\bar{p}p \to \bar{p}p$ were found to be (9.9±2.0)

(a)
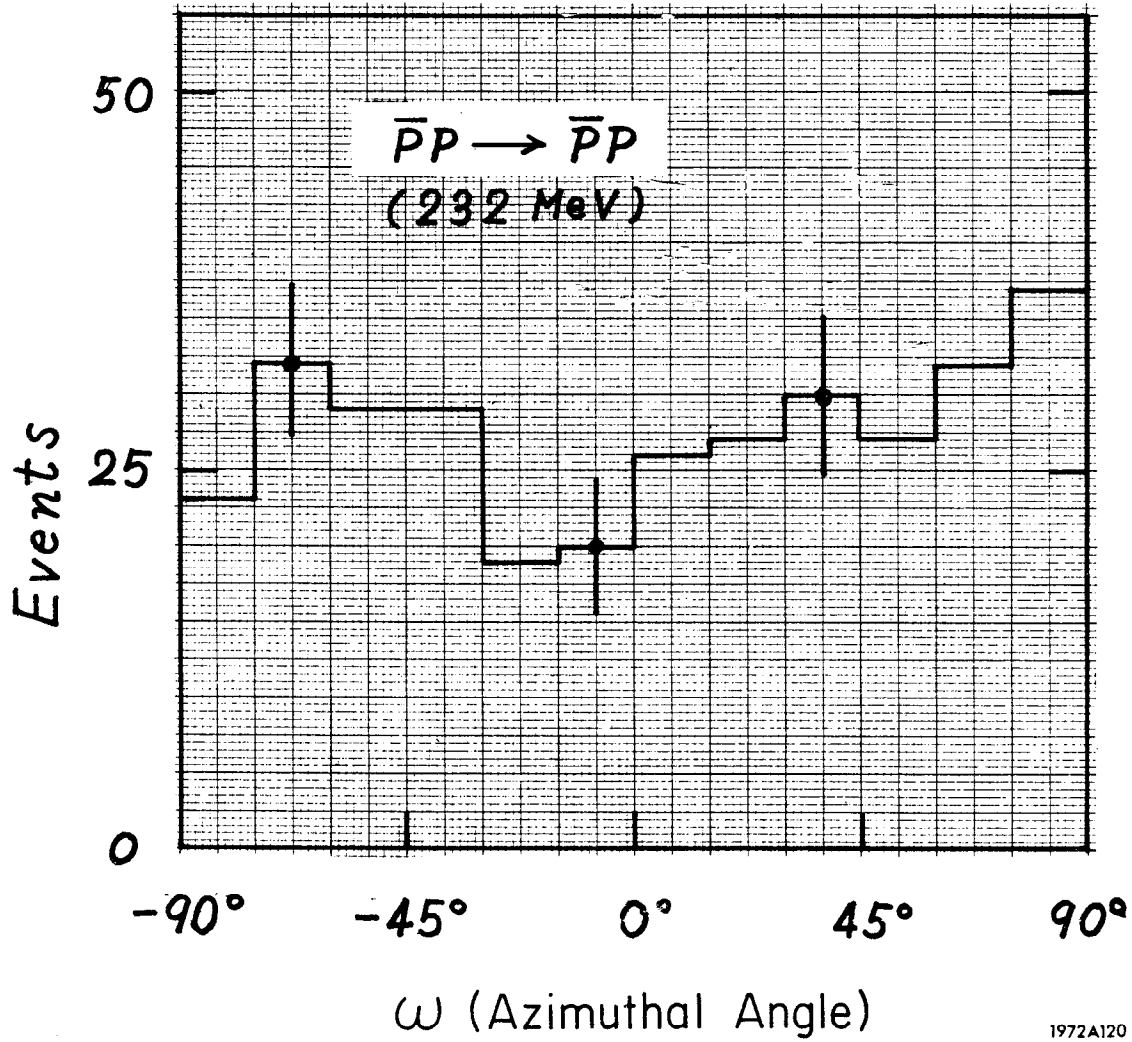
FIG. 2--Distribution of the scattered p̄ (a) and the odd prongs (b) in
the azimuthal angle (ω) measured around the beam direction.
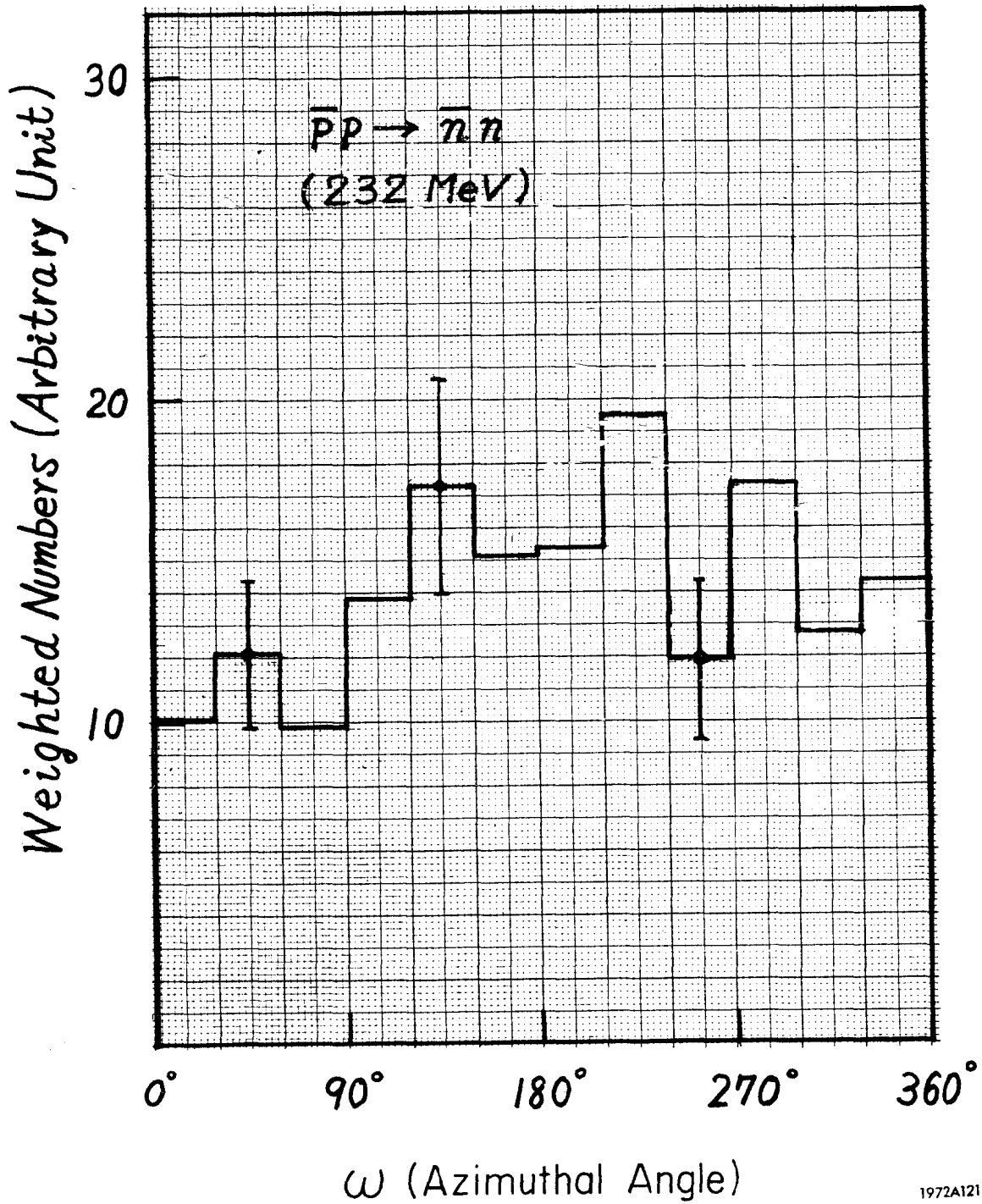
FIG. 2--continued.

(b)

$\overline{P}P \rightarrow \overline{n}n$
(232 MeV)

Weighted Numbers (Arbitrary Unit)

ω (Azimuthal Angle)

1972A121
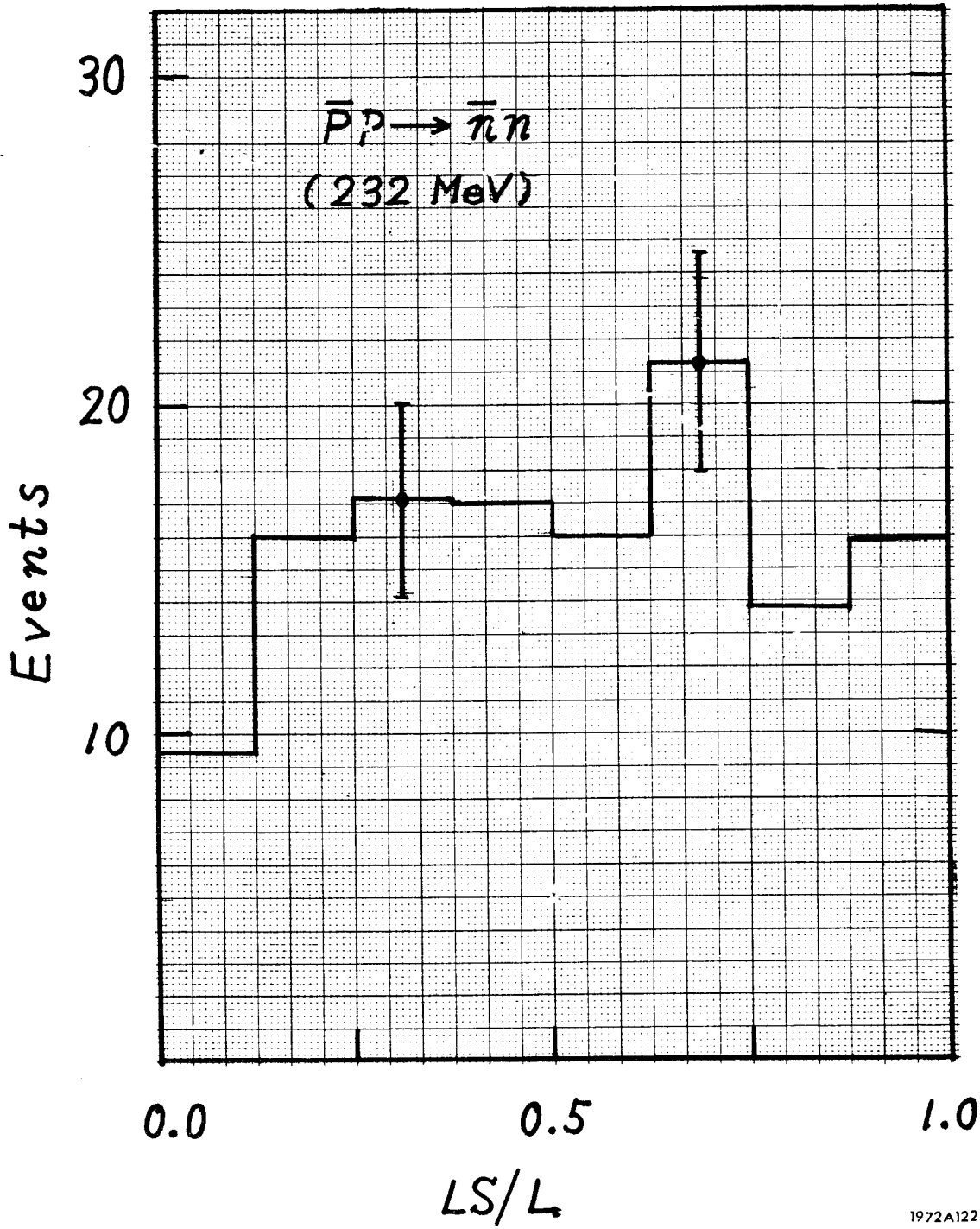
FIG. 3--Distribution of LS/L. LS and L are described in Fig. 1.

14-7

mb and (53.3±3.0) mb, respectively. $\sigma(\bar{p}p \to \bar{n}n)_{tot}$ may contain some systematic errors mainly due to the uncertainty in the $\bar{n}p$ annihilation cross sections used.

Results and Discussion

In Table 1, the total cross sections for various final states are presented. They are consistent with the available data. The angular distributions as a

Table 1: Partial and Total Cross Sections

Energy (MeV)	---	(700 ± 20) MeV
0-prong		
σ (charge exchange)		9.9 ± 1.1 mb
σ (annihilation)		2.2 ± 0.7 mb
2-prong		
σ (elastic)		53.5 ± 3.0 mb
σ (annihilation)		27.0 ± 4.0 mb
σ (4-prong)		35.7 ± 2.6 mb
σ (6-prong)		3.1 ± 0.5 mb
σ (Total)		131.4 ± 5.9 mb

function of the four-momentum transfer t and the center-of-mass angle θ^* are shown in Fig. 4 and Fig. 5, respectively, where the errors indicated are statistical only. The t-dependence of the cross section is represented by the diffraction model:

$$\frac{d\sigma}{dt} = A J_1^2 \left[\left(\frac{a + \lambdabar}{\hbar} \right) \sqrt{|t|} \right] / t , \qquad A = b + c\lambda .$$

The Roma-Trieste group determined $a = 1.04$ fm, $b = 29.4$ mb and $c = 49.5$ mb fm^{-1} by fitting the forward peak of $\bar{p}p \to \bar{p}p$ at energies lower than 180 MeV. The forward peak is well reproduced at 232 MeV with these parameters and $\lambda = 0.60$ fm. The sharp diffraction peak appears in $\bar{p}p \to \bar{p}p$ (Fig. 4a) but not in $\bar{p}p \to \bar{n}n$ (Fig. 4b). Assuming charge independence, the scattering amplitudes T are expressed as

$$T(\bar{p}p \to \bar{p}p) = \frac{1}{2} T_0 + \frac{1}{2} T_1$$

$$T(\bar{p}p \to \bar{n}n) = \frac{1}{2} T_0 - \frac{1}{2} T_1$$
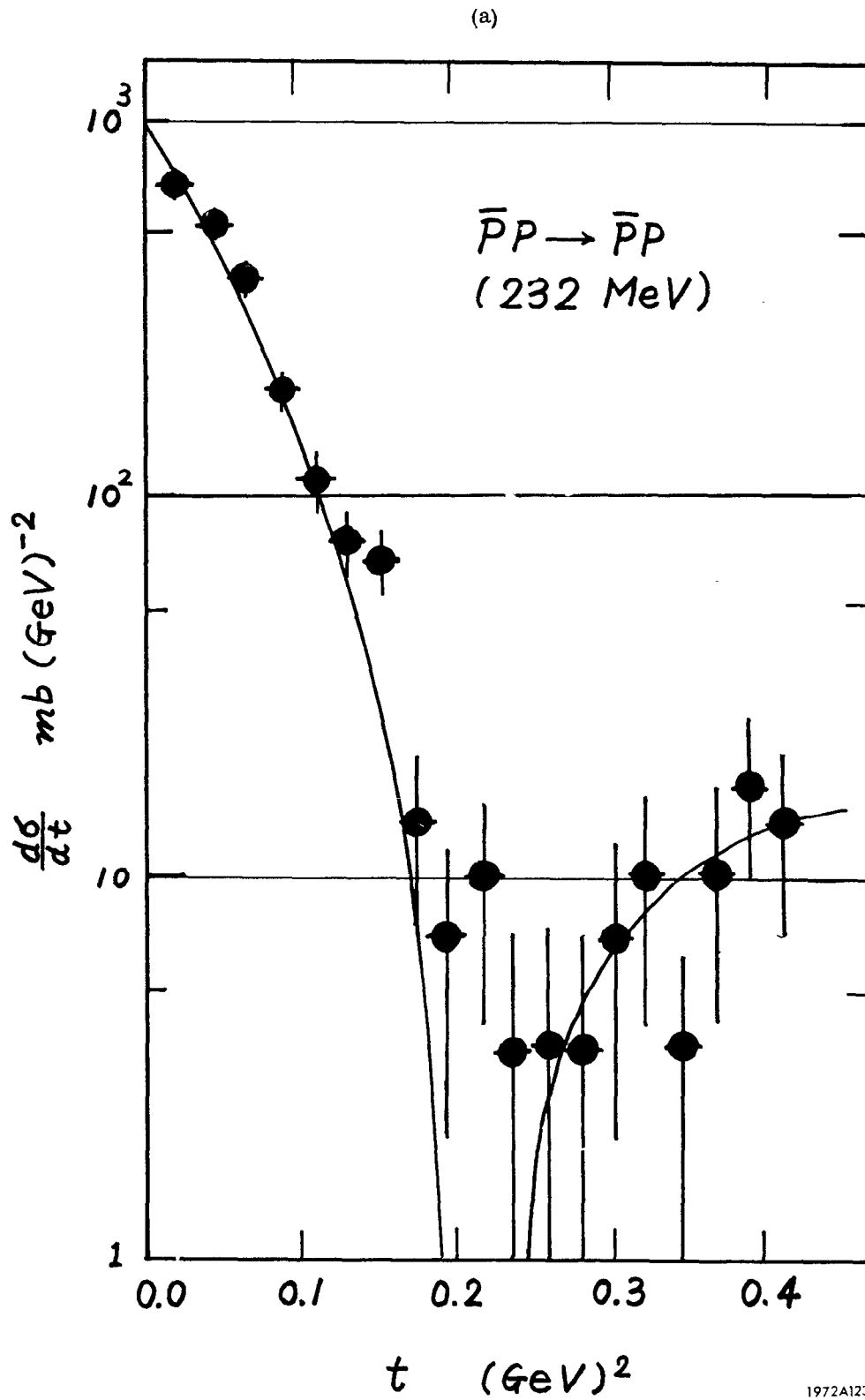
FIG. 4--Differential cross section dσ/dt for $\bar{p}p \rightarrow \bar{p}p$ (a) where the solid curve is calculated by a diffraction model and for $\bar{p}p \rightarrow \bar{n}n$ (b); the straight line is drawn by hand.

FIG. 4--continued.

(b)
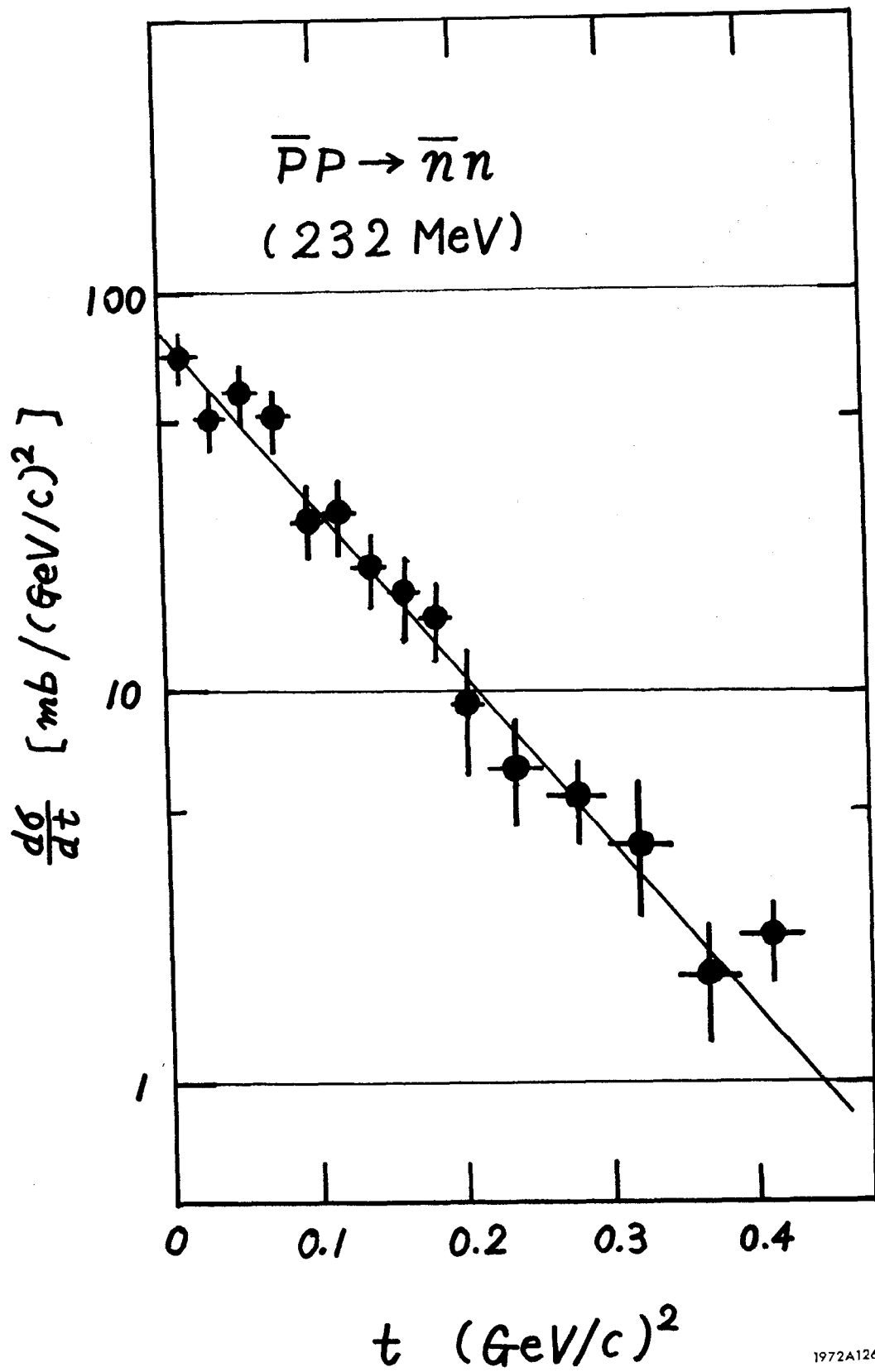
$$\overline{P}P \rightarrow \overline{n}n$$
$$(232 \text{ MeV})$$

1972A126
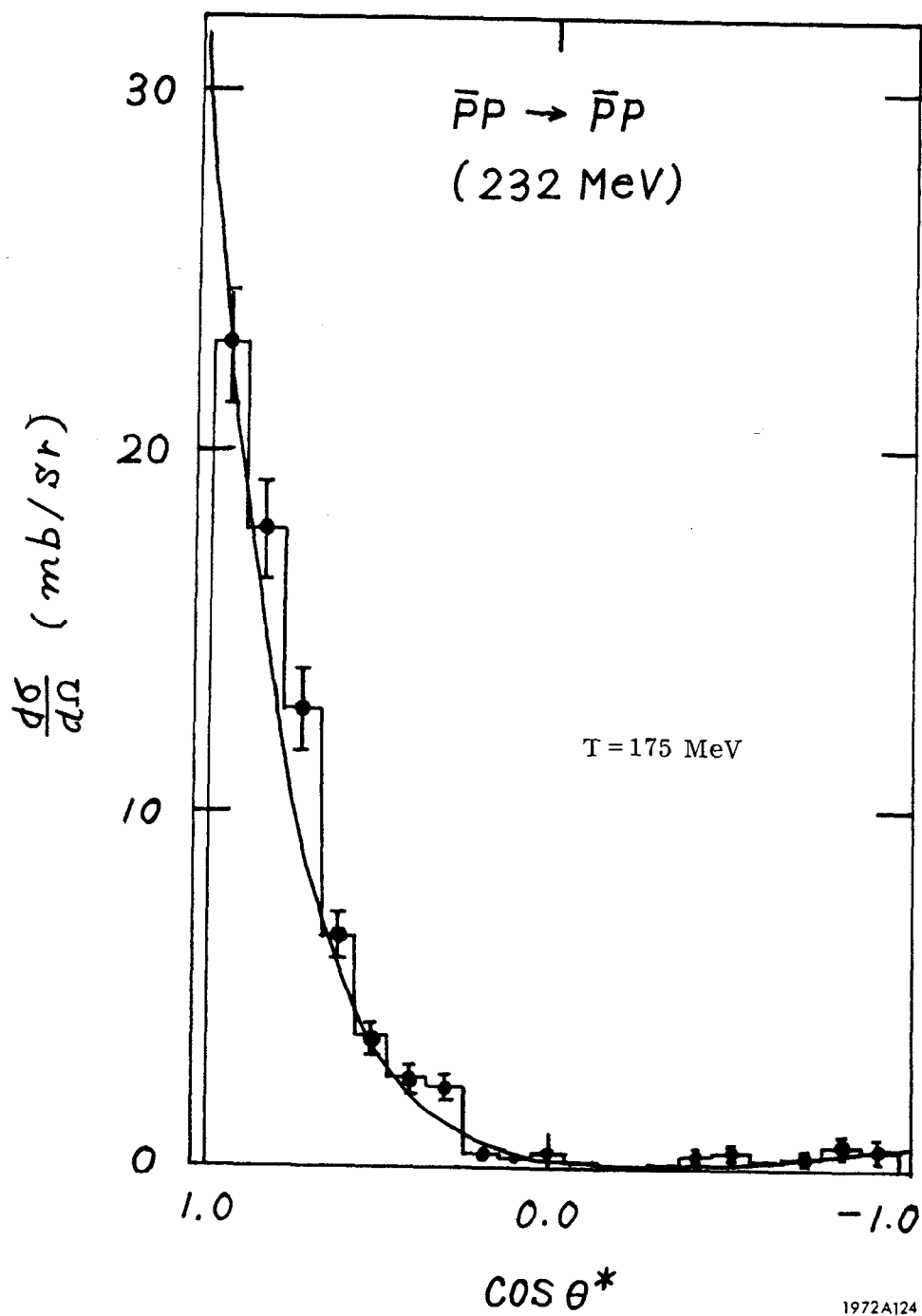
FIG. 5--Center-of-mass differential cross section dσ/dΩ for p̄p → p̄p (a) and for p̄p→ n̄n (b). Only statistical errors are shown. The curves are the Bryan and Phillips theoretical predictions.

FIG. 5--continued.

(b)

$\overline{p}p \rightarrow \overline{n}n$

(232 MeV)

T = 150 MeV

1972A125

14-12
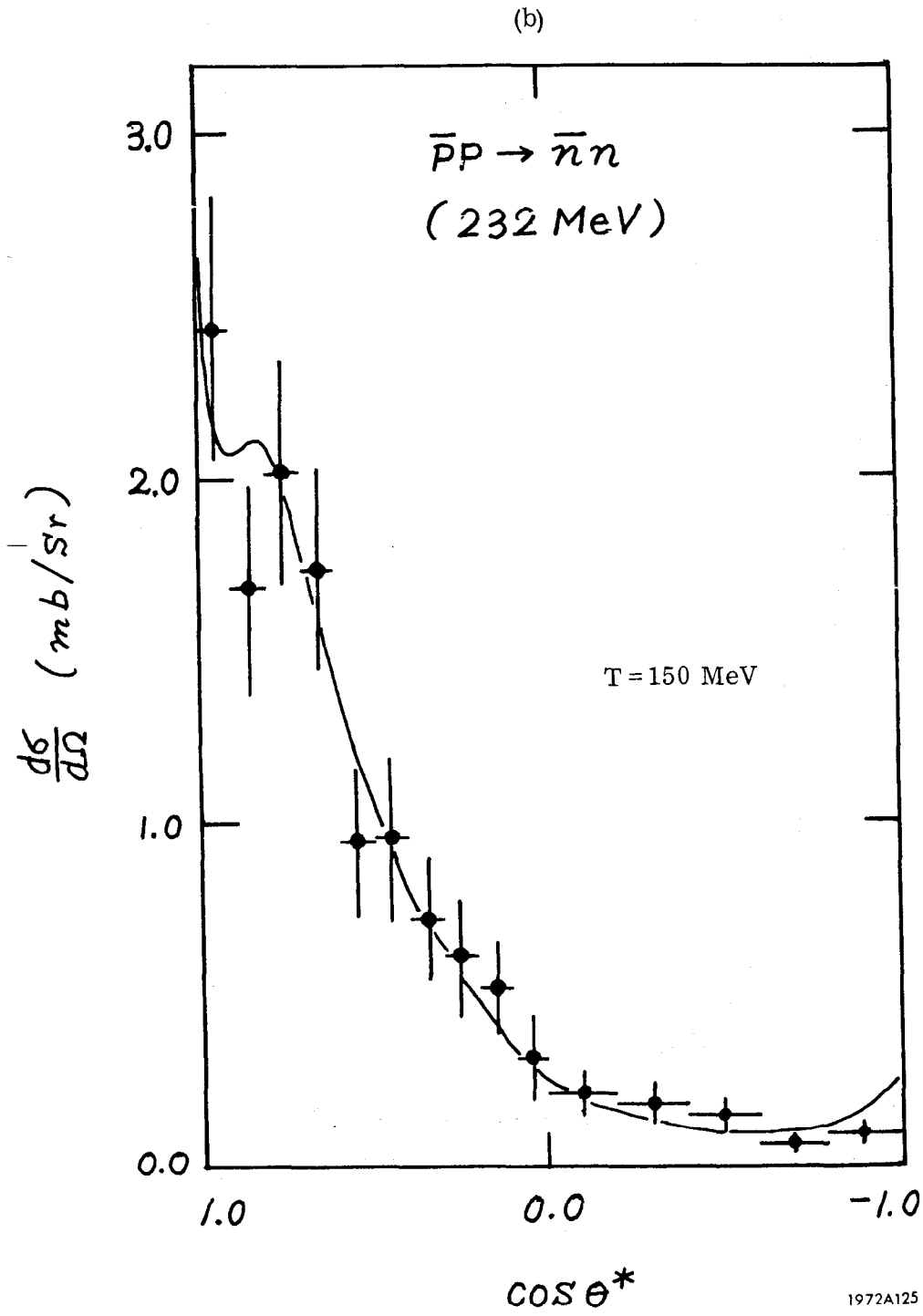
where T_0 and T_1 represent the amplitudes for isospin I=0 and I=1, respectively. The cancellation of the two diffraction amplitudes may explain $\sigma(\bar{p}p \to \bar{n}n)$ being five times smaller than $\sigma(\bar{p}p \to \bar{p}p)$. Recently, Bryan and Phillips have successfully explained the experimental data on the $\bar{N}$-N interaction. They introduced a phenomenological imaginary potential of the Wood-Saxon shape in addition to the real potential taken from one boson exchange as in N-N. Our data show a bump in the forward direction for $\bar{p}p \to \bar{n}n$ at around $\cos \theta^* \approx 0.9$ and a small backward peak in $\bar{p}p \to \bar{p}p$ as Bryan and Phillips predicted. It is necessary to accumulate many more events to make clear these points. Moreover, in order to understand the $\bar{N}$-N interaction in more detail, it is important to obtain information on the spin dependence of the interactions by means of experiments such as measuring the $\bar{p}$ polarization and the triple scattering of $\bar{p}$. We are going to measure the $\bar{p}$ polarization, and expect to have 3×10^3 double scattering events in 1.2×10^5 frames. We are also doing theoretical investigations, particularly with regard to the spin and isospin dependence of the imaginary potential.

Discussion

<u>Plano</u>: Do you have an explanation for the bump in $\cos \theta^*$ (Fig. 5b)?

<u>Hirose</u>: As a guess, it is due to the mixing of angular momentum states of different ℓ, but it is not clear what ℓ values give the bump.

<u>Yamagata</u>: In the calculation of Bryan and Phillips, if you assume one-pion exchange and a real potential, you get the peak and the bump. One-pion exchange alone does not give the observed structure.

MULTIPLE PARTICLE PRODUCTION IN 12.6 GeV/c K^-p REACTIONS

M. Teranaka, S. Konishi, T. Konishi, O. Kusumoto, F. Ochiai,
H. Okabe, S. Ozaki, N. Ushida and J. Yokota

Osaka City University
Osaka, Japan

Introduction

As Feynman has pointed out,[1] there are two methods for studying multiple-particle production, that is, the inclusive and the exclusive methods. Typical examples of the inclusive method are counter experiments, and those of the exclusive method are bubble chamber experiments. In the exclusive analysis, a final state of an interaction is usually completely assigned. Through this method, information has been obtained on resonance contributions to a reaction, the existence of diffraction dissociation, the validity of the multi-Regge picture, and so on. However, the number of the events which allow the assignments of their final states through the kinematically constrained fits is quite small. For example, in the four-prong events, only 10% of them can be determined. This limitation is more serious as the prong number increases. Therefore, in this type of analysis, it can be said that we see only part of the multiple particle production. We want to emphasize that, to understand the nature of the multiple particle production, we have to use some analytical method through which we can inspect all of the events. This standpoint is "inclusive", since we cannot always assign final states to all of the events. The bubble chamber is useful in inclusive experiments, in particular in the study of events with a V^o or kink. We will report some results of a study along this line for K^o production in the many-body process induced by the 12.6 GeV/c K^-p interaction.

In the following, first, we will mention the general features of the K^o production at 12.6 GeV/c, comparing them with the results previously obtained, and then discuss some interesting features we found.

Experimental Procedures and Results Obtained

We examined the reaction $K^-p \rightarrow K^o_s +$ anything (anything means in our case the final states including two or more charged particles). In order to do this, we used 10 K frames which were taken in an exposure of the Brookhaven National Laboratory 80" liquid-hydrogen bubble chamber to the rf separated K^- beam at 12.6 GeV/c. Two thousand frames were scanned, yielding 2000 events with

0 to 10 prongs. Scanning was done twice. From this, the scanning efficiency was estimated to be more than 95%.

The total K^-p cross section is evaluated to be 22.4 ± 0.5 mb. This value is in good agreement[2] with those reported around 12.6 GeV/c. The topological cross sections are shown in Table 1. For comparison, results obtained at 9 GeV/c are also shown.[3] We see that the cross sections for the events with $\geq$ 4 prongs increase with energy.

Table 1

Total cross section	22.4 ± 0.5 mb	
Topological cross section		
Number of prongs	Cross section in mb	
	12.6 GeV/c K^-	9 GeV/c K^-
0	0.40 ± 0.06	
2	6.6 ± 0.3	
4	8.4 ± 0.3	7.25 ± 0.17
6	3.6 ± 0.2	1.90 ± 0.08
8	0.51 ± 0.07	0.176 ± 0.025
Cross section for K^o_s production	0.89 ± 0.05 mb	
Cross section for Λ^o production	0.58 ± 0.04 mb	

Also 10 K frames were scanned twice to detect only the events associated with the V^o-particles; 318 events of K^o_s + anything and 207 events of Λ^o + anything were found. The K^o or Λ^o was identified as follows. Firstly, the line-of-flight of the V^o has to pass within one bubble diameter of the K^-p vertex. Secondly, the invariant mass of the V^o was evaluated assuming the positive charged particle to be a proton or a pion. From this, about 90% of the Vee's were identified as K^o's or Λ^o's. For the remaining 10% of the Vee's, a bubble density measurement was applied. In this application, the dip angle of a track was limited within 30 degrees. By this measurement, about 20% of the remaining Vee's were identified. Therefore, about 92% of all the Vee's observed were finally identified. The lifetimes derived from these K^o_s's or Λ^o's were well within their known lifetimes. This is shown in Fig. 1. The abscissa is the flight length, L, in cm before decay, and the ordinate shows the number of events. The solid curves show the relation $e^{-c\tau}$ where τ is the mean life of K^o_s or Λ^o. Using the deviation

Λ° Cτ DISTRIBUTION

Cτ = 7.54 cm

K$^{\circ}$
Cτ DISTRIBUTION

Cτ = 2.59 cm
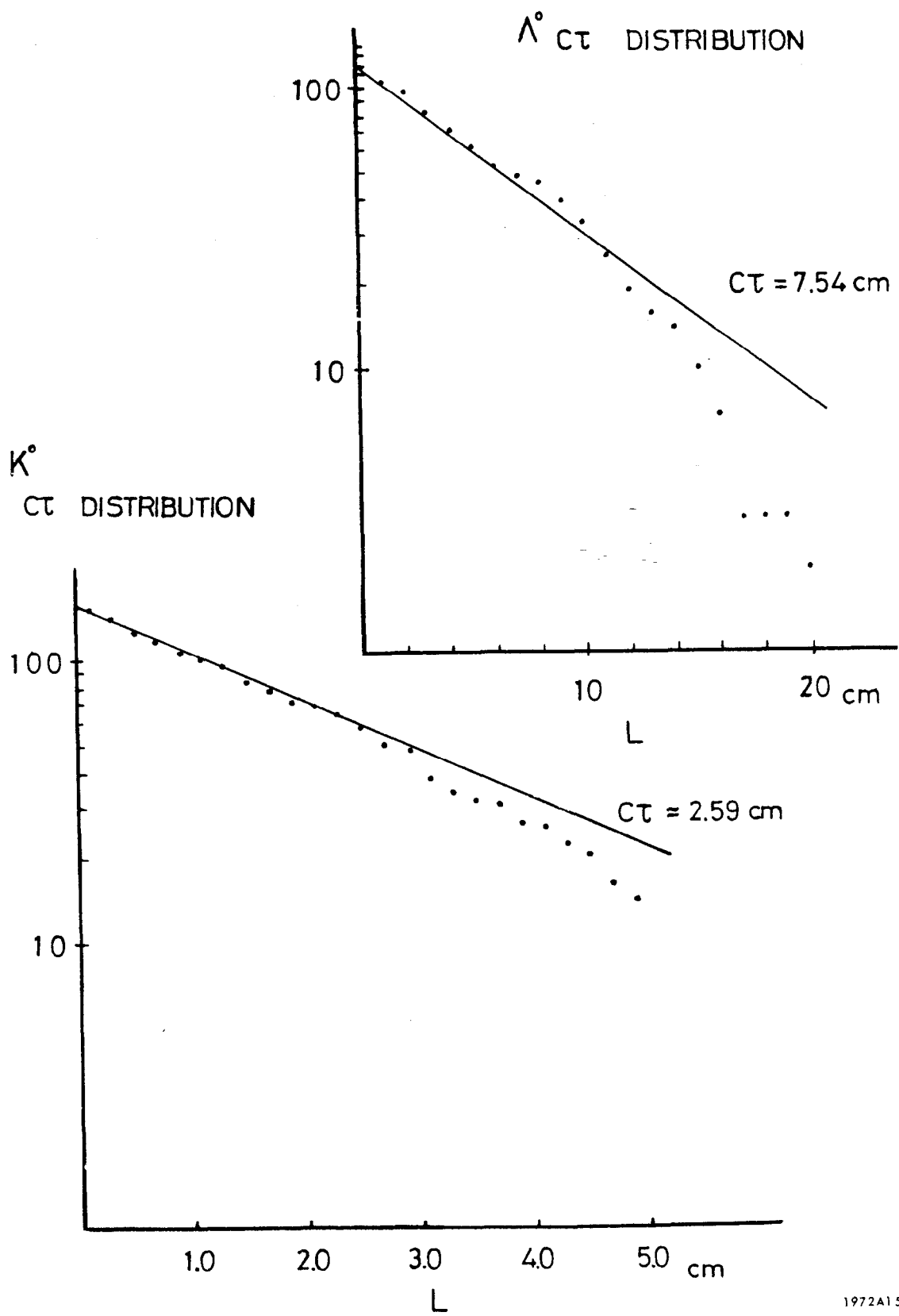
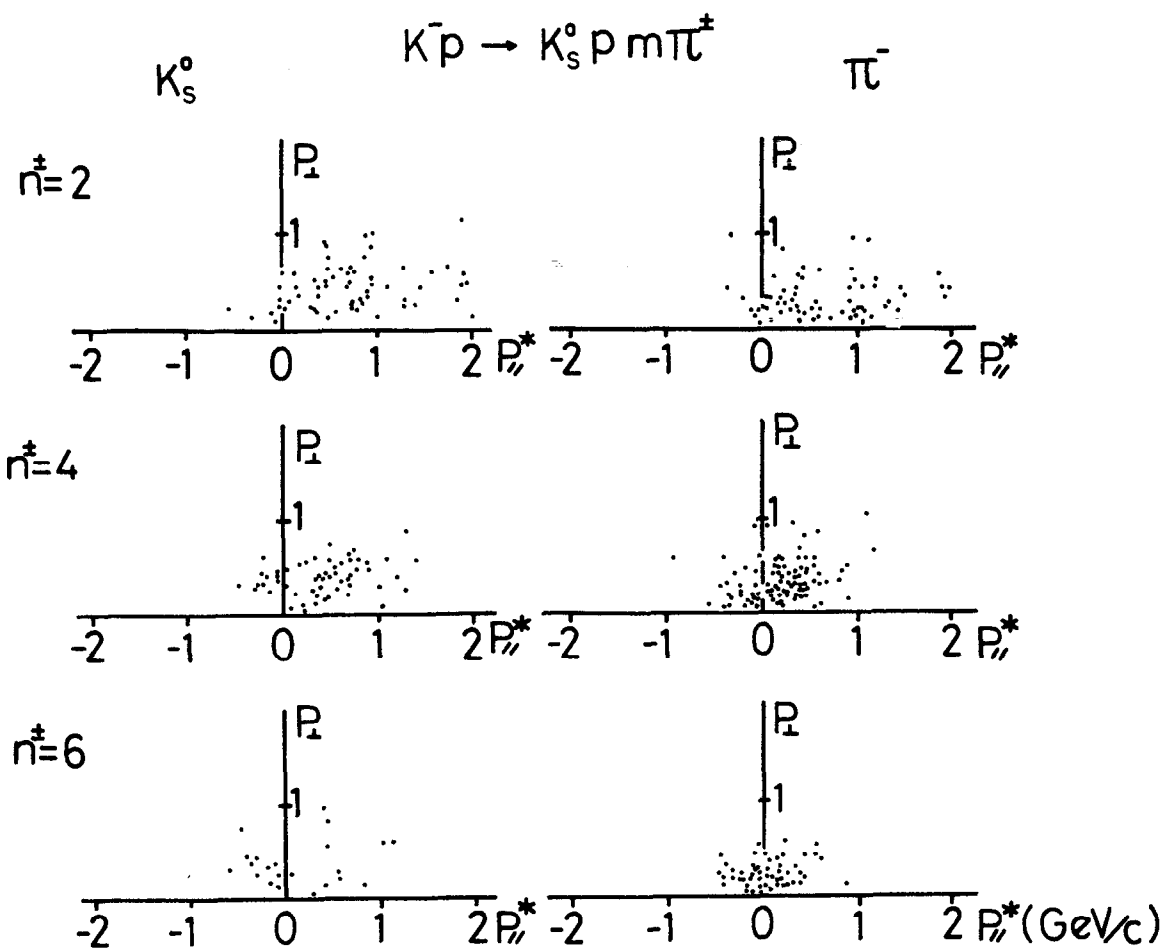FIG. 1--Integral distribution of flight length, L in cm, before decay for K_s^0's and Λ^0's.

between observed and expected values at large L, we can estimate the loss of K_s^0- or Λ^0-decays to be less than 5%. In Table 1, we show also the cross sections for K_s^0 and Λ^0 productions. They are corrected for missing probability and for the neutral decay modes.

In Fig. 2, we show Peyrou plots of K_s^0, $\pi^\pm$ and p for the $K_s^0 p \pi^-$, $K_s^0 p 3\pi^\pm$ and $K_s^0 p 5\pi^\pm$ channels. In these channels, the contribution of the neutral particles other than K^0 is not taken into account. From these figures, we can see that the K_s^0's have the character of leading particle, that is, they take away relatively high momenta and move in the forward direction of the $K^- p$ c.m.s. Though this tendency is suppressed as the prong number increases, this is to a large extent due to the influence of kinematics and phase-space factors. It could be said, therefore, that these interactions are peripheral. According to the Peyrou plots, the negative pions are also emitted in the forward direction. Therefore, the production correlations of K_s^0 and π^- were examined. The contribution of the K^{*-} resonances plus the Deck-type interactions was estimated from the distribution of the invariant mass of $K^0 \pi^-$. This is shown in Fig. 3. From a comparison with pure phase space, the contribution of the K^{*-} resonance plus the Deck-type effect around the invariant mass of 890 MeV was estimated to be less than 15%. This rate corresponds to the K^* production cross section of 0.2 mb. The results obtained at 10 GeV/c (Ref. 4) show the cross section for the reaction $K^- p \rightarrow K^{*-} p$ to be about 0.2 mb. In our case, other types of interactions are included. From these, we see that the contributions of the resonance and Deck-type interactions are small.

Figure 4 shows plots of the mean number of charged prongs versus t, where t is the four-momentum transfer squared from K^- to K_s^0. Though the statistics are poor, there seems to be a tendency for the mean prong number to level off at $t \sim 1.5$ (GeV/c)^2. This tendency is also seen if we separate all K^0-events into two groups according to the effective mass of the proton side and then make the same plots. Two groups are tentatively separated in such a way that each group has an equal number of events. The effective mass of the proton side, M^*, is defined as

$$M^* = \left(M_p^2 + 2\epsilon\, M_p^2 + t \right)^{1/2}$$

$$K^- p \rightarrow K^o_S \, p \, m\pi^{\pm}$$

K^o_S π^-

$n^{\pm} = 2$ $P_{\perp}$ $P_{\perp}$

1   1

-2   -1   0   1   2 $P^*_{//}$ -2   -1   0   1   2 $P^*_{//}$

$n^{\pm} = 4$ $P_{\perp}$ $P_{\perp}$

1   1

-2   -1   0   1   2 $P^*_{//}$ -2   -1   0   1   2 $P^*_{//}$

$n^{\pm} = 6$ $P_{\perp}$ $P_{\perp}$

1   1

-2   -1   0   1   2 $P^*_{//}$ -2   -1   0   1   2 $P^*_{//}$ (GeV/c)

1972A152

FIG. 2--Plots of $p_{\perp}$ vs. $p^*_{//}$ in c.m.s. for K^o_S, $\pi^{\pm}$ and p in the $K^o_S p (m\pi^{\pm})$ channels. $n^{\pm}$ means the number of charged particles, that is, $n^{\pm} = m+1$ for these channels.

FIG. 2--continued.

(b)

$$K^- p \rightarrow K^0_s p m \pi^{\pm}$$

π^+ p

$n^{\pm} = 2$

$n^{\pm} = 4$

$n^{\pm} = 6$

1972A153

15-6
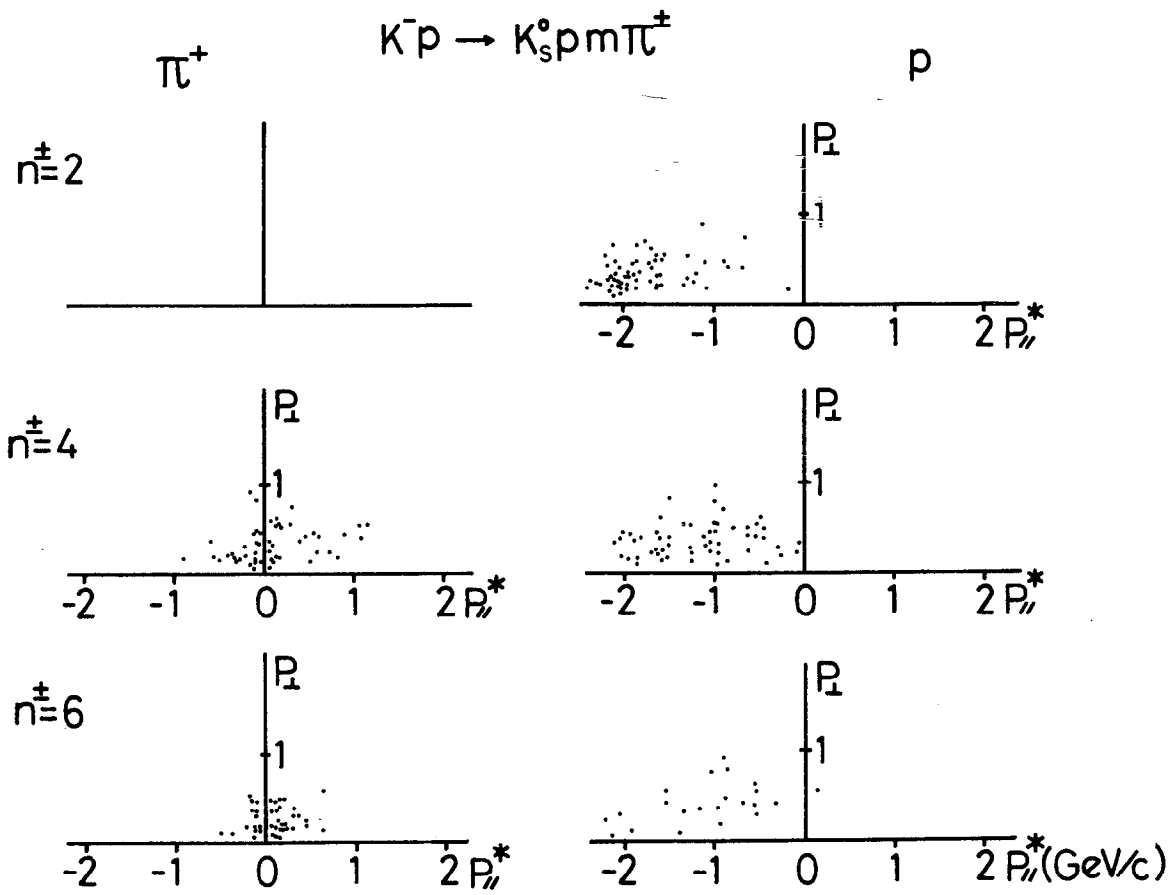
INVARIANT MASS M(K°π⁻) DISTRIBUTION

FIG. 3--Distributions of the invariant mass of $K^0\pi^-$ for different numbers of charged particles, $n^\pm$.
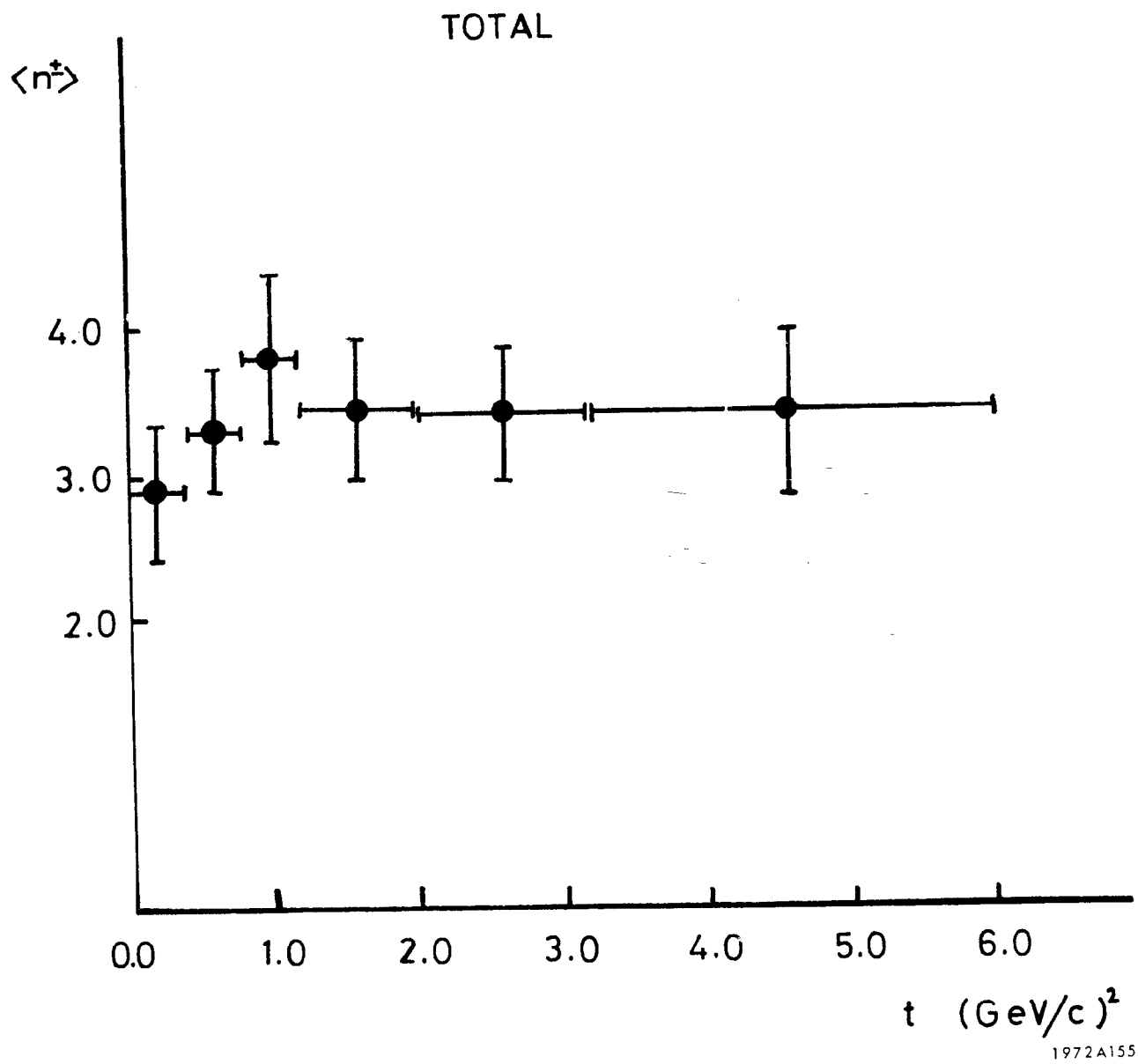
FIG. 4--Plots of mean number of charged particles, $\langle n^{\pm} \rangle$ vs. squared four-momentum transfer to kaons, t.

(a) The case of the total events examined.

FIG. 4--continued.
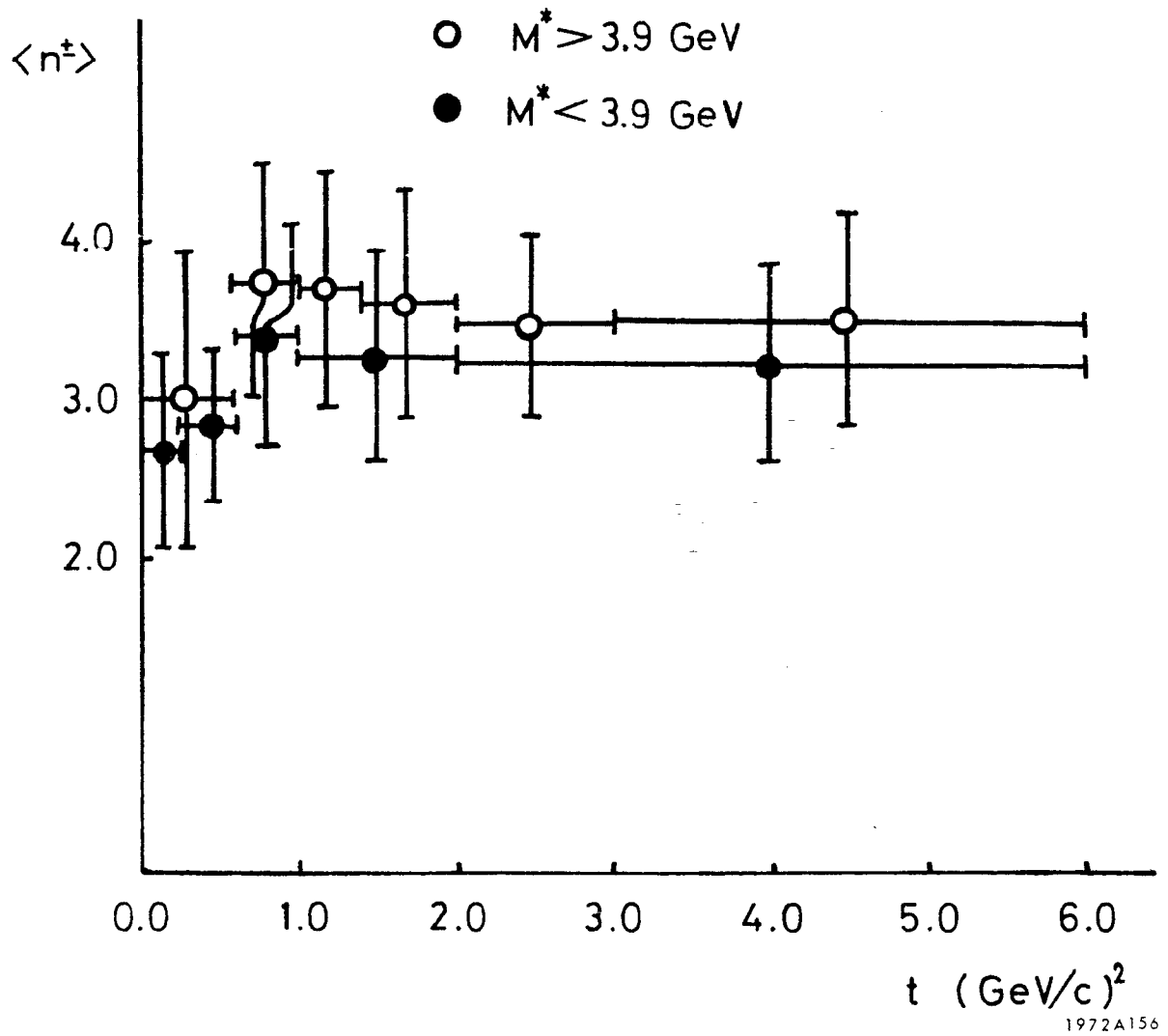
(b) The cases separated into two different M* regions at M*=3.9 GeV.

where ϵ is the energy transferred from K^- to K^o and M_p the proton mass. If the mean prong number is leveling off at $t \sim 1.5$ $(GeV/c)^2$, the t-distributions for different multiplicities should be similar in shape at $t \gtrsim 1.5$ $(GeV/c)^2$. This is seen in Fig. 5. The same feature is recognized in the 8 GeV/c π^+p, and 16 GeV/c π^-p reactions[5,6] where the t-distributions to protons are examined for the events with charged particles of up to eight. According to Czyzewski,[7] this fact seems to mean that part of the matrix element responsible for the behavior of leading particles is similar for different multiplicities. In our case, as seen in the Peyro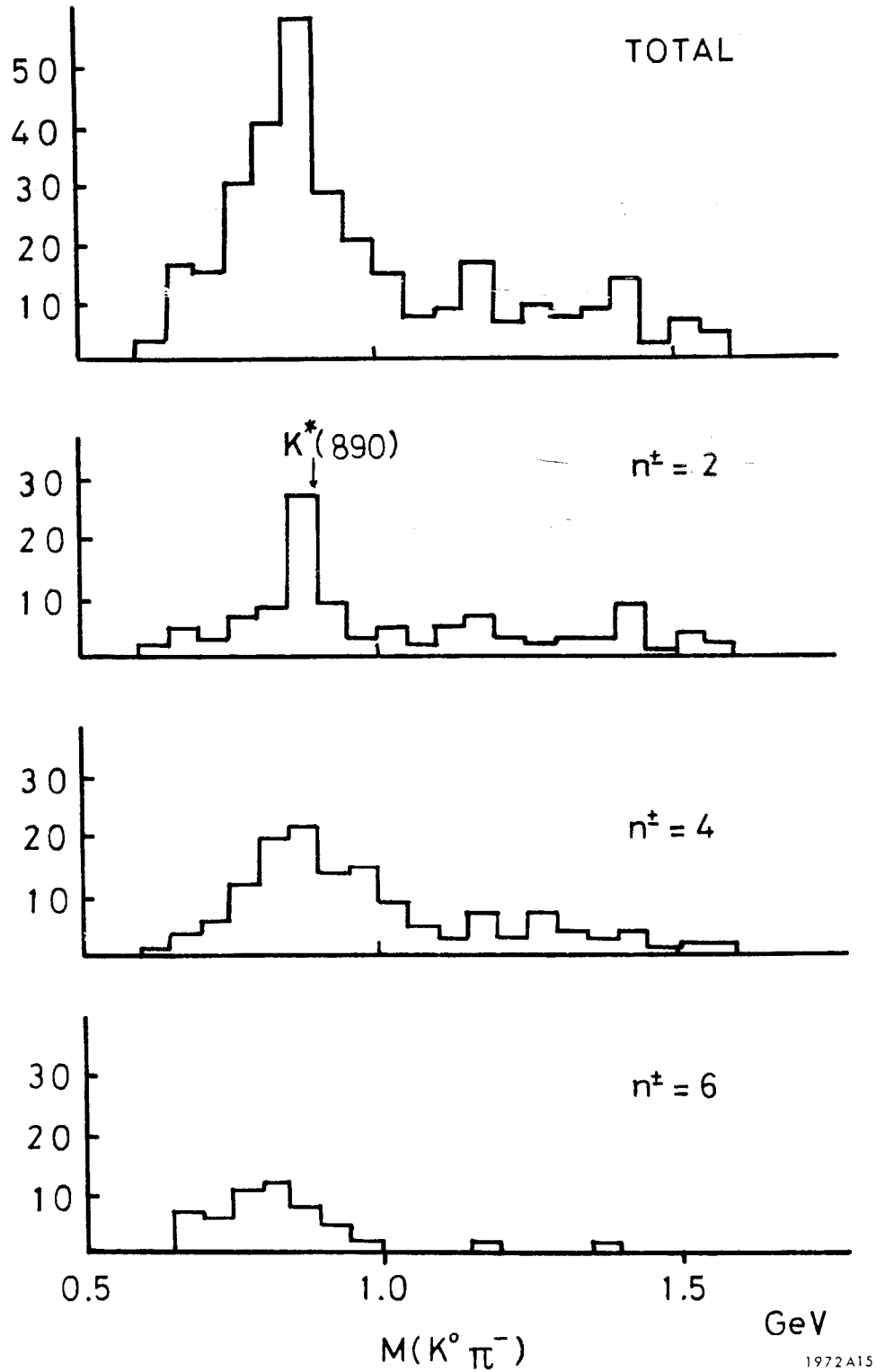u plots, protons behave also as leading particles in the backward hemisphere of c.m.s. Therefore, it should be noted that the t-distributions to protons will have similar features to those of kaons.

In Fig. 6, we show the t versus X plots where X is defined by $t/2\epsilon$. The solid lines in this figure show the kinematical limits of X for different multiplicities. Maximum and minimum values of X due to kinematical requirements for n-body channel are given approximately by

$$X_{max} \simeq M_p t / \left[2M_p (nm_\pi) + (nm_\pi)^2 \right]$$

$$X_{min} \simeq t/2E_0$$

where m_π and E_0 are the pion mass and the incident energy in LS. In Fig. 6, we see that at $t \lesssim 1.5$ $(GeV/c)^2$ data points distribute closely along the line of X_{min}. This means that at $t \gtrsim 1.5$ $(GeV/c)^2$ the transfer energy is nearly constant and equal to ϵ_{max}. This fact does not contradict a small mean inelasticity of about 0.5, since we consider only the K^o-production among all types of interactions induced by the 12.6 GeV/c K^-p collisions and further, in the K^o-production, the events with $t \lesssim 1.5$ $(GeV/c)^2$ have relatively small mean inelasticity. However, it can be said that the mean inelasticity of kaons for K^o-production is considerably larger than 0.5. In Fig. 7, the X-t plots for different multiplicities are shown. We can see in these figures that the feature under discussion is independent of prong number.

In Fig. 8, the distribution of X is shown. We can see a sharp peak at $X = 50 \pm 5$ MeV and there seems to be a small bump around $X \simeq 110$ MeV. The contributions of the events for which the invariant mass of $K^o_s \pi^-$ is in the region 890 ± 50 MeV, is shown in the same figure by the shaded portion. In Fig. 9, we show the X-distribution in two different t-regions, that is, for t less than or

t DISTRIBUTION
(INTEGRAL)
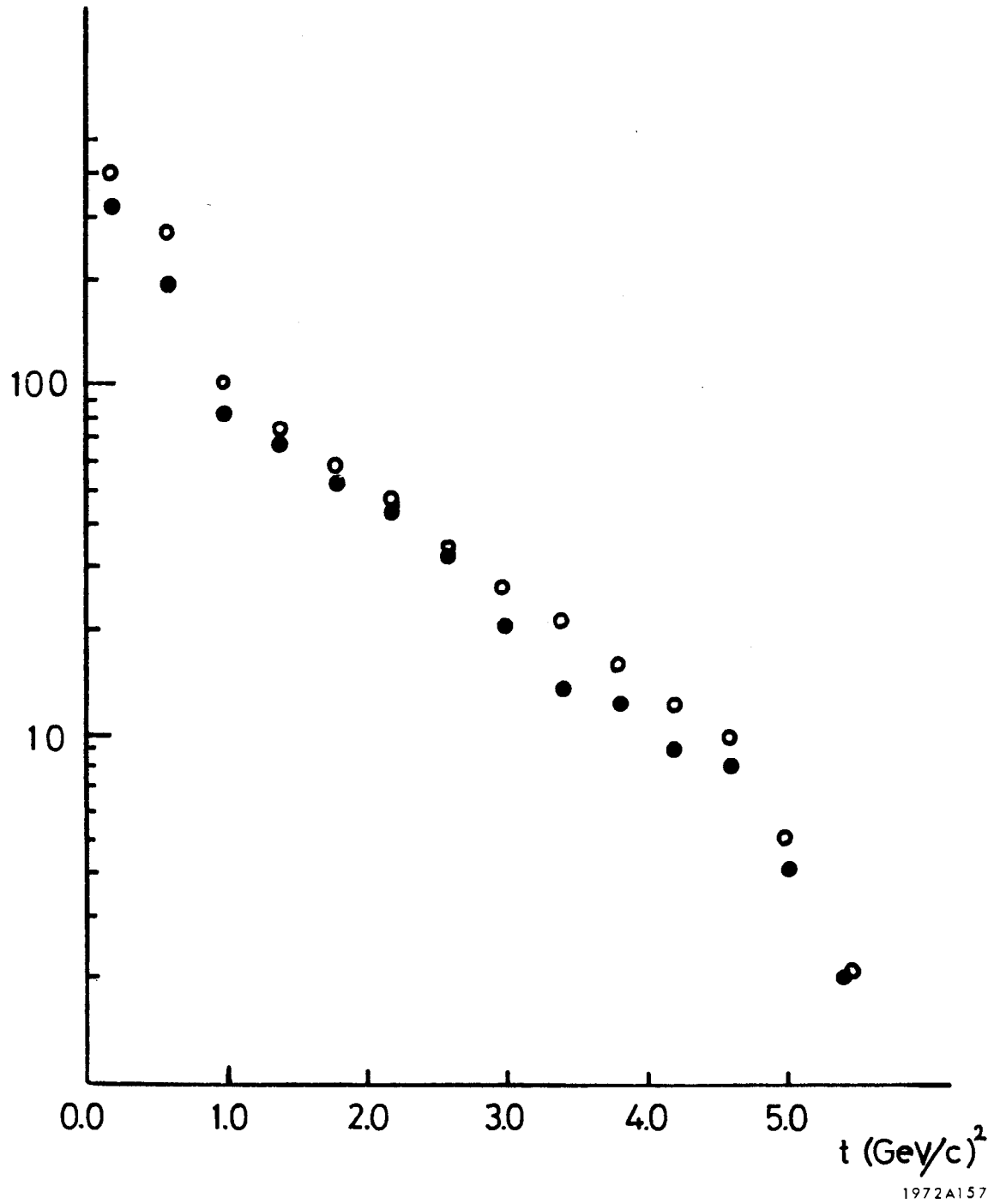
FIG. 5--Integral t-distribution for $n^\pm = 2$ and $n^\pm \geq 4$.
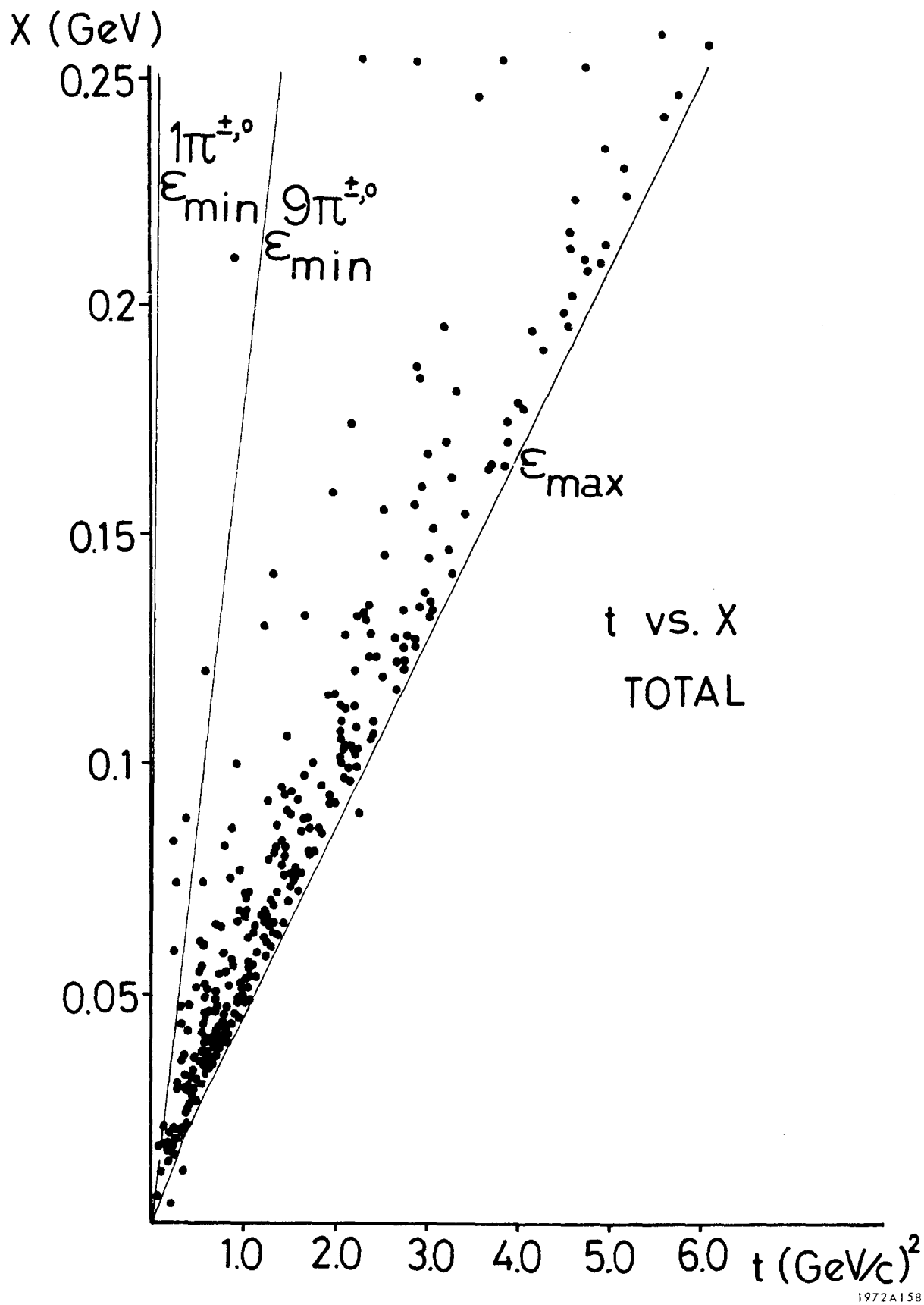
FIG. 6--t vs. X plots where X means $t/2\epsilon$. ϵ is the transfer energy of K^- to K_S^0.
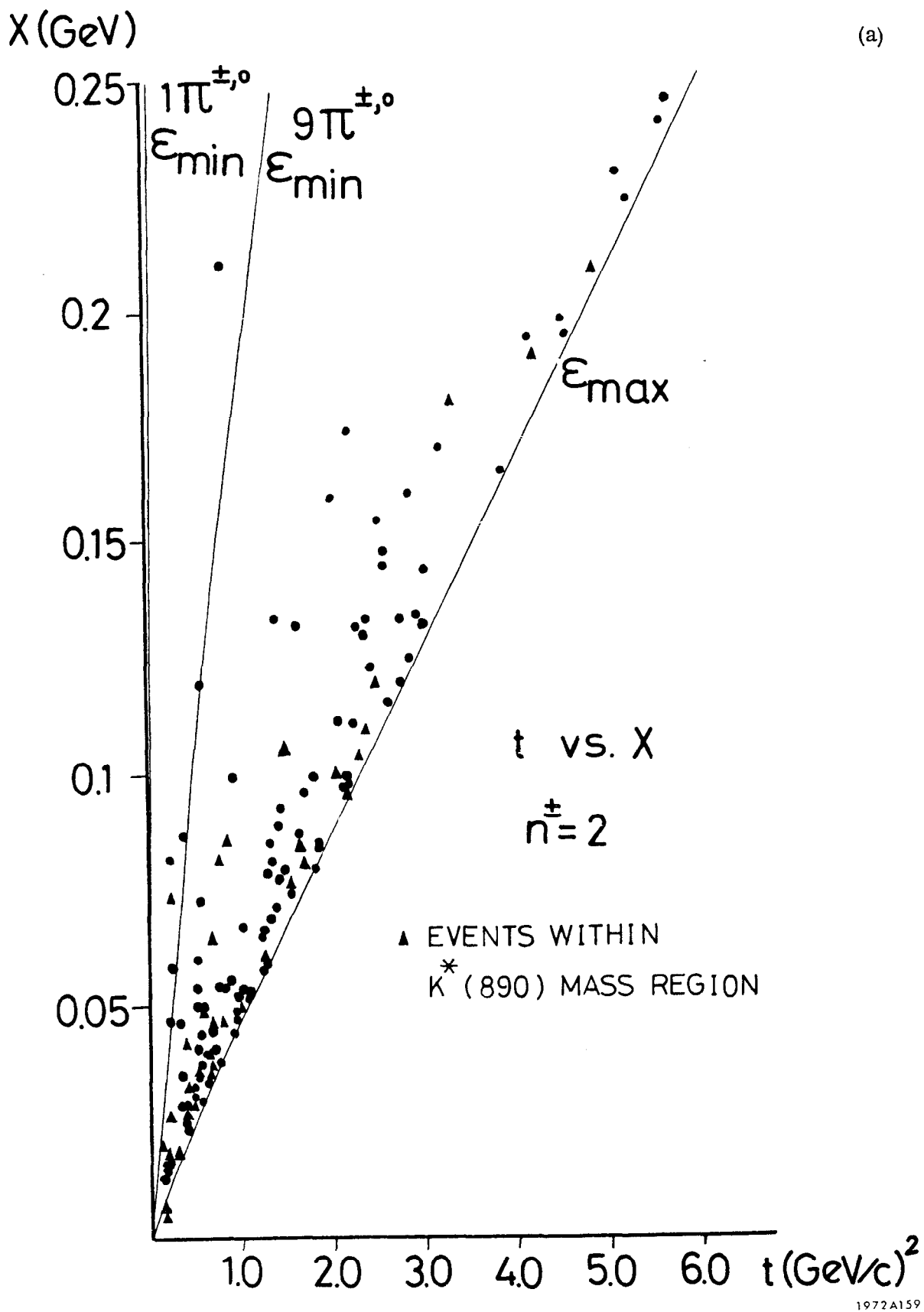
FIG. 7--t vs. X plots for different $n^{\pm}$'s.

FIG. 7--continued.

FIG. 7--continued.

X (GeV)

$1\pi^{\pm,o}$ ε_{min}

$9\pi^{\pm,o}$ ε_{min}

ε_{max}

t vs. X

$n^{\pm} = 4$

▲ EVENTS WITHIN $K^{*}(890)$ MASS REGION
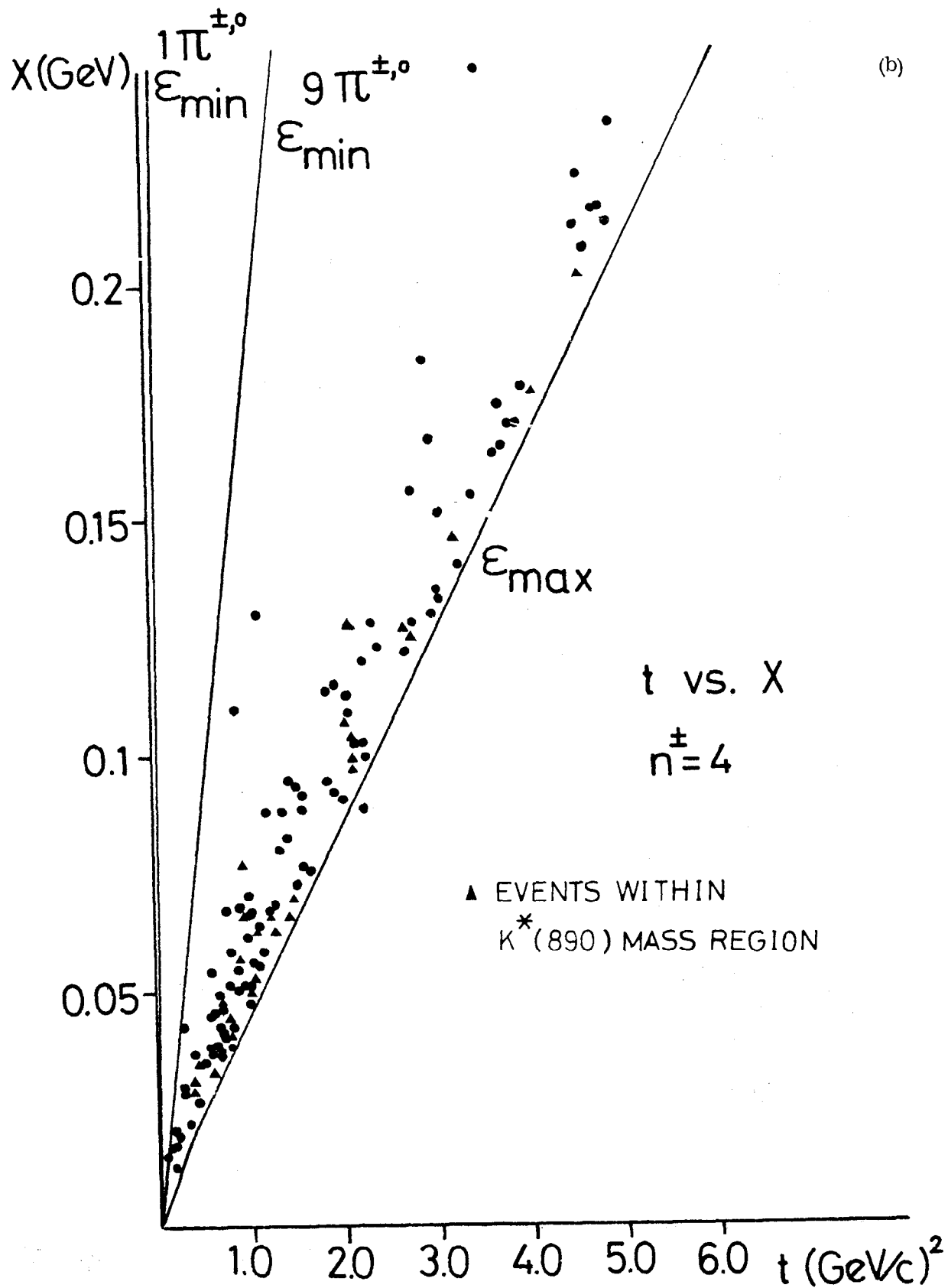
t (GeV/c)^2

1972A160

FIG. 7--continued.

(c)

1972A161

X DISTRIBUTION

TOTAL
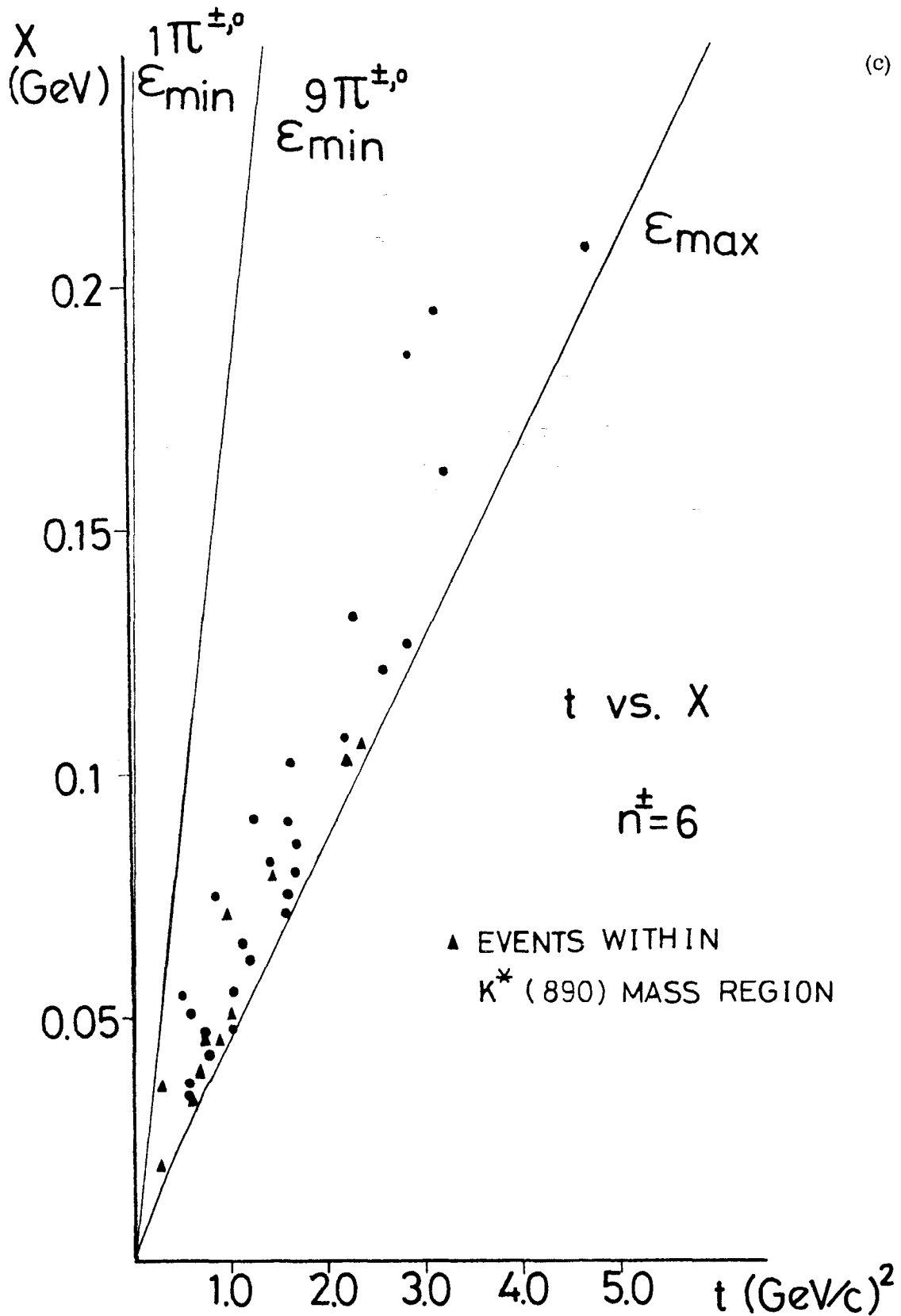
EVENTS WITHIN
$K^*(890)$ MASS RIGION
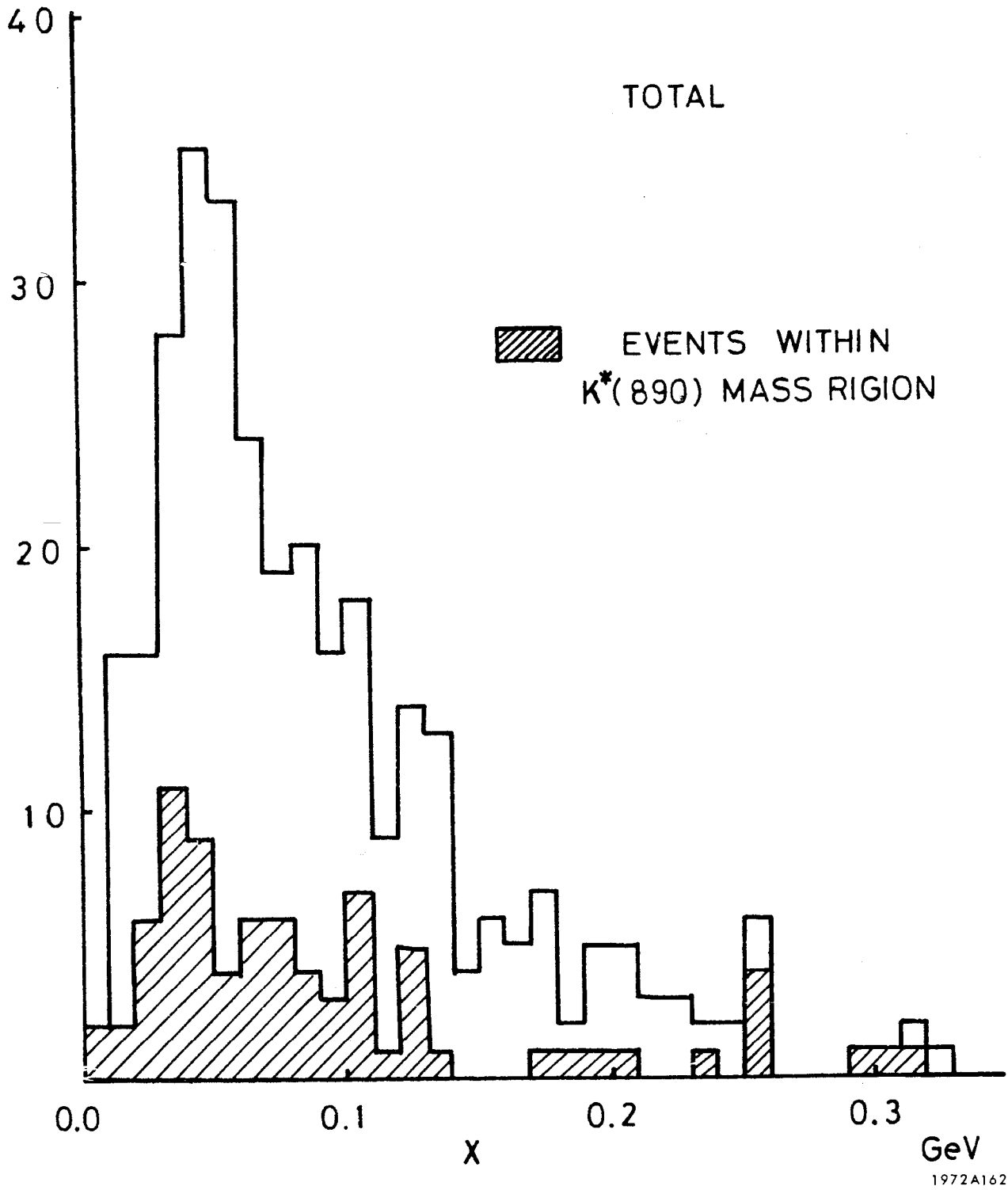
FIG. 8--X distribution for total events with $n^{\pm} \geq 2$.

1972A162

X DISTRIBUTION

$n^{\pm} = 2$

$t > 1.5 (GeV/c)^2$

ε_{max}

10

0.1   0.2   0.3

X   GeV

$t < 1.5 (GeV/c)^2$

30

20

10

0.1   0.2   0.3

X   GeV
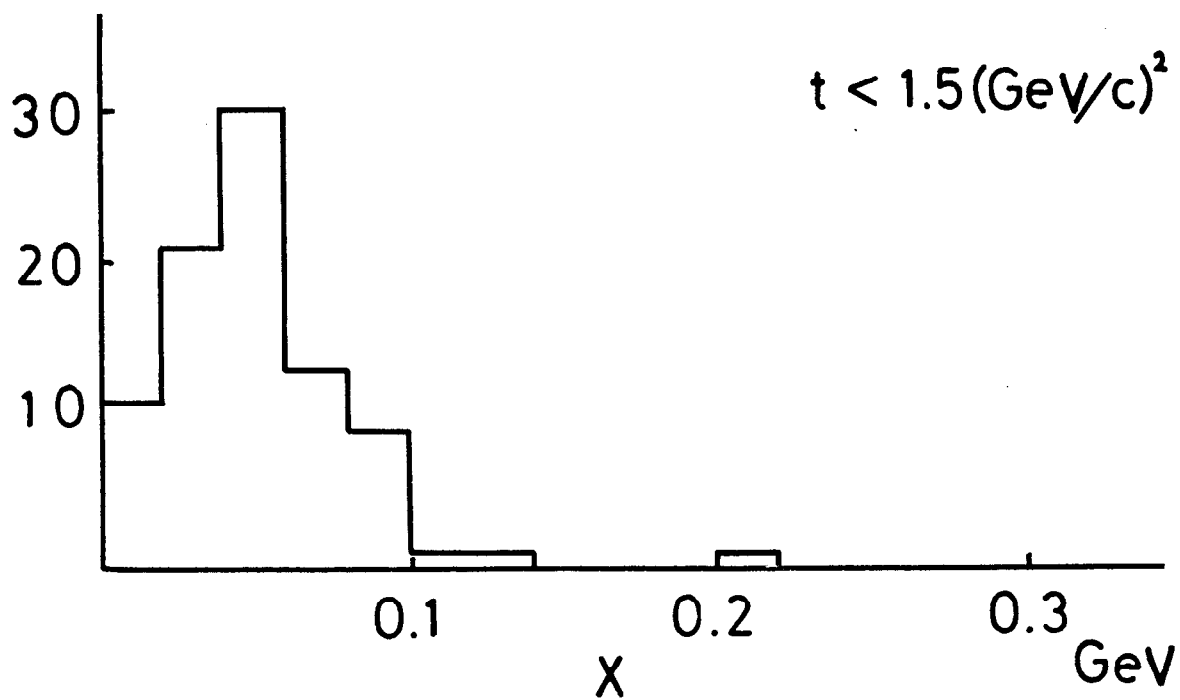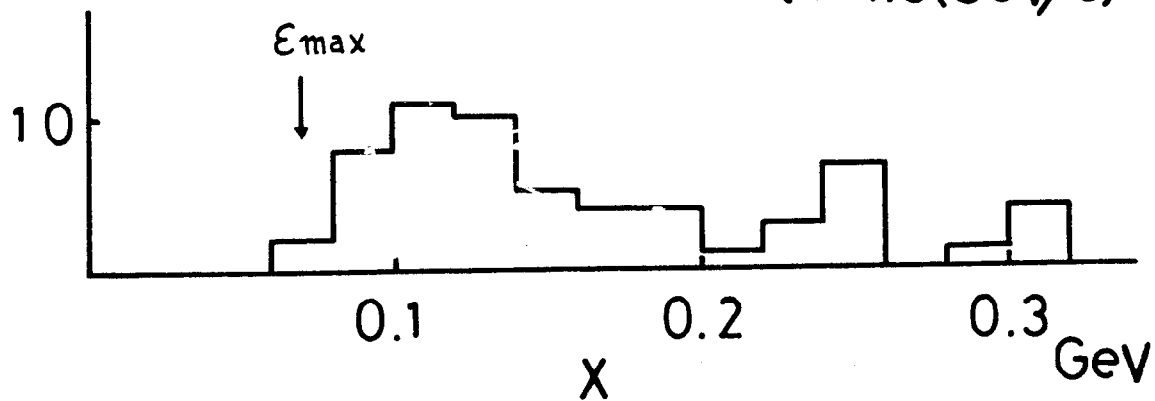
1972A163

FIG. 9--X distributions separated by t at 1.5 $(GeV/c)^2$ for different $n^{\pm}$'s.

FIG. 9--continued.

(b)
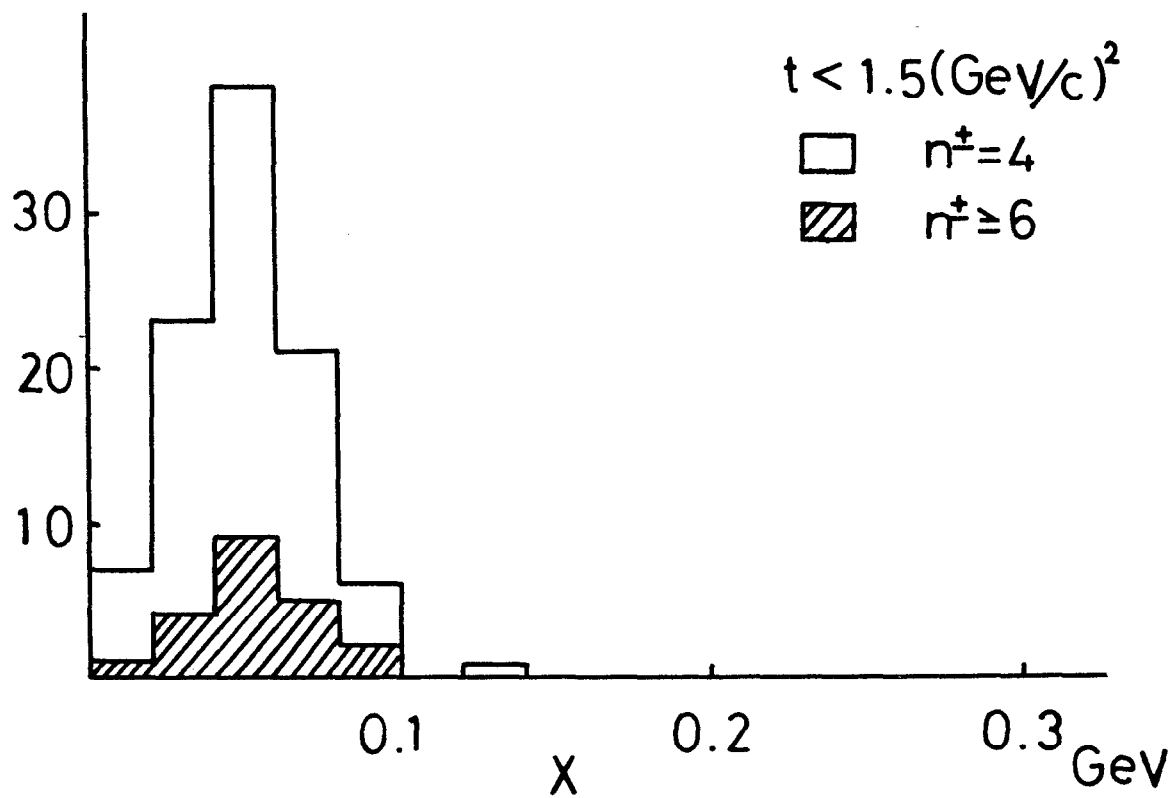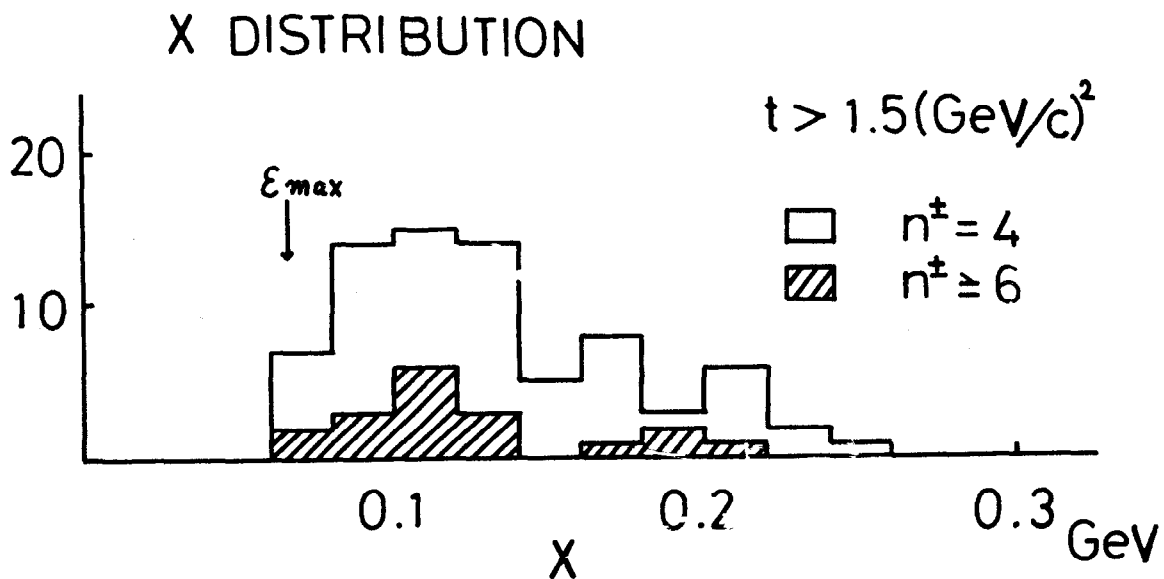
X DISTRIBUTION

more than 1.5 $(GeV/c)^2$. We see that, at small t, the X-distribution has a sharp peak at X = 50 ± 5 MeV and, at large t, the distribution is broad and has a broad peak at X = 110 ± 10 MeV/c. Kinematically, when t $\lesssim$ 1.5 $(GeV/c)^2$, X-values should be distributed up to an X_{max} of about 1 GeV and, at larger t the distribution spreads out in the region 0.065 $\lesssim$ X $\lesssim$ 1 GeV. Here, it must be emphasized that the X-distributions for different multiplicities are similar (see Figs. 8 and 9).

Conclusions

The results we obtained in the study of $K^- p \to K^0_s$ + anything (anything means that $n^{\pm} \geq 2$ where $n^{\pm}$ shows prong number) at 12.6 GeV/c are summarized as follows.

We first discuss the t-dependence of the data. For $\iota \gtrsim$ 1.5 $(GeV/c)^2$, the mean number of charged particles associated approaches a value of 3.4. In this t-range, the transfer energy also saturates to its maximum value available. On the other hand, as seen in the X-distribution, X-values are small compared with the kinematically allowable limit. The peak value of X is 110 ± 10 MeV and, as seen in the X-t plot, X is approximately proportional to t. All of these features except for the mean prong number versus t plot are independent of the mode of K^0-production.

Since the β of the incident K^- is 0.9992 and t is more than 1.5 $(GeV/c)^2$, if we can take a viewpoint that the reactions under consideration satisfy the conditions of both high energy and highly inelastic limits in the lowest order, it might be allowed to say that X represents the target mass of the proton side against which the incident negative kaon undergoes the charge-exchange scattering. Then, we may state that the present results are very suggestive of the sub-particle structure of the proton.

At t $\lesssim$ 1.5 $(GeV/c)^2$, the interactions have the gross feature that, irrespective of the multiplicity of particles produced, X-distributions have the same sharp peak at 50 ± 5 MeV. This might reflect the fact that in this small t-region, K^0-production is initiated by a process similar to that occurring in the high t region.

We wish to continue further the present work of studying the hadron structure and to extend the present results to a higher energy region.

Acknowledgement

References

1. R. P. Feynman, Phys. Rev. Letters 25, 1415 (1969).

2. J. V. Allaby et al., Phys. Letters 30B, 500 (1969).

3. Private communication through K. Takahashi.

4. M. Aderholz et al., Nucl. Phys. B5, 567 (1968).

5. R. Honecker et al., Proceedings of the 14th International Conference on High-Energy Physics, Vienna, 1968, edited by J. Prentki and J. Steinberger, paper 465.

6. T. Coghen et al., Proceedings of the 14th International Conference on High-Energy Physics, Vienna, 1968, edited by J. Prentki and J. Steinberger, paper 755.

7. O. Czyzewski, Proceedings of the 14th International Conference on High-Energy Physics, Vienna, 1968, edited by J. Prentki and J. Steinberger, paper 367.

MULTIPARTICLE PRODUCTION AT 12 GeV/c

M. W. Peters

University of Hawaii
Honolulu, Hawaii   USA

The following data are from a sample of 190,000 frames of $\pi^- p$ at 12 GeV/c in the SLAC 82" LHBC. This corresponds to 9.2 events/μbarn. We have found 34,800 6-prong events, which implies a cross section of 3.8 mb. The events are measured on SMP's, fitted with TVGP-SQUAW, and resolved using automatically measured track density and gap frequency.

The analysis of the ionization data involves a two-stage process. First, a normalization for each view of the event is determined from all tracks in the event, with inconsistent tracks rejected. Then, each track is treated separately, using this normalization to determine the maximum likelihood value of the ratio between predicted and observed track density and gap frequency. The distribution of this quantity for a sample of 4C events is given in Fig. 1. This indicates that for tracks near minimum ionization we determine the relative ionization with a standard deviation of about 0.2.

Finally, we obtain 955 accepted 4C events and 4300 accepted 1C events with a missing π^0. The corresponding cross sections are 160 μbarn and 700 μbarn.

The CERN missing mass spectrometer experiment observed an enhancement at a mass of 2400 MeV which decayed into 5 or more charged particles 25% of the time (labeled U^-). From their data, we estimate $\sim$ 2-3 μbarn as a cross section for $U^- \to$ 5 charged particles (or more). This would predict 15-20 events in our sample. Figure 2 is the distribution of $(5\pi)^-$ mass for our 955 examples of $\pi^- p \to p\pi^+ \pi^+ \pi^- \pi^- \pi^-$. There is a suggestion of structure in the right mass region and with the right number of events, but low statistics prevents any definite conclusion. If the U^- or a similar particle had even G-parity it could decay into 6 pions including a π^0 and appear in our 1C (π^0) events. That mass plot is shown in Fig. 3. No structure is evident near 2400 MeV.

A negative G-parity U^- might also be observed in our data after production by the process $\pi^- p \to U^- p\pi^0$. The mass of all five charged pions in our 1C(π^0) events is plotted in Fig. 4. Here a cut $-t <$ 2.2 $(\text{GeV/c})^2$ has been
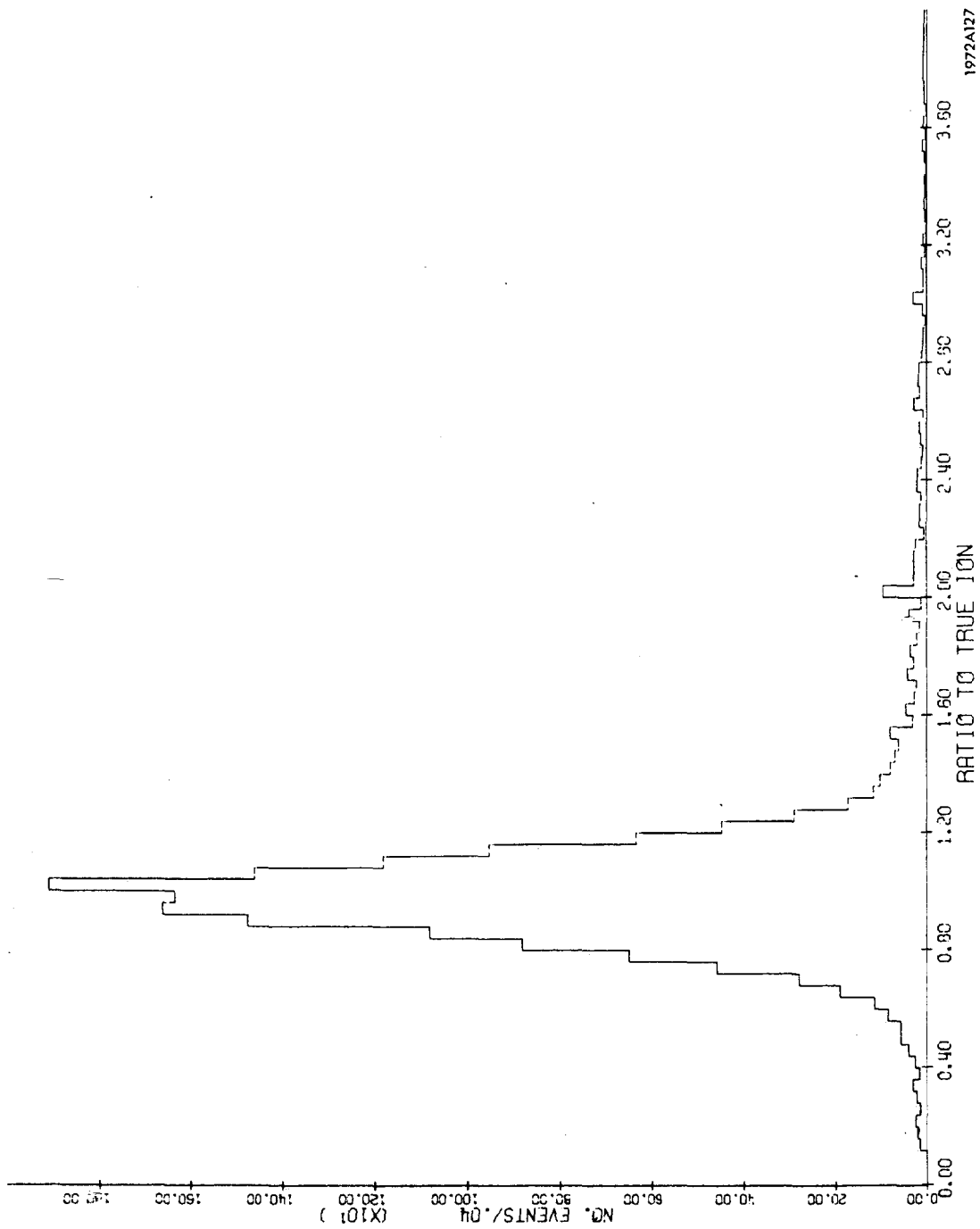
FIG. 1--Ratio between predicted and observed track density.
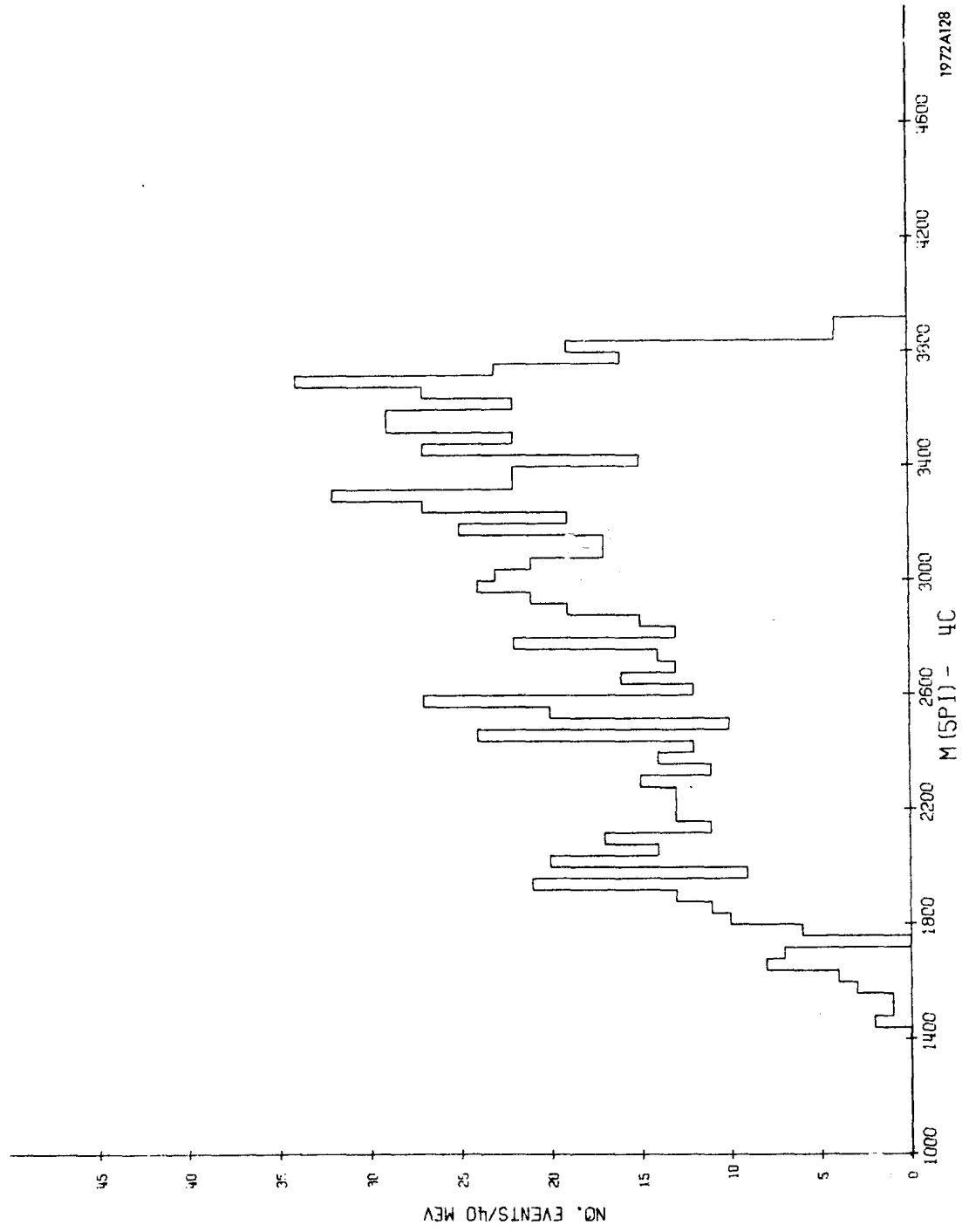
FIG. 2--Reaction $\pi^- p \to p 2\pi^+ 3\pi^-$. $(5\pi)^-$ mass distribution.
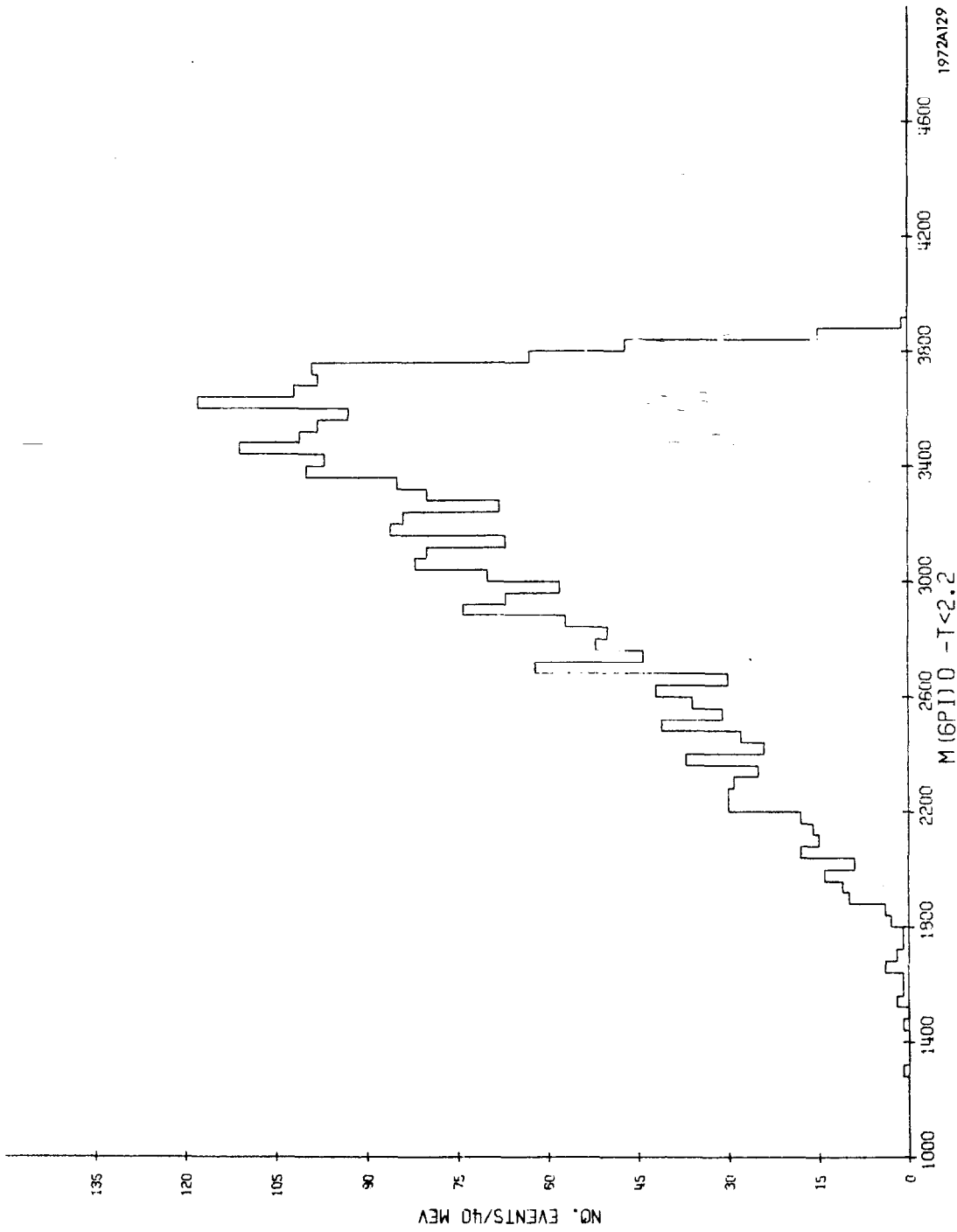
FIG. 3--Reaction $\pi^- p \to p 2\pi^+ 3\pi^- \pi^o$. $(6\pi)^-$ mass distribution for $|t| < 2.2$ GeV^2.

16-4
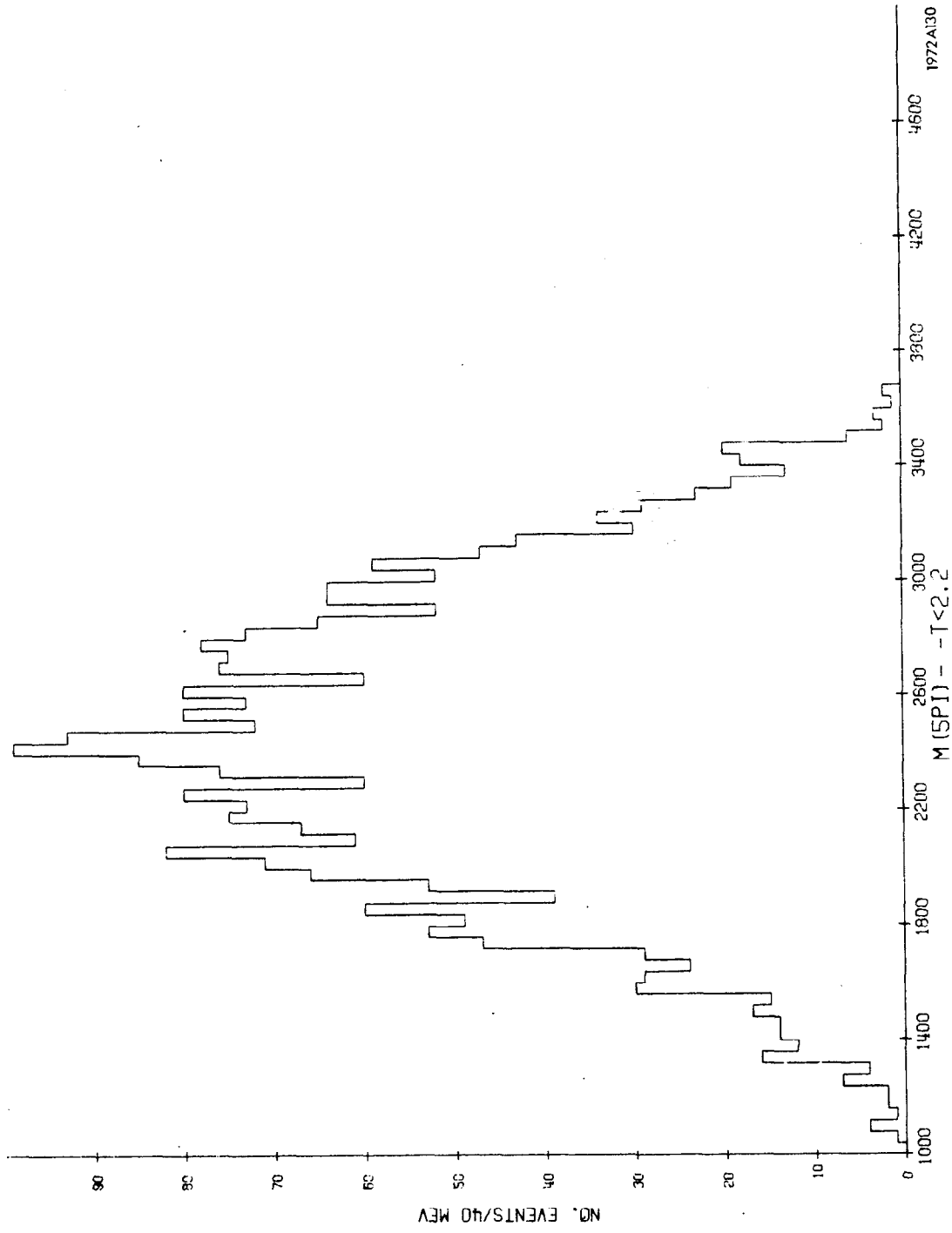
FIG. 4--Reaction $\pi^- p \rightarrow p 2\pi^+ 3\pi^- \pi^0$. $(5\pi)^-$ mass distribution for $|t| < 2.2 \text{ GeV}^2$.

16-5

applied to ensure that we are able unambiguously to resolve the proton by our ionization technique. There is a suggestion of an enhancement near 2400 MeV. We estimate from this plot that we see a signal of about 54 events above background, corresponding to a cross section of $8.6 \,\mu$barn, about 4 times greater than that calculated for the direct production as seen in the MMS. (Of course, we may not even be seeing the same particle.)

In order to investigate possible decays of this U^- state, we have made plots of the $(5\pi)^-$ mass involving zero, exactly one or two ρ^0 combinations, where only disjoint combinations are counted. The results are shown in Figs. 5, 6 and 7. The U^- enhancement appears in both the one and two ρ^0 plots. The distribution between the two plots is consistent with a decay $U^- \rightarrow \rho^0 \rho^0 \pi^-$, since with our ρ cut (650 MeV - 850 MeV) and estimated mass error (30 MeV) only 38% of all true $\rho^0 \rho^0$ events would be included in the two ρ^0 plot, the remainder appearing mainly in the one ρ^0 plot. The curve on Fig. 7 is a weighted least squares fit of a cubic polynomial to the central region of the plot (not required to be normalized). The probability of a fit as bad or worse is .004.

An analysis based on the use of side band subtractions results in quite large errors on the branching ratio for $U^- \rightarrow \rho^0 \rho^0 \pi^-$, but the result is close to 100%. If a large fraction of the decays are indeed $\rho^0 \rho^0 \pi^-$, a search for resonances between the two ρ^0's or between one ρ^0 and the π^- might be instructive. We have carried this out, and find no strong indications for dominance by one such channel. In other words, if the decay is actually two body, with $\rho^0 \rho^0 \pi^-$ as an intermediate state on the way down to five π's, then more than one or two 2-body modes must be involved. If true, this might suggest support for the "meson towers" proposed in connection with the Regge picture. In that case, several states with varying spins and parities would be mass degenerate, and we would not separate them. Calculations based on angular momentum barrier ideas suggest that a pure state would have at most two important decay modes involving two ρ^0's.
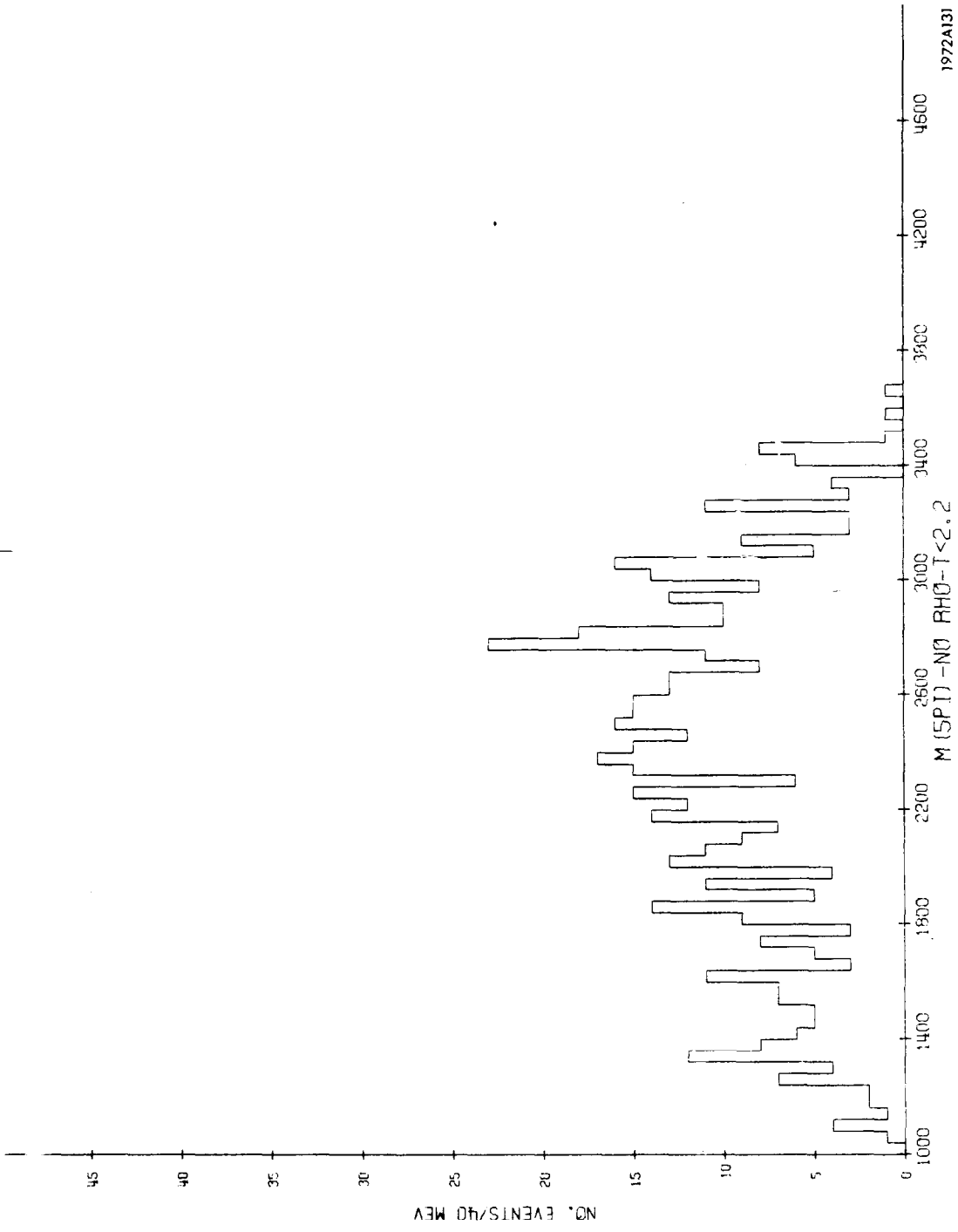
FIG. 5--Reaction $\pi^- p \rightarrow p2\pi^+3\pi^-$. $(5\pi)^-$ mass distribution for no ρ^0 combinations and $|t| < 2.2$ GeV^2.
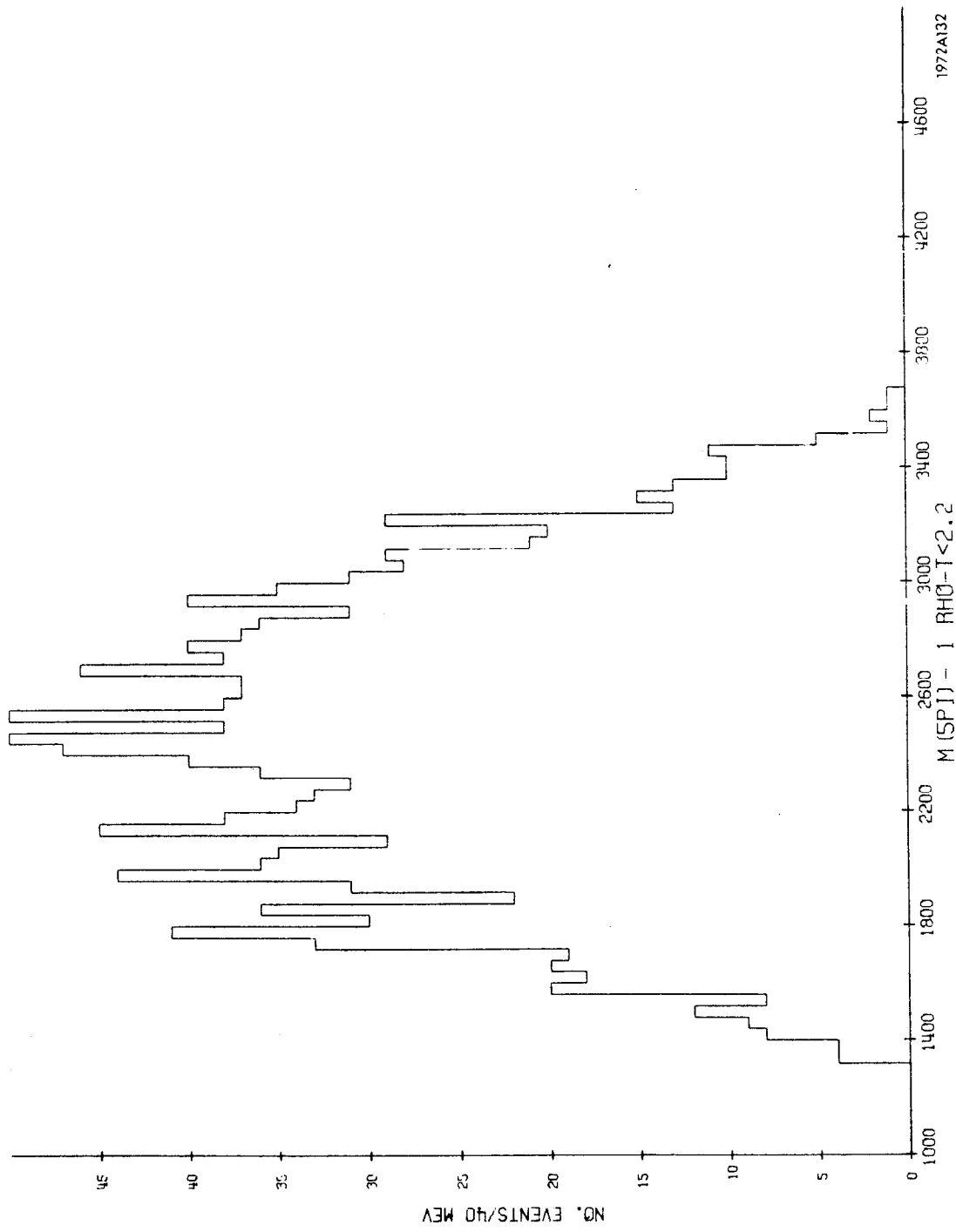
FIG. 6--Reaction $\pi^- p \rightarrow p2\pi^+3\pi^-$. $(5\pi)^-$ mass distribution for one ρ^0 combination and $|t| < 2.2$ GeV^2.

16-8
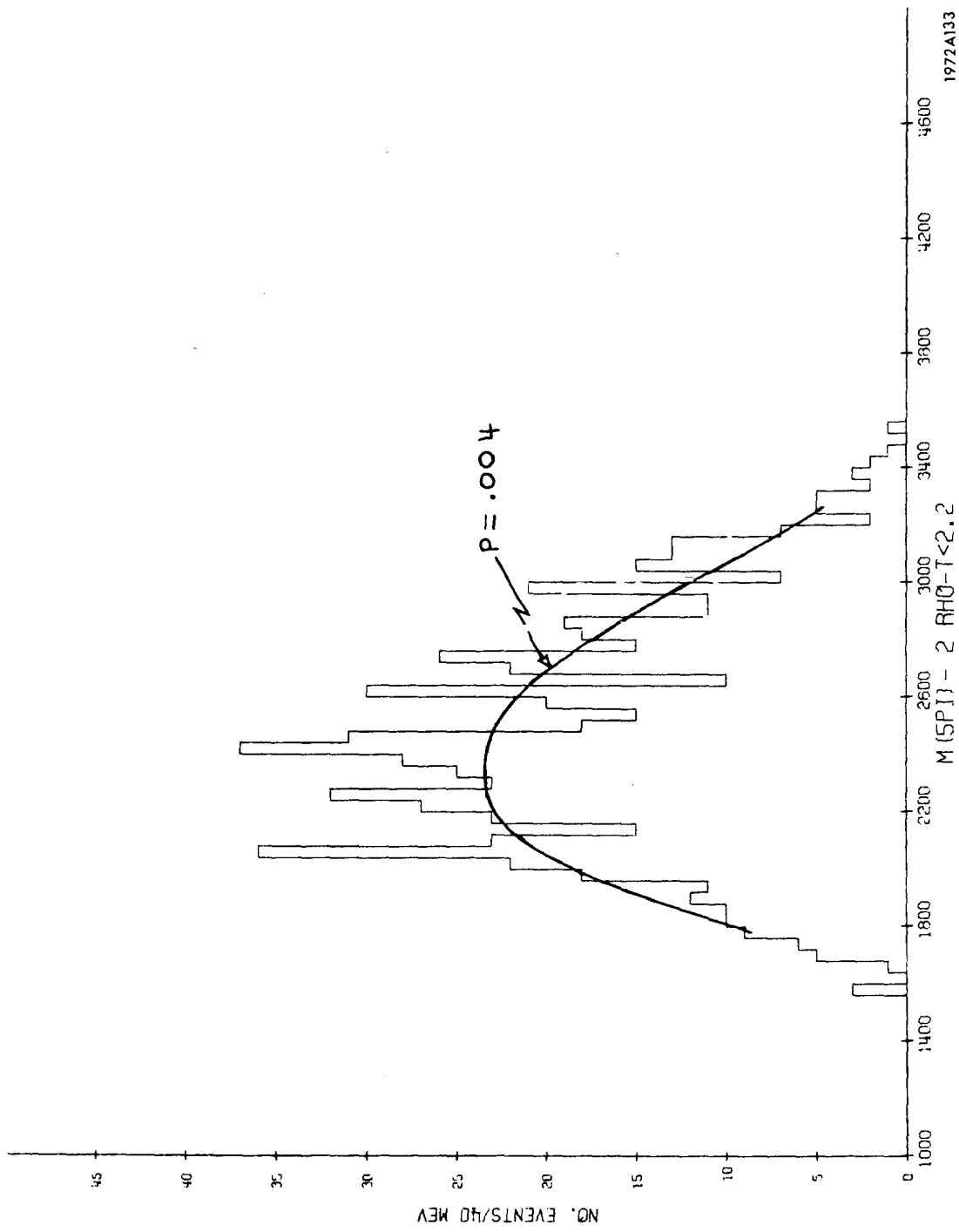
FIG. 7--Reaction $\pi^- p \to p 2\pi^+ 3\pi^-$. $(5\pi)^-$ mass distribution for two ρ^o combinations and $|t| < 2.2$ GeV^2.

Discussion

Pless: At what momentum can you distinguish a π from a proton?

Peters: About 1 GeV/c — our basic limitation is that the S. M. P. samples only a small fraction of the track.

Unknown Speaker: Is this your total statistics?

Peters: We will have four times this number finally.

Ferbel: Did you make the t-cut before or after you saw the peak in Fig. 6?

Peters: The peak was evident before any cuts and before ionization cuts were applied.

Pless: Is that the best curve? (Fig. 7)

Peters: This is a Chebychev polynomial not necessarily normalized to the same area. It is the curve giving the lowest χ^2.

Pless: Did you look at $p\pi^+$ to see if you have N^*'s?

Peters: We do have N^*'s in this data. We've tried cutting them out and find that then the resonances tend to go away.

Takeda: Are you going to say that there are indications of several resonances?

Peters: I'm going to say that there are indications of five or possibly even six resonances, but I'm not going to claim their existence.

Takeda: Sometimes you have one prominent resonance, here there are several resonances, each one is not significant statistically. I don't know which way is the better indication for the existence of one resonance. The probability of having at least one resonance may be large here. Experimentalists now-a-days seem to be biased toward eliminating resonances.

Peters: It is very hard to establish the existence of even one resonance.

Harari: The question is what is the probability that this sample has at least one resonance without deciding which one it is. Possibly it's very high.

Peters: This would have to be a severe fluctuation, 0.4% probable, which is not impossible these days. I would point out that the other plots from the same data have peaks which are consistent with statistics. You somehow have to have all the fluctuations crowded into this one plot.

Harari: There is a very fundamental point here that makes one look differently at this picture then at the mass of the A_2 for example. All models would suggest real structure at ~2 GeV — at least as rich as at 1 GeV for example. In contrast to the A_2 region — there should be lots of resonances here.

Ferbel: How do you know that?

Harari: Any type of picture — historical analogy. Fitting this with polynomials is really using a bias which you should not use. If you should have any bias it should be in favor of trying to see what are the properties of those peaks rather than trying to get rid of them as quickly as possible.

Baltay: The standard procedure is: 5-6 standard deviations establish an effect, 3 should be made public as it needs confirmation from other experiments, 1.5-2 I would not publish.

Plano: A number of bumps must have a different statistical weight, if there is an a priori reason to expect them there, than just one alone.

Peters: Let me tell you how far I've gone. I plotted the peaks as a function of M^2 and computed the Fourier transform of the mass distribution because that's a figure that measures this periodic structure with one number. One can also calculate the statistical errors for the coefficient and indeed it looks significant. This is an attempt to say something about the periodicity which would not be expected from random statistical fluctuations.

PHOTOPRODUCTION OF VECTOR MESONS IN THE BUBBLE CHAMBER*

G. Chadwick

Stanford Linear Accelerator Center
Stanford University, Stanford, California USA

In this talk I will describe some aspects of a bubble chamber study of photoproduction in the 82" LRL-SLAC hydrogen bubble chamber using the SLAC backscattered laser beam. I will try to show why the bubble chamber was the best technique to use, investigate its shortcomings, and inquire into the future prospects of this type of experiment.

The usual source of high energy photons is from bremsstrahlung of high energy electrons in a thin radiator: unless the photon reaction is associated with a measurement of the energy loss of the electron (tagging) the photon energy is unknown. Tagging reduces the allowable data collection rate considerably. Therefore, counter experiments generally have used the "step" method with bremsstrahlung to measure photoproduction of a resonance plus one particle, say a proton, by measuring the proton energy at a fixed angle. The "line" in the proton spectrum expected for a narrow resonance produced by a monochromatic γ is transformed into a step, as shown in Fig. 1.[1] For zero-width particles the cross section is very precise, but the shape of the step cannot be determined well for large width resonances. However, if the shape is known the step can give the cross section accuracy needed.

Analogous problems exist in the case where the resonance decay products are observed. As an example, Fig. 2 shows the dipion spectrum found by the DESY-MIT group[2] for the reaction $\gamma p \rightarrow \pi^+ \pi^- + $ anything. In this experiment the π^+ and π^- energy and angles are measured, giving $E_+ + E_-$, $\cos\theta_{+-}$, and M_{+-}. The problem is to isolate the reaction

$$\gamma p \rightarrow \pi^+ \pi^- p \tag{1}$$
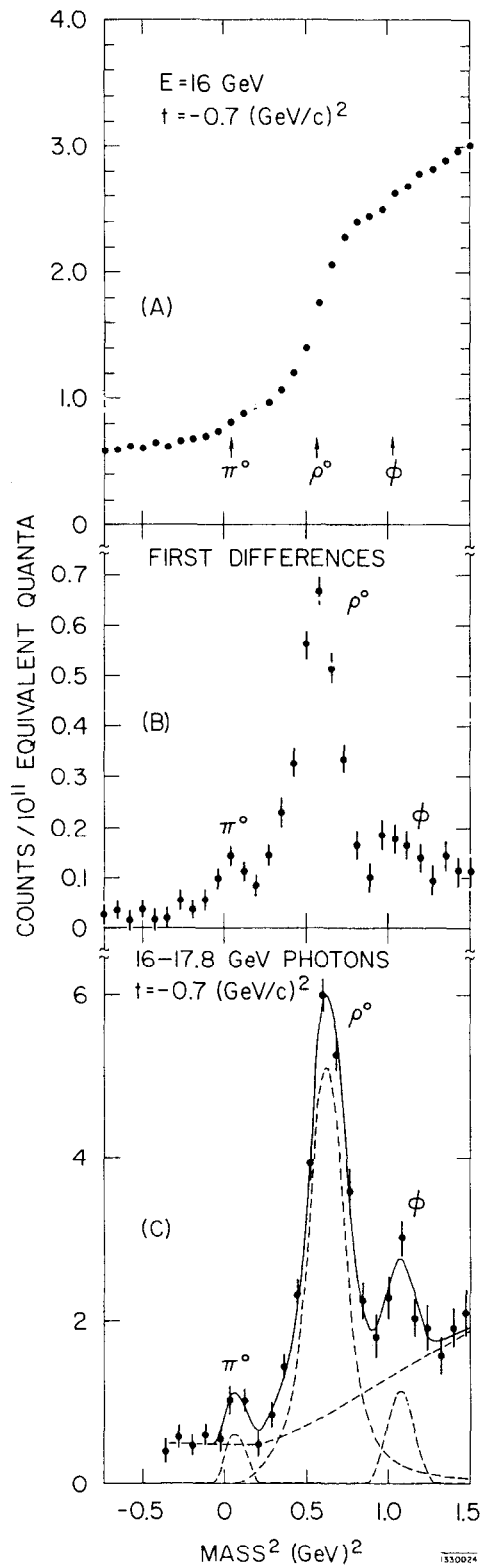
FIG. 1--Data of Ref. 1 illustrating the "step" method for measuring two body
reactions with a bremsstrahlung beam. The first differences of the
step must be used to determine the resonance shape.
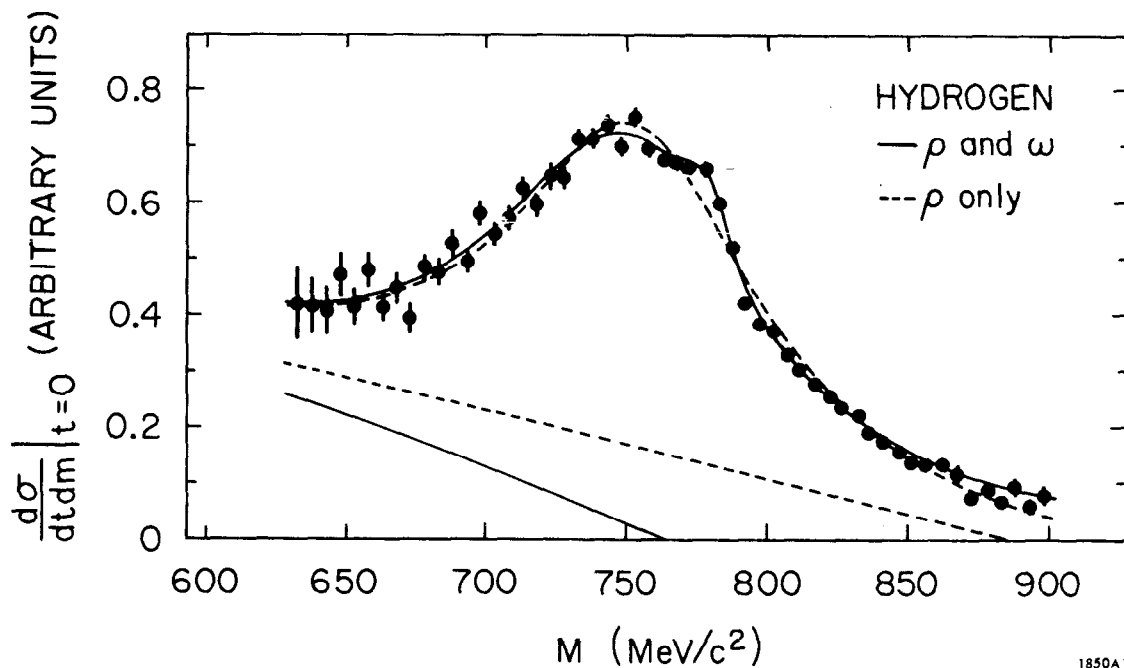
FIG. 2--Data of Ref. 2 on the reaction $\gamma p \rightarrow \pi^+ \pi^-$ + anything, corrected for spectrometer acceptance. The authors assume 100% transverse ρ^0 production, and do not include a possible 10% systematic normalization error owing to an uncertain spectrum shape. The solid lines show the shapes assumed by the authors for reaction (1) and background, including ρ-ω interference effect. The broken lines show the same for no ρ-ω interference.

by removing backgrounds from the reactions

$$\gamma p \rightarrow \pi^+ \pi^- \ (p. \ldots) \tag{2}$$

$$\rightarrow \pi^+ \pi^- \ (n. \ldots) \tag{3}$$

where the dots represent at least one extra pion. This was done by fitting the data to a sum of an <u>expected</u> ρ shape and an arbitrary smooth background. In Fig. 2 the solid and broken lines through the data show two shapes assumed by these authors for dipion masses of reaction (1) and the lower solid and broken lines the corresponding backgrounds (in this case a distorted Breit-Wigner with and without the $\rho-\omega$ interference effect). The cross section is different for the two cases, and clearly it would help to measure the proton as well in this reaction. As will be seen, we question their background forms, based upon our bubble chamber study of vector meson photoproduction.

Of course, present counter techniques have a hard time with multibody states. These can be studied in the bubble chamber and provide an important side dividend. But here I am concerned with a direct comparison of a bubble chamber experiment in the domain of the counter.

For our experiment, the beam used the Compton scattering at 180° of a Q-switched ruby laser light beam from a high energy electron beam. If the laser light is optically polarized, the 180° scattered photons are nearly 100% polarized as well as taking a good fraction of the electron energy. For a ruby laser (1.78 eV photon) and 20 GeV electrons we can obtain up to 7.5 GeV back-scattered photons. With the ruby light frequency doubled, we can obtain 10 GeV.

In the present system the ruby laser delivers 1-2 joules of light at 2 pps, limited by the strength of the ruby in intensity, and by average heat dissipation in rate. The yield of high energy photons is up to $\sim$ 200/pulse, all within 30 nsec of the Q-switch trigger. These properties make the beam well matched to the bubble chamber: the short burst is no drawback (but terrible for counters), and a long chamber gives the most efficient use of a limited flux.

The beam has been described previously[3] so I will only give a few properties. The electron beam phase space is defined by two collimators to be $\sim$ 1 cm $\times$ 10^{-5} radians in the interaction region. The laser light is directed by remotely adjustable mirrors to intersect the electron beam at about 3 mrad. The

electrons have a focus at a collimator near the chamber (subtending $\pm 10^{-5}$ radians) but are dumped after the interaction, so photons scattered into the beam direction converge to pass through the final collimator. To improve photon energy resolution, then, both electron and photon collimators would have to be smaller, cutting intensity according to the fourth power of the improvement ratio. To have $\sim 50 - 70$ photons per burst we have to settle for $\pm 2.5\%$ energy resolution at 2.8 GeV and $\pm 4\%$ at 4.7 GeV.

Foregoing many important experimental details for lack of time, I will only say that we will have 2.2 million pictures, giving 90, 150, and 250 evts/μb at 2.8, 4.7, and 9.3 GeV respectively. Cross sections are obtained by comparing the number of events to the number of e^+e^- pairs found in the same fiducial volume, and using the pair production cross sections, known to 0.5%, for flux normalization.

I now will describe some results obtained on reaction (1) and specifically on the reaction

$$\gamma p \rightarrow p\rho^0 \tag{4}$$

Figure 3 shows the dipion spectrum for all events of reaction (1) obtained in the 9.3 GeV film on hand. One might deduce that any background is negligible under the clear ρ^0 signal. However, note the low mass skewing of the resonance shape, and the almost complete absence of a high mass tail we should expect to see. As will be seen, we interpret these features as due to a subtle form of interfering background. If a large, normal, nonresonant background were present, we might miss the true complexity of the situation. Also, if a counter experiment does not give the overall view available to a bubble chamber, it will have problems of interpretation which no amount of statistical superiority can overcome.

The first measurement I will describe is that of the contribution σ_N and σ_U to the ρ^0 production cross section σ. For forward ρ^0 the polarization dependence in the matrix element for exchange of any trajectory in the natural parity sequence ($P=(-1)^J$) will involve the polarization vectors, $\vec{\epsilon}$, of γ and ρ in the form $\vec{\epsilon}_\gamma \cdot \vec{\epsilon}_\rho$. For unnatural parity exchange ($P=(-1)^{J+1}$) the form must be the pseudoscalar $(\vec{\epsilon}_\gamma \times \vec{k}) \cdot \vec{\epsilon}_\rho$. These lead to the angular distributions in the ρ^0 rest frame

$$d\sigma_N/d\Omega \sim \sin^2\theta \cos^2\psi$$

$$d\sigma_U/d\Omega \sim \sin^2\theta \sin^2\psi$$
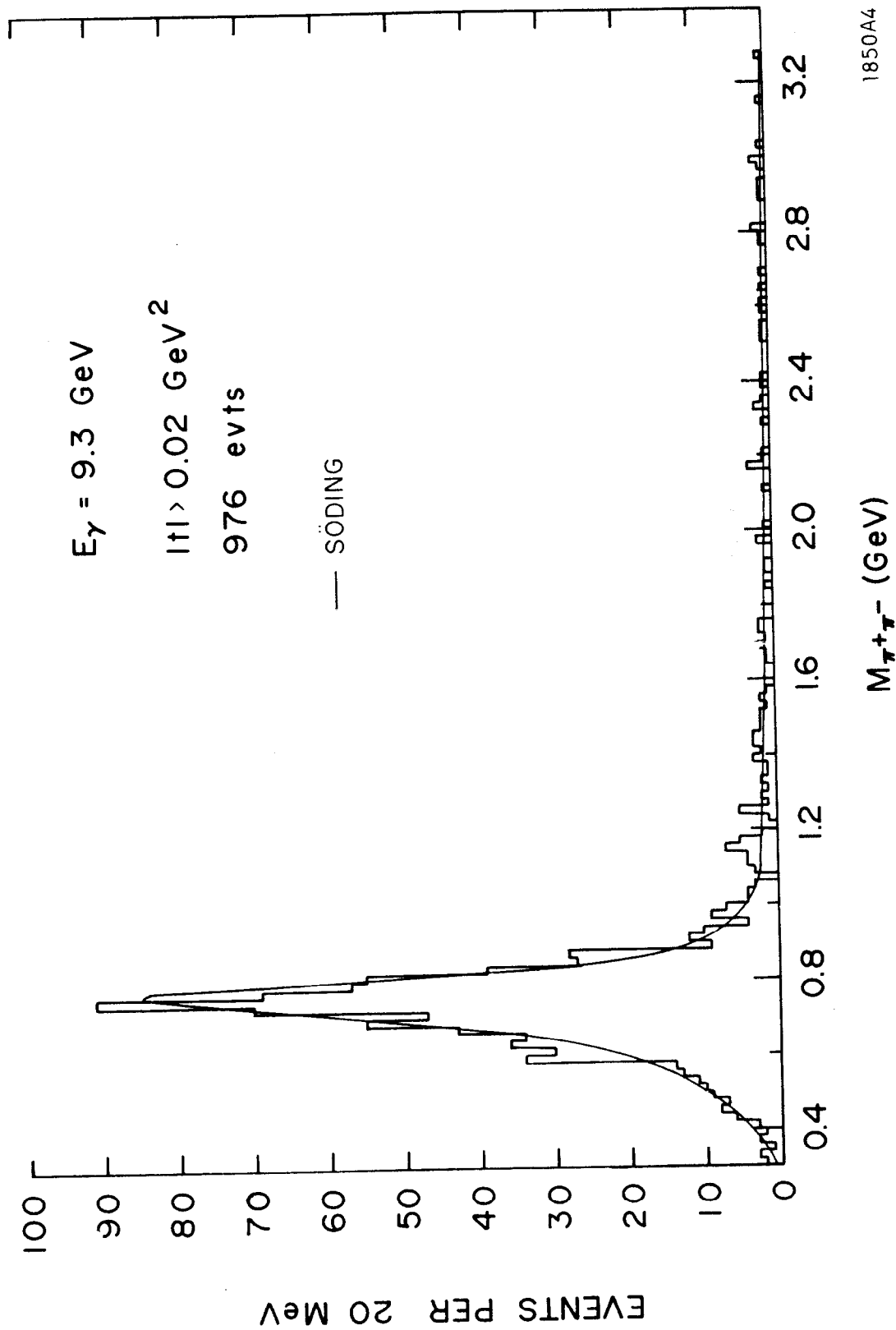
FIG. 3--Dipion mass spectrum of reaction (1) obtained in the bubble chamber for $E_\gamma = 9.3$ GeV.

where θ is the angle of the π^+ in the ρ^0 rest frame with respect to the c.m.s. ρ^0 direction, and ψ is the azimuth of the π^+ with respect to the photon polarization plane. Thus the natural and unnatural cross sections are separable and we define the parity asymmetry

$$P_\sigma = \frac{\sigma_N - \sigma_U}{\sigma_N + \sigma_U}$$

For nonforward production the definition of ψ is more complicated but analogous.[4,5] Figure 4 shows the decay distribution for ρ^0 with $|t| < 0.4$ GeV^2. It is evident that natural exchange dominates; in fact, the isotropic parts are consistent with coming from background and the unpolarized beam component. The counter experiments[6,7,8] measure the cross section for symmetric ($\theta = \frac{\pi}{2}$) ρ^0 decay at two azimuths, $\psi = 0$ and $\psi = \frac{\pi}{2}$, obtaining $\sigma_{||}$ and $\sigma_\perp$ respectively. As can easily be seen, if flip terms are zero, the azimuthal asymmetry ratio

$$\Sigma = \frac{\sigma_{||} - \sigma_\perp}{\sigma_{||} + \sigma_\perp}$$

is a measure of the difference between natural and unnatural exchange. Figure 5 compares the bubble chamber and counter data, and all are consistent with $\Sigma = 1$. Note that one bubble chamber event not near $\psi = 0$ or $\frac{\pi}{2}$ is statistically worth less than one counter event at those angles, but no great superiority can be seen from the error bars. The counter data does suggest a finite unnatural exchange part. We will refer to this later.

In the bubble chamber data we can isolate contributions to P_σ due to helicity flip because they have a $\cos^2\theta$ dependence. These are lost in the counter data where such terms must be assumed zero (only then will $P_\sigma = \Sigma$). This turns out to be correct from the bubble chamber data but is not a priori necessary except in the forward direction.

In the bubble chamber we can see the effects of ρ helicity flip, since any sign of longitudinally polarized ρ, e.g., in any density matrix element with a zero, must imply helicity flip at the $\gamma-\rho$ vertex. Looking at the density matrix elements in Fig. 6, we see that in the helicity system no helicity-flip term is significantly different from zero for $|t| < 0.4$ GeV^2. Hence we have shown that the diffractively produced ρ^0 is consistent with conservation of the s-channel helicity of the photon. It was quickly noticed by Gilman et al.[9]
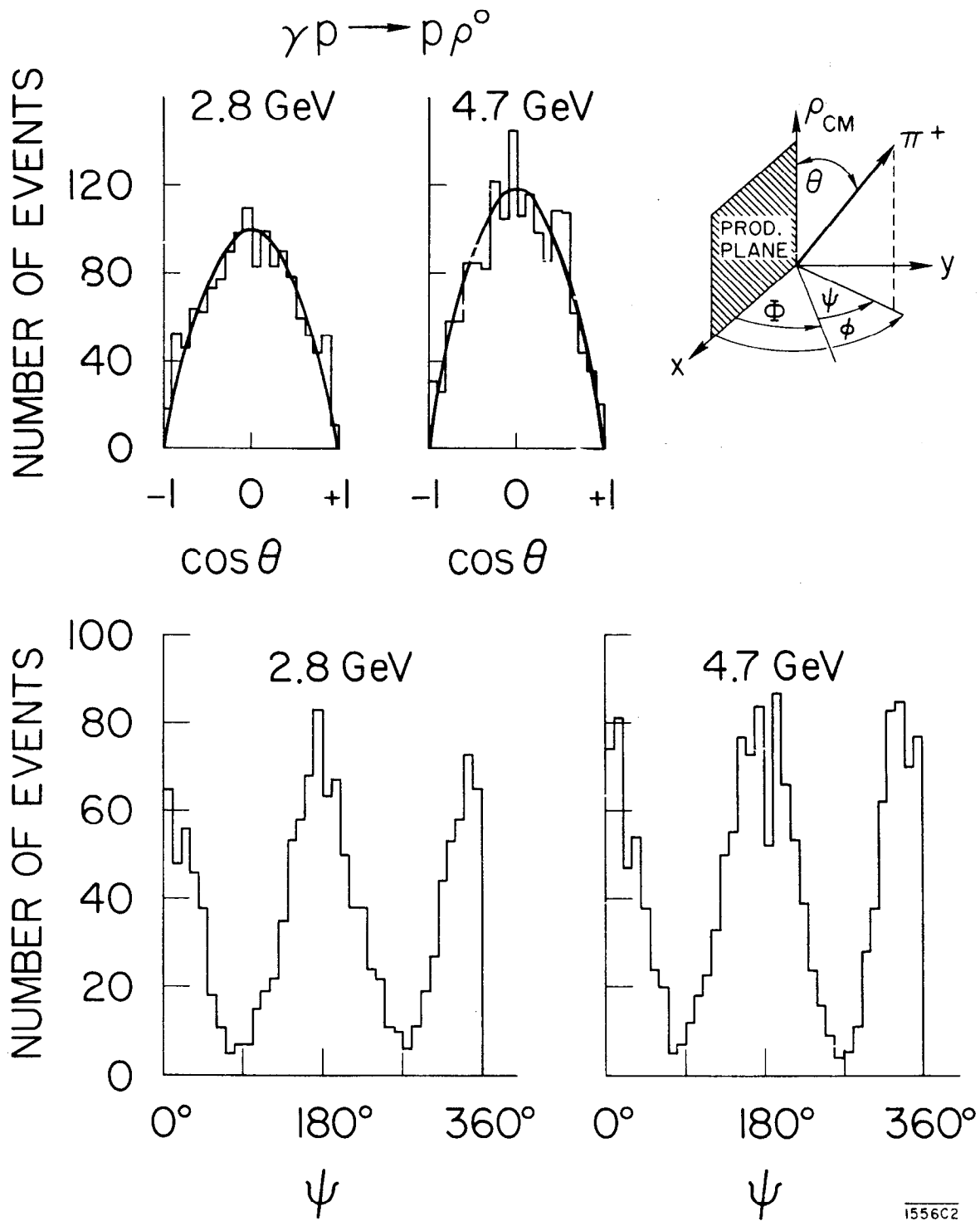
FIG. 4--c.m.s. helicity system decay distributions as seen in the ρ^0 center-of-mass system for $E_\gamma = 2.8$ and 4.7 GeV, for $|t| < 0.4$ GeV^2. The definition of angles may be seen from the inset.

Eγ = 4.7 GeV

○ Cornell, Eγ = 3.5 GeV

185083

Eγ = 2.8 GeV

This Exp
DESY I
DESY II

Σ

0   0.1   0.2   0.3   0.4   0   0.1   0.2   0.3   0.4

1.0   0.8   0.6   0.4   0.2   0

|t| GeV^2
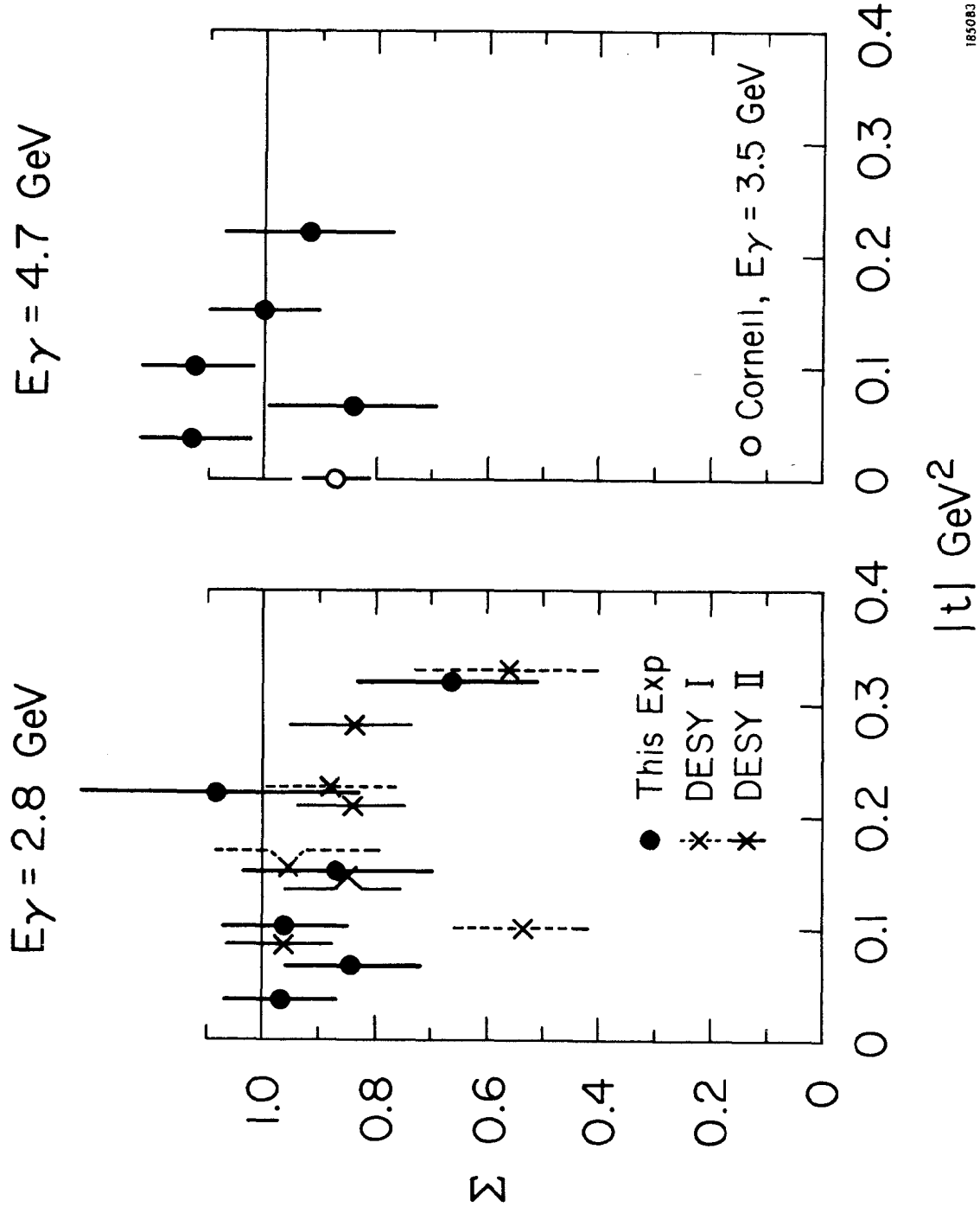
FIG. 5—Comparison of the bubble chamber result for Σ, the azimuthal asymmetry defined in the text, with counter results with polarized crystal beams. The counter experiments are: DESY I from Ref. 6 (2.0 < Eγ < 2.5 GeV); DESY II from Ref. 7, a repeat of the DESY I experiment (2.1 < Eγ < 2.4 GeV); CORNELL from Ref. 7 (Eγ = 3.5 GeV).
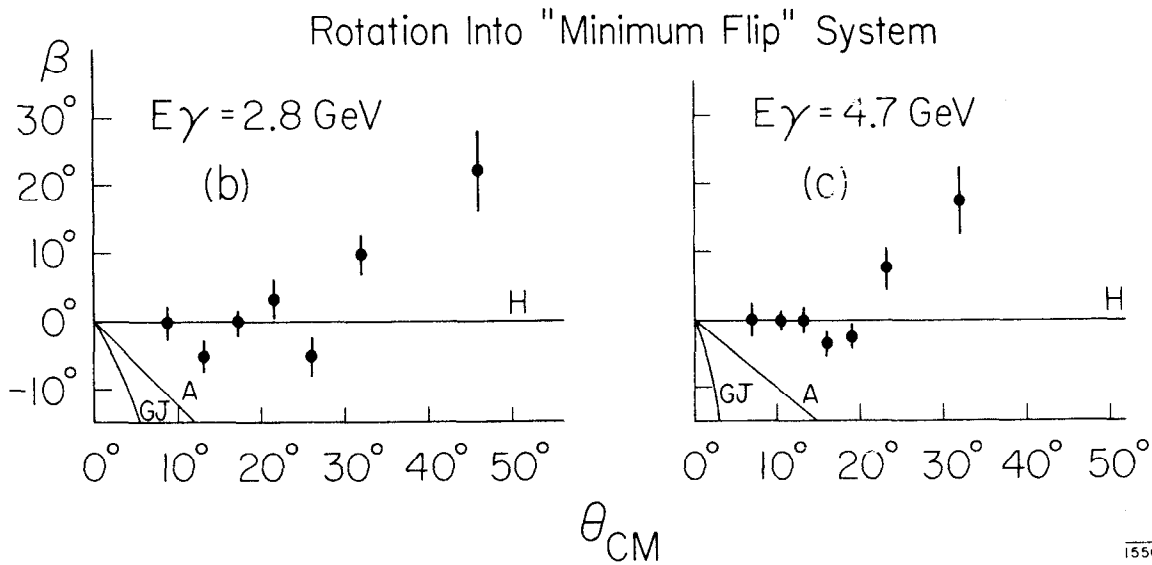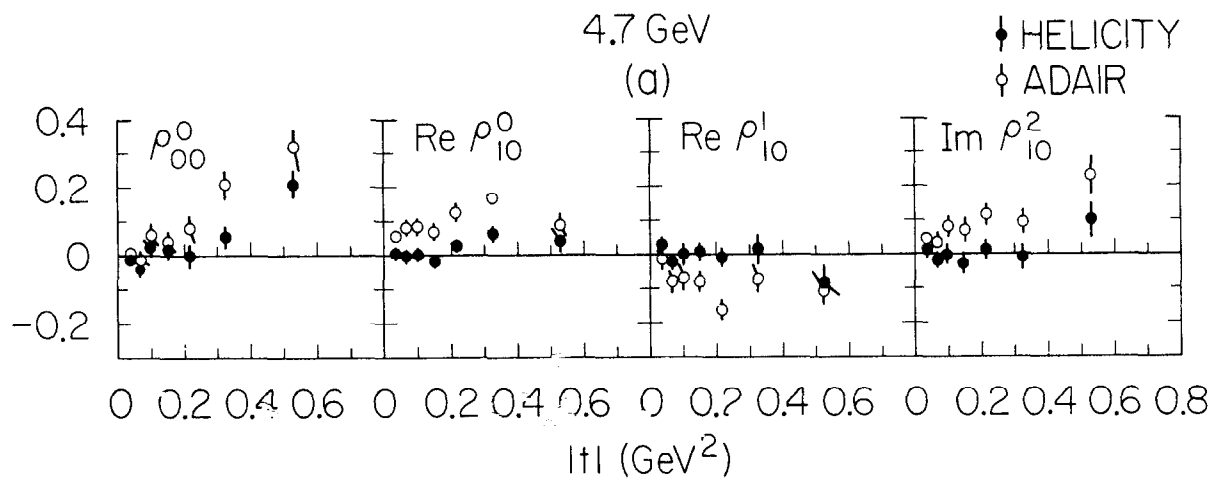
FIG. 6--(a) The ρ^0 density matrix elements which become nonzero if spin-flip is present. For c.m.s. helicity conservation these are zero in the helicity system, while for "spin independence" the Adair system would be favored. For t-channel helicity conservation, the Gottfried-Jackson system should have these elements zero, but the values in that system are not shown because they are very large. The helicity and Adair systems nearly coincide in our range of t values and here our experiment can decide for the helicity frame. (b) The angle β by which the frame must be rotated away from the helicity axis to minimize the spin-flip elements shown in (a). This shows that the helicity system is preferred over all other frames.

that in πp diffractive scattering the s-channel helicity-flip amplitudes also tend to zero with increasing energy, suggesting (using factorization) that Pomeron exchange is helicity conserving.

Now we turn to the question of the ρ cross section. Evidently we must account for the skewed distribution found in the dipion mass spectrum. Ross and Stodolsky[10] suggested that a kinematic factor $(M_\rho/M_{\pi\pi})^n$, with $n = 4$, could be introduced by the ρ beginning life with zero mass. We checked this hypothesis by fits which allowed n to be a function of t. The result for n is shown in Fig. 7 as a function of t. Evidently $n \sim 5.6$ at $t = 0$, and changes rapidly with t. Also shown is the measured t-slope as a function of $M_{\pi\pi}$.

The next hypothesis is that the ρ interferes with a background with a different t dependence from the ρ and with relatively constant phase, as was suggested by Söding.[11] He suggested the Drell[12] mechanism, where non-resonant pion pairs are produced, as the background. We have found that this model can reproduce enough of the features of the data that we believe at least the interference explanation is the most likely one.[5] The consequence of this conclusion is that, if the background were "turned off" the ρ peak would become an unskewed Breit-Wigner containing fewer events, at our energies, than are seen in the experimental enhancement.

We note again that these conclusions are derived from the overall view of the reaction given us by the bubble chamber. Some of the counter people are now beginning to use this model.

Unfortunately we don't measure many events in the precisely forward direction. In fact, such events have rather short protons and are easily confused with wide-angle electron pairs up to $|t| \sim 0.02$ GeV^2, so to give a forward cross section we must bridge the gap by extrapolation. The result, when compared with the DESY-MIT values[2] as in Fig. 8, shows a considerable discrepancy, with nothing to do with models. What is the source of the problem?

We first explore the possibility that "inelastic" ρ production from reactions (2) and (3) gives a background, by simulating as best we can the experimental resolution of the spectrometer and applying it to our results.[13] Figure 9 shows the result of selecting $\pi^+\pi^-$ pairs with transverse momentum p_T, satisfying $p_T^2 < 0.05$ (GeV/c)^2. The shaded events are from excluding reaction (1) and hence are from the background reactions (2) and (3). The counters might

$E_\gamma = 9.3$ GeV

---- EMPIRICAL

$n(t) = 5.6 + 10\,t$

---- WITH $\left[\dfrac{M_\rho}{M_{\pi\pi}}\right]^{n(t)} e^{A_\rho t}$
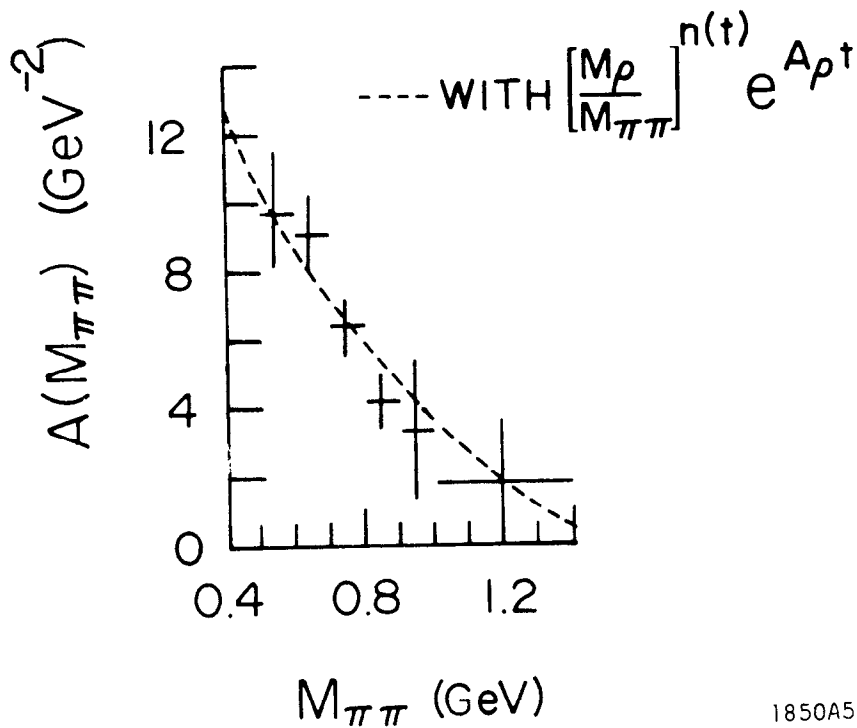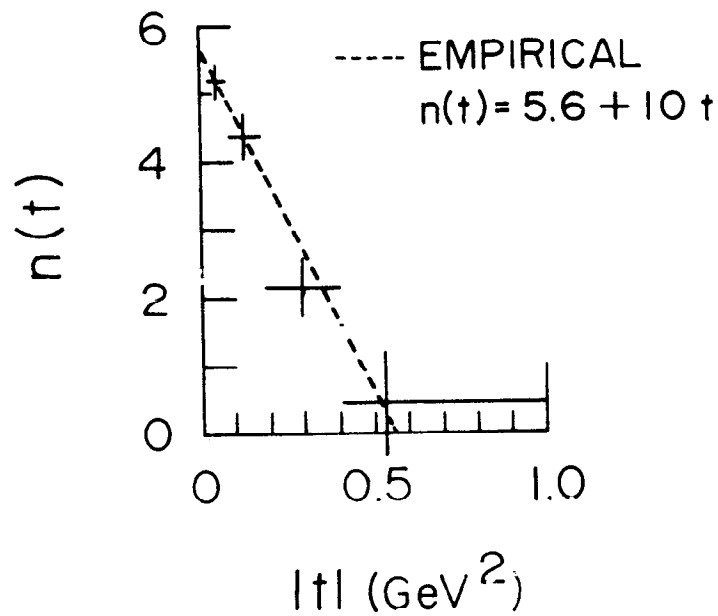
1850A5

FIG. 7--Values of n, as a function of t, needed to fit a form of the dipion mass spectrum to $(m_\rho/m_{\pi\pi})^n$ times a p-wave Breit-Wigner form. It should be noted that such fits give an excellent description of the data.
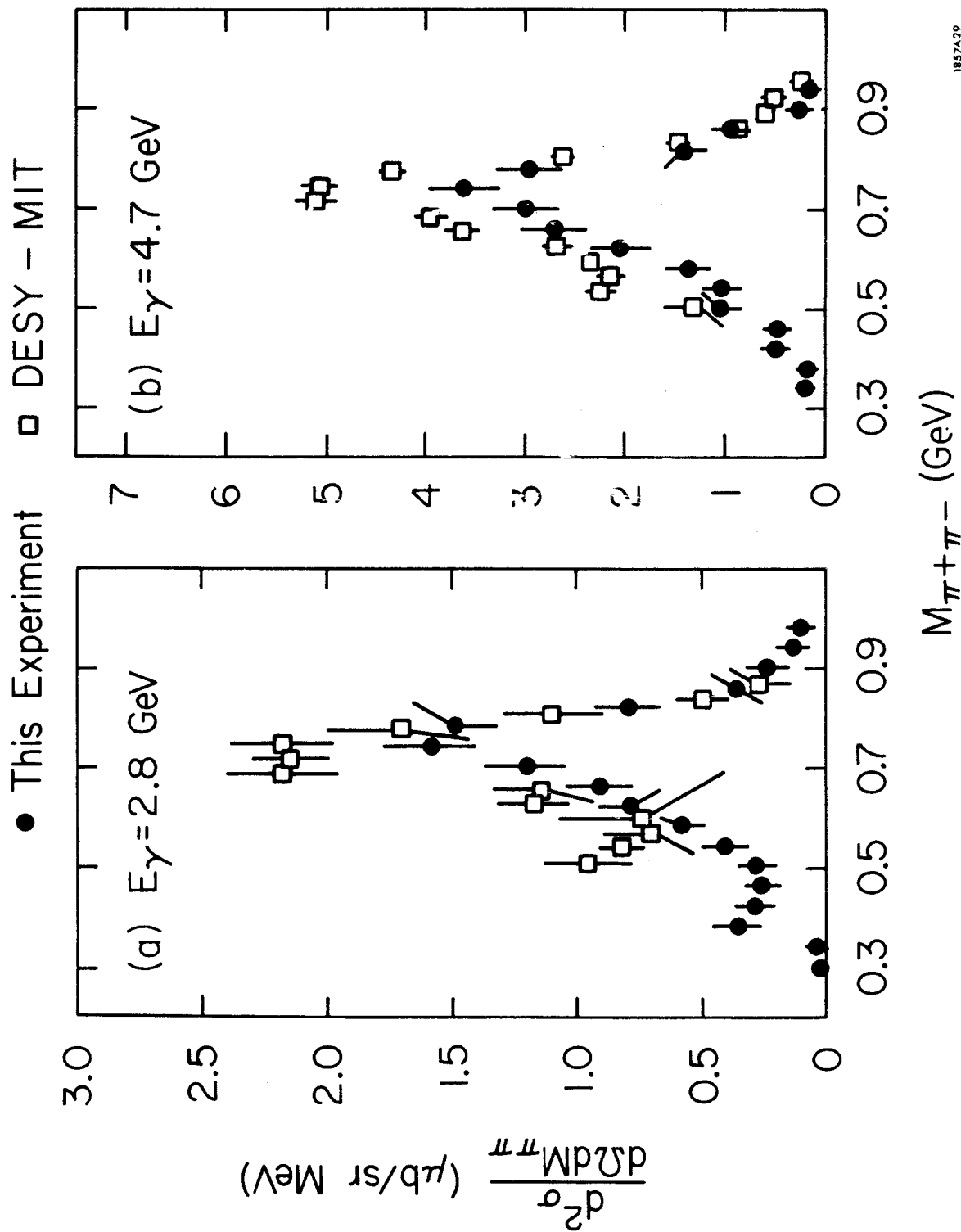
FIG. 8—Comparison of the data of Ref. 1 on the forward cross section for reaction (1) with that obtained in our experiment using a dependence $d^2\sigma/dmdt = A \exp(Bt)$ and extrapolating to $\theta=0$. The discrepancy is discussed in the text.
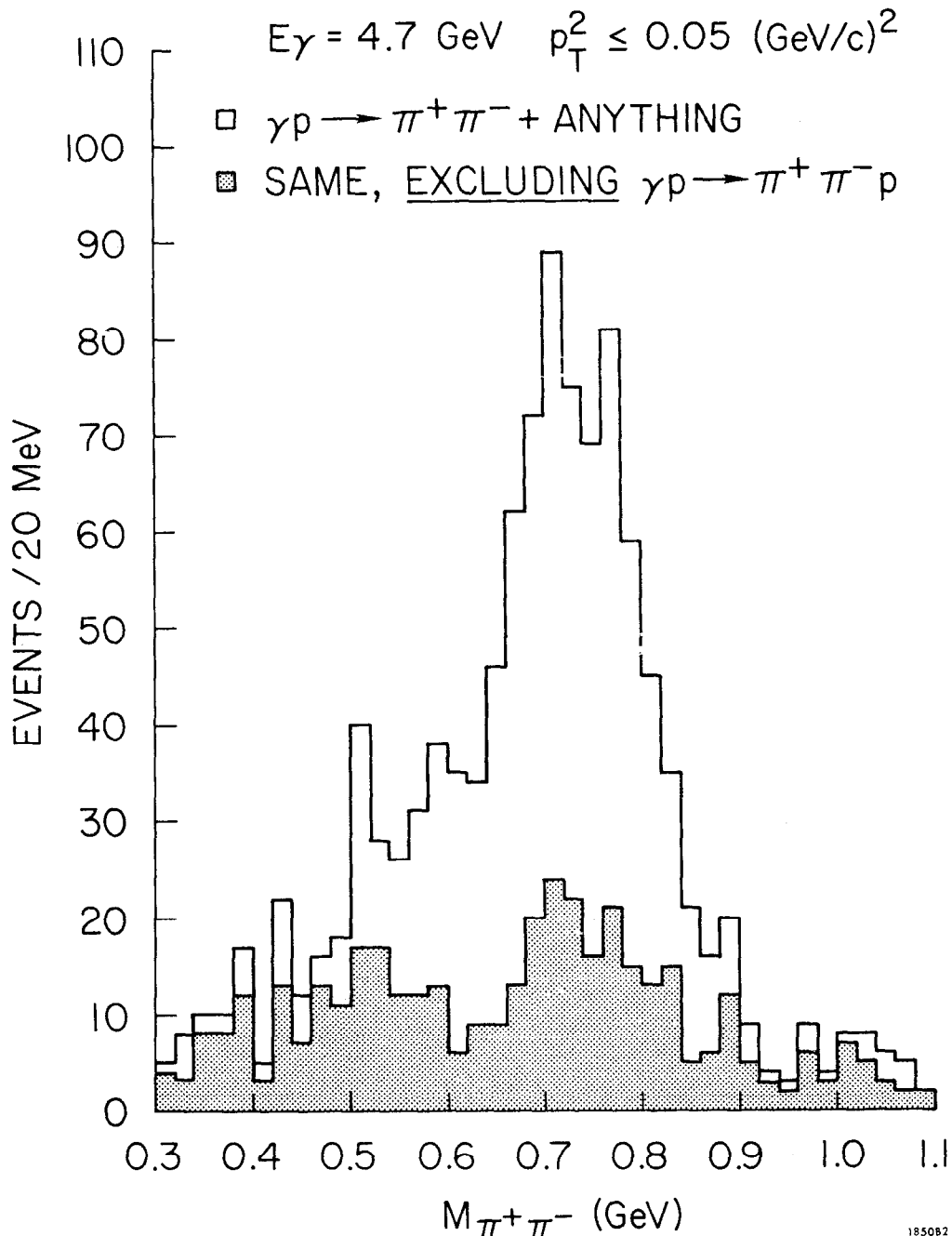
FIG. 9--Simulation of the dipion mass spectrum reported in Ref. 1 using all
bubble chamber events. Since the photon spectra differ, the "spec-
trometer" setting was taken as $\bar{E} = E_{\gamma max}/1.08$ to compensate, and
the requirement $|\bar{E} - (E_+ + E_-)| \leq 0.18 (E_+ + E_-)$ imposed. To obtain
sufficient events, all decay angles were taken and the transverse
momentum p_T of the dipion pair required to obey $p_T^2 < 0.05$ $(GeV/c)^2$
instead of < 0.01 $(GeV/c)^2$ as obtained in the counter experiment.
The inelastic events are not observed to have a strong decay angle
distribution and have a fairly flat dependence on p_T. The unshaded
distribution shows all such selected events while the shaded areas
are from reactions (2) and (3).

17-14

be seeing the ρ peak in the background which could be 20-30% of the total signal. I say "could be" because again there are few events in the exact forward direction, and the very small t dependence of the background is not established. Such a background could also simulate $\Sigma \neq 1$ for the polarized counter experiments.

Next, what evidence have we that our overall normalization is correct? Our total hadronic cross section[3] agrees very well with a counter experiment done by UCSB at SLAC.[14] The cross sections for the entire channel also are in agreement with previous determinations. Hence we seem to be on firm ground.

The third possibility is that $d\sigma/dt$ has not just a linear exponential dependence with t, but rather peaks up at very small angles. Here the combination of counter and bubble chamber results suggests a further experiment might be very profitable. It also illustrates the drawback of the bubble chamber in not identifying particle masses.

Now I turn to the future for photoproduction experiments in the bubble chamber. In the short range, there is much to be done. These studies would benefit from high statistics, there are deuterium reactions to study, and at low energies there is the important question of the electromagnetic couplings to the nucleon resonances requiring both hydrogen and deuterium. After considerable study it has been concluded that even single π production in the resonance region is best done in a bubble chamber. Thus the chamber is assured of at least two years of photoproduction work.

In the long range it is not clear that the bubble chamber is going to be able to carry the load. The requirement in all cases will be at least an order of magnitude increase in statistics. But for every hadronic interaction at high energies, almost 200 pairs are produced. This electromagnetic stuff is very messy, and can easily swamp a triggering system. With advancing laser technology it appears that a 100 pps laser may be built, so that the match of beam and chamber is no longer so obvious. However, it is important to retain most of the bubble chamber features to keep the overall view shown to be so useful in this experiment. We now are expecting to turn to the streamer chamber or the rapid cycling chamber for the needed increase in statistics. The conclusion is that visual techniques in photoproduction will be required for even the long range future.

References

1. R. Anderson et al., Phys. Rev. $\underline{D1}$, 27 (1970).

2. H. Alvensleben et al., paper submitted to the Kiev Conference on High Energy Physics, Kiev (1970); see also Phys. Rev. Letters $\underline{23}$, 1058 (1969).

3. J. J. Murray and P. Klein, SLAC-TN-67-19. See also J. Ballam et al., Phys. Rev. Letters $\underline{23}$, 498 (1969).

4. K. Schilling et al., Nucl. Phys. $\underline{B15}$, 397 (1970).

5. For a fuller description of the experiment, see H. H. Bingham et al., Phys. Rev. Letters $\underline{24}$, 955 (1970) and J. Ballam et al., Phys. Rev. Letters $\underline{24}$, 960 (1970).

6. L. Criegee et al., Phys. Letters $\underline{28B}$, 228 (1968) (DESY I).

7. L. Criegee et al., Phys. Rev. Letters $\underline{25}$, 1306 (1970) (DESY II).

8. G. Diambrini-Palazzi et al., Phys. Rev. Letters $\underline{25}$, 478 (1970) (Cornell).

9. F. J. Gilman et al., Phys. Letters $\underline{31B}$, 387 (1970).

10. M. Ross and L. Stodolsky, Phys. Rev. $\underline{149}$, 1172 (1966).

11. P. Söding, Phys. Rev. Letters $\underline{19}$, 702 (1965).

12. S. Drell, Phys. Rev. Letters $\underline{5}$, 278 (1960).

13. See the analysis of G. Wolf, DESY report 70/64 (unpublished).

14. D. O. Caldwell et al., Phys. Rev. Letters $\underline{25}$, 609 (1970); $\underline{25}$, 902 (1970, Erratum).

$K^o_L p$ INTERACTIONS FROM 1-10 GeV/c[*]

SLAC Group B[**]
Presented by J. S. Loos
Stanford Linear Accelerator Center
Stanford University, Stanford, California USA

1. Introduction

I would like to present a progress report on the SLAC $K^o_L p$ interaction experiment for which data have been acquired over the past two years in three separate exposures of the SLAC 70-inch hydrogen bubble chamber to a neutral beam. We now have some 800,000 photographs on hand which will represent a $K^o_L p$ equivalent of about 40 events/μb when fully analyzed. The K^o_L beam, described below, is distributed over a momentum spectrum covering the range from 1 GeV/c to 10 GeV/c with the peak flux near 4 GeV/c. Since all momenta are analyzed with the same technique and since we have a good understanding of our K^o_L beam spectrum, our experiment will provide data over this wide momentum region free from the systematic normalization problems usually encountered when comparing data from different experiments at different energies. Thus, we expect that the data from our experiment will provide stringent tests on both the s and t behavior of various theoretical models.

At present, the following reactions[1] are under study:

$$K^o_L p \rightarrow K^o_S p \qquad (1300) \qquad (1)$$

$$\overline{K}^o p \rightarrow \pi^+ \Lambda \qquad (1600) \qquad (2)$$

$$\overline{K}^o p \rightarrow \pi^+ \Sigma^o \qquad (1000) \qquad (3)$$

$$K^o p \rightarrow K^+ \pi^- p \qquad (2500) \qquad (4)$$

$$\overline{K}^o p \rightarrow K^- \pi^+ p \qquad (3500) \qquad (5)$$

$$K^o_L p \rightarrow K^o_S p \pi^+ \pi^- \qquad (5500) \qquad (6)$$

$$\overline{K}^o p \rightarrow \Lambda \pi^+ \pi^+ \pi^- \qquad (2000) \qquad (7)$$

The number of events now on hand is indicated for each reaction. The final numbers of events are expected to be increased by factors from 2 to 4. The direction of the K_L^o, but not its momentum, is measured for each event so all of the above reactions have 3 kinematic constraints except (3) which has 1 kinematic constraint. A number of other reactions are also of potential interest, such as:

$$\bar{K}^o p \rightarrow \Sigma^\pm \pi^\mp \pi^+ \tag{8}$$

$$\bar{K}^o p \rightarrow \Xi^- K^+ \pi^+ \tag{9}$$

$$\bar{K}^o p \rightarrow \Xi^o K^+ \tag{10}$$

$$K_L^o p \rightarrow K_S^o K^+ \Lambda \tag{11}$$

$$K_L^o p \rightarrow K_S^o p K^+ K^- \tag{12}$$

$$\bar{K}^o p \rightarrow \Lambda \pi^+ K^+ K^- \tag{13}$$

$$K^o p \rightarrow p K^+ \pi^+ \pi^- \pi^- \tag{14}$$

$$\bar{K}^o p \rightarrow p K^- \pi^+ \pi^+ \pi^- \tag{15}$$

I shall restrict today's talk to our results on reactions (1), (2), (4), (5), and (6). Briefly, our results on reaction (1) show for the first time the details of the entire t distribution, and give firm information concerning ω exchange; reaction (2) is useful for model studies on K* and K** exchange and may shed some light on the question of exchange degeneracy of the two trajectories by comparison to the line-reversed reaction; reactions (4) and (5) provide interesting information on K*p, $\bar{K}$*p, and ΔK production; and (6) gives a comparison of $Q^o p$ and $\bar{Q}^o p$ production up to 10 GeV/c. Note that because the K_L^o beam is made up of equal components of strangeness +1 and -1 our data can have no normalization error in comparing $K^{*o}p$ and $\bar{K}^{*o}p$, or $Q^o p$ and $\bar{Q}^o p$ at the same energy. This point is not trivial when one considers the difficulty of comparing $K^+ p$ and $K^- p$ results in absolute magnitude.

2. Production of a K_L^o Beam at SLAC: the K_L^o Momentum Spectrum

The K_L^o particles are produced by impinging the SLAC electron beam on a low-Z target. The detailed production is quite complicated but probably is due to a combination of associated ΛK and ΣK photoproduction and ϕ meson photoproduction.[2] The K_L^o mesons resulting from these processes are

18-2

produced mainly at laboratory angles of a few degrees or less. In contrast the neutrons arise mainly through isotropic breakup of the target nuclei and have only a small contribution from $N\overline{N}$ pair production. As a result, the SLAC neutral beam contains a very favorable K_L^0/n ratio, especially above about 2 GeV/c.

A schematic picture of the neutral beam is shown in Fig. 1. The electron beam passes through a charge monitor (used for beam monitoring and for a rough beam normalization) and a vertical bending magnet (used to provide the production angle and to safely steer the beam to a radiation dump) onto a target made of beryllium (targets of 0.6 and 1.8 radiation lengths were used). The electromagnetic component of the secondary beam is removed by an absorber made of tungsten, lead, and lithium hydride. The charged particles are swept with magnets and the neutrals are suitably collimated to fill the bubble chamber volume located 55 meters downstream of the target. The K_L^0 angles are known within 1 mrad at the bubble chamber.

The K_L^0 momentum spectrum is determined by observing $K_L^0 \rightarrow \pi^+ \pi^- \pi^0, \mu^\pm \pi^\mp \nu$ and $e^\pm \pi^\mp \nu$ decays in the bubble chamber.[3] No attempt is made to identify the decay mode on an event-by-event basis. Rather, a distribution is accumulated for the visible momentum, defined as $p_{VIS} = (\vec{p}_1 + \vec{p}_2) \cdot \hat{K}_L^0$, where $\vec{p}_1$ and $\vec{p}_2$ are the momenta of the observed charged tracks and $\hat{K}_L^0$ is the beam direction. Crudely speaking, p_{VIS} has on the average two thirds of the parent momentum, regardless of the decay mode. This idea can easily be made quantitative by generating a large number of K_L^0 decays via Monte Carlo in proportion to the known decay rates. Then the Monte Carlo decays may be Lorentz-transformed to the laboratory to give p_{VIS} distributions corresponding to given K_L^0 momenta. Finally, the theoretical p_{VIS} distributions may be added appropriately to yield a unique fit to the experimental p_{VIS} data. An example of the technique is displayed in Fig. 2, where the theoretical p_{VIS} distributions arising from the fitted K_L^0 momentum components are summed to give the solid curve imposed on the experimental p_{VIS} spectrum. The K_L^0 momentum spectrum is then found from the fitted K_L^0 components after correcting for the effect of having observed K_L^0 decays over a fixed length in the bubble chamber.

FIG. 1--Schematic layout of K^O production at SLAC.

K$_L^o$ Momentum, Events

(a) 0.0-0.4   24
(b) 0.4-0.6   51
(c) 0.6-0.8   86
(d) 0.8-1.0   129
(e) 1.0-1.4   355
(f) 1.4-1.8   465
(g) 1.8-2.2   552
(h) 2.2-2.6   602
(i) 2.6-3.0   625
(j) 3.0-3.4   572
(k) 3.4-4.2   952
(l) 4.2-5.0   740
(m) 5.0-5.8   562
(n) 5.8-6.6   392
(o) 6.6-7.4   267
(p) 7.4-8.2   176
(q) 8.2-9.0   115
(r) 9.0-10.0   91
(s) 10.0-11.0   55

(a)-(s) K$_L^o$ Momentum Components
of P$_{VIS}$ Distribution

(t) Experimental P$_{VIS}$ Distribution,
6797 Events

——— Sum of Curves (a)-(s)

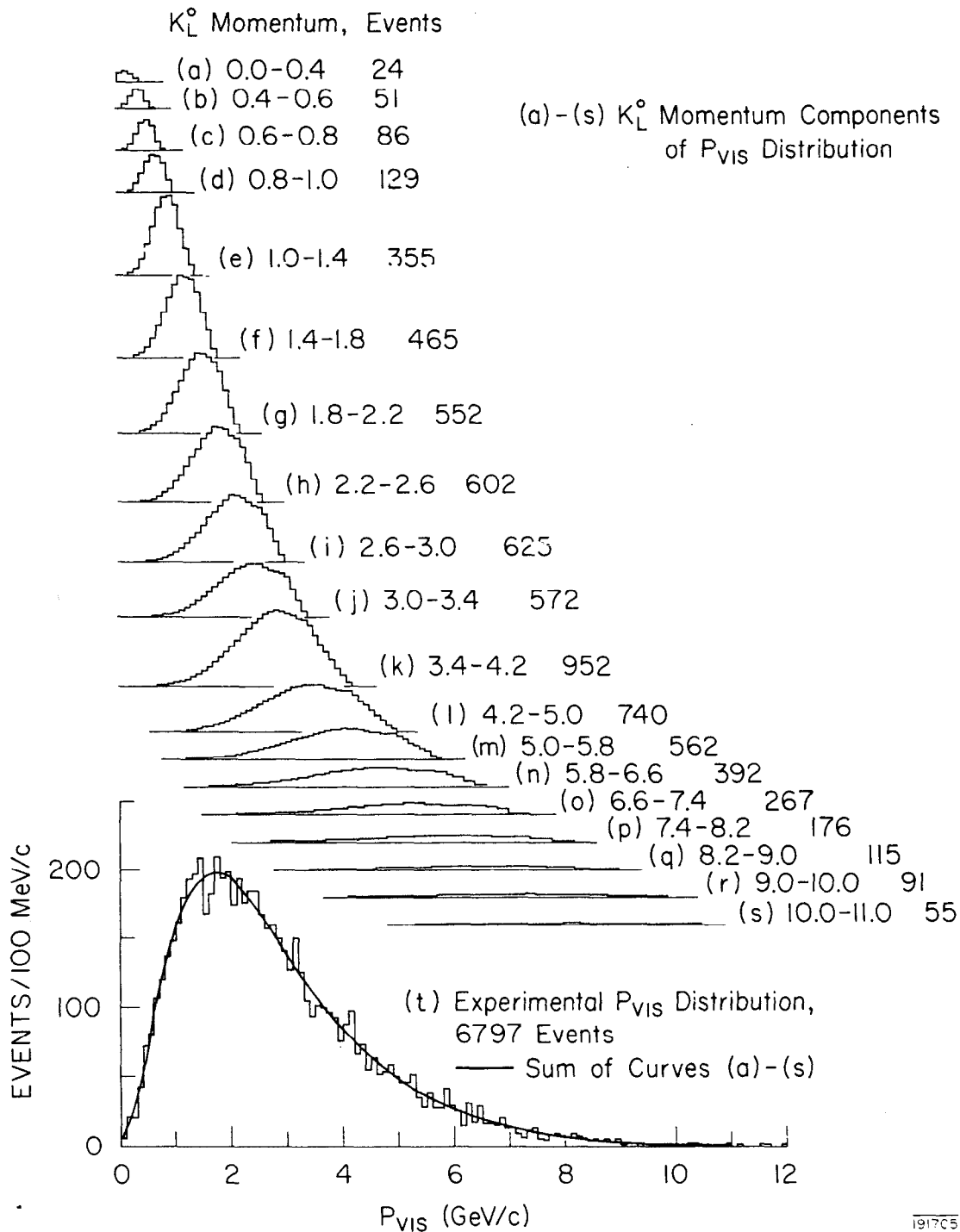FIG. 2--P$_{VIS}$ distribution used to determine the K^o momentum spectrum.
P$_{VIS}$ is the visible momentum from the three body K^o decays, as
explained in text. (a) - (s) Monte Carlo component histograms
from narrow momentum intervals found in a fit to the experi-
mental P$_{VIS}$ spectrum. (t) Experimental P$_{VIS}$ spectrum. Solid
curve is the summation of the fitted component histograms.

The K_L^0 beam momentum spectrum for the film on hand is shown in Fig. 3 in units of events/μb/GeV/c. The scope of the experiment is pretty well summed up by this figure.

3. The Reaction $K_L^0 p \rightarrow K_S^0 p$

This reaction is known to weak interaction experts as "K_S^0 regeneration in hydrogen" but is in fact a very interesting member of the class of inelastic scattering reactions between pseudoscalar mesons and baryons. The possible t channel exchanges are highly restricted; in fact, the only known candidates are the members of the vector nonet (ρ, ω, and ϕ) since the exchanged object must have both natural spin-parity and odd charge conjugation. As first pointed out by Gilman[4], ω exchange is expected to dominate over ρ in the forward direction while ϕ exchange is expected to be small because of the experimentally small $\phi \bar{N} N$ coupling. Thus our data on this reaction provide important new information on the properties of ω exchange. In particular, we use the forward point of the differential cross section to determine the phase of the forward amplitude, and consequently, the intercept of the effective Regge trajectory. The data are also interpreted within the framework of two distinctly different theoretical models.

The results which I will now show on $K_L^0 p \rightarrow K_S^0 p$ are being prepared for publication elsewhere[5] and are based on an analysis of 200,000 photographs yielding 571 events in the momentum interval 1.3-8.0 GeV/c. We have been careful to apply corrections for the effects of K_S^0 lifetime and steeply dipping proton tracks and have made a thorough study of the K_L^0 momentum spectrum for this sample of film.

The cross section, $\sigma(K_L^0 p \rightarrow K_S^0 p)$, versus p_{LAB} is shown in Fig. 4a. As indicated by the solid line the data are well described by the empirical law, $\sigma \sim p_{LAB}^{-n}$, with n = 2.1 $\pm$ 0.2, a value typical of many inelastic meson exchange reactions. Figure 4b shows the same data used in a test of the Pomeranchuk theorem by Finklestein and Roy.[6] If one assumes that the Pomeranchuk theorem is violated in such a way that $\Delta \sigma \equiv \sigma_T(K^- n) - \sigma_T(K^+ n) =$ 2.25 mb at infinite energies (as suggested by recent experiments at Serpukhov), then a lower bound (dot-dashed line) may be predicted for $\sigma(K_L^0 p \rightarrow K_S^0 p)$ simply from unitarity and analyticity considerations. The extrapolation of our data (dashed line) penetrates the bound at $p_{LAB} \sim 15$ GeV/c
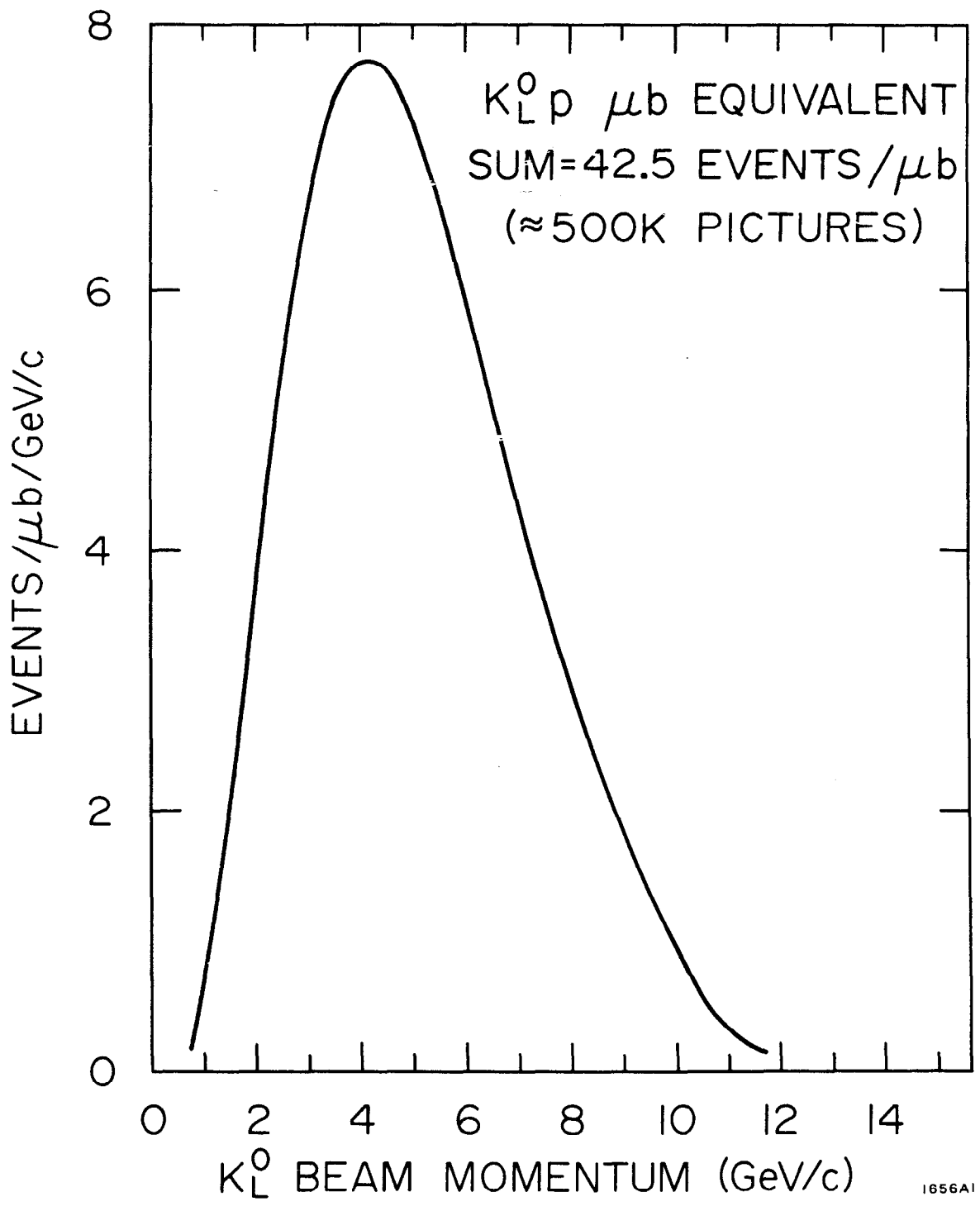
FIG. 3--K^O momentum spectrum.

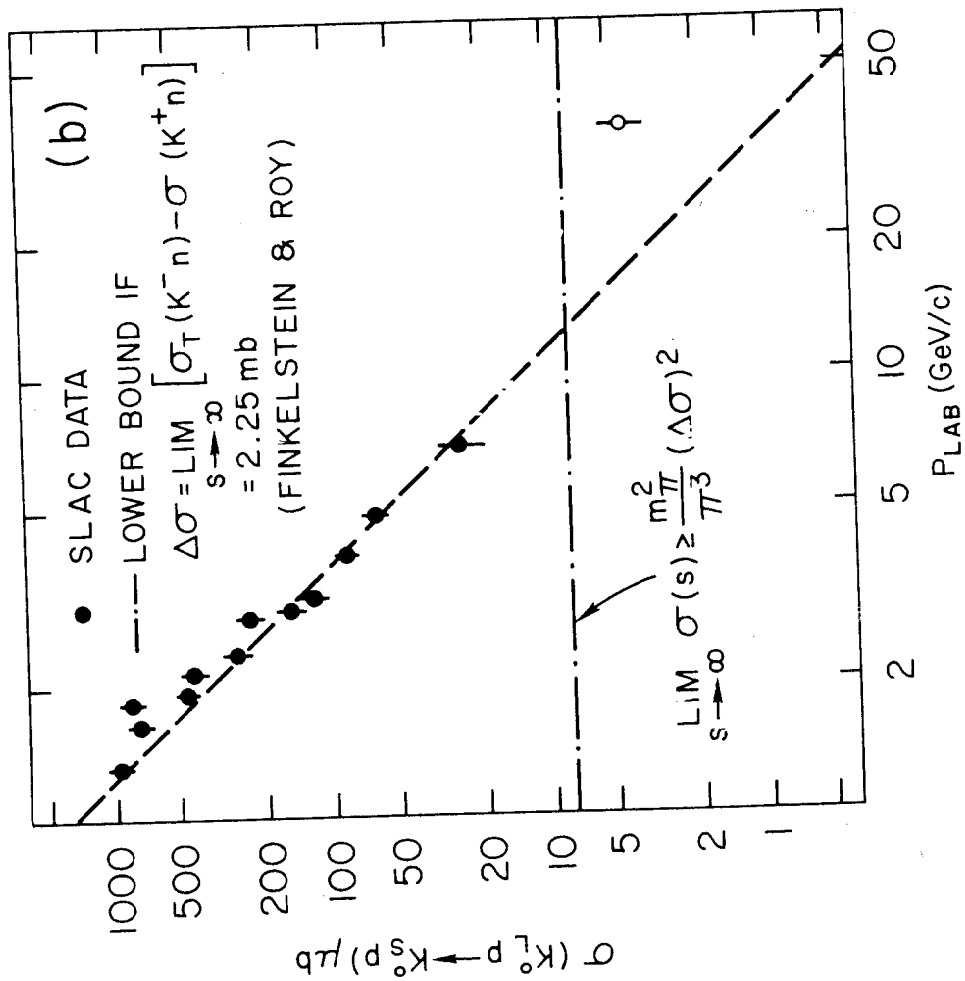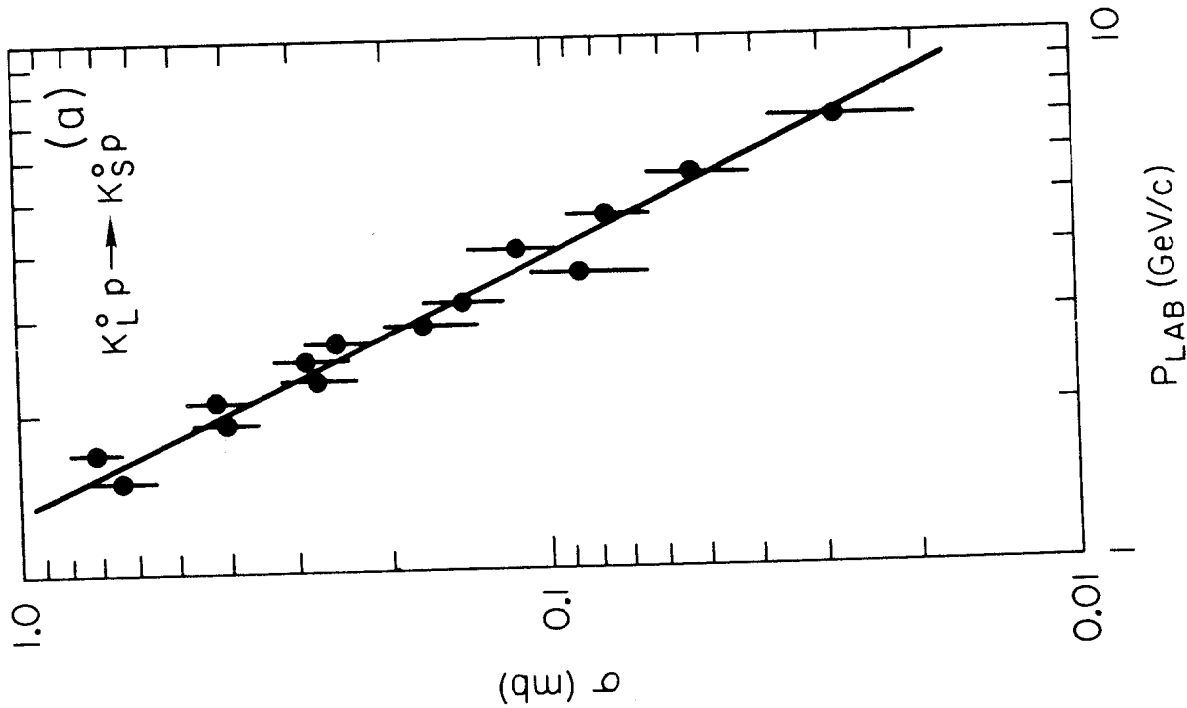FIG. 4--(a) Cross section for $K^0_L p \rightarrow K^0_S p$ versus p_{LAB}. The solid line corresponds to $\sigma \propto p^{-n}_{LAB}$, with $n = 2.1 \pm 0.2$. (b) Comparison to lower limit implied from high energy KN total cross sections (see Ref. 6).

indicating that either $\sigma(K_L^0 p \to K_S^0 p)$ must not continue to fall as p_{LAB}^{-2} or the difference $\Delta\sigma$ must be less than 2.25 mb at infinite energy. The open circle on Fig. 4b is an estimate from the recent Serpukhov experiment[7] assuming

$$\sigma \simeq \frac{1}{b}\left(\frac{d\sigma}{dt}\right)_0 ,$$

where $\left(\frac{d\sigma}{dt}\right)_0$ is the Serpukhov measurement, and b is the slope of the forward differential cross section taken from the SLAC experiment ($b \simeq 10$ GeV^{-2}). If I were to make a bet, I would wager that $\sigma(K_L^0 p \to K_S^0 p)$ will continue to fall like p_{LAB}^{-2} right past the bound and that eventually the experimental value for $\Delta\sigma$ will prove to be much less than 2.25 mb.

The differential cross sections are shown in Fig. 5a, averaged over 3 momentum intervals: 1.3-2.0 GeV/c (upper points), 2.0-4.0 GeV/c (middle points), and 4.0-8.0 GeV/c (lower points). The principal features are a sharp forward peak with an average slope of 10 ± 2 GeV^{-2}, a distinct shoulder in the interval $0.3 < |t| < 0.7$ GeV^2, and a rapid fall off for $|t|$ greater than 1.0 GeV^2. The differential cross section falls as $\sim p_{LAB}^{-1.3}$ in the forward direction and as $\sim p_{LAB}^{-2.5}$ for $|t|$ near 1.0 GeV^2.

The values for $(d\sigma/dt)_0$ from our experiment have been determined in a smooth way over the entire energy interval by a fit to the forward data using an empirical form which I will not describe here.[5] Figure 5b shows the differential cross section for the forward region together with the results of the fit. A slight shrinkage of the forward peak from 8.7 to 11.0 GeV^{-2} over the momentum range from 2.0 to 8.0 GeV/c is indicated by the fit.

The experimental values for $\left(\frac{d\sigma}{dt}\right)_0$ as a function of p_{LAB} are shown by the shaded region in Fig. 6 where the solid curve represents our experimental values for $\left(\frac{d\sigma}{dt}\right)_0$ and the dashed lines represent the uncertainty. The data given by the diamonds are from the recent transmission regeneration experiment by Darriulat et al.,[8] in which both K_S^0 regenerated events and $K_L^0 \to \pi^+\pi^-$ decay events were observed in a wire chamber spectrometer. The two experiments agree, but our experiment has much smaller error bars. The comparison of these two experiments makes good propaganda for bubble chamber techniques when one considers that Darriulat et al. obtained over two million triggers from which only about 500 $K_S^0 \to \pi^+\pi^-$
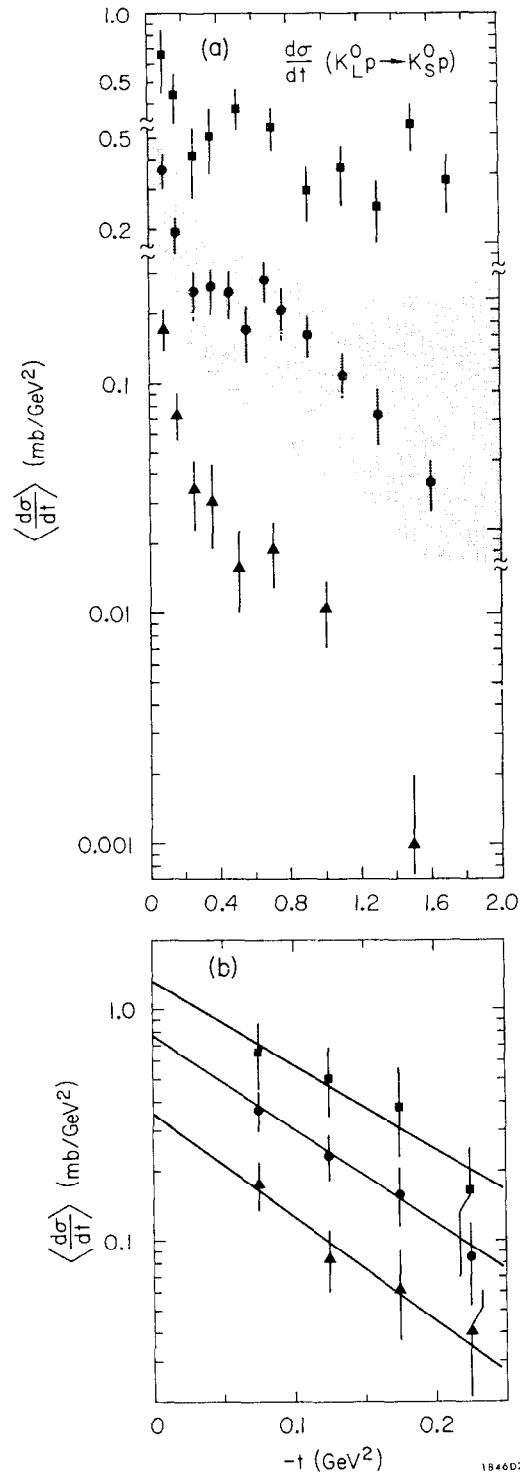
FIG. 5--Differential cross sections for $K^0_L p \to K^0_S p$. The data are averaged over three momentum intervals: $1.3 \leq p_{LAB} \leq 2.0$ GeV/c ($\blacksquare$); $2.0 \leq p_{LAB} \leq 4.0$ GeV/c ($\bullet$); $4.0 \leq p_{LAB} \leq 8.0$ GeV/c ($\blacktriangle$). (a) Full t region. Note the breaks in the ordinate scale as indicated by the shaded area. (b) Small t region. The curves result from a fit used to determine $(d\sigma/dt)_{t=0}$.

18-10
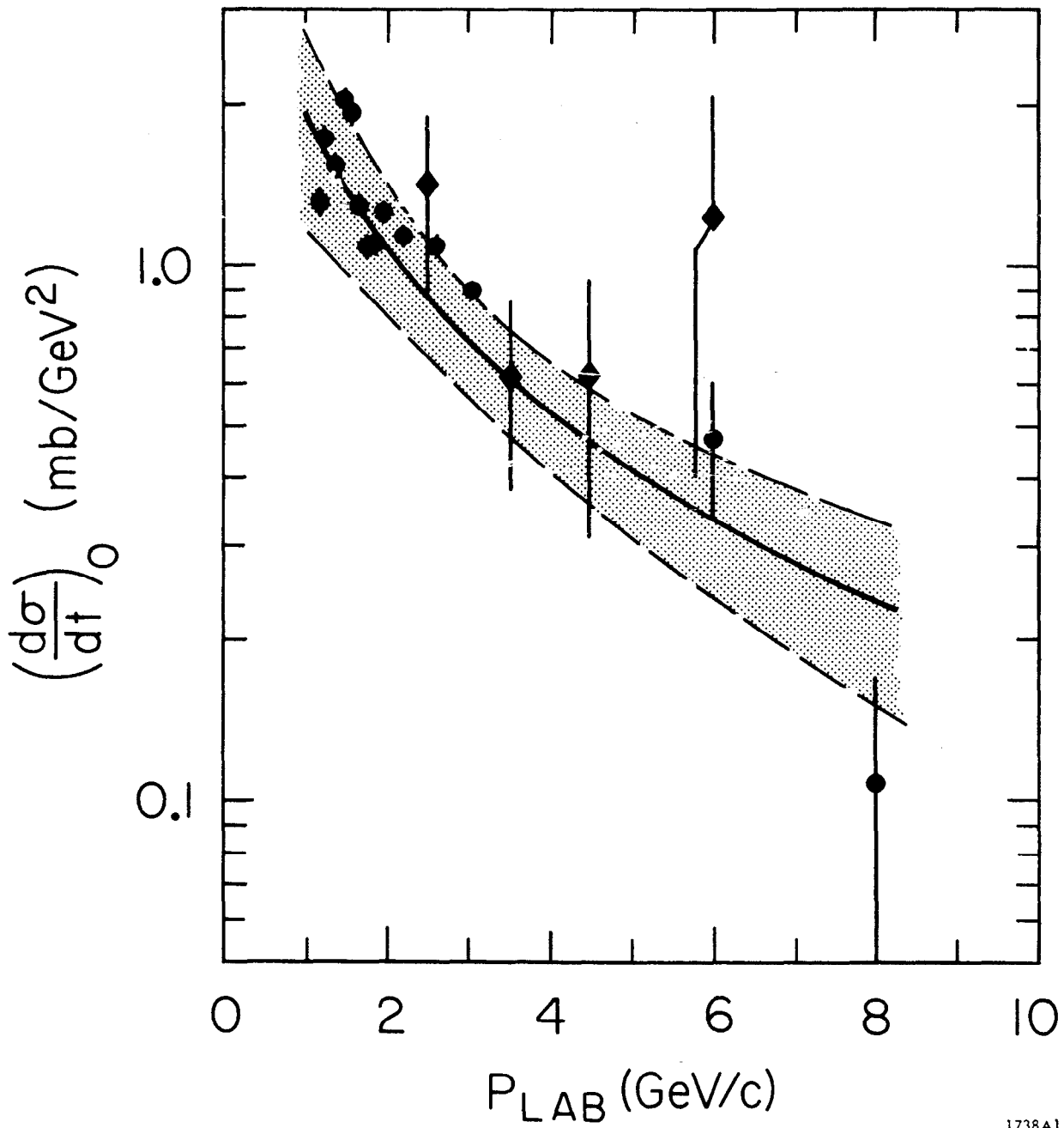
FIG. 6--Forward differential cross section for $K^O_L p \rightarrow K^O_S p$. The data are summarized by the smooth curve and the uncertainties by the dashed curves. For comparison, we show the results of Ref. 8 (▲) and the optical points (multiplied by a factor of two) calculated from the total cross sections of Ref. 9 (♦).

regenerated decays and 500 $K_L^O \to \pi^+\pi^-$ C P-violating decays were found. Thus the bubble chamber provides competitive event statistics and in addition observes the full t region for $K_L^O p \to K_S^O p$.

The phase of the forward amplitude is defined as

$$\phi = \tan^{-1} (\text{ImA}/\text{ReA}),$$

where $A(K_L^O p \to K_S^O p)$ is the forward amplitude. The SLAC experiment provides measurements of ϕ through the relation

$$\left| \frac{\text{ReA}}{\text{ImA}} \right| = \left\{ \left[\left(\frac{d\sigma}{dt}\right)_0 \bigg/ \left(\frac{d\sigma}{dt}\right)_{\text{OPT}} \right] - 1 \right\}^{1/2} ,$$

where

$$\left(\frac{d\sigma}{dt}\right)_0 = \frac{\pi}{k^2} \left[|\text{ReA}|^2 + |\text{ImA}|^2 \right] ,$$

$$\left(\frac{d\sigma}{dt}\right)_{\text{OPT}} = \frac{\pi}{k^2} |\text{ImA}|^2 ,$$

and

$$\text{ImA} \left(K_L^O p \to K_S^O p \right) = \frac{k}{8\pi} \left[\sigma_T(K^+n) - \sigma_T(K^-n) \right] .$$

The last expression follows simply from isospin invariance and the optical theorem.

If you look again at Fig. 6 you will find optical points (solid circles) computed from total cross section data[9] and multiplied by a factor of two. Since $\left(\frac{d\sigma}{dt}\right)_0$ and $2 \times \left(\frac{d\sigma}{dt}\right)_{\text{OPT}}$ agree well in magnitude it is clear that $|\text{ReA}/\text{ImA}| \approx 1$ over the entire momentum range. For an average value over the interval 1.3–8.0 GeV/c, we find

$$|\text{ReA}/\text{ImA}| = 0.82 \pm 0.20.$$

This ratio implies an average phase angle:

$$\phi = -(133 \pm 8)^{\text{O}} ,$$

and an average value for the intercept of the effective Regge trajectory:

$$\alpha(0) = 0.47 \pm 0.09 .$$

If ω exchange is assumed to dominate the forward amplitude,[4] $\alpha(0)$ may be identified with the ω trajectory intercept and is <u>consistent with a linear trajectory of unit slope passing through the physical ω mass.</u> The ρ exchange

contribution is expected to be small on the basis of SU(3) symmetry and should have only a minor influence on our determination of $\alpha(0)$ for the ω trajectory. In fact, if one writes $A = A_\rho + A_\omega$, then from SU(3) one finds

$$\frac{A_\rho}{A_\omega} \simeq - \frac{(1 + d/f)}{(3 - d/f)} \,,$$

where d/f is the ratio of the symmetric to antisymmetric nonflip couplings at the baryon vertex. The d/f ratio is generally believed to be such that $|A_\rho/A_\omega| \sim 20\%$. I shall return to the d/f ratio again shortly since the SLAC experiment determines a new measurement of this ratio by a comparison to $\pi^- p$ charge exchange.

Let us turn now to theoretical descriptions of the reaction $K_L^0 p \to K_S^0 p$. We have analyzed our data in terms of two distinctly different Regge models. The first is the model of Ahmadzadeh and Kaufmann [10] (hereafter called AKM) and the second is the strong cut Regge absorption model (SCRAM).[11] Both have been successful in describing $\pi^- p$ charge exchange as well as other reactions and we have extended these models to $K_L^0 p \to K_S^0 p$.[12] Briefly, both models involve the exchange of primary trajectories (mainly ω with a small admixture of ρ), and both require "secondary" effects to adequately describe the experimental data. However, the secondary effects are presumed to have completely different origins: in AKM they are due to lower lying Regge trajectories (ω' and ρ') whereas in SCRAM they are caused by absorptive cut corrections. I might add that we have unsuccessfully tried simpler models involving only the exchange of leading Regge trajectories. Just as for $\pi^- p$ charge exchange, the simple Regge pole models seem to be unable to provide good detailed descriptions.

The results of the fits are compared to the data in Figs. 7 and 8 where the solid (dashed) curves refer to AKM (SCRAM). The parameters of the fits[12] were determined from the SLAC data in the interval 2-7 GeV/c. The differential cross sections (Fig. 7) are well described by both models. Even below 2 GeV/c, where s-channel resonances are expected to be important, good agreement is found for $|t| \gtrsim 1.0$ GeV^2. The forward differential cross sections below 10 GeV/c are well reproduced both in magnitude and in energy dependence (Fig. 8a). For comparison to the preliminary high energy measurements from Serpukhov[7] the models have been extrapolated to 50 GeV/c
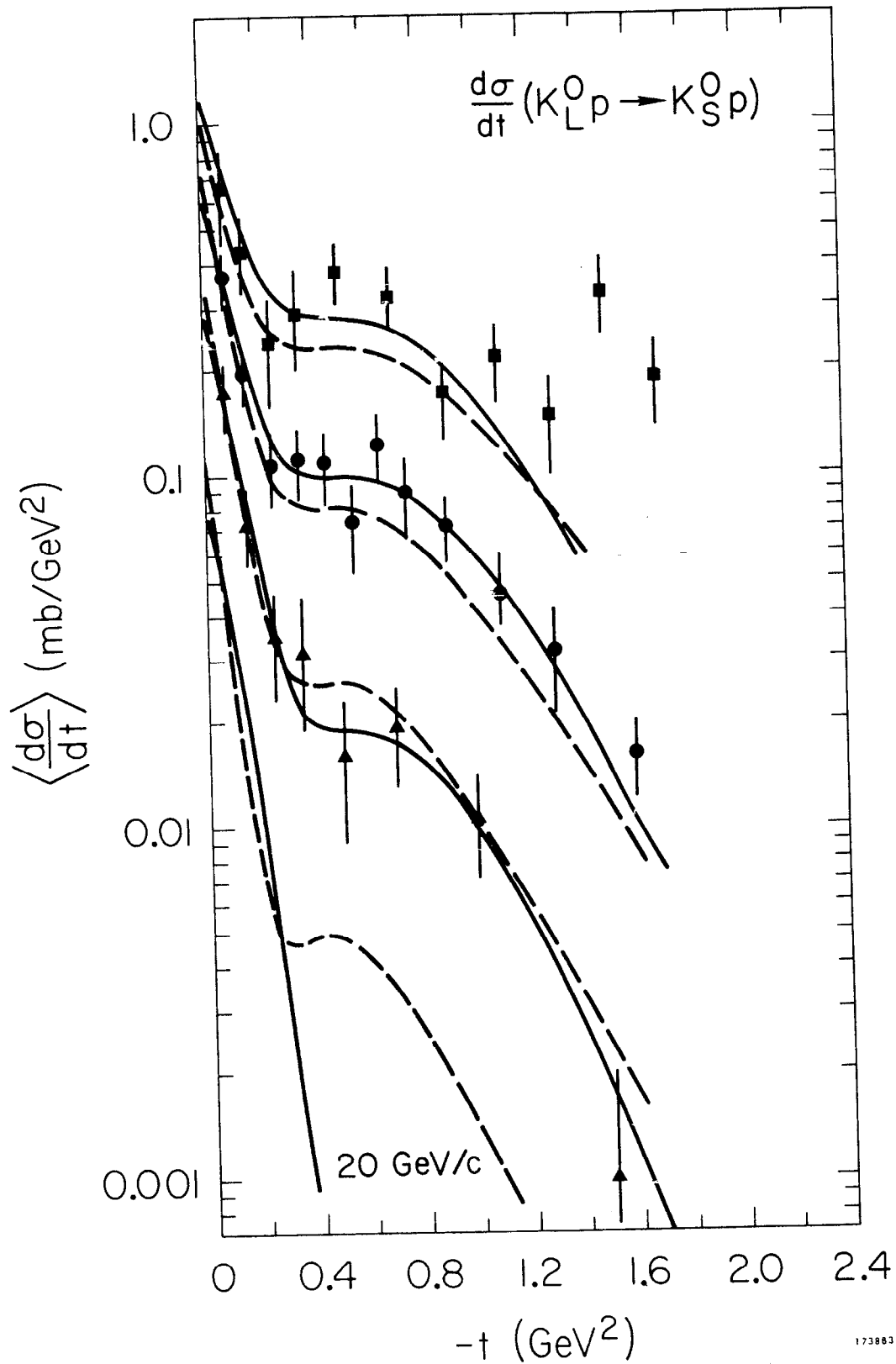
FIG. 7—Comparison of theoretical models to $d\sigma/dt\,(K_L^0 p \rightarrow K_S^0 p)$. The solid (dashed) curves here and in Fig. 8 are the result of a fit with the AKM (SCRAM) model (see text).
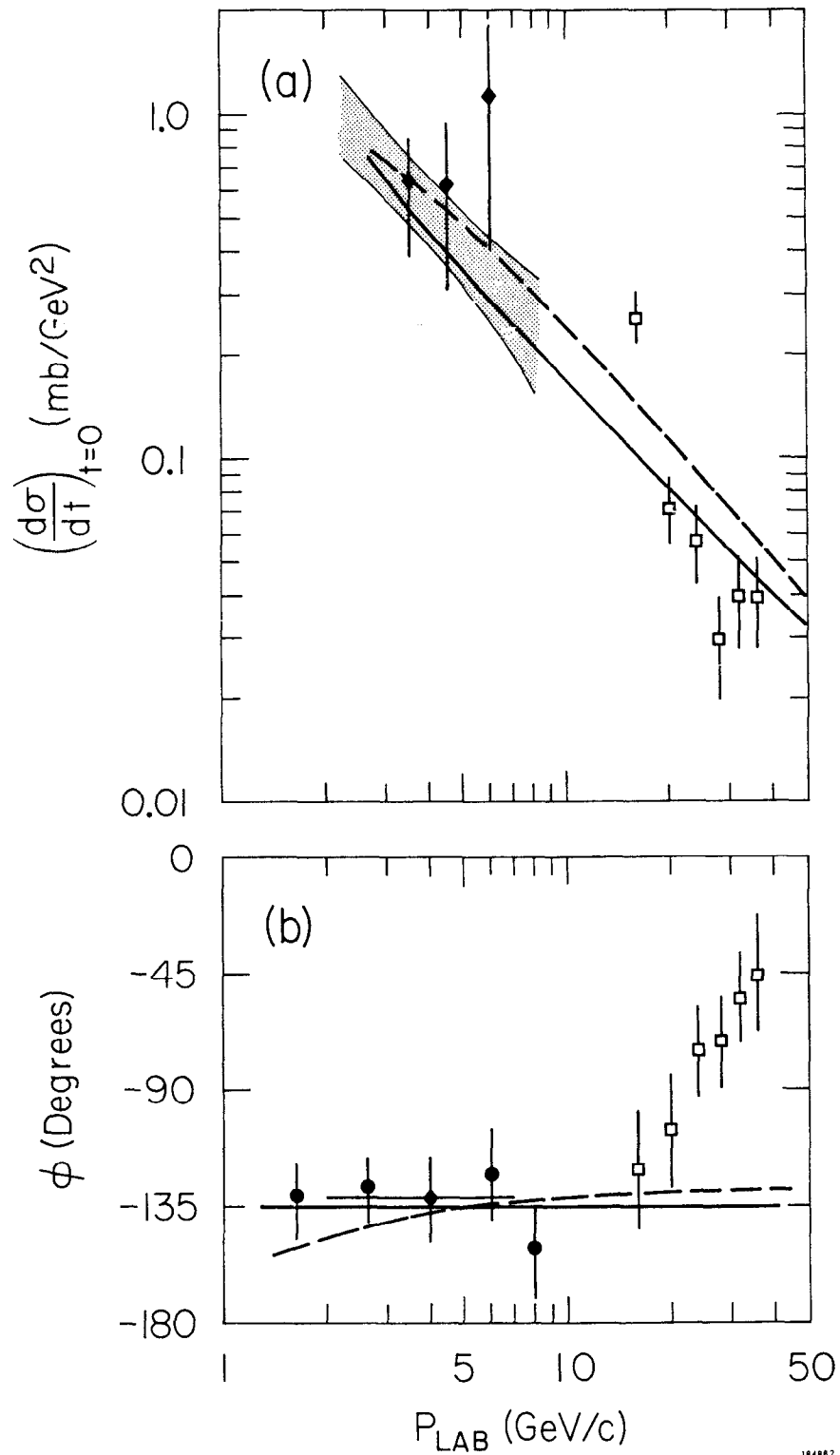
FIG. 8—(a) Forward differential cross section for $K_L^0 p \rightarrow K_S^0 p$. The results of the Regge model fits for $2 \leq p_{LAB} \leq 7$ GeV/c are extrapolated to 50 GeV/c. The data are from SLAC (shaded region), Ref. 8 ($\blacklozenge$), and Ref. 7 (ϕ). (b) Phase of the forward amplitude. The SLAC data are shown by solid circles ($\blacklozenge$).

and are found to be consistent with the data. The phase of the forward amplitude (Fig. 8b) also is well fitted below 10 GeV/c, but the extrapolations of the models to high energy are clearly incompatible with the measured phases. My personal prejudice on the matter is that the final values for ϕ at high energy will come into line with the low energy measurements. If, however, the preliminary Serpukhov results are confirmed, the validity of most Regge models, including AKM and SCRAM, will be in serious doubt,[13] and we will have a very interesting situation indeed.

Both models give equally good descriptions of $K_L^0 p \to K_S^0 p$ below 10 GeV/c and we cannot favor one over the other. Measurements of $d\sigma/dt$ in the vicinity of 20 GeV/c or higher will certainly be helpful in evaluating the models.

Finally, the forward cross sections for $K_L^0 p \to K_S^0 p$ and $\pi^- p \to \pi^0 n$[14] may be used to find a value for the SU(3) f/d ratio for the coupling of vector mesons to baryons. The experimental values for the forward differential cross sections for the two reactions are consistent with equality for all available data, as shown in Fig. 9. The ratio

$$R \equiv \left[\frac{d\sigma}{dt} (K_S^0 p) \, / \, \frac{d\sigma}{dt} (\pi^0 n) \right]_{t=0}$$

is found to have an average value of 0.91 ± 0.12. The f/d ratio may be expressed in terms of the experimental value of R. The value obtained is shown in Fig. 10 along with a synopsis of other values which have appeared in the literature. It is no surprise to find that f/d is somewhat model dependent. Nevertheless, the available estimates are all consistent with a value in the vicinity of -4 to -8.

4. The Reaction $\bar{K}^0 p \to \Lambda \pi^+$

Figure 11 shows the values for $\sigma(\bar{K}^0 p \to \Lambda \pi^+)$ versus p_{LAB}. Good agreement is found with the values for $\sigma(K^- n \to \Lambda \pi^-)$ and $2 \times \sigma(K^- p \to \Lambda \pi^0)$. The model of Sarma and Reeder[18] predicts values which are too low by a factor of two or three.

The differential cross section, averaged over three different momentum intervals is shown in Fig. 12. The main feature to note here is that the forward peak shrinks as energy increases, although we certainly need more events to reduce the errors.
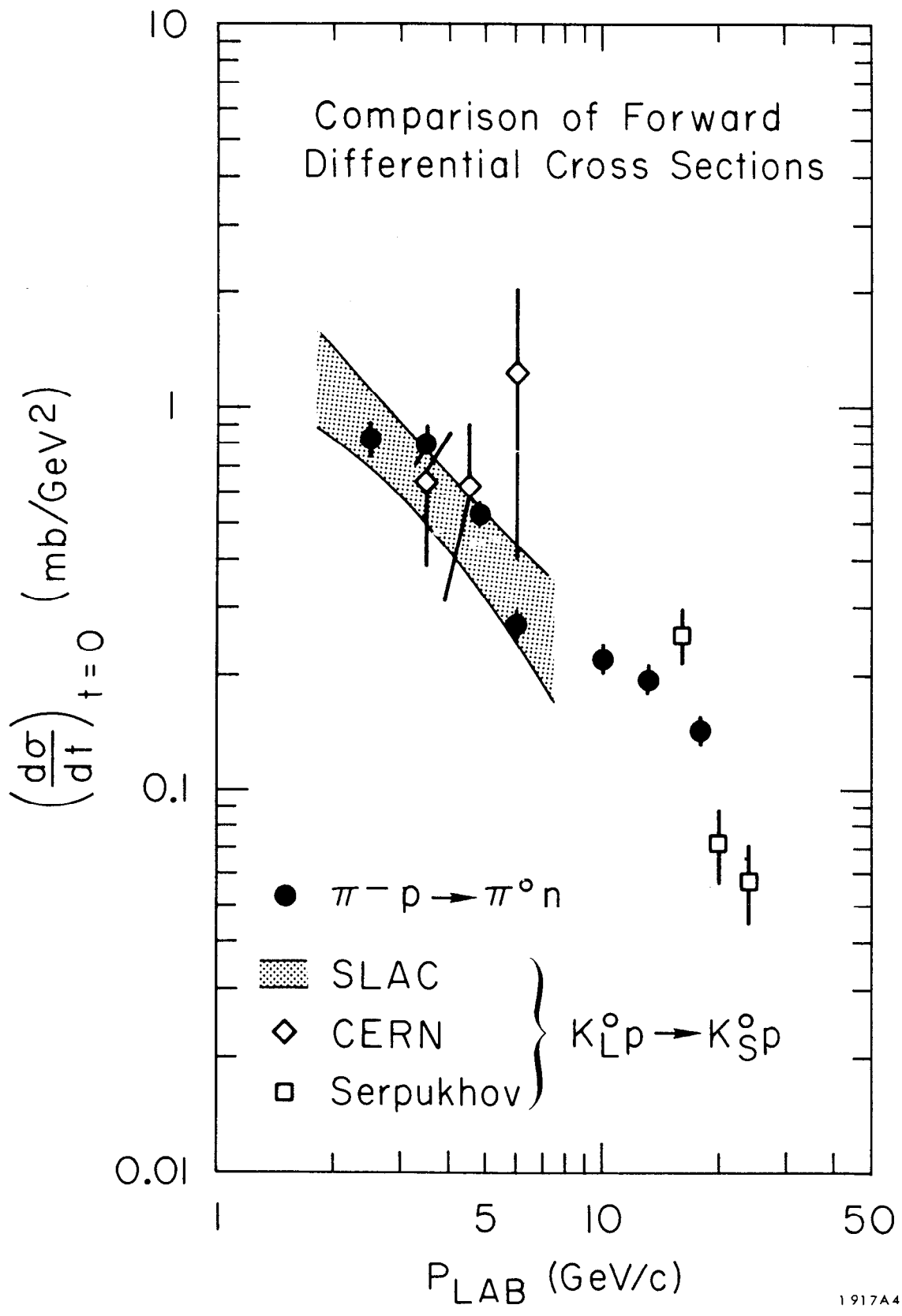
FIG. 9--Comparison of forward differential cross sections for $K_L^o p \rightarrow K_S^o p$ and $\pi^- p \rightarrow \pi^o n$.

Technique	Value	Reference
$f/d = \dfrac{1 + \sqrt{2R}}{1 - \sqrt{2R}}$ $R = \left[\dfrac{\dfrac{d\sigma}{dt}\ (K^0_L p \to K^0_S p)}{\dfrac{d\sigma}{dt}\ (\pi^- p \to \pi^0 n)}\right]_{t=0}$	$-6.8\ ^{+1.3}_{-2.0}$	12
$f/d = \dfrac{\Delta\sigma(\pi p) + \Delta\sigma(KN)}{\Delta\sigma(\pi p) - \Delta\sigma(KN)}$ $\Delta\sigma(\pi p) = \sigma_T(\pi^- p) - \sigma_T(\pi^+ p)$ $\Delta\sigma(KN) = \sigma_T(K^- n) - \sigma_T(K^+ n)$	-3 to -5	15
Regge Analysis of $K^0_L p \to K^0_S p$ and $\pi^- p \to \pi^0 p$: $\quad$ AKM $\quad$ SCRAM	-7 $\left\{\begin{array}{l}-2.1\ \text{Sol. I}\\ -3.5\ \text{Sol. II}\end{array}\right\}$	10, 12 11, 12
Regge Analysis of σ_T for πN, KN, and NN	-2.0 ± 0.4	16
Regge Analysis of $\pi N \to YK$ and $\overline{K} N \to Y\pi$	-11	17

FIG. 10--Summary of f/d determinations for nonflip coupling of vector mesons to baryons.
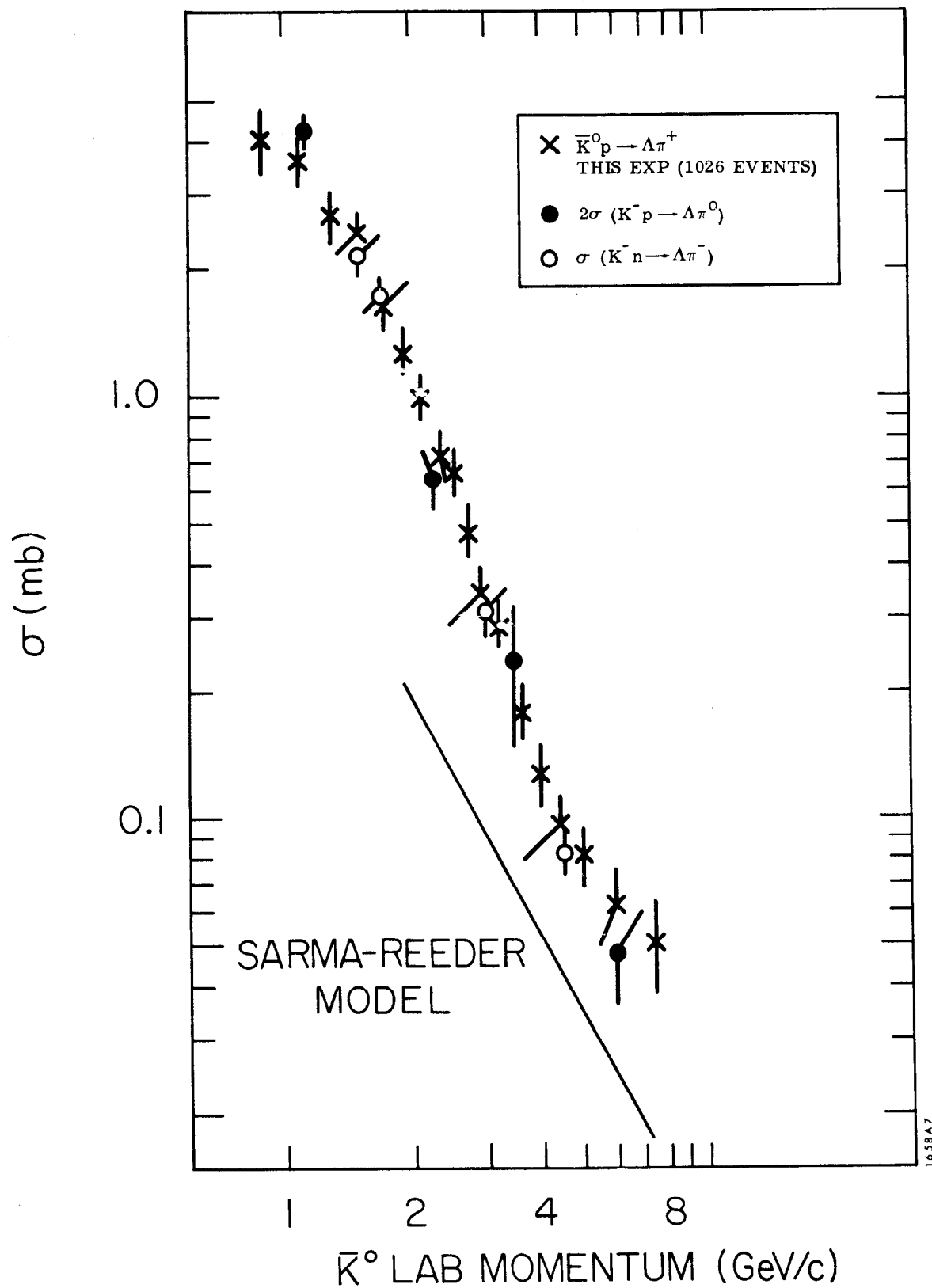
FIG. 11--Cross section for $\bar{K}^0 p \rightarrow \Lambda \pi^+$ versus p_{LAB}. The curve is the prediction of Ref. 18.
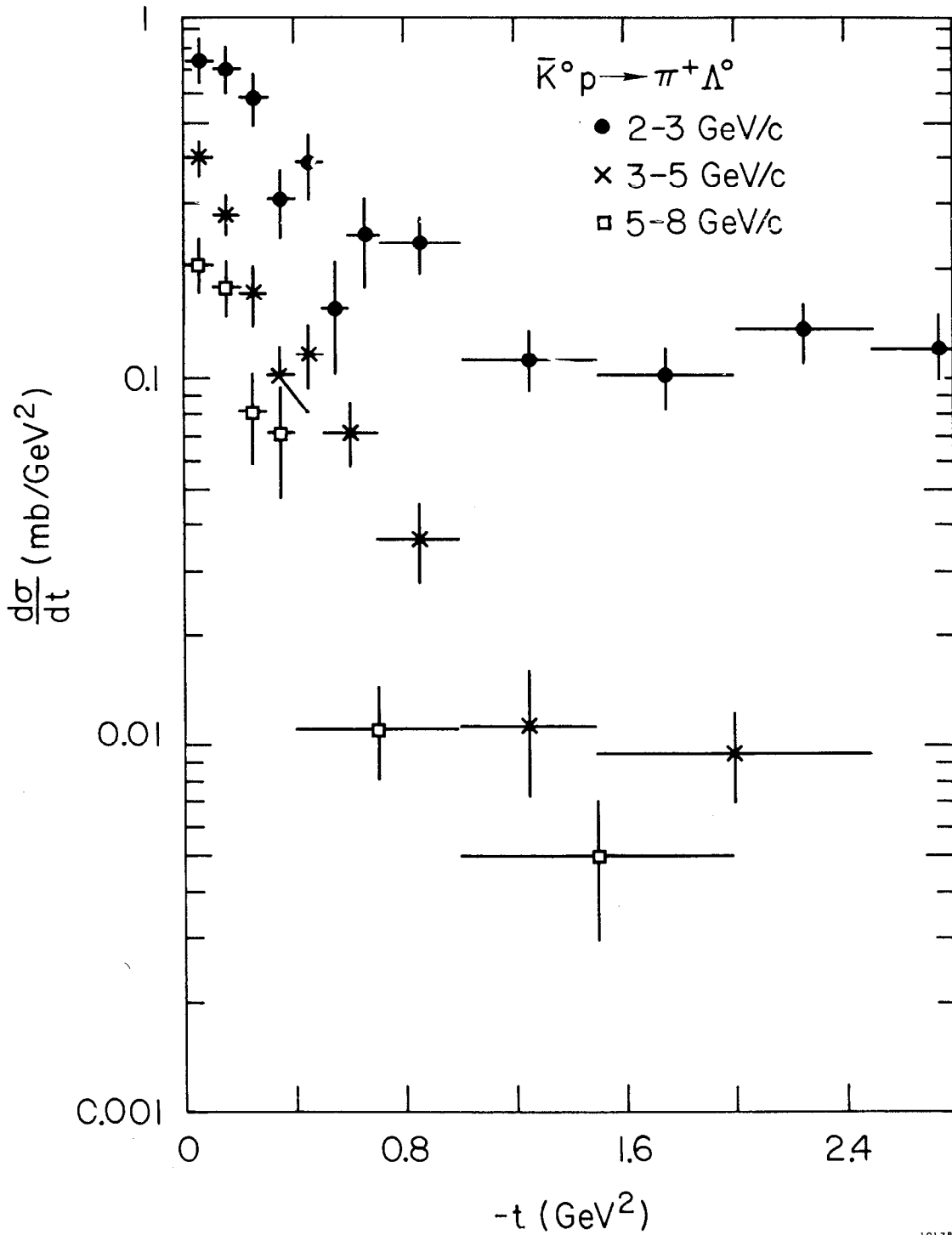
FIG. 12—Differential cross sections for $\bar{K}^o p \to \Lambda \pi^+$ averaged over momentum intervals: $2 < p_{LAB} < 3$ GeV/c ($\bullet$), $3 < p_{LAB} < 5$ GeV/c ($*$), $5 < p_{LAB} < 8$ GeV/c ($\square$).

By comparing $\overline{K} N \rightarrow \Lambda \pi$ and the line-reversed $\pi N \rightarrow K \Lambda$ reactions, one can test the ideas of exchange degeneracy (EXD) of the K^* and K^{**} trajectories. The weak form of EXD predicts equal differential cross sections for these two reactions. Lai and Louie[19] have shown that at low energies the EXD hypothesis does not work very well, as is illustrated in Fig. 13, which shows an average slope parameter of ~ 8 GeV^{-2} for $\pi N \rightarrow K \Lambda$ and ~ 4 GeV^{-2} for $\overline{K} p \rightarrow \Lambda \pi$. Since the SLAC data indicate shrinkage one finds the intriguing possibility that EXD may be working better above about 5 GeV/c. However, $\sigma(\overline{K} N \rightarrow \Lambda \pi)$ still seems larger than $\sigma(\pi N \rightarrow K \Lambda)$ by a factor of 1.5 to 2.0 at 6 GeV/c, so this is a definite problem for EXD.

The Λ polarizations, shown in Fig. 14, are large and positive away from the forward region both at low energy and at high energy. The SLAC polarizations are in agreement with the published polarization measurements for $K^- n \rightarrow \Lambda \pi^-$. The Sarma-Reeder model is seen to fail for $|t| > 0.3$ GeV^2.

We have not made very much effort as yet to fit the data with other models that might work (such as AKM or SCRAM) since the data are in a rather preliminary form. In the near future we expect to have good experimental measurements across a wide momentum interval for both $\overline{K}^0 p \rightarrow \Lambda \pi^+$ and $\overline{K}^0 p \rightarrow \Sigma^0 \pi^+$. Taken together, these data should provide a rigorous challenge to any model which employs K^* and K^{**} exchange.

5. Reactions $K^0 p \rightarrow K^+ \pi^- p$ and $\overline{K}^0 p \rightarrow K^- \pi^+ p$

Cross sections for the three body $K \pi p$ production are shown in Fig. 15. The negative strangeness state has a slightly larger cross section but the two seem to be approaching one another for $p_{LAB} \sim 10$ GeV/c. Good agreement is found with cross section measurements from $K^\pm n$ experiments.[20] Let me remind you that the SLAC experiment has exactly equal components of positive and negative strangeness in the beam so that there can be no systematic error between the two cross sections arising from beam normalization problems.

These final states provide data on $K^{*0} p$, $\overline{K}^{*0} p$ and $\Delta^{++} K^-$ production across a wide momentum interval. Figure 16 gives the cross sections for $\sigma(\overline{K}^{*0} p)$ and $\sigma(K^{*0} p)$ along with available values from $K^\pm n$ experiments.[20] Note that the cross sections for S = -1 clearly exceed those for S = +1 in contrast to what has been found for other pairs of particle and antiparticle
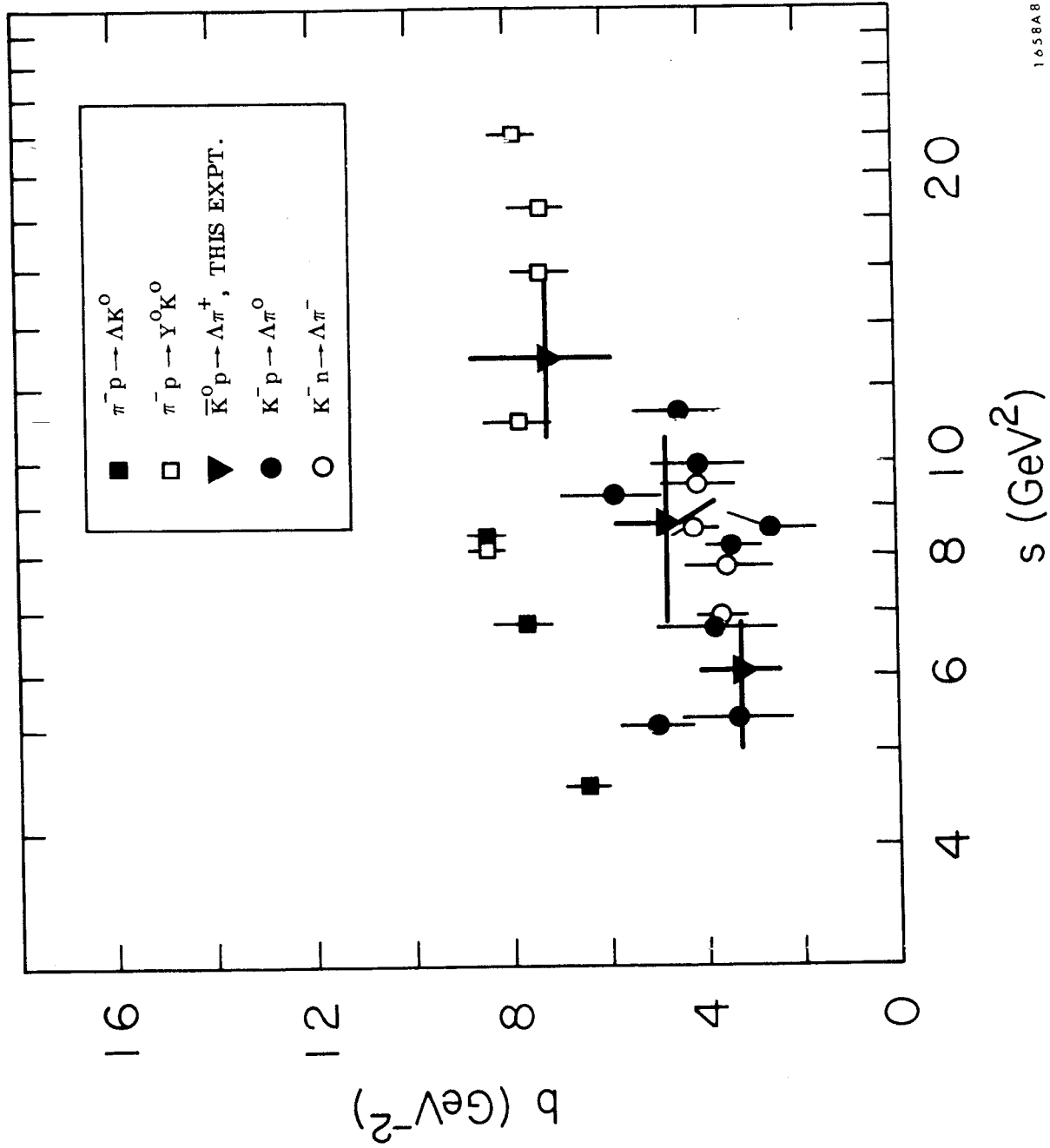
FIG. 13-- Exponential slope parameters of the forward differential cross sections from $\pi N \to KY$ and $\bar{K}N \to Y\pi$ reactions.
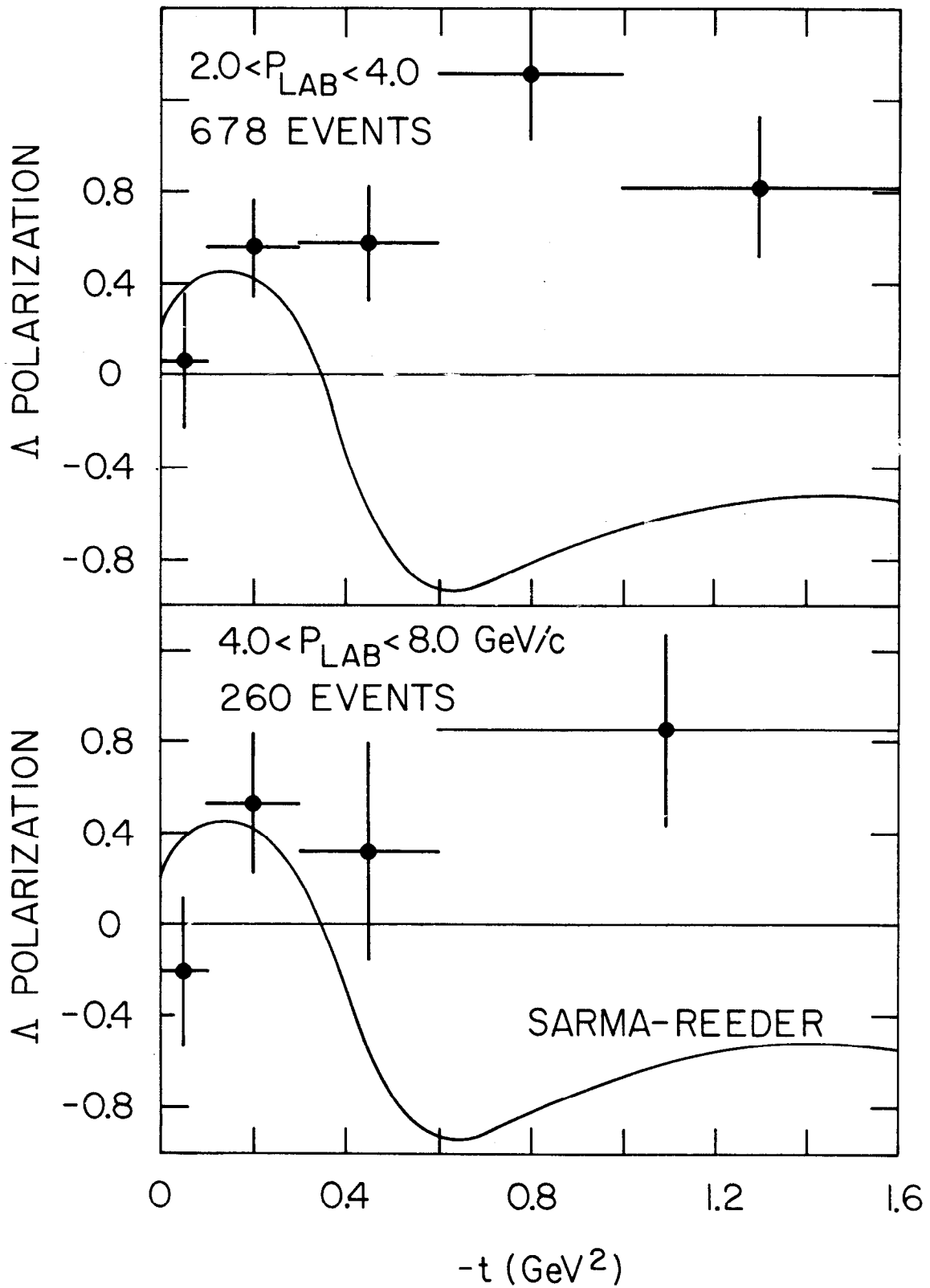
FIG. 14--Polarization of Λ in $\bar{K}^0 p \rightarrow \Lambda \pi^+$ averaged over the indicated momentum intervals. The curves are predictions from Ref. 18.
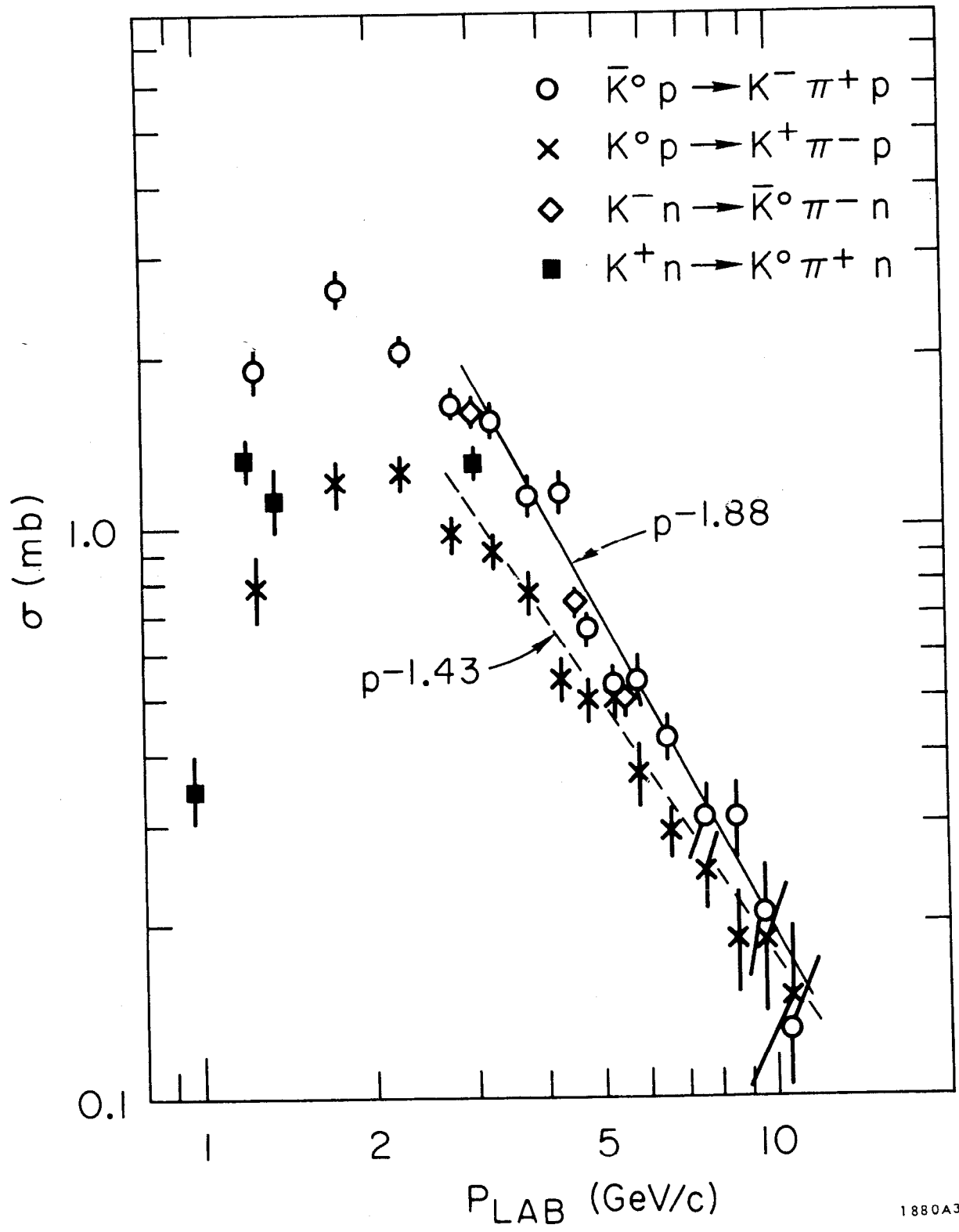
FIG. 15--Cross sections versus p_{LAB} for $\bar{K}\, p \to K^- \pi^+ p$ and $K\, p \to K^+ \pi^- p$.
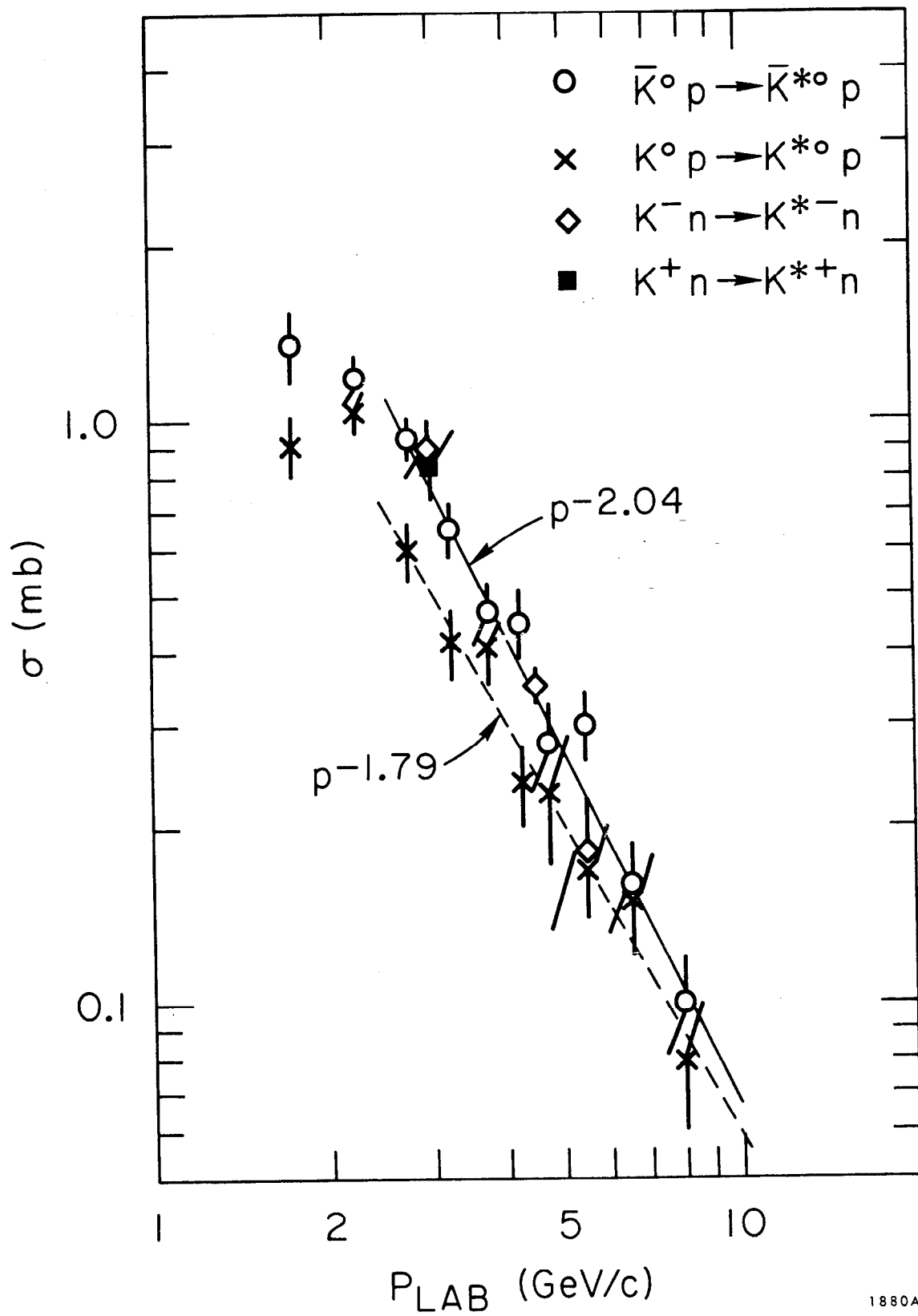
FIG. 16--Cross sections versus p_{LAB} for $K^{*0}p$ and $\bar{K}^{*0}p$ production.

1880A1

18-25

cross sections. Harari[21] has suggested that the antiparticle reactions must have the smaller cross sections because absorption is larger than for the particle reaction. The SLAC data upset this simple scheme especially at low p_{LAB}. The situation is more dramatically summarized by Fig. 17 where I have plotted all available $K^{*+}p$,[22] $K^{*-}p$,[23] $K^{*0}p$, and $\bar{K}^{*0}p$ cross sections multiplied by p_{LAB}^2. All four reactions were fitted to the form $\sigma = A\, p_{LAB}^{-n}$, where a common value for n was assumed for all reactions. The fitted curves indicate $\sigma(K^{*+}p)/\sigma(K^{*-}p) \simeq \sigma(\bar{K}^{*0}p)/\sigma(K^{*0}p) \simeq 1.4$, and $\sigma(K^{*+}p)/\sigma(K^{*0}p) \simeq 2.2$. I know of no explanation for these curious ratios. There should be no relative error between the $K^{*0}p$ and $\bar{K}^{*0}p$ points, but because the SLAC $K\pi p$ data is rather preliminary there may be systematic errors of $\sim 20\%$ between the neutral and charged K^* data.

The differential cross section and density matrix elements for K^* production, averaged over two momentum intervals, are presented in Figs. 18-19. The curves are predictions of Dass and Froggatt[24] based on a Regge fit to $K^{\pm}p$ data. The model gives good predictions for the shape and magnitude of $d\sigma/dt$, except that it predicts $\frac{d\sigma}{dt}(K^{*0}p) > \frac{d\sigma}{dt}(\bar{K}^{*0}p)$, contrary to experiment. The density matrix elements are in good agreement with other K^*N data and show evidence for unnatural spin-parity exchange (presumably π) for low t and natural spin-parity exchange (ω) for high t.

The reaction $\bar{K}^0 p \to K^- \Delta^{++}$ is an interesting reaction for the study of EXD for ρ and A_2 trajectories. Figure 20 presents the cross section versus p_{LAB} for this reaction along with available data on the companion line-reversed reaction, $K^+ p \to K^0 \Delta^{++}$.[22] The values for $\sigma(K^0 \Delta^{++})$ are about 20 percent greater than $\sigma(K^- \Delta^{++})$ on the average, in fair agreement with EXD. The differential cross section, shown in Fig. 21 has nearly the same forward slope parameter $(b = 4.0 \pm 0.5 \text{ GeV}^{-2})$ as found for $K^+ p \to K^0 \Delta^{++}$. Thus the EXD idea may be working fairly well for this pair of reactions, though not perfectly. The density matrix elements are given in Fig. 22. Note that they are consistent with the M1 dominance concept of Stodolsky and Sakurai[25] away from t=0 (the predicted values are $\rho_{33} = 0.375$, Re $\rho_{3-1} = 0.21$, Re $\rho_{31} = 0$). The solid curves imposed on Figs. 21-22 are predictions from a Regge model due to Krammer and Maor.[26] The model employs (nondegenerate) ρ and A_2 trajectories with the parameters determined by fits to the reactions

COMPARISON OF K* (890) PRODUCTION

$$\sigma_i = A_i \, P_{LAB}^{-n}$$

$$n = 2.00 \pm 0.10$$

$K^+ p \rightarrow K^{*+} p$
A = 11.9 ± 1.3

$K^- p \rightarrow K^{*-} p$
A = 8.7 ± 0.8

$\bar{K}^0 p \rightarrow \bar{K}^{*0} p$
A = 7.0 ± 0.7

$K^0 p \rightarrow K^{*0} p$
A = 4.8 ± 0.5

(y-axis) $P_{LAB}^2 \cdot \sigma \, (K^* p)$ mb $(GeV/c)^2$

(x-axis) P_{LAB} (GeV/c)

1880810
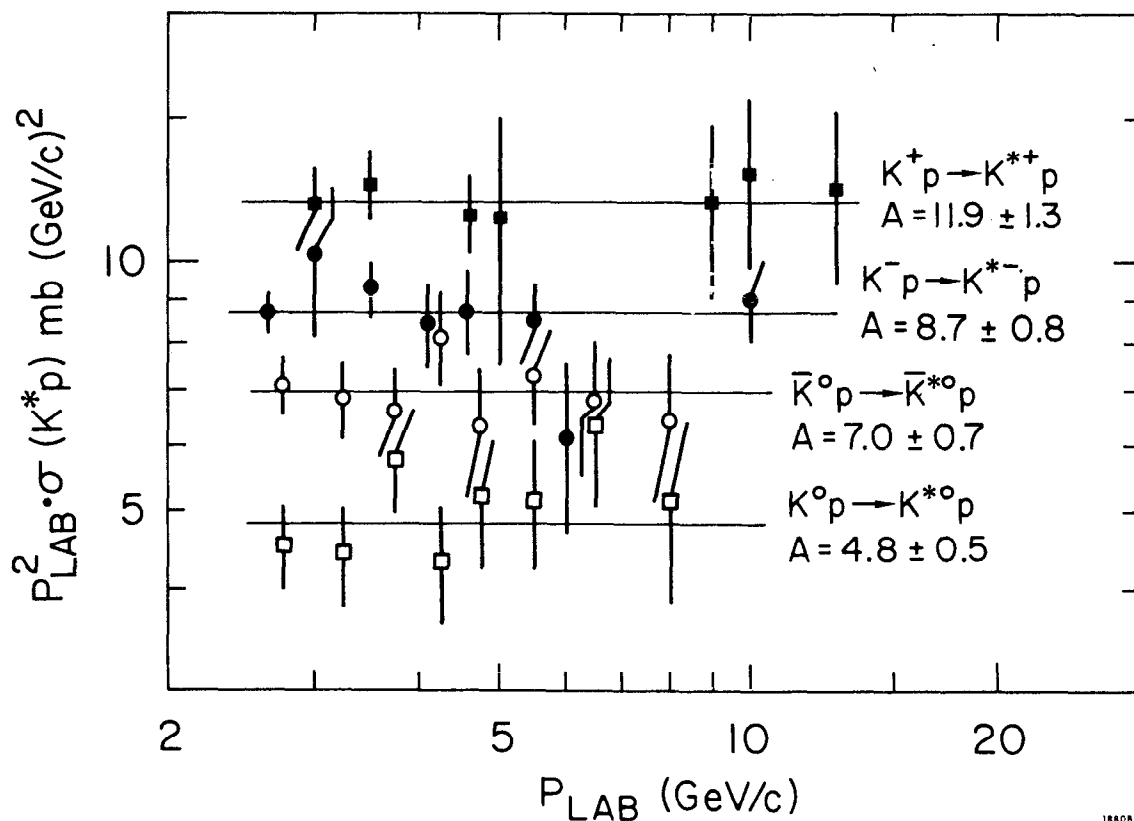
FIG. 17--Comparison of K*p cross sections produced through neutral
exchange. For ease of illustration the cross sections have
been multiplied by p_{LAB}^2.

18-27
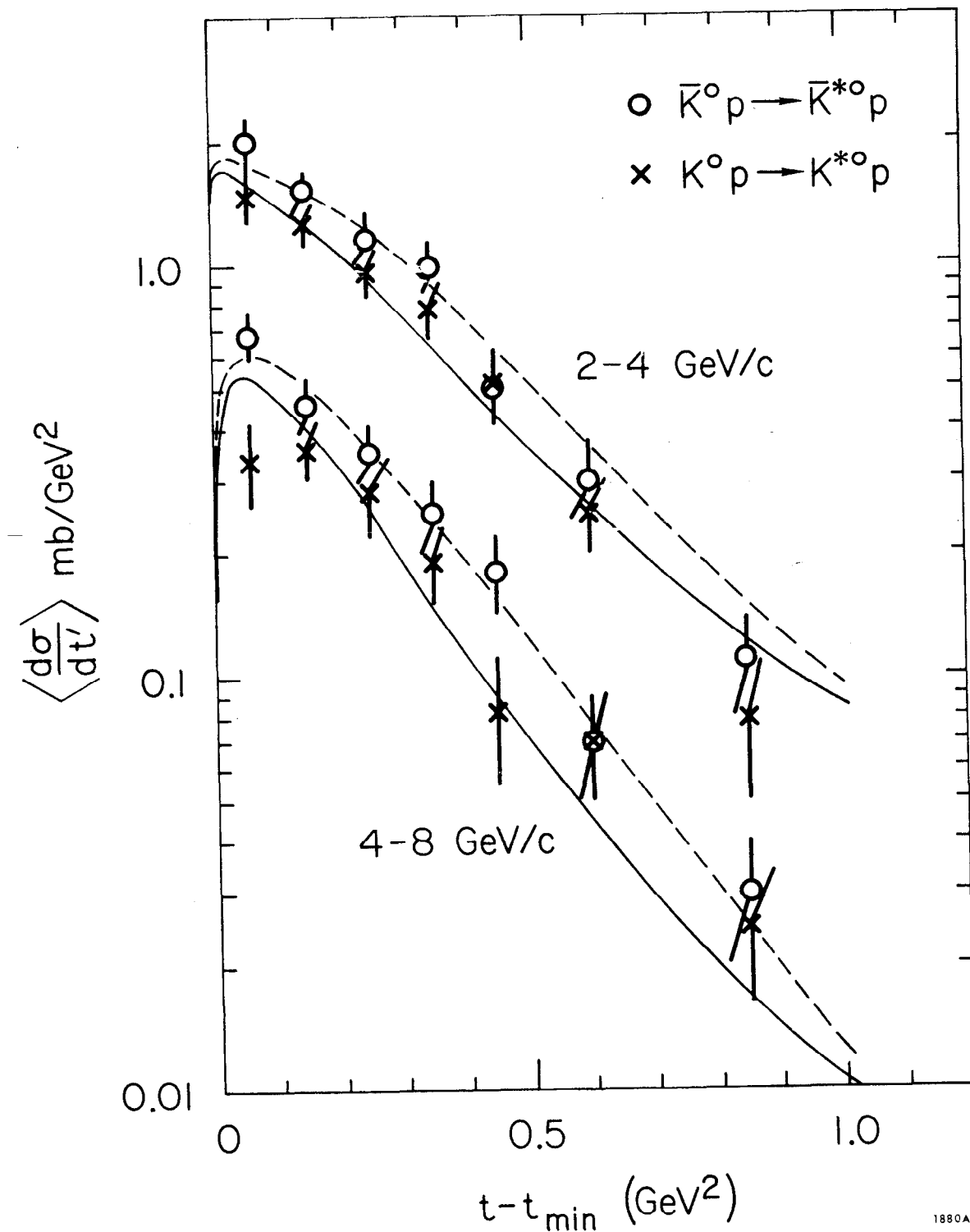
FIG. 18--Differential cross section versus p_{LAB} for $\bar{K}^{*0}p$ and $K^{*0}p$ production averaged over the indicated p_{LAB} intervals. The curves in this and the following figure are predictions of Ref. 24 (dashed curve, $K^{*0}p$; solid curve, $\bar{K}^{*0}p$).
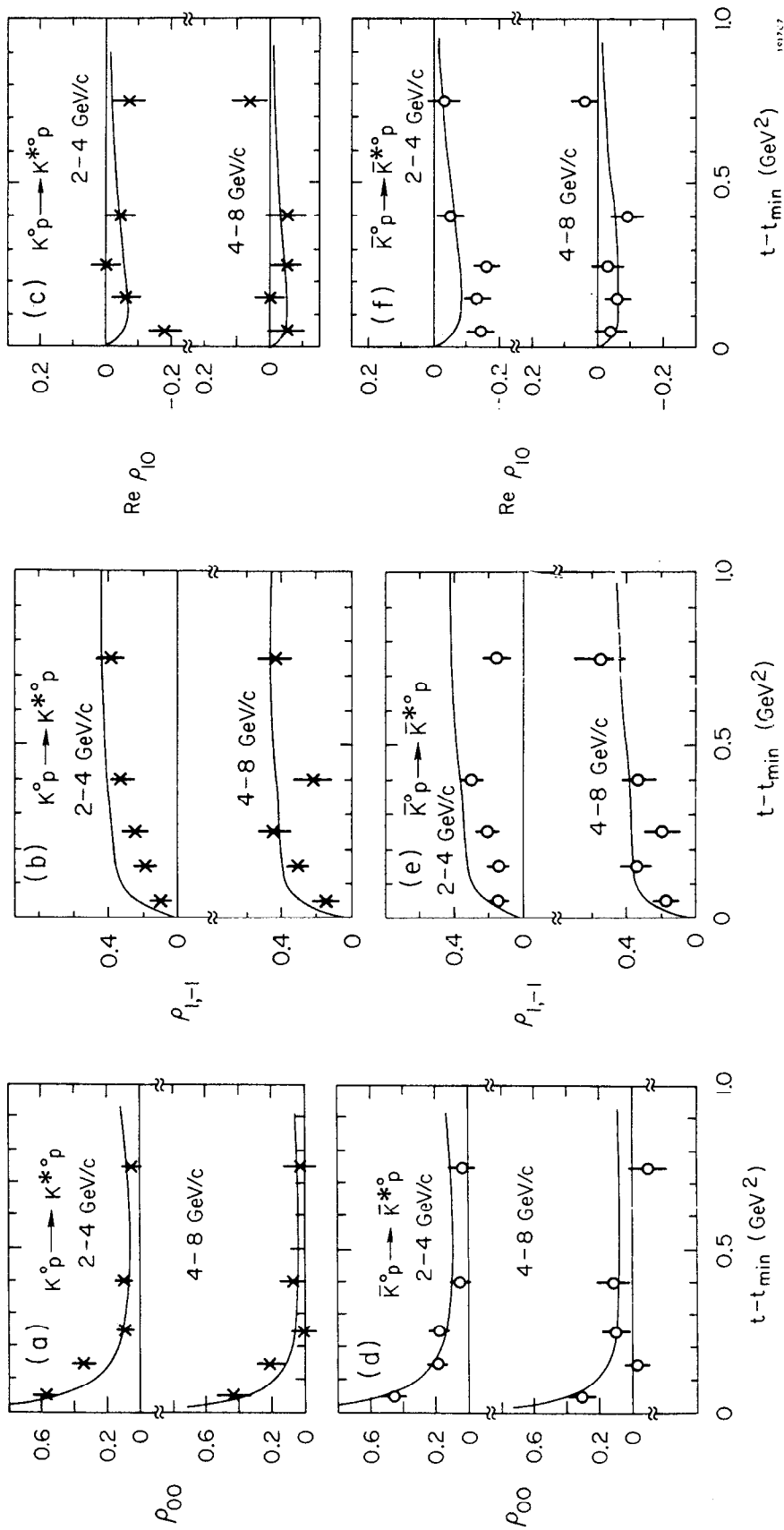
FIG. 19--Density matrix elements for K* production in the Gottfried-Jackson frame. (a)-(c) $K^{*0}p$, (d)-(f) $\bar{K}^{*0}p$.
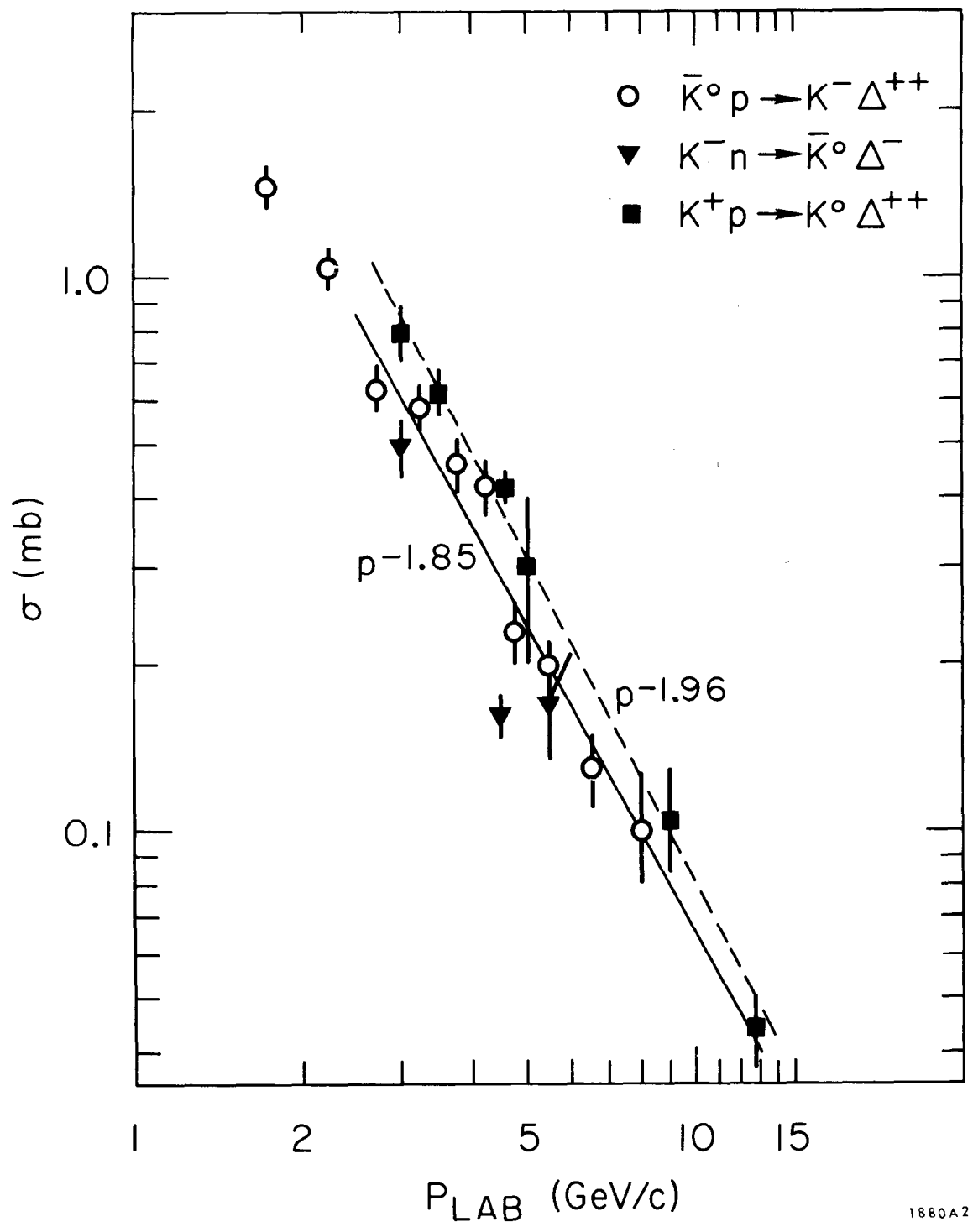
FIG. 20--Cross section versus p_{LAB} for $\bar{K}^0 p \to K^- \Delta^{++}$ compared to the line-reversed reaction $K^+ p \to K^0 \Delta^{++}$.
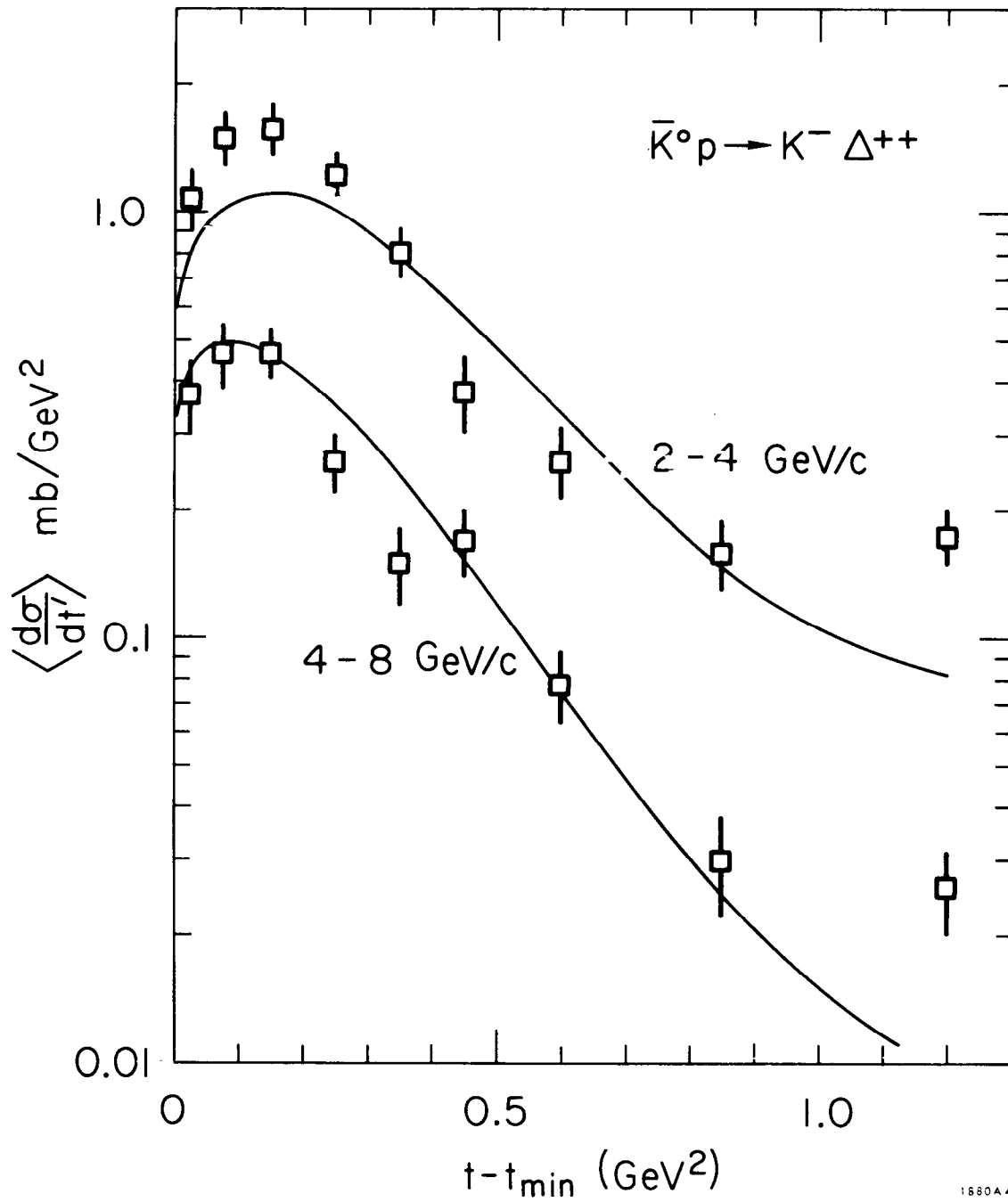
FIG. 21--Differential cross section for $\bar{K}^0 p \rightarrow K^- \Delta^{++}$ averaged over the indicated momentum intervals. The curves in this and the following figure are from Ref. 26.
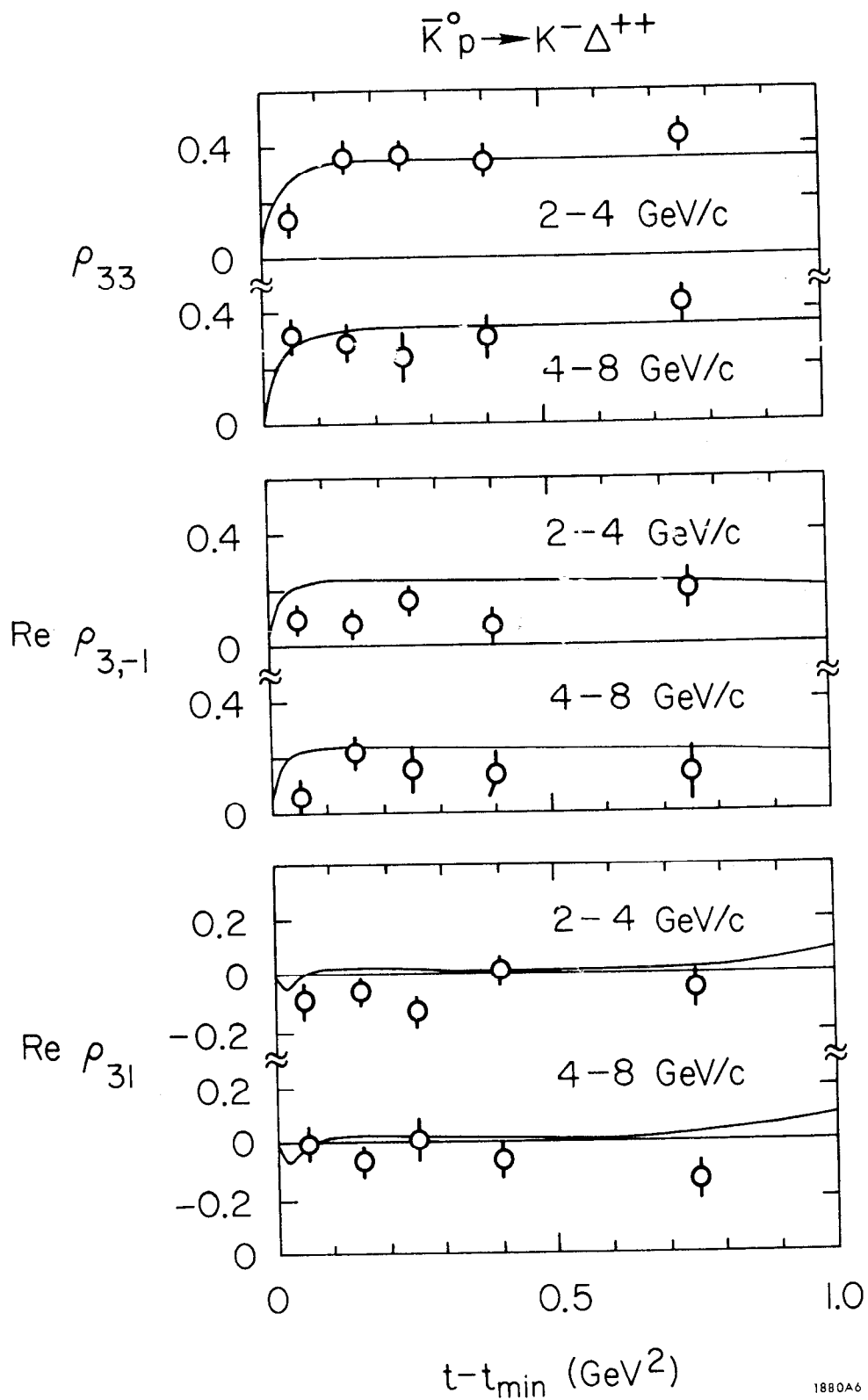
FIG. 22--Density matrix elements in the Gottfried-Jackson frame for
$\bar{K}^0 p \rightarrow \Delta^{++} K^-$ averaged over the indicated momentum intervals.

$K^+p \rightarrow K^o \Delta^{++}$ and $\pi^+p \rightarrow \pi^o\Delta^{++}$. The predictions are quite good for both $d\sigma/dt$ and ρ_{ij} except that the predicted cross section falls a little too slowly with energy.

6. The Reaction $K^o_L \rightarrow K^o_S p\pi^+\pi^-$

Our analysis on this reaction is quite preliminary as yet so I will show only a glimpse of our results on Q^op and $\overline{Q}^o$p production. In Fig. 23 we see the $K^o_S\pi^+\pi^-$ mass spectrum summed from 2 to 12 GeV/c excluding Δ^{++} events (1130-1340 MeV). The characteristic Q enhancement at low mass having a width of 300–400 MeV is observed. There is no evidence for L production. The mass plot is divided into four p_{LAB} regions in Fig. 24 and an additional cut on the proton momentum transfer ($\Delta^2_{p \rightarrow p} < 0.6$ GeV^2) is imposed. Aside from phase space changes, the mass spectrum looks very much the same at all energies. With more events, we hope to be able to answer some questions concerning the energy dependence of the mass spectrum in the Q region.

As has been noted at this conference[27] there seems to be an indication that $\sigma(K^+p \rightarrow Q^+p)$ is greater than $\sigma(K^-p \rightarrow Q^-p)$. Our data on this question show equal values for $\sigma(Q^o p)$ and $\sigma(\overline{Q}^o p)$ as illustrated by Fig. 25, where the $K^o_S\pi^+$, $K^o_S\pi^-$, and $\pi^+\pi^-$ mass spectra are shown for events from the Q region (1050 < $K^o_S\pi\pi$ < 1450 MeV). The SLAC experiment has a clear advantage on the cross section question since we have equal S = +1 and S = -1 components in the beam.

We are proceeding on the analysis of the Q events. We are particularly interested in whether the forward slopes of Q^op and $\overline{Q}^o$p are similar to those for K^+p and K^-p elastic scattering. But we have to compile more statistics and carefully analyze our data before we can say much more on this topic.
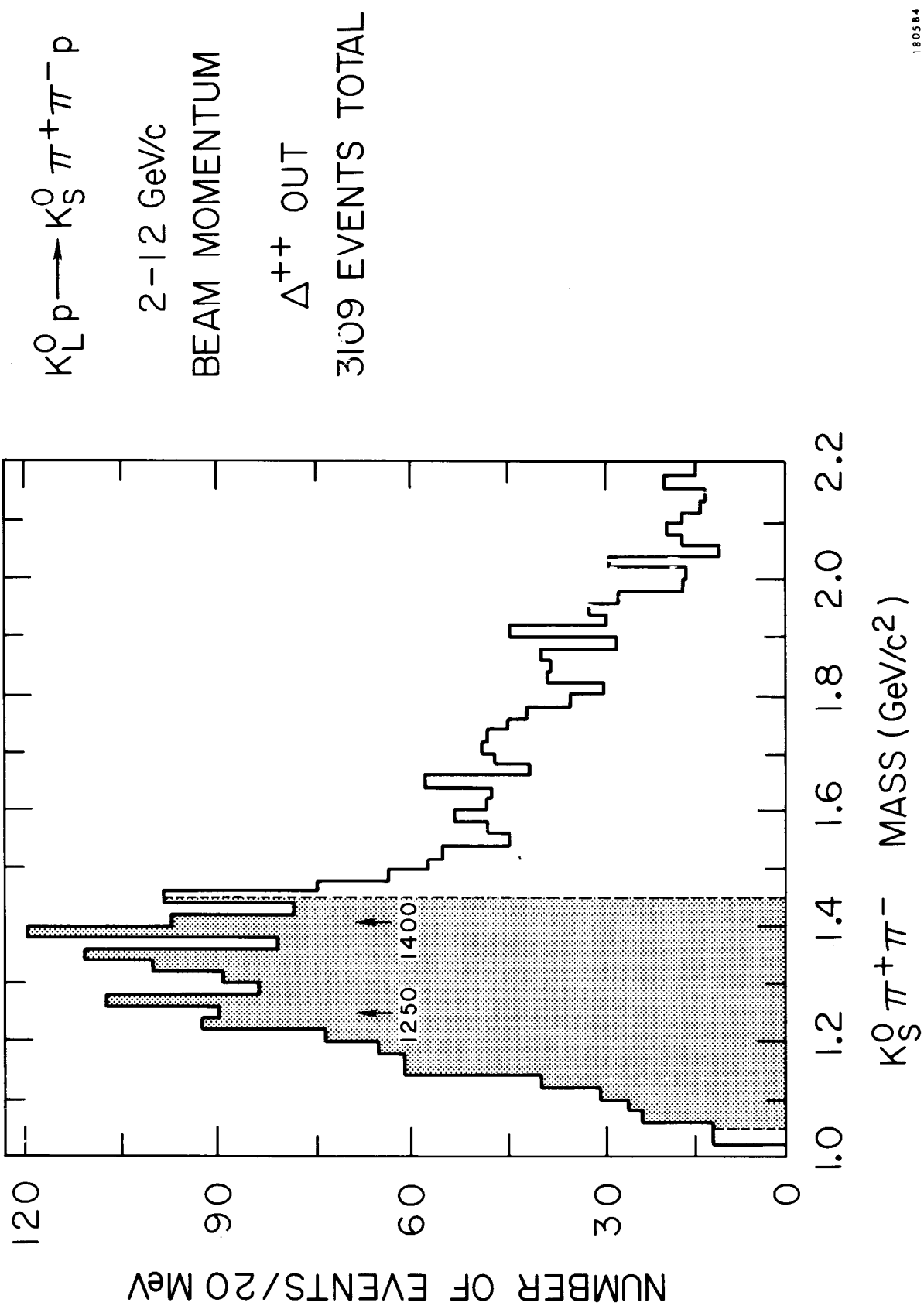
FIG. 23--$K_S^0 \pi^+ \pi^-$ mass spectrum from $K_L^0 p \rightarrow K_S^0 p \pi^+ \pi^-$ summed over the interval $2 < p_{LAB} < 12$ GeV/c, but with Δ^{++} events excluded.

$$K^0_L p \longrightarrow K^0_S \pi^+ \pi^- p$$

Δ^{++} Out

$\Delta^2_{p \rightarrow p} < 0.6 \ (GeV/c)^2$

$K^0_S \pi^+ \pi^-$ MASS

vs

Beam Momentum

8-12 GeV/c
(273)

6-8 GeV/c
(538)

4.5-6 GeV/c
(563)

3-4.5 GeV/c
(468)

NUMBER OF EVENTS / 40 MeV

$K^0_S \pi^+ \pi^-$ MASS

1805C5
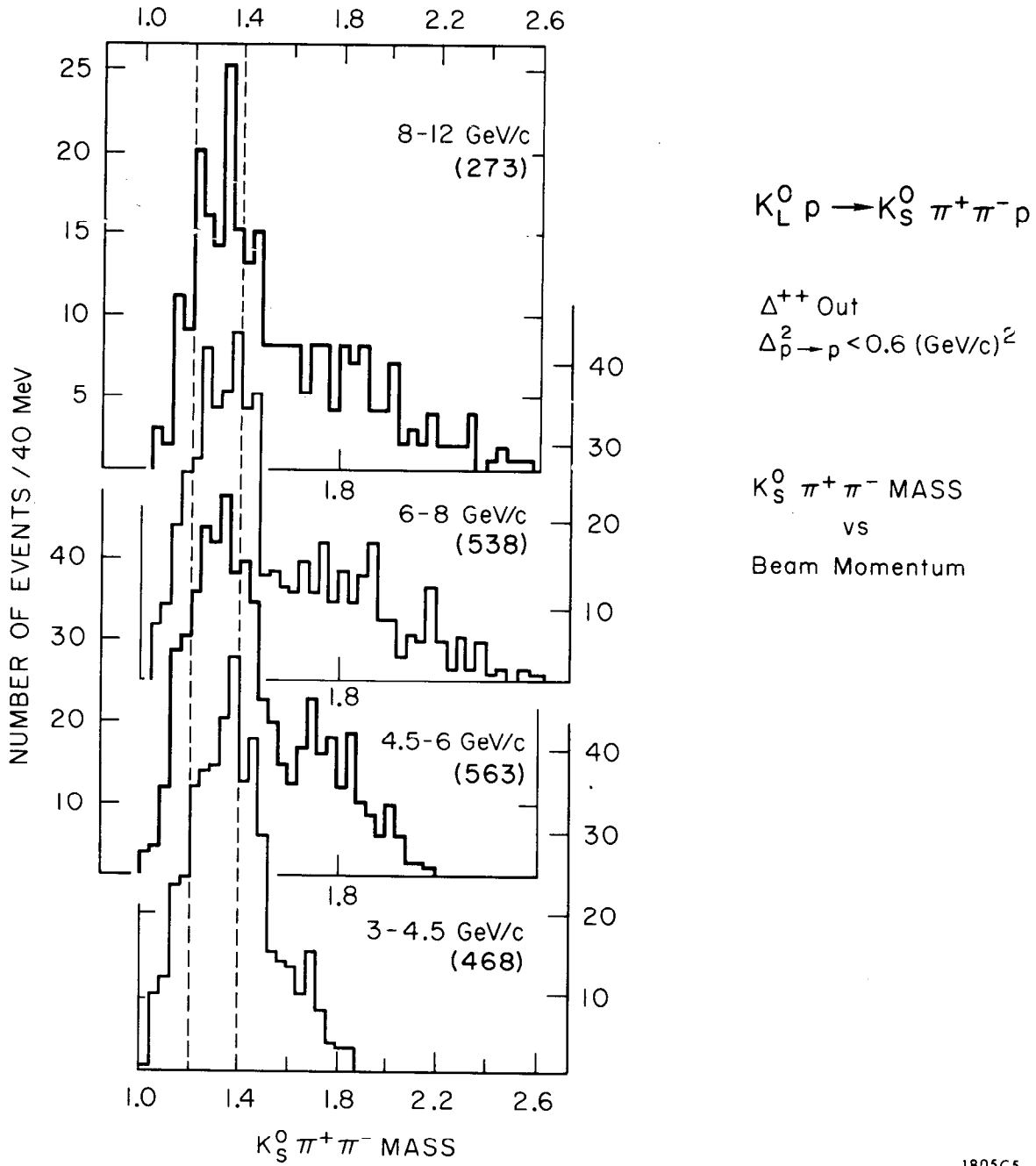
FIG. 24--$K^0_S \pi^+ \pi^-$ mass spectrum in narrow p_{LAB} intervals.
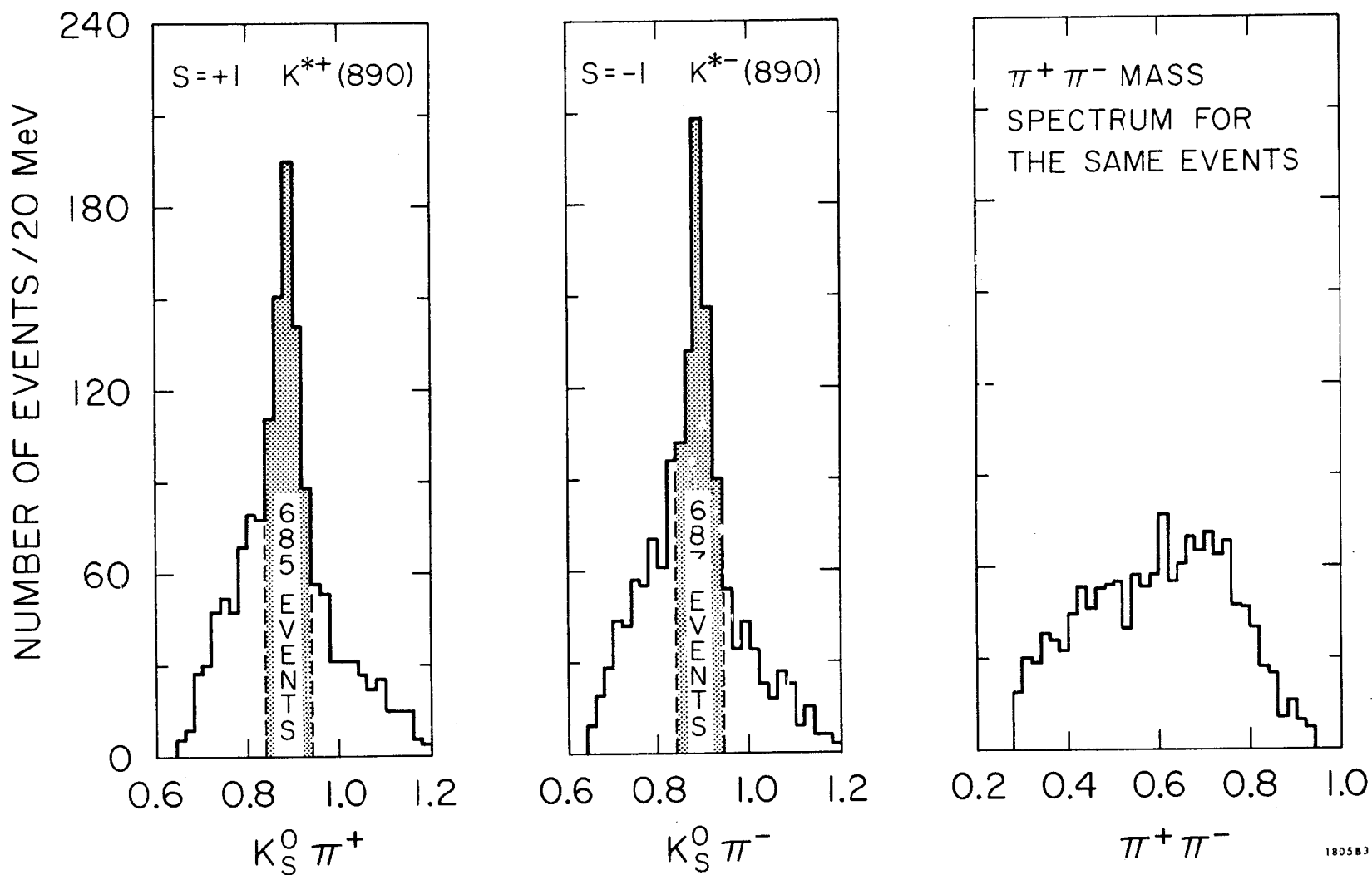
FIG. 25—Two body mass spectra for $K_L^0 p \rightarrow Q^0 p$ or $\bar{Q}^0 p$.

References

1. A. D. Brody, et al., contribution to the Proceedings of the XV International Conference on High Energy Physics, Kiev, USSR, 1970.

2. Y. S. Tsai, Stanford Linear Accelerator Center Users Handbook, Stanford University, Stanford, California, 1966 (unpublished).

3. A. D. Brody et al., Phys. Rev. Lett. 22, 966 (1969).

4. F. J. Gilman, Phys. Rev. 171, 1453 (1968).

5. A. D. Brody et al., Phys. Rev. Lett. 26, 1050 (1971).

6. J. Finklestein and S. M. Roy, CERN-TH 1279, 1971 (to be published).

7. Dubna-Serpukhov Collaboration, contribution to the Proceedings of the XV International Conference on High Energy Physics, Kiev, USSR, 1970 (Atomizdat., Moscow, to be published); see J. V. Allaby, CERN Report No. 70-2989, 1970 (unpublished).

8. P. Darriulat et al., Phys. Lett. 33B, 433 (1970).

9. W. Galbraith et al., Phys. Rev. 138, B913 (1965); R. L. Cool et al., Phys. Rev. D1, 1887 (1970); R. J. Abrams et al., Phys. Rev. D1, 1917 (1970).

10. A. Ahamadzadeh and W. B. Kaufmann Phys. Rev. 188, 2438 (1969).

11. F. Henyey et al., Phys. Rev. 182, 1579 (1969).

12. W. B. Johnson et al., Phys. Rev. Lett. 26, 1053 (1971).

13. Several possible explanations for the unexpected energy dependence of the phase have been suggested by V. Barger and R. J. N. Phillips, Phys. Lett. 33B, 452 (1970).

14. A. S. Carroll et al., Phys. Rev. 177, 2047 (1969); M. A. Wahlig and M. I. Mannelli, Phys. Rev. 168, 1515 (1968); P. Sonderegger et al., Phys. Lett. 20, 75 (1966); A. V. Stirling et al., Phys. Rev. Lett. 14, 763, (1965).

15. V. Barger and M. H. Rubin, Phys. Rev. 140, B1365 (1965).

16. V. Barger and M. Olsson, Phys. Rev. 146, 1080 (1966).

17. Ph. Salin, Nucl. Phys. B3, 323 (1967).

18. D. D. Reeder and K. V. L. Sarma, Phys. Rev. 172, 1566 (1968).

19. K. W. Lai and J. Louie, Nucl. Phys. B19, 205 (1970).

20. K^+n references: Allan A. Hirata et al., Phys. Rev. Lett. 21, 1485 (1968), (0.86 to 1.36 GeV/c); CERN-Bruxelles - München Collaboration,

Nucl. Phys. <u>B16</u>, 125 (1970), (3.0 GeV/c); K⁻n references:
S. A. B. R. E. Collaboration, Nucl. Phys. <u>B18</u>, 403 (1970), (3.0 GeV/c);
D. D. Carmony et al., Purdue Report No. C00-1428-166 (1970),
(4.5 GeV/c); B. Musgrave, private communication, (5.5 GeV/c).

21. H. Harari, Phys. Rev. Lett. <u>26</u>, 1079 (1971).

22. M. Ferro-Luzzi et al., Nuovo Cimento <u>36</u>, 1101 (1965), (3.0 GeV/c);
CERN-Bruxelles Collaboration, Nuovo Cimento <u>46</u>, 539 (1966), (3.0,
3.5, 5.0 GeV/c); CERN-Bruxelles Collaboration, Nuovo Cimento <u>51A</u>,
401 (1967), (3.5 GeV/c); C. Fu, J. MacNaughton, and G. H. Trilling,
Nucl. Phys. <u>B28</u>, 528 (1971), (4.6 GeV/c); V. Gordon Lind et al.,
UCRL-1928 (1969), (9.0 GeV/c); K. W. J. Barnham et al., Nucl.
Phys. <u>B28</u>,171 (1971), (10.0 GeV/c); J. C. Beriinghieri et al.,
Nucl. Phys. <u>B8</u>, 333 (1968), (12.7 GeV/c).

23. J. R. Ficenec, H. A. Gordon, and W. P. Trower, Phys. Rev. <u>175</u>,
1725 (1968), (2.65 GeV/c); Saclay-Paris-Amsterdam Collaboration,
Report C. E. A. R3037 (1966), (3.0 GeV/c); F. Schweingruber et al.,
Phys. Rev. <u>166</u>, 1317 (1968), (4.1 and 5.5 GeV/c); Y. W. Kang, Phys.
Rev. <u>176</u>, 1587 (1968), (4.6 GeV/c); Birmingham-Glasgow-London
(I. C.)-München-Oxford-Rutherford Collaboration, Nuovo Cimento <u>53A</u>,
522 (1968), (6.0 GeV/c); Aachen-Zeuthen-Geneva-London-Vienna
Collaboration, Nucl. Phys. <u>B5</u>, 567 (1968), (10.0 GeV/c).

24. G. V. Dass and C. D. Froggatt, Nucl. Phys. <u>B19</u>,611 (1970).

25. L. Stodolsky and J. J. Sakurai, Phys. Rev. Lett. <u>11</u>, 90 (1963).

26. M. Krammer and U. Maor, Nuovo Cimento <u>52A</u>,308 (1967).

27. T. Ferbel, "Diffraction Production of Bosons", presented to this con-
ference.

Discussion

Ferbel: Is there a dip in $d\sigma/dt$ near 0.15 GeV^2?

Loos: No, our data show no evidence for a dip near 0.15 GeV^2. Certain Regge models have a "crossover zero" built into the amplitude for ω exchange which would mean that if we are really looking at ω exchange then $d\sigma/dt$ must go to zero at this point. Our data, therefore, do not support the notion of a crossover zero in the ω amplitude.

Ferbel: Does the dip near 0.4 GeV^2 move with energy?

Loos: There is a break in the data near 0.4 GeV^2 at all energies, but I would call this structure a "shoulder" rather than a "dip".

Ferbel: Do you get a large contribution for the cut in the SCRAM fit for $K_L^0 p \rightarrow K_S^0 p$?

Loos: Yes, this is the "strong cut" model and there $\underline{is}$ a strong cut.

Chadwick: Doesn't the SCRAM model give a cut contribution larger than the pole contribution at large t?

Loos: Yes. The cut also plays a significant role at small t since it interferes destructively with the pole.

Ferbel: It seems peculiar that such a model can fit for a reaction which has an energy falloff like a pole.

Harari: The cut and the pole should have the same energy dependence, at least in the forward direction.

Takahoshi: Have you considered the Argonne weak cut model of Arnold in trying to fit your data?

Loos: No. No one knows the right model. My personal feeling is that on all of these inelastic pseudoscalar-baryon reactions what is really needed is a model that can explain them all at once. Explaining reactions piecemeal may be useful but is not necessarily the answer. It is very important to get complete sets of data with small experimental errors on all of the reactions so that we can really pin down the right model when it comes along.

Takeda: Have you looked for $K_L^0 p \rightarrow K_S^0 p$ backward scattering which would involve Z exchange?

Loos: Not yet. We need more events, and the question is further complicated because both S = +1 and S = -1 exchange is allowed for backward scattering.

18-39

STATUS OF HIGH ENERGY PHYSICS IN JAPAN

Toshio Kitagaki

Tohoku University
Sendai, Japan

First I would like to thank the National Science Foundation and Dr. R. R. Ries for supporting this seminar. One of the purposes of this kind of meeting is to get to know each other, and so I am going to tell you about the present status of high energy physics in Japan.

First, I would like to mention something about the number of high energy physicists in Japan. There are about 500 theorists, plus 250 people each in cosmic ray research and in high-energy physics research. But these numbers are nominal: the effective numbers are about half of them.

Next I shall speak of the new accelerator. We have been trying to get a high-energy accelerator in Japan for the last ten years. In 1961 we proposed a 12 GeV proton synchrotron with high intensity, then changed the plan into one for a 40 GeV machine. But there was trouble in getting a large enough budget for the plan. Finally, at the beginning of last year, the advisory committee of the Ministry of Education reached a decision on the proposal and cut the budget by a factor of 1/4. This cut reduced the size of the project to that of an 8 GeV accelerator. The revised plan, finally approved last December, allows for increasing the maximum energy eventually to 12 GeV. This is possible because the diameter of the machine is rather large compared to its energy. It is 108 meters. The machine is of the so-called separated function type, and this is why the machine has such a large diameter. In this respect this machine is like the accelerator at NAL. For general interest, the separated function accelerator is based on my work which was published in Physical Review in 1953. So we thought that the new Japanese machine should be of this type.

Figure 1 shows the layout of the accelerator. It has a 20 MeV linear accelerator as an injector and has a 500 MeV booster. The experimental area and the bubble chamber area are also shown in Fig. 1. It was decided that the site of the machine should be in the Tsukuba area which is shown on the map in Fig. 2. The site, located about 50 miles northeast of Tokyo, has a total area of 500 acres, and therefore has room for a still larger ring.

N

1 CONTROL ROOM
2 PRE-INJECTOR
3 LINAC
4 BOOSTER
5 MAIN RING
6 EXPERIMENTAL HALL
7 BUBBLE CHAMBER

1972A110

FIG. 1

SEA OF JAPAN

●SENDAI
(TOHOKU UNIV.)

TSUKUBA SITE
FOR 8 GeV PS

●TOKYO

KYOTO ●NAGOYA

HIROSHIMA ●OSAKA
●NARA

PACIFIC OCEAN

N

0   100   200   300 Km

- 4 -
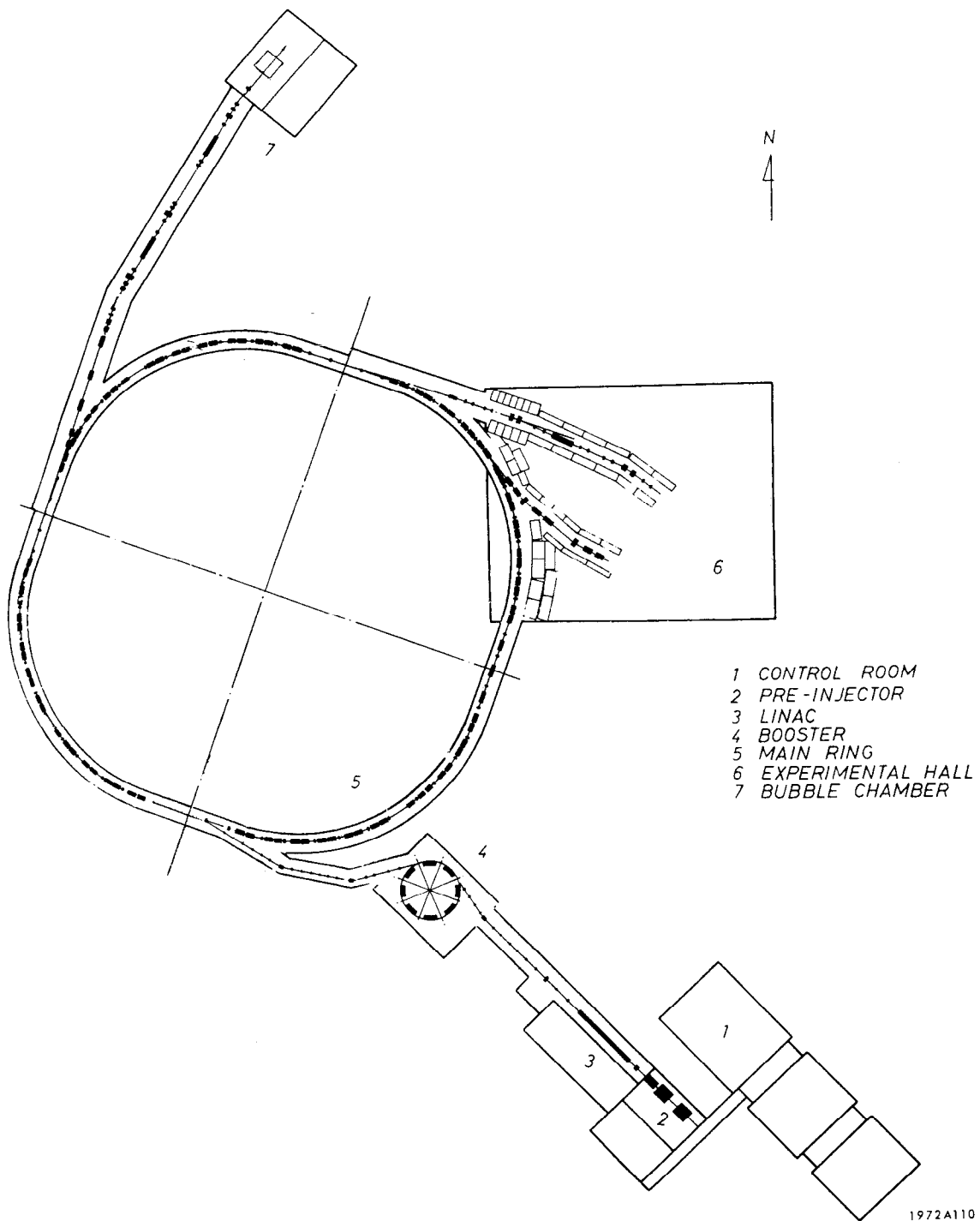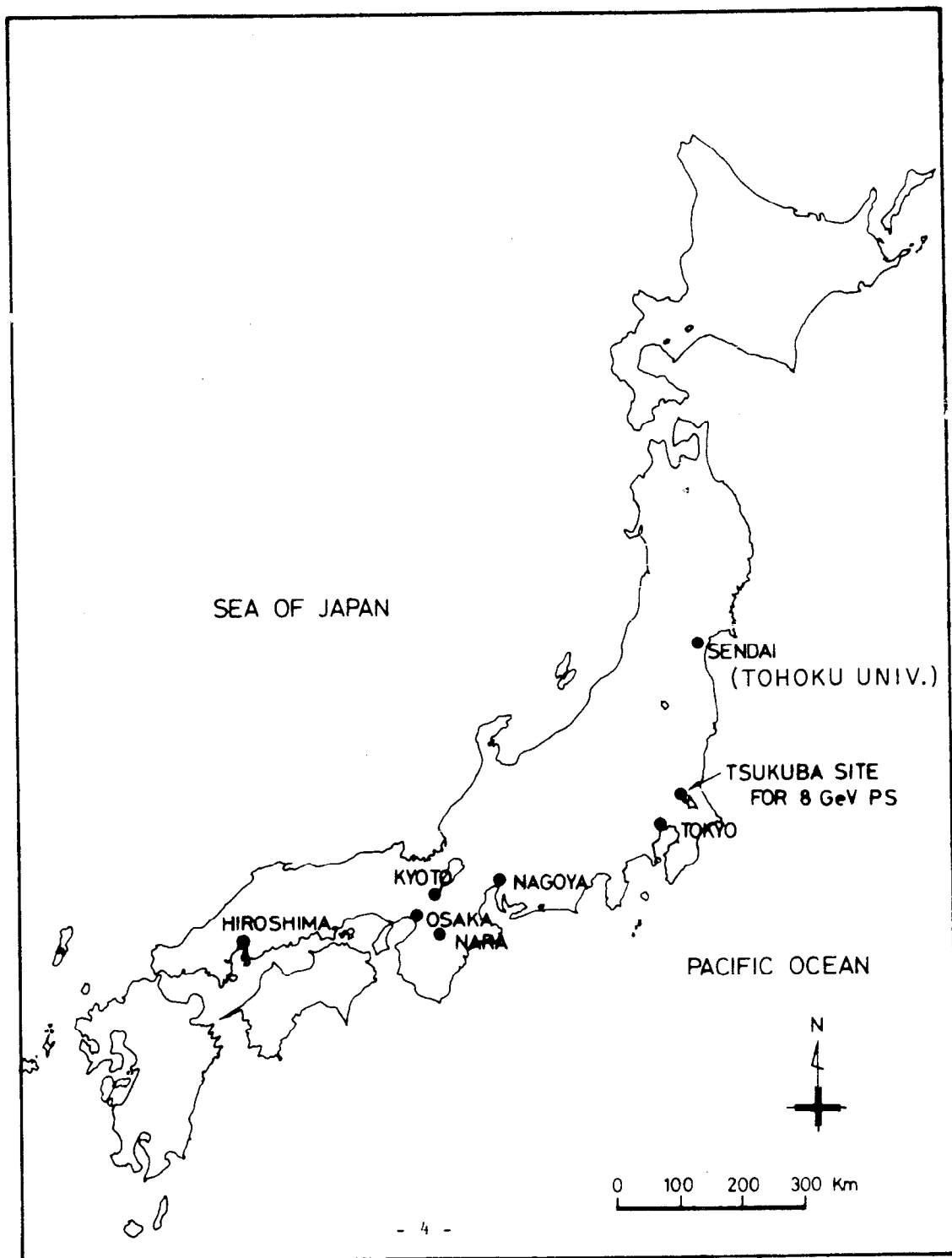
1972A111

FIG. 2--Japan.

Dr. Suwa will be the director of the laboratory which is called the National Laboratory for High Energy Physics. The total budget for this project is about 24 million dollars.

Next I would like to describe the bubble chamber being built at the Institute for Nuclear Study in Tokyo, where they have a 1.3 GeV electron synchrotron. The bubble chamber, now nearly complete, is housed in the experimental area near the 1.3 GeV accelerator and will be tested with electron beams.

Figure 3 shows the cross section of the Japanese 75 cm bubble chamber. Originally it was intended to be a test chamber for a larger one to be built for the 40 GeV accelerator. Because of the budget cut, we plan to use this chamber with the 8 GeV accelerator. Although the nominal size of the chamber is 75 cm in diameter, we intend to increase its length in the beam direction to about 1 meter. The magnet, giving a 17.8 kG magnetic field, was so designed that it could be used on a 1 meter chamber. Another feature which is now under discussion is adding a perpendicular view using a mirror. Scotchlite is used for a light reflector (see Fig. 3). The first test run was successfully performed last October.

Next I will go on to describe the bubble chamber analysis groups in Japan. Some people who could not wait out the four years until the accelerator is completed have started bubble chamber analysis work, including myself. Of course, all of the groups are at a very early stage of development. At present there are three major groups now doing analysis work: namely the Tohoku group, the low energy $\bar{p}p$ group and the Osaka group. Another four groups are just about to start.

Some work of the low energy $\bar{p}p$ group was reported by Dr. Hirose yesterday afternoon. People in this group are mostly inside Tokyo with the exception of the people from the University of Hiroshima. Prof. Yamagata is a leader of the group. The facilities of the group consist of one standard Vanguard Measuring Projector and another Japanese made measuring machine, which uses the so-called D-Mac digitization which is widely used in Germany. This measuring projector measures two-prong events at a rate of 10 to 15 eV/hour. The least count of the machine is 5 microns. Their 700 MeV/c $\bar{p}$ film was exposed at CERN. The number of physicists involved in this experiment is given in Table 1.
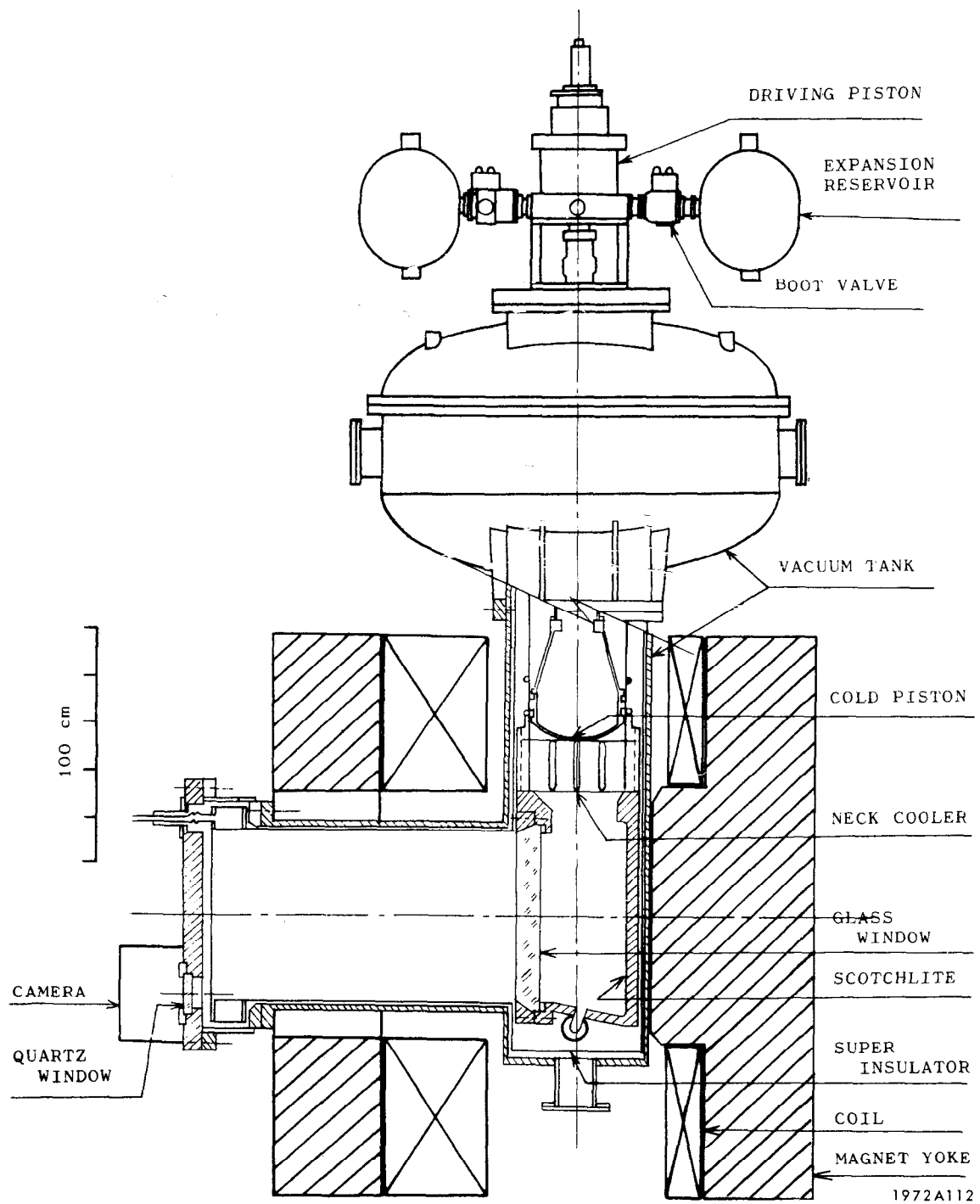
FIG. 3--Japanese 75(100) cm bubble chamber.

TABLE 1

Groups		Members		Equipment			
		Staff	Grad. Stud.	Used SP	MP	Under Construction SP	MP
Low Energy p̄p Group	Tokyo	6		1	1	3	2
	Hiroshima	2	6	1	1	1	1
Osaka Group		5	4	1	1	2	1
Groups being built, 4 Groups		7	2			1	2
Tahoku Univ. Group		5	7	3	5	3 + T. V. FSD	
		25	19	6	8	7	10

As is shown in Table 1, the $\bar{p}p$ group is constructing two more measuring machines and three scanning projectors. One of the measuring machines under construction, designed by Prof. Yamagata, deserves special note. It is named CAMP (Computer Aided Measuring Projector), and I will describe it briefly.

The light beam from the projector is first divided into two, one of which goes to a scan-measure table of the Mangespargo type. If we measure for example three points on a track, the computer works out roughly how to follow the track to be measured, which is done using the other half of the light signal. It goes through a rotating dove-prism measuring device which allows the perpendicular scan to the track. The principle of the device is shown in Fig. 4. Thus, measurements are going on under computer control using the information from rough digitization, like in Franckenstein track following. The machine is nearly ready for production.

Next some words about the Osaka Group. The structure of the group is shown in Table 1. Their study of multiparticle production in 12.7 GeV $K^{-}p$ interactions was reported on by Dr. Teranaka yesterday. Other physicists in Osaka University are doing cosmic ray experiments, which is one reason for their interest in multiparticle production processes at high energy. In these multiparticle production studies, bubble counting is one of the essential problems. Figure 5 shows their bubble density counter and outlines its function.

Now I will briefly speak about the four groups now building up. These four groups are at: 1) Tokyo University, under Dr. Yamamoto, who just came back from the U.S. last year; 2) Nagoya University; 3) Nara Women's University and 4) Tohoku Gakuin University.

Let me now give a brief description of our Tohoku University group. Figure 6 shows a view of our Bubble Chamber Analysis Center at Tohoku University. Figure 7 shows our image plane digitizing measuring-projectors at work. They have X- and Y- coordinate digitizers, utilizing a magnetic scale. Our group at present is using five measuring projectors. Three of them were shown in Fig. 7, while the other two use film plane digitizing. All are Japanese made.

We are now constructing three more measuring machines. One of these is of special type, which we call a "Concentric Reader". The film is projected

TO SCREEN

DOVE PRISM

MERCURY LAMP

HALF MIRROR

SLIT 2

MAIN LENS

SLIT 1

FILM

PHOTOTUBE 1

GRATING

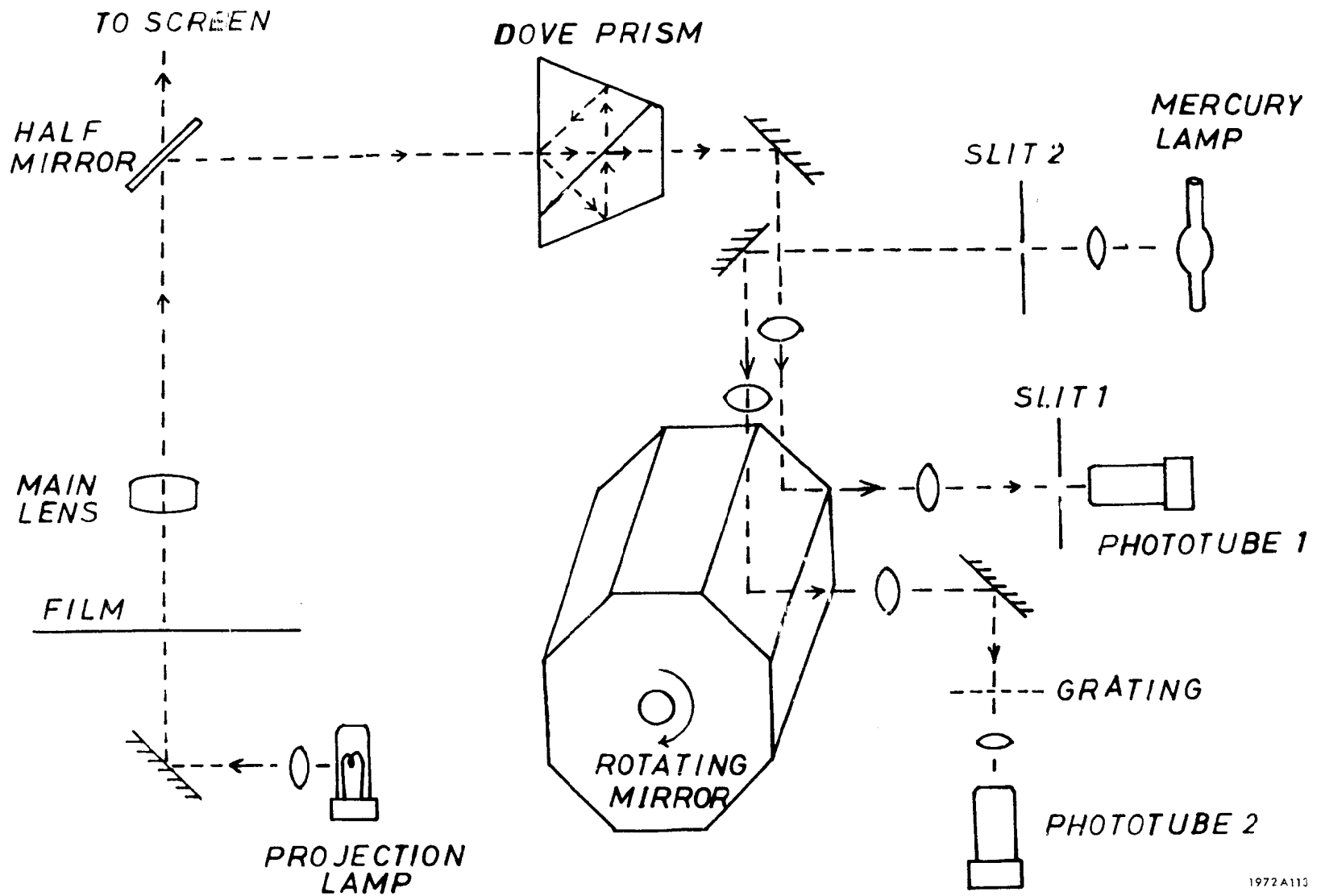ROTATING MIRROR

PHOTOTUBE 2

PROJECTION LAMP

19-8

1972 A113

FIG. 4
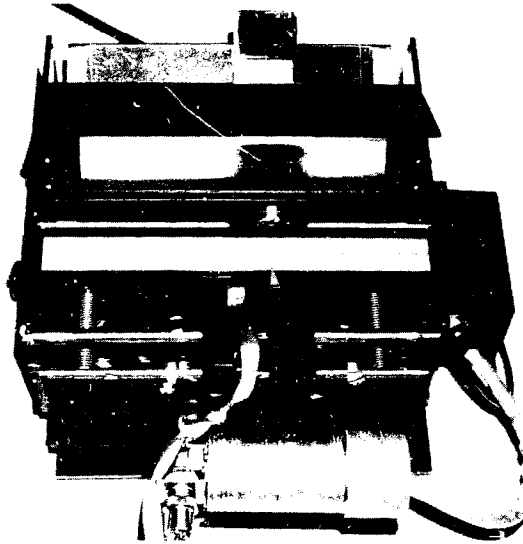
(a) Bubble density measuring equipment,
Osaka City University.

TRAVELING DIRECTION
OF SLIT

SLIT, width 0.1~0.4mm(variable)
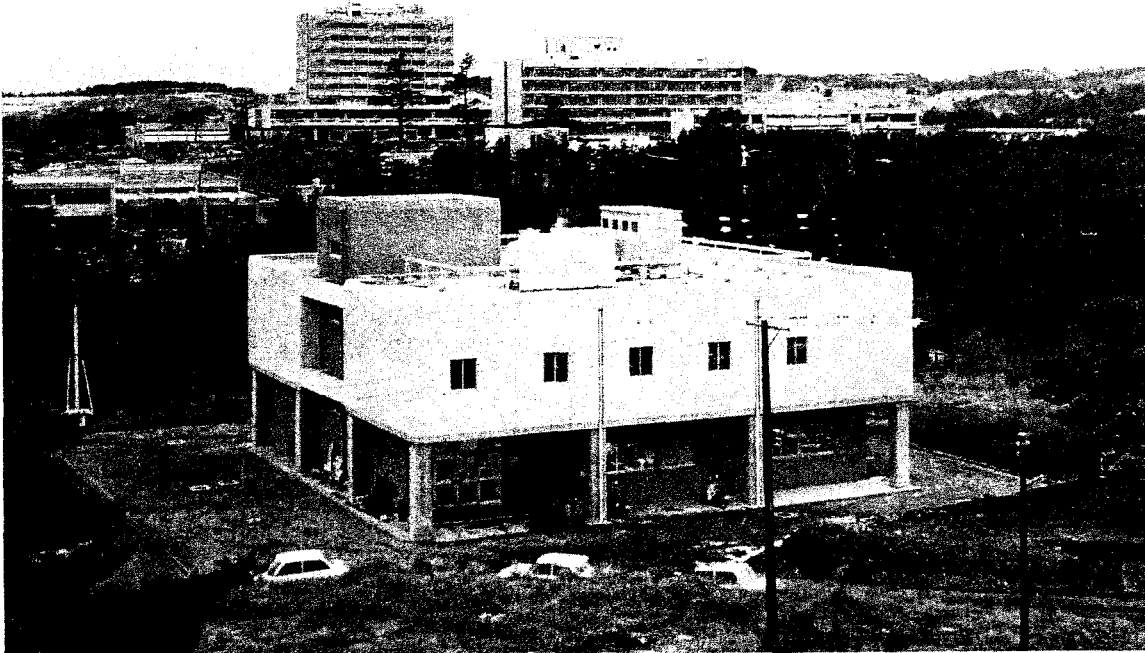
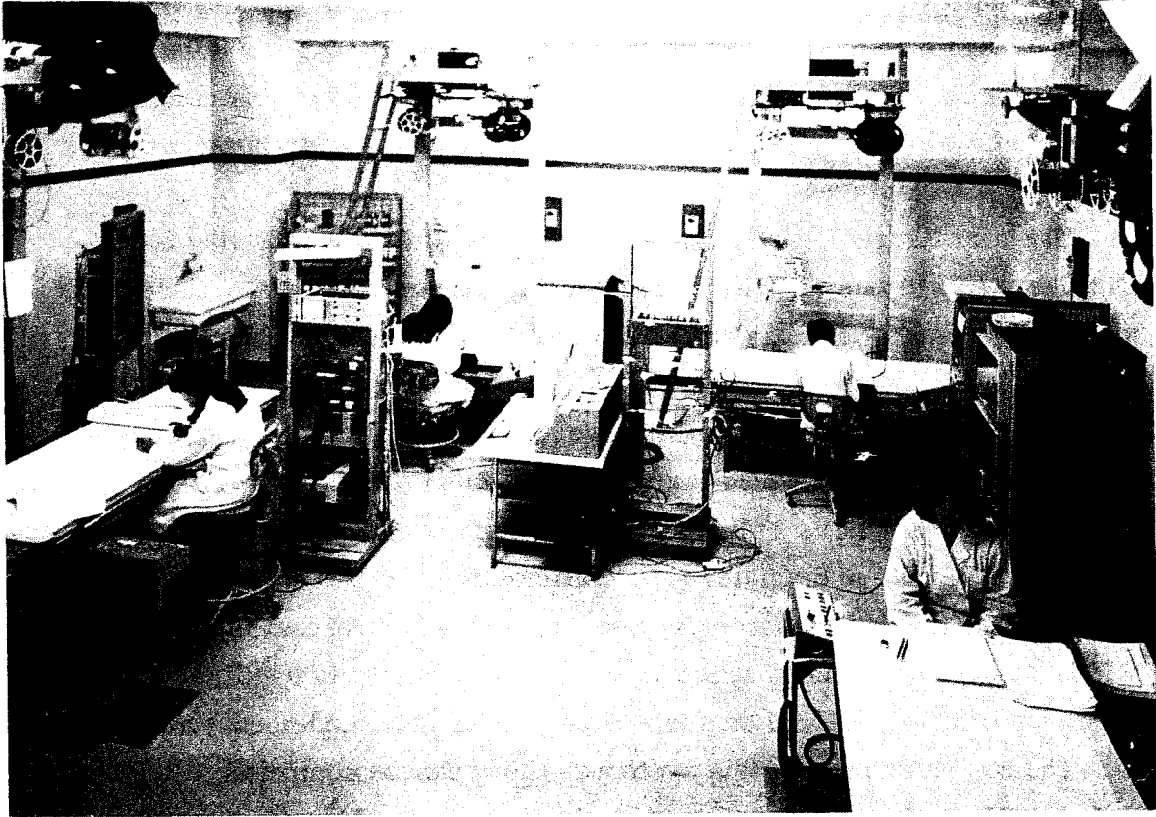SLIT LENGTH ~ 5mm

TRACK
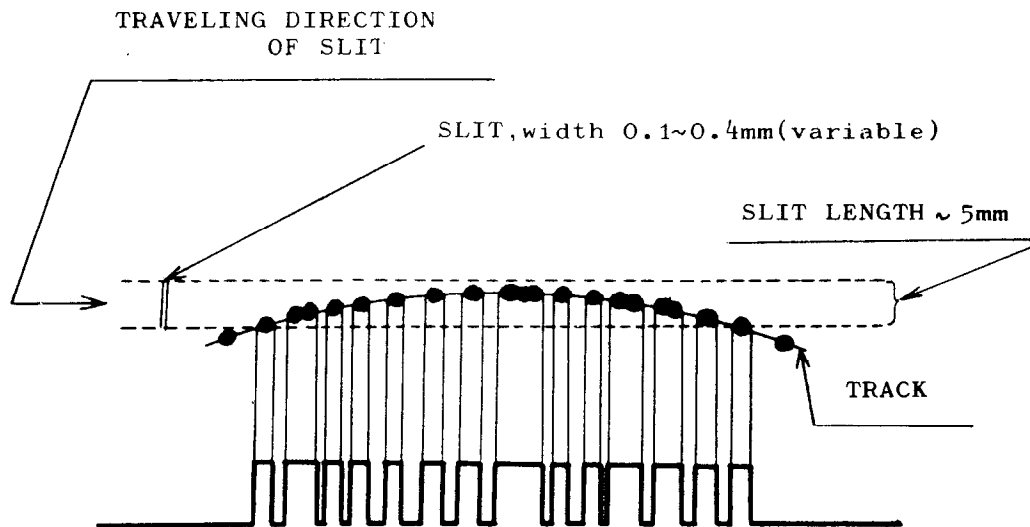
SHAPED PULSES FOR BUBBLES

1972114

(b) Bubble density measurement.

FIG. 5

1972A115

FIG. 6--The new building for bubble chamber physics,
Tohoku University.

1972A116

FIG. 7

onto the measuring table with the vertex of the event at the center of a group
of concentric rings. Each ring can be rotated so that a hole in the ring is
set on the track to be measured. Light from the projected image goes
through the hole in each ring, and reaches the photomultiplier when a rotating
slit underneath the table passes the hole, and the track is detected. The
rotation angle of the slit gives X and Y coordinates of the track at each ring
by means of its radius (γ) and rotation angle (θ) as $X = X_0 + \gamma \cos\theta$, and
$Y = Y_0 + \gamma \sin\theta$, where X_0 and Y_0 are the X- and Y- coordinates of the
vertex point which is measured by a stage-position digitizer attached onto
the X and Y film stages.

The next figure (Fig. 8) shows a schematic view of our Flying Spot
Digitizer (FSD) system. The main features are very similar to those of the
usual FSD system. Rotating and fixed slits to make a flying spot, X and Y
scanning lines and so on. One of the big difference between ours and most of
others in the rest of the world is that we are constructing three identical
FSD's and we will use one for each view and thus do three view scanning. Our
design of the machine is influenced by this feature. For example, our rotating
disc has rather large diameter (650 millimeters) compared with conventional
ones, and so the rotation speed is also much slower than that in the usual
FSD. Also, the rotational speed is controlled by a quartz oscillator with the
precision of 10^{-5}. Figure 9a shows some of the parts under construction.

The computer used in this system is the Japanese computer
called a TOSBAC 3400/41 and is made by the Toshiba Electric Company. The
machine which is shown in Fig. 9b, is most comparable to the IBM 7090 or to
the PDP-10. This computer will mostly be used for on-line use with the FSD
system in daytime and will be used at night for general off-line use. For some
computing jobs this computer is not big enough. For these we use a bigger
machine at the Tohoku University Computing Center. This machine is made
by NEC and named NEAC 2200/model 700. This machine has a speed 15 times
faster than the IBM 7090 and is very similar in size to the CDC-6600.

As you can see, our present status is that of the very beginning of
construction. We will need quite a lot of effort for development. Someone
told us in this seminar, the physics we do now is more or less "bread and
butter" physics, but for our physics status in Japan, I prefer to say that we
are preparing "iron-pot and pan" for our physics, since we use an iron-pot
for boiling rice and a pan for soup in a Japanese daily life.

Number of slits in disk – 24 (10 μ width)
Distance of slits from center – 253 mm
Magnification of projector lens – 1:1
Scanning range – 54 mm
Measurement – 50 mm
Disk rotation – 232 rpm
Scanning time – 10.8 msec
  (effective – 8.6 msec)
Resolving power – 1.54 μm
  (4 MHz clock)
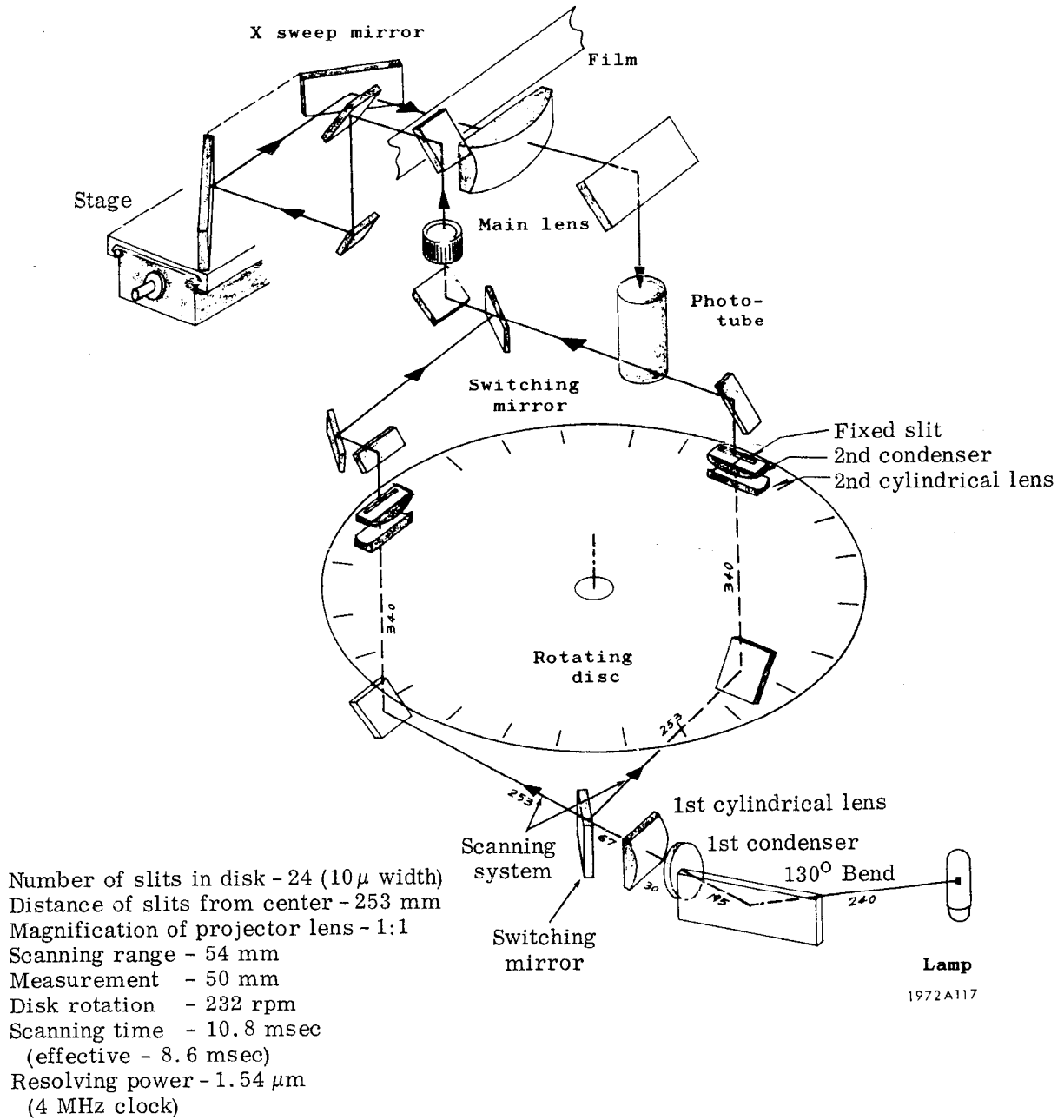
FIG. 8--Schematic view of FSD, Tohoku University. A set of three
FSD scans three views simultaneously.

PRESENT STATUS OF BUBBLE CHAMBERS IN THE U.S.

J. Ballam

Stanford Linear Accelerator Center
Stanford University, Stanford, California USA

1. Introduction

U. S. bubble chambers are now almost exclusively cryogenic. There are, for example, no plans to build large heavy liquid chambers such as Gargamelle (CERN) or the corresponding chamber being constructed at Dubna for the Serpukhov accelerator. The chambers shown in Table 1 are now in operating condition. In addition there are two further chambers in construction: the NAL 168" and the SLAC 15" rapid cycling chamber.

2. Picture Taking Capacity

On the basis of a considerable amount of experience with all sorts of chambers, we now have an idea of the efficiency of picture taking, i.e., for the entire system: chamber, beam and accelerator. The result is that on the average a chamber will take useful pictures for about 25% of the time it is scheduled to run. Using this efficiency factor, it is possible to calculate the picture taking capacity per year as

$$N = TRr\epsilon$$

where
- T is the scheduled time for BC running in seconds
- R is the accelerator pulse rate per second
- r is the number of expansions per pulse
- ϵ is the efficiency (25%)

For BNL and ANL

$$T = 2.25 \times 10^7 \quad (75\% \text{ of the calendar time})$$

$$R = 1/3 \qquad r = 2 \text{ (double pulsing)}$$

For SLAC

$$T = 1.5 \times 10^7 \quad (50\% \text{ of calendar time})$$

$$r = 1$$

$$R = 2 \quad (\text{Limited by cameras})$$

The result, shown in Table 1 comes out as an impressive 38,000,000/year. I have assumed that BNL would not run the 30" and 31" simultaneously.

Table 1

Picture Taking Capacity of U. S. Chambers Per Year,
Derived From the Formula in the Text

Laboratory	Chamber	Pictures/year	Actually taken in 1970
SLAC	82"	$9 \cdot 10^6$	$4 \cdot 10^6$
SLAC	40"	$9 \cdot 10^6$	$0.5 \cdot 10^6$
BNL	80"	$4 \cdot 10^6$	$1.1 \cdot 10^6$
BNL	30/31"	$4 \cdot 10^6$	$2.6 \cdot 10^6$
BNL	84"	$4 \cdot 10^6$	----
ANL	30"	$4 \cdot 10^6$	$2.3 \cdot 10^6$
ANL	168"	$4 \cdot 10^6$	----
	Total	$38 \cdot 10^6$	$10.5 \cdot 10^6$
	Event Rate		$7.0 \cdot 10^{6*}$

* Assuming 1 event/picture in the 80" and 82", 1/3 event/picture in the others.

If we look at the actual performance in 1970, shown also in Table 1, we find that, excluding the two large BNL and ANL chambers, the actual rate is ~ 1/3 of maximum--a pretty good record considering financial limitations as well as difficulties with the 80". Normalizing to one chamber and to an average number of tracks (as explained in Table 1) this rate produced about 7,000,000 events/year.

3. Data Analysis Capacity--U. S. Bubble Chamber Groups

Now what kind of a match is this to the U. S. data analyzing capacity which we hope to have in the near future? Table 2 shows a list of all U. S.

Table 2

U. S. Bubble Chamber Groups 1970

Institutes

*Argonne National Laboratory

*Brookhaven National Laboratory

*Lawrence Radiation Laboratory

*Stanford Linear Accelerator Center

Universities

Brandies University

*Calif. Institute of Technology

Carnegie Institute of Technology

*Columbia University

*Duke University

Florida State University

*Johns Hopkins University

*Massachusetts Inst. of Technology

Michigan State University

*Purdue University

*Rutgers University

Stevens Institute of Technology

SUNY, Stony Brook

Syracuse University

Tufts University

Vanderbilt University

Western Reserve University

*Yale University

Univ. of Calif. , Berkeley

Univ. of Calif. , Davis

Univ. of Calif. , Irvine

Univ. of Calif. , Los Angeles

*Univ. of Calif. , Riverside

Univ. of Colorado

*Univ. of Hawaii

*Univ. of Illinois

*Univ. of Indiana

*Univ. of Maryland

Univ. of Massachusetts

Univ. of Michigan

*Univ. of Pennsylvania

Univ. of Rochester

*Univ. of Washington

*Univ. of Wisconsin

Totals

34 Universities   4 Institutes   38 All

*Now have, either on order or in use, an automatic measuring machine of the types Spiral Reader, PEPR, POLLY, FSK, HPD.

bubble chamber groups. I have indicated which of these have automatic measuring devices either in operation or on order. Assume the University groups with automatic measuring equipment can measure 250,000 events/year, that the Institutes do 500,000 events/year, and that the more conventional systems do 100,000 events/year. Also assume that 20% of the events are re-measures. The capacity C is then:

$$C = 0.8 \left[4 \times 500,000 + 16 \times 250,000 + 18 \times 100,000\right]$$

$$\cong 6,200,000 \text{ events/year.}$$

This is to be compared with the data taking rate of 7,000,000 events/year. This is a good match since perhaps one half of the events are uninteresting, unmeasurable or otherwise not processed.

I realize that LRL, BNL and ANL can probably do more than 500,000 events/year. But on the other hand, not all the University groups can do 250,000 or 100,000. Therefore, I feel that 6,000,000/year is a reasonable estimate. Incidentally, it was not that big in 1970.

Finally, I have also made an attempt to list the groups that have left or entered BC physics. This is shown in Table 3. Although the statistics are

Table 3

Universities Leaving Bubble Chamber Work

| Harvard | Iowa State | UCLA |
| Princeton | Chicago | |

Universities Entering Bubble Chamber Work

Calif. Institute of Technology   SUNY, Stony Brook

poor, I believe the trend is obvious. There will be fewer BC groups in the future, and the tendency will be for the larger groups to consolidate and to increase their analysis capacity. Personally, I feel this is quite in line with the task to be done in this field.

4. Looking into the Future

Without a major breakthrough in measuring rates, I cannot imagine increasing the yearly capacity to more than about 9,000,000 events/year. Considering that there will be three new, large chambers with a capability of supposedly 2-3 million pictures/year each, it would seem that more events per year could be taken than can be analyzed.

How can we best use our equipment that has taken so long to assemble? There are several ways out of the dilemma:

1. Neutrino Physics--All three large chambers are scheduled for a large amount of neutrino running with events rates of hundreds per day. They can thus effectively use their pulsing capacity while the event rate can easily be handled by present measuring capacity.

2. Triggered Chambers--As fast cycling, multiple pulsing and hybrid systems become more available, selective triggering of the lights of chambers by counters and spark chambers can get us the rarer but more interesting types of event.

Triggered experiments have been tried out at ANL and at the 15" chamber of Princeton. At SLAC we have three setups utilizing these techniques which I will briefly describe.

We have a K_2^o beam at SLAC, containing energies between 4 and 7 GeV/c and with a 1:2 ratio of K_L^o to neutrons. The SLAC accelerator can be made to give a pulse of electrons of 1 nsec width so as to provide a time-zero marker. We have done time-of-flight measurements of the K^o and neutron events using counters placed as shown in Fig. 1. About 100K pictures were taken, triggering on events in the "time-late" cutoffs shown in Fig. 2. As an example, in a particular neutron event it was found that the 3c fit gave a time-late of 27.6 nsec, while the uncorrected time-late direct measurement was 30 nsec.

The second example is a hybrid experiment setup with the 40" HBC. The beam and spark chamber setup is shown in Fig. 3. In this experiment the Cal-Tech group will look at $\pi^- p \rightarrow N^* +$ fast π^-. They have 2 msec to decide whether or not to flash the lights. The cross section is such that the lights should trigger every 50 expansions. Thus a 200,000-event experiment of peripherally-produced N^*'s which would normally require 10 million photographs can be done by taking 4-500,000 photographs (assuming a 50% efficiency in the trigger).
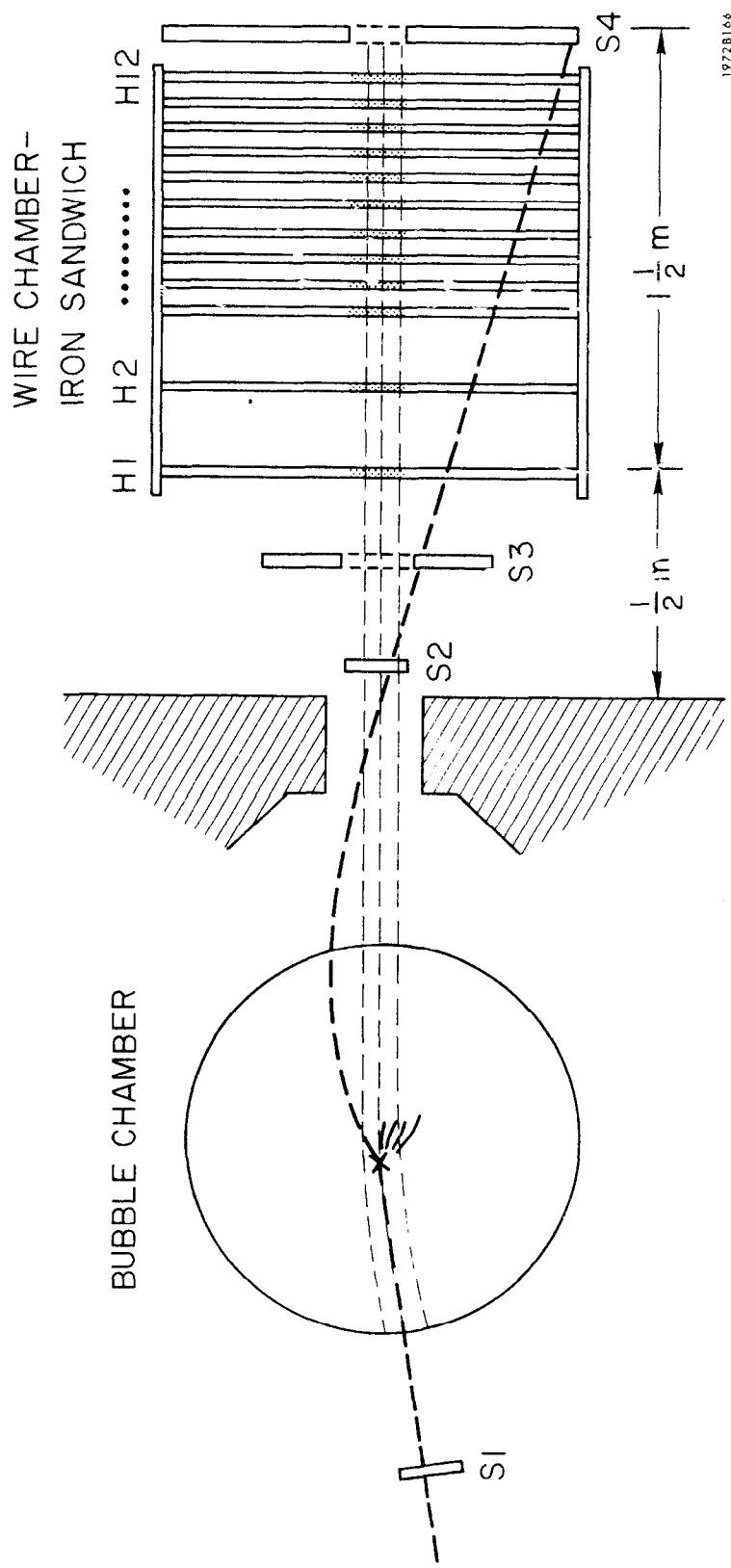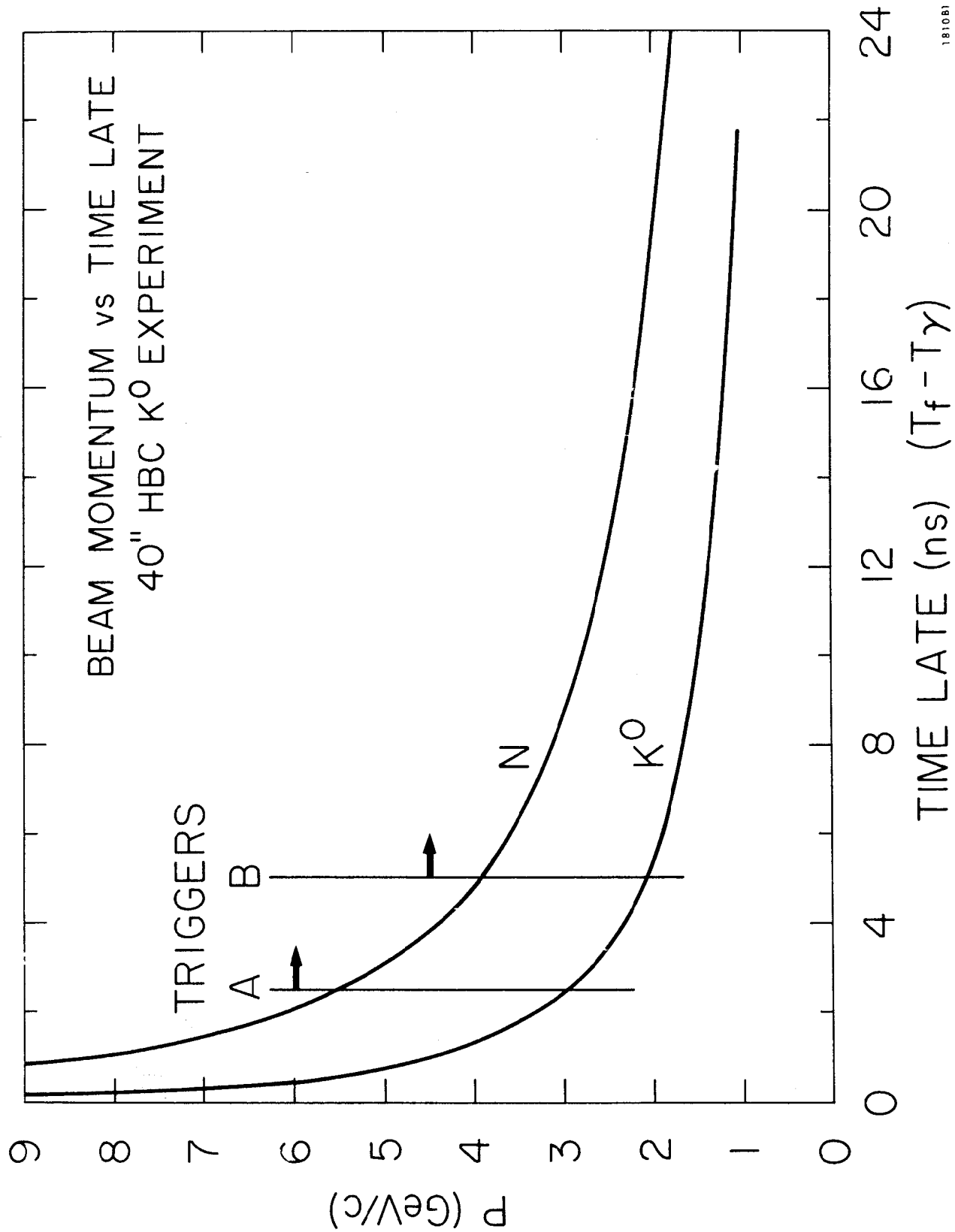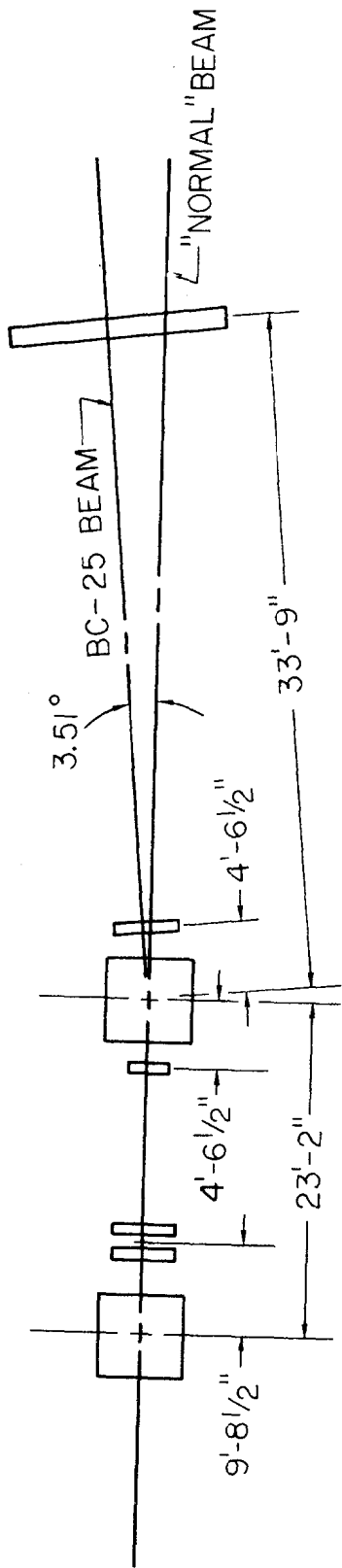
FIG. 1—SLAC 40" HBC with K^o counters.

FIG. 2—Beam momentum vs. time late with time cutoffs for K⁰ experiment.

PLAN
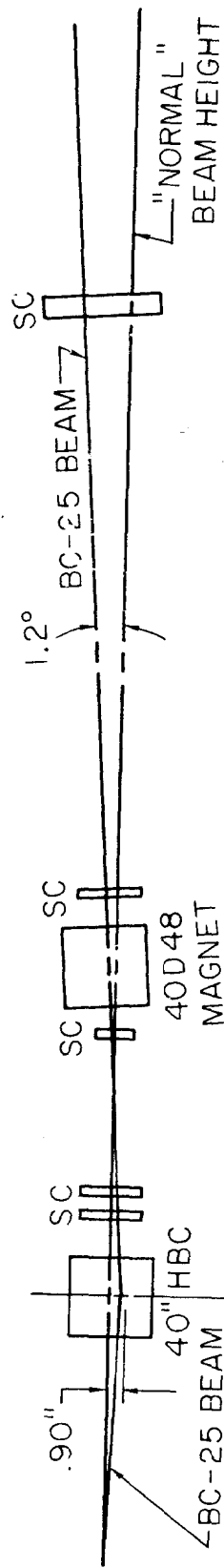
ELEVATION

FIG. 3--The beam for experiment BC-25 at SLAC.

A similar setup will be used to do μ-p inelastic scattering with the system. Here we will run 50-100 μ's per pulse and try to run the 40'' at 10-20 pulses/second (1000 μ's/second). In this experiment we would trigger on 1 event every 500-1000 expansions and end up with several thousand high-momentum-transfer events with the advantage of 4π geometry.

Lastly, we are in the process of building what amounts to a visible hydrogen target which is a 15'' diameter, 5'' deep, thin-walled rapid cycling chamber capable of going 60-90 pps. We have successfully run a 4'' model. Figure 4 shows a drawing of the chamber.

The first proposed experiment will trigger this chamber on fast neutrons:

$$\pi^+ p \rightarrow \pi^+ \pi^+ n$$
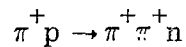
In 400 hours of running we would obtain 150 events/μb but wish only 30-50,000 events to be measured.

5. Present Status of Conventional Experiments

Coming back to more conventional bubble chamber experiments, I have updated a series of charts, first prepared by I. Pless for a PEPR Conference, held in May 1970. In these charts I have tried to graph the present status of completed and approved (not yet done or only partially finished) experiments for $\pi^\pm p$, $\pi^\pm d$, $K^\pm p$, $K^\pm d$, $p^\pm p$ and $p^\pm d$ done at SLAC, ANL and BNL. These are shown in Figs. 5, 6 and 7. I have left out of consideration the very extensive work that has been done at energies below 3 GeV--such as stopping K's and $\bar{p}$'s, as well as the phase-shift analysis of formation reaction in $\pi^\pm p$ and $K^\pm p$ processes. It is my belief that the general survey experiment at these lower energies has now been done, with the possible exception of some highly specific processes.

These charts show some obvious characteristics. First, there is a notable lack of high statistic exposures for pp and $\bar{p}$p at intermediate energies. Second, there is a need for high energy (12-25 GeV) $K^\pm$ exposures. Presumably BNL will supply some of these when the high intensity conversion is complete. Third--in spite of a rather heavy attack on the remaining regions-- there is still a need for 10-20 high-statistic 750-1000K exposures. I have some ideas on where these could be taken, but obviously much thought could and should be given to the subject of proper selection of momenta. Obtaining
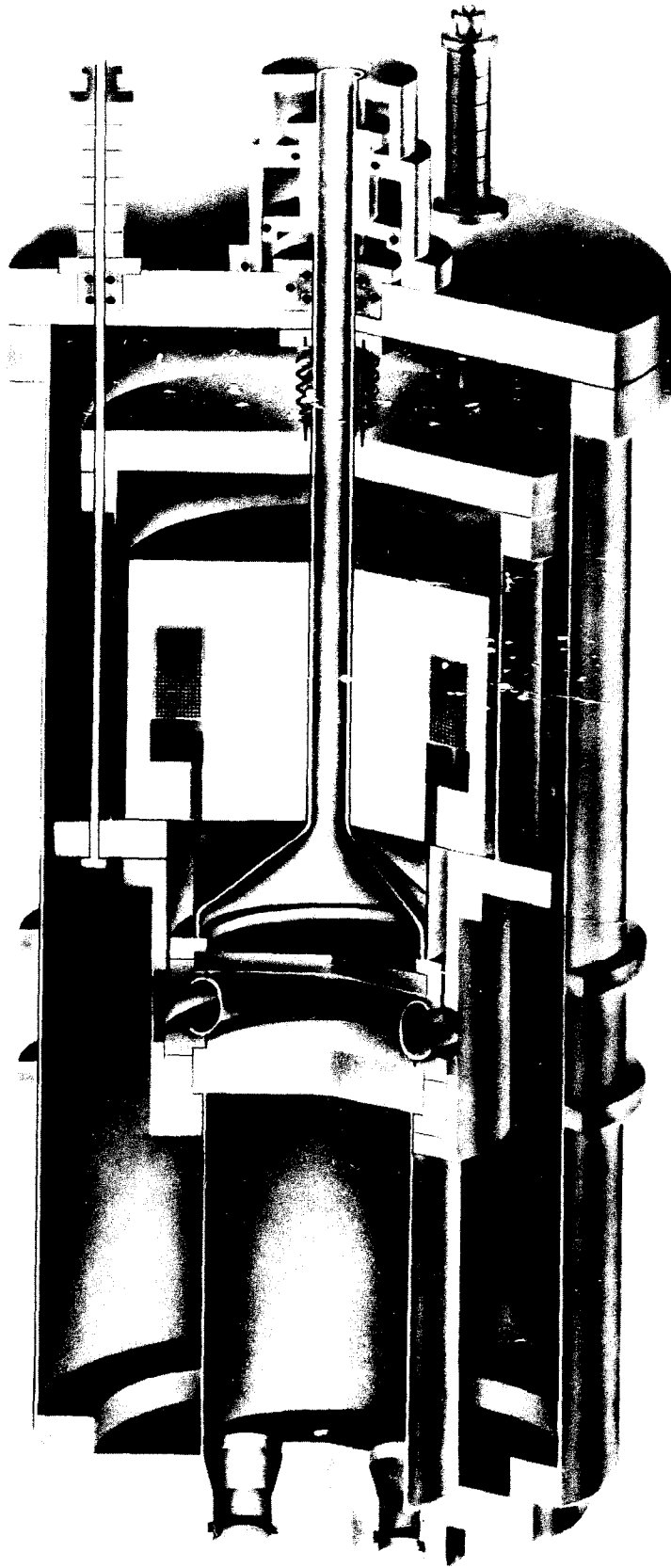
1768A1

FIG. 4--SLAC rapid cycle bubble chamber.
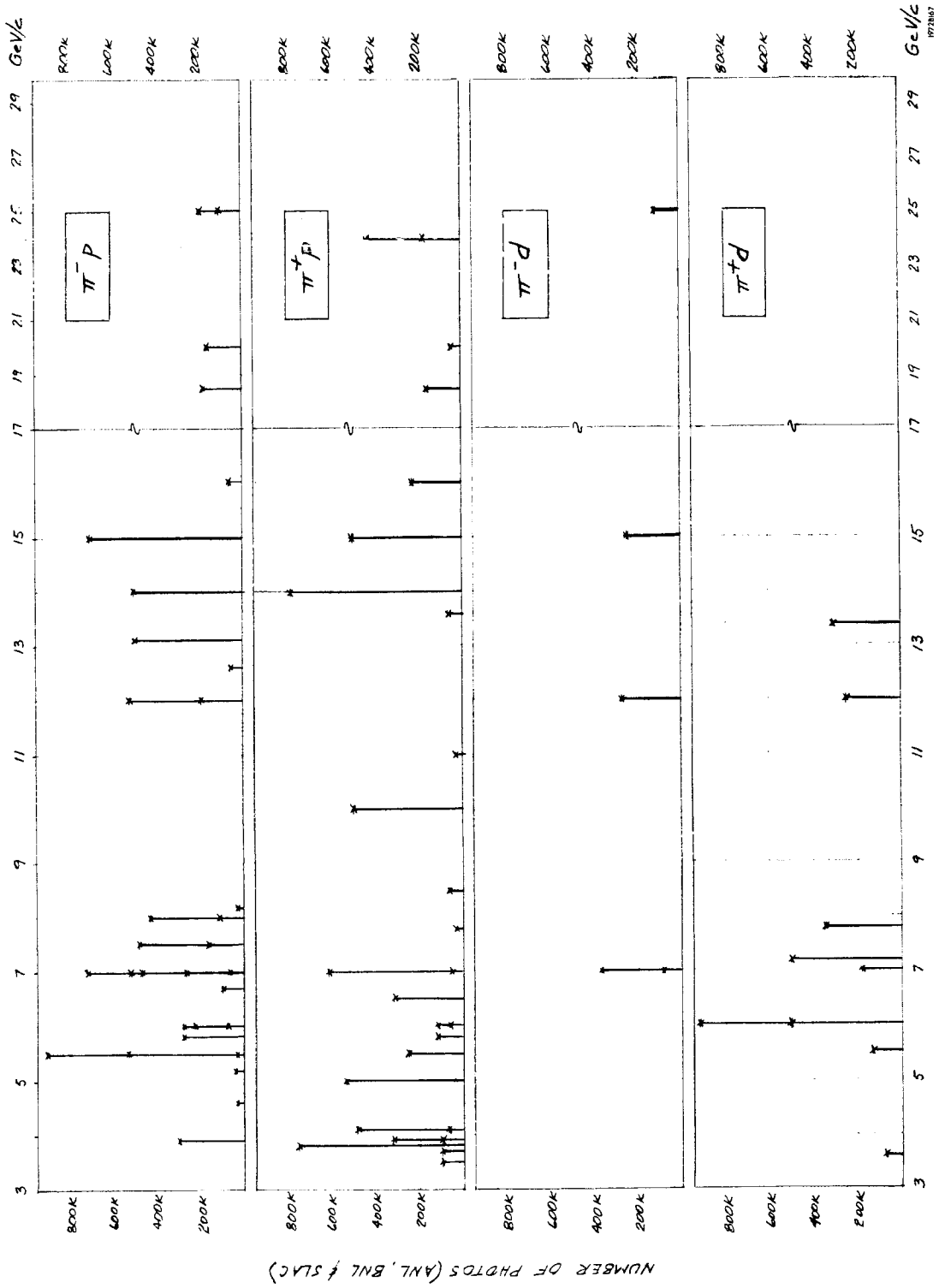
FIG. 5--Charged pion exposures completed or approved at ANL, BNL and SLAC (Jan. '71).
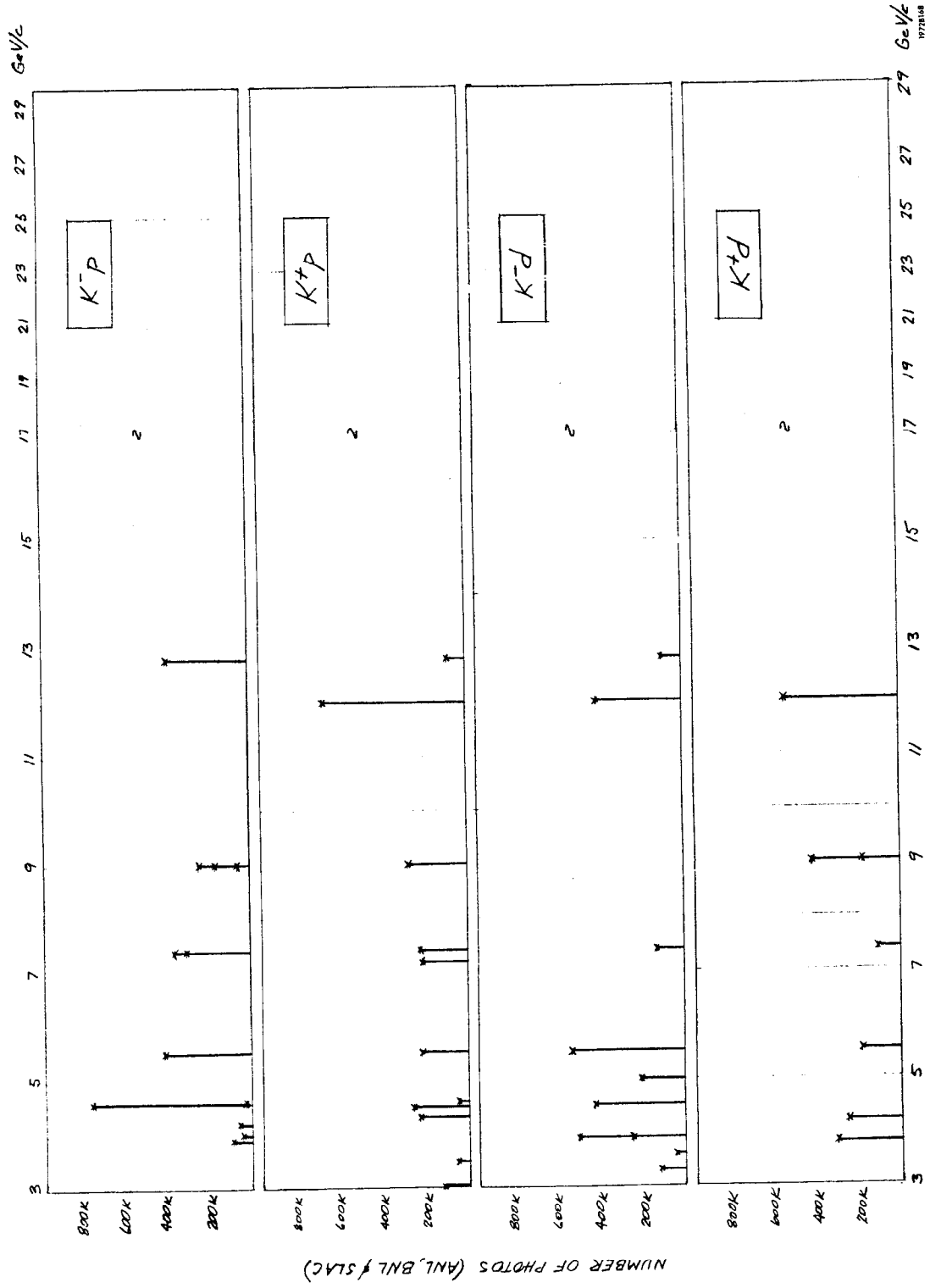
FIG. 6--Charged kaon exposures completed or approved at ANL, BNL and SLAC (Jan. '71).
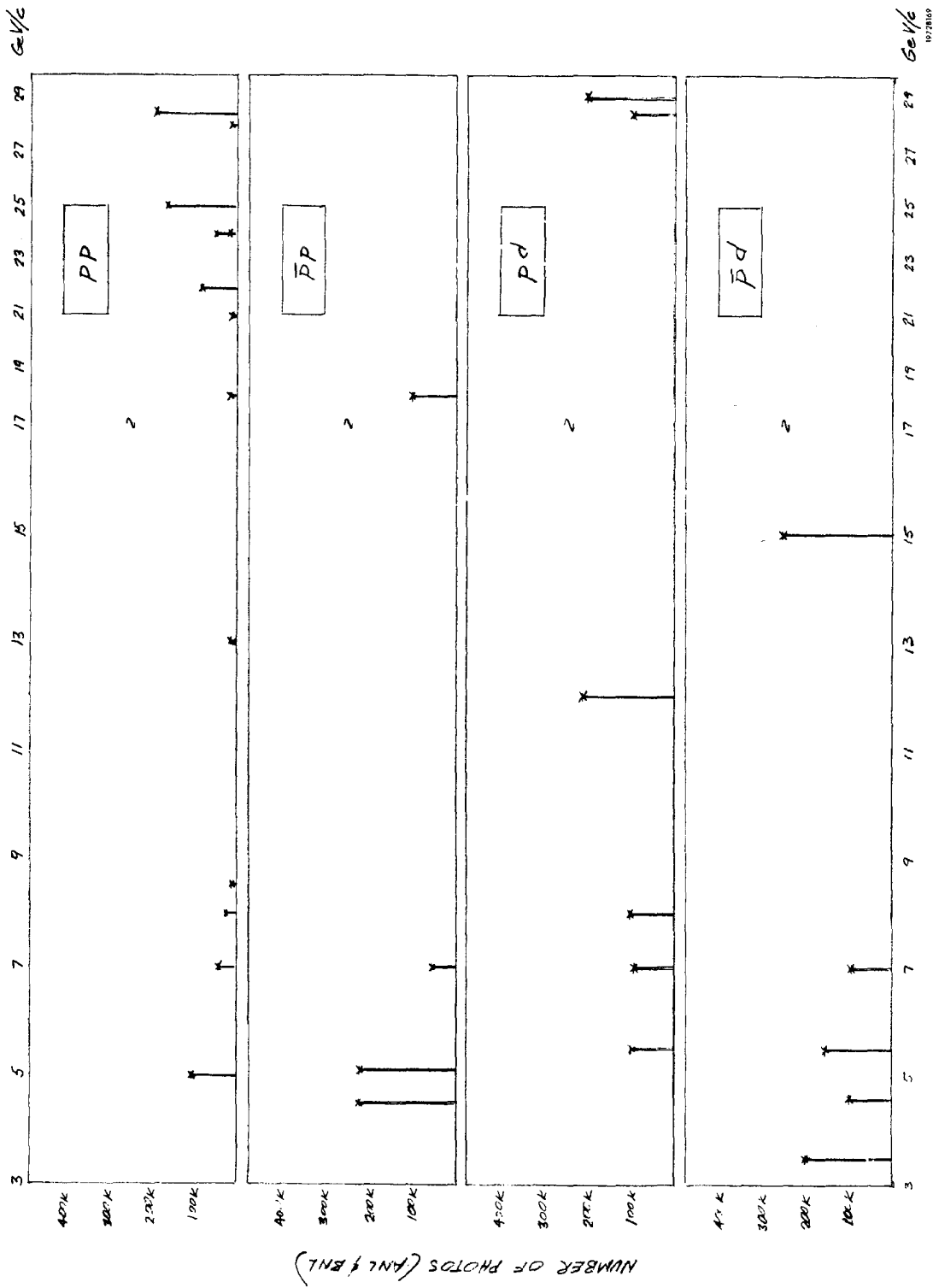
FIG. 7—Proton and antiproton exposures completed or approved at ANL and BNL (Jan. '71).

20-13

these pictures should take 2-3 years, and I think they should be done by large collaborations with good analysis ability. By that time, the work with the large chambers should tell us whether to continue at the higher energies.

6. General

Another field which has remained virtually unexplored is channels with several π^0's. A serious attempt to make track-sensitive targets work has been made at BNL, SLAC and several European laboratories--but no large experiment has been done. There are several extensive experiments approved at BNL to use a track sensitive target in the 80", but none as yet for the SLAC 40".

If the TST's do not work it will be necessary to make hybrid systems which consist of shower detectors surrounding the bubble chamber. The chamber is needed to locate the event origin and for the measurement of wide-angle, slow, charged particles.

In this talk I have made no attempt to discuss the physics status of our field--leaving that hopefully to the people who will summarize the Seminar and to the general discussion following the formal program.

Discussion

Pless: Did the overall measuring capacity go up or down in 1970?

Ballam: My feeling is that it has gone down slightly.

Derrick: Another solution [to the mismatch of picture potential and measuring] is to turn off half the chambers.

Ballam: I've assumed some chambers will turn off, but even with half the potential there may be a serious problem.

Pless: If you fund (or overfund) the automatic measuring program you could quadruple the output. For example, we could run PEPR on two or more shifts.

Ballam: I don't agree. I think 9×10^6 events/year is really an upper limit. My point is that the gap is widening.

Baltay: At NAL the neutrino beams may give one event every 3 pictures, which won't help the gap.

Pless: You seem to say that in 5 years it's going to be all over!

Ballam: No. We'll take another look.

Harari: So the present question is, should you fill the gaps [shown in Figs. 5-7] or, say, triple the statistics in regions already done?

Ballam: This can only be decided by the physics justification in the proposals.

A QUALITATIVE DESCRIPTION OF TWO-BODY INTERACTIONS
AT INTERMEDIATE ENERGIES*

H. Harari **

Stanford Linear Accelerator Center
Stanford University, Stanford, California USA

Abstract

A simple qualitative model for hadronic two-body amplitudes is discussed. The model combines the two-component theory of duality with the main ideas of the absorption model. The imaginary parts of all two-body hadronic amplitudes are described as a sum of two components — a Pomeron term dual to the s-channel background, and an ordinary exchange term dual to the s-channel resonances. The latter term is assumed to be dominated by the most peripheral partial waves within the range of interaction ($\ell \sim qr$, where q is the c.m. momentum; $r \sim 1$ fermi). The model reproduces correctly the qualitative features of the elastic differential cross sections and polarizations as well as the dip systematics of inelastic two-body reactions.

References

H. Harari, Ann. Phys. 63, 432 (1971).

H. Harari, Report No. SLAC-PUB-837, Proc. of the 1970 Int'l. School of Physics Ettore Majorana, Erice (Academic Press, New York, in print).

M. Davier and H. Harari, Phys. Letters 35B, 239 (1971).

H. Harari, Phys. Rev. Letters 26, 1400 (1971).

H. Harari, Report No. SLAC-PUB-914, Int'l. Conf. on Duality and Symmetry in Hadron Physics, April, 1971, Tel-Aviv, Israel (in print).

BUBBLE CHAMBER PHYSICS AT RUTGERS-STEVENS

Richard J. Plano

Department of Physics
Rutgers University
New Brunswick, New Jersey USA

1. Introduction

I will present no physics results today, but would like to describe the current Rutgers-Stevens bubble chamber research program and make a few general comments on bubble chamber physics which I hope will be useful or at least helpful in stimulating discussion.

This group has two probably unique features in that:

(1) We joined with Stevens to form a single larger group with sufficient power to rapidly and economically carry out the increasingly difficult and lengthy experiments we are interested in. Ten Ph.D.'s are currently in the joint group.

(2) We own and maintain a large PDP-6 time-sharing computer facility which controls the digitized measuring machines, runs a PEPR device, and in addition carries out all the normal computing needs of the group. We find this to be an extremely convenient and economical mode of operation in spite of occasional servicing and administrative difficulties due to the inadequate technical staff. Our complete control of the computer is probably a major factor in the success of this mode of operation.

2. Experimental Program

We are currently analyzing four major exposures. The first is an old exposure of the BNL 80" chamber to 25 GeV protons originally conceived in 1962 to study the highest energy reactions available. The lack of definitive results has been somewhat discouraging. In particular, we have studied $pp \rightarrow pp\pi^+\pi^-$ to test the multi-Regge model and study the $N^*(1470)$ and $N^*(1700)$. The large and unknown "backgrounds" have prohibited definitive conclusions and we are now increasing the statistics and attempting the prism analysis described by Pless[1] in an attempt to clarify the situation. As I discussed at Kiev,[2] I believe detailed fits to many final states including coherence effects are essential if production experiments are to contribute appreciably to our

knowledge of nucleon resonances. We are also studying the inclusive reactions $pp \rightarrow \Lambda^0 \gamma X$ and $pp \rightarrow pK^0 X$ in an attempt to study the Y^*'s in the $\Lambda^0 \gamma$ and pK^0 decay modes with a mass resolution of 5-10 MeV as well as to obtain data suitable for testing multiparticle production models.

The reaction $dd \rightarrow dd\pi^+\pi^-$ at 25 GeV/c in the BNL 80" chamber is being used to study the $I=0$ $\pi\pi$ interaction, although the small number of events without deuteron break-up make the statistics marginal.

$\bar{p}d$ reactions at 15 GeV/c are being studied in collaboration with Strasbourg to test the double-Regge model using the favorable reaction $\bar{p}n \rightarrow \bar{p}p\pi^-$ which will complement work at BNL on the reaction $pn \rightarrow pp\pi^-$. We are also attempting to use the bubble chamber as a missing mass spectrometer to search for bosons of mass around 5.5 GeV produced in the reaction $\bar{p}d \rightarrow p_s X^-$. Due to the Fermi motion of the neutron the $\bar{p}n$ system will have a spread of invariant masses, and we will search the region 5.2-5.8 GeV with a mass resolution of about 20 MeV. About 12 MeV is contributed by the $1/2\%$ beam spread and the remainder by the measurement uncertainty of the spectator proton angle. An error of 1^0 in angle on a 1 cm proton contributes about 8 MeV to the error in the missing mass. To obtain this accuracy, we are applying three techniques: (1) Obtaining the vertex position from the intersection of the beam track and a fast transverse prong whenever possible. (2) Using the knowledge of the curvature of the spectator proton obtained from its range in reconstructing this track. This reduces the error in the azimuth angle by a factor of $\sqrt{13}$ over a fit in which the curvature is a free parameter when measurement error is dominant. (3) Using the full error matrix on those tracks for which multiple scattering is important. This can reduce the angle error by a factor of 2 or more. These techniques can easily improve our mass resolution from 50 MeV to less than 20 MeV and thus are of crucial importance in efficiently detecting narrow resonances. Such techniques are of importance to the highest energies due to the ubiquitous slow proton. If the leading trajectory remains straight to a mass of 5.5 GeV ($s \sim 30$ GeV^2), if the corresponding mesons are narrow and coupled to the $\bar{p}n$ state ($kr \sim 13$ for $r = 1$ f.), we may detect 5 new mesons.

Our major effort, however, is directed to a study of the T(2190) meson region produced in a formation experiment by $\bar{p}p$ interactions in the BNL 31"

chamber around 1.3 GeV/c. We are uniformly sensitive to the invariant mass region 2165 to 2215 MeV with a total sensitivity of 10 events/μb. This corresponds to one million events. We plan to measure at least half these events in our PEPR device which currently is stumbling through its first 1000 events. We believe the importance of unraveling a possible meson tower and thereby gaining real insight into the structure of mesons justifies an effort of this rather sobering magnitude. Previous experiments with as little as 10 times fewer events have uncovered strong indications of a complex structure thereby motivating and guiding this work. The complexity of such final states as $\rho^0\rho^0\pi^0$ and $K_1^0 K_1^0 \omega$ as well as the importance of cascade decays and spin-parity determinations make this a study ideally suited to the bubble chamber. Note that the 1/2% beam spread gives us a mass resolution of 2.5 MeV. Probably more data will be required to extend or complete this study. Unfortunately, as the BNL 31" chamber is shutting down, no chamber in this country can currently provide such pictures.

We also plan to study backward $\bar{p}p$ elastic scattering, $\rho-\omega$ interference (perhaps 500 $\omega \to 2\pi$ events), the A_2 meson (10^4 $A_2 \to 3\pi$ expected), $\bar{n}p$ interactions, and a far out try to observe C noninvariance using $T \to K_1 K_1 \omega(C = -1)$ interference with $T \to \rho^0\rho^0\pi^0$ (C $= + 1$) as suggested by Barshay.

3. Opinion

I have an intuitive feeling that 4C physics will continue to be of the greatest importance to the highest energy and admit to a queasy uncertainty concerning inclusive experiments. Many examples could be given to justify this feeling, but the clearest is perhaps given by Ferbel's discussion[3] of the longitudinal asymmetry of the π^- produced in π^+p reactions. Observing only the π^-, these results could easily be taken as strong evidence for the validity of the quark picture (and were so taken). A detailed (exclusive) study, however, showed rather convincingly, I believe, that the asymmetry can be explained by resonance production and is independent of quarks. Further, as I and others have shown, 4C physics is quite feasible at NAL energies in a large and precise chamber which is practical to build.

Finally, I would like to show some calculated errors in invariant masses. The problem is conveniently divided into Formation and Production type experiments.

A. <u>Formation</u>: a particle of mass m_1, energy E_1 striking target of mass m_2:

$$M^2 = m_1^2 + m_2^2 + 2m_2 E_1$$

$$\delta M^2 \approx 2m_2 E_1 k \approx M^2 k \quad \text{at high energy}$$

where k is the fractional error on the beam momentum.

$$\delta M = \frac{1}{2} Mk.$$ Taking $k = 10^{-3}$ gives the following

p_1 GeV/c	1.3	15	60	200
M GeV	2.18	5.47	10.69	20
δ M MeV	0.5	2.55	5.2	10

B. Production: final particles 1 and 2 have opening angle θ in the chamber:

$$M^2 = m_1^2 + m_2^2 + 2(E_1 E_2 - p_1 p_2 \cos\theta)$$

$$\approx 2p_1 p_2 (1 - \cos\theta)$$

$$\delta M^2 \approx (2p_2 \delta p_1 + 2p_1 \delta p_2)(1 - \cos\theta) + 2p_1 p_2 \sin\theta \, \delta\theta.$$

For the case $p_1 = p_2 = p$, $\delta p_1 = \delta p_2 = kp$

$$\delta M^2 \approx 4p^2 (1 - \cos\theta)k + 2p^2 \sin\theta \, \delta\theta$$

$$\approx 2M^2 k \quad \text{if} \quad \delta\theta = 0.$$

Hence $\delta M \approx Mk$.

For 1 m tracks with p<4 GeV/c and taking $k = 10^{-2}$ the error for M=2400 MeV is ~ 25 MeV. For a 90° opening angle, and $\delta\theta \sim 10^{-3}$, $\delta M \sim 30$ MeV. Constraint fitting at these energies gives little improvement, but is critical for identifying events.

Note that in both cases δM increases linearly with M, and δM^2 increases proportionately with M^2.

References

1. Talk by Pless at this conference (Paper No. 5).

2. Nonstrange Baryon Resonances (Experiment), Richard J. Plano, Rapporteur's Review Talk, XVth International Conference on High Energy Physics, Kiev U.S.S.R., (October 1970). (Preprint).

3. Talk by Ferbel at this conference (Paper No. 13).

A SUMMARY OF THE SESSIONS

Gyo Takeda

Tohoku University
Sendai, Japan

First I would like to thank those who organized this meeting which has
been very fruitful for me. Through the meeting I have learned quite a lot
about current and future problems in particle physics with bubble chamber
detectors and the limitations of present bubble chamber experiments. I shall
summarize our discussions and talks by making several comments.

(1) Everybody working in the field of particle physics would like to look
for something which is more fundamental than what we know at present. Are
all the fundamental conservation laws already discovered by now? Are there
particles of a completely new kind? Such questions were briefly touched in
Prof. Sakurai's talk. Experiments with high energy neutrinos as discussed
by Prof. Baltay and Prof. Derrick or coming experiments on the NAL accel-
erator could be relevant for these questions. Although searches for more
fundamental particles or laws are a kind of gambling at present, it would be
rather surprising if nothing more fundamental comes out from future
experiments.

(2) There are two different attitudes when we look at the present status
of elementary particle physics. Some people seem to think that nothing quali-
tatively new is left in hadron physics unless we go to extremely high energies.
Others think that almost nothing is known at present in particle physics. I
shall rather take the latter point of view. Let us take, e.g., SU(3) symmetry
in hadron physics. The symmetry and its breaking are understood rather
well in the low mass hadron spectrum. On the other hand no deep understand-
ing has been obtained at present as to the cause of the symmetry and its
violation. If our future experiments prove that the symmetry is more exact
when we go to higher energies as conjectured some years ago, it would be
important progress in our understanding of the symmetry.

(3) Prof. Pless gave us a very impressive talk, in which he argued for
making use of the full information supplied by each bubble chamber event.
If we make use of four variables in the case of three-body final states and

seven variables in the case of four-body final states, remarkable reductions of backgrounds result as were shown in some of his new plots of experimental data. Another impressive result was obtained by Dr. Chadwick. He showed the cross section for ρ-production by photons at 9.3 GeV ($\gamma p \to \rho p$), where the background seemed absent at first appearance but still affected the data. Since our ignorance of the nature of backgrounds has been one of main causes preventing further progress in hadron physics, I believe that the experiments mentioned above suggest some means to break through this ignorance. In fact, Dr. Chadwick was able to make a reasonable estimate of the magnitude of background contributions by making use of his beautifully complete data. There may be some bias coming from the choice of which theoretical physicists he believes.

(4) To evaluate experimental results obtained with bubble chambers is something like to appreciate modern paintings. Each physicist would like to look at results in his own way, so that there is some room for personalities to enter. Let us take, e.g., the question of whether many resonances do exist in the intermediate mass region. If we find five peaks, each being 2 standard deviations away from the background, then the probability for at least one of them being a real resonance is almost equal to the probability for one prominent peak, 4.5 standard deviations away from the background, being a real resonance. Everybody has to believe in the existence of a resonance when one sees a prominent peak many standard deviations away from the backgrounds. On the other hand, when one sees many peaks, each of which is statistically insignificant, there are two different points of view. One man would disregard all of these peaks, because the physics behind him does not attribute any significance to any possible resonance at present. Another would like to regard five peaks as an evidence for the existence of at least one resonance in the mass region, because such evidence is very important to their physical interpretation. Throughout the discussions of the last three days I have been amused to find how personalities come into physics with bubble chambers. I am not saying this is bad. Rather this reflects our vivid life with bubble chamber physics.

(5) Prof. Flatté told us what has happened with bubble chamber physics in the last few years. During this meeting we have heard many interesting talks in which you talked about your present and future interests. The subjects

talked about more or less cover the subjects discussed by Prof. Flatté's talk and no more than that. Presumably physics with bubble chambers in the 1970's will not be much different from physics in the 1960's.

(6) Improvement of energy resolution, accumulation of large numbers of events, and presentation of experimental data in adequate ways are of very much concern to us, since we Japanese have started physics with bubble chambers rather late and, therefore, we have to do precision experiments. I have heard a new unit, namely, one Flatté (50 events/μb) as a measure for precision of experiments. Our Japanese unit at present may be one tenth of a Flatté. I am sure that our unit will become about one third of a Flatté in the near future. However, it will take quite a while before we get the exchange rate of one to one. In any case, whether we can get much more physics by improving present energy resolution and statistics by significant factors remains to be seen.

Finally I would like to say that the meeting has been very successful and fruitful. Everybody participated actively in the discussions, which proves the usefulness of having a small meeting like this.

Discussion

Flatté: A personal comment. When you spoke of these five-standard-deviation effects (from 5 two-standard-deviation peaks), I didn't know what you were referring to.

Takeda: They were specifically in Prof. Peters' talk. While you were away, some of us were a little critical of your attitude (toward small effects).

Flatté: So many plots are being presented that it just isn't worthwhile to follow up each such effect, even two dozen a year. You judge on a personal basis what the significance is. If you have 100 bins in a distribution, a two-standard-deviation effect is a virtual certainty.

Ferbel: He's referring to the fact that a smooth curve has an extremely low probability to fit Peters' data.

Flatté: You can make such a test and state the significance, perhaps prove there is structure, but you haven't shown which is real.

Harari: That was his point.

ROUND-TABLE DISCUSSION ON THE PROSPECTS
FOR BUBBLE CHAMBER WORK IN JAPAN

[Editor's Note: The final afternoon of the seminar was devoted to the degegates' ideas on whether a heavy emphasis on bubble chamber work at the new Japanese National Accelerator Center was advisable, and if so what kinds of work would be done. Note that the accelerator will be completed five years from the present and therefore the fruits of the effort would be realized in the next 8 - 10 years. The discussion was lead by Malcolm Derrick. It has in many places been paraphrased, and the delegates are free to claim misunderstanding if they want to change their minds.]

Derrick: I have set down four topics for this discussion, representing the questions we might try to answer. They are:

1. Establishing bubble chamber user groups in Japan.
2. The possible physics program of the 8 GeV accelerator.
3. Technical question: precision needed, special beams, heavy liquids or track sensitive targets, analysis procedures.
4. Competing techniques, e.g., wire chambers, streamer chambers.

I shall begin with some comments on the first topic. What are the arguments in favor of bubble chamber user groups? Well, they could get training in the techniques which could be used in the machine at home. Counter groups would have to work at machines outside the country and so would be away for long periods and, let's face it, they may never return.

Yamagata: I would think that we need to join in collaborations with other countries in order to get the required experience.

Derrick: You need cooperation at least. I am thinking of the use of SLAC by the Israeli groups, who use SLAC without actually collaborating. Also Canada has a group with people already at NAL and they do not expect to collaborate with in-house groups.

Ballam: What you need is to set up the capacity for analyzing as much film as you possibly can, then ask for a million pictures and get all groups together analyzing as fast as they can, so that everyone gets experience and some good physics.

Yamamoto: I suggested this, but there was considerable opposition. Everyone wants a little film all to themselves. Also there seems to be money for equipment, but none for going abroad. And it's hard to get money for scanner's salaries for the machines already funded.

Derrick: That's an argument for bubble chamber analysis. It would require the least travel money: people just go out and collect the film and return.

Yamamoto: No money even for that.

Kitagaki: We hope discussions like these will help change the situation.

Derrick: I'd like to make another point. The Rutherford Lab bubble chamber group got its film from CERN, and so had no interest in running chambers at their own lab. Consequently the whole chamber program there has pretty well stopped. I opposed using outside film at ANL, even though it meant a much slower startup.

Pless: With the new machine, 8 GeV, 10^{12} particles/sec and 1 sec repetition rate, you don't have a special machine at all. I think it is right to build it but it would be a mistake without a National program (since you can't rely on individual inspiration). For example, the DESY machine came in late but is a big success because they have a big continuing program and lots of money and people (a bit at the expense of outside groups). In the U.S. the support is spread over several machines. I recommend the Japanese government follow the German lead. I'm prejudiced, but I imagine, listening to the preceding talks, that the 8 GeV energy region will be less interesting to the U.S. people than 500 GeV neutrino and special bubble chamber techniques. If the available money stays constant, the 8 GeV high multiplicity events will just not get done.

So I say, concentrate on high multiplicity events and really do a job. There is the question: is it worth while? I think it is but I'm glad I don't have to decide. Perhaps the theorists will help. If you decide to do it, at, say, the rate of 5×10^{6} events/year, you must begin preparing now. Collect the techniques for prism plots, for example. It's a gamble, but the worst thing is to do nothing.

Yamamoto: What is the alternative to the gamble?

Pless: Not to go into bubble chambers at all, and if not 5×10^{6} events worth per year, get out now before the investment gets too big.

Derrick: That's too strong. They could do say 10^{6} per year in cooperation with CERN or the U.S. instead.

24-2

Pless: No, no, no.

Ballam: Why not? It means no chambers at the 8 GeV machine which does counter work exclusively, but they take interesting bubble chamber exposures at other machines.

Pless: I don't believe the Japanese government is ready to pour lots of money into anything the physicists want to do.

Ballam: Why not? The French don't use Saclay for bubble chambers and get lots of film from CERN.

Pless: Well, for 50 million the Japanese could effectively buy a big piece of NAL. But if they did a good job at 8 GeV they could argue better for going to higher energies.

Takeda: I have been involved in the Japanese accelerator for 13 years now. We chose 8 GeV because of budget, secretly hoping to achieve 12 GeV. One can't be certain that a detailed study in this region will yield anything very new. The present questions are at the 20% level as we have heard. We hope that bringing the data to the 5 - 10% level will help our understanding. At present our level is only 0.1 Flatté-units (i.e., 1/10th of 50 events/μb). In five years maybe one Flatté.

Derrick: If present experiments are repeated with better statistics, how important are things like better resolution, such as the Rutherford Laboratories 70 kG proposal.

Pless: (To Takeda) Will 1 MeV resolution help find your structures?

Takeda: 1 MeV is not essential, but definitely we need better than 10 MeV.

Flatté: Then present chambers are sufficient. We had enough resolution to settle the A_2 question for example.

Takahashi: We need more theoretical resolution to use and improve experimental resolution. The separation of resonances from background will not be helped by 1 MeV mass determination, for example the background under the photoproduced ρ. Tell us how to do it, theorists!

Ballam: You'll have to catch a theorist and lock him up.

Pless: You won't keep one that long on such a dull problem.

Ballam: Another point, what about proton beams? There are many gaps in exposures taken. Can anyone say why?

Pless: There's always two baryons and no resonances — three-body final states are hard to analyze.

24-3

Ballam: What about N* - N* ?

Derrick: It's a matter of fashion. Look at $\bar{p}$'s for example, all done by Europeans while the U.S. ignores them.

Pless: I'd say that it's because πp phase shifts are known and π-π phase shifts are needed. The lack of $\bar{p}$ work is to me more striking.

Takeda: I hope that you won't all rush out and do them [protons] because we have to wait five years for our machine!

Flatté: [To Derrick] What will you do in five years with the very comparable ZGS?

Derrick: I can only say anything about the next five years. We will exploit the 12-foot chamber (the only one we have left), doing neutrino and K^0 experiments. We will build 12 GeV/c beams and a 6.5 GeV/c K beam.

Flatté: What program is there for other techniques?

Derrick: Our counter and spark chamber experiments will be very similar to BNL's, about in the 3 - 7 GeV range compared to 10 - 15 GeV. We will exploit polarized targets strongly. There is no systematic exploration — it is foreign to the American nature.

Ballam: Is there any sense in putting polarized protons into a chamber?

Kitagaki: We plan to make an accelerated polarized beam.

Derrick: We used a polarized beam for Λ^0 studies. It worked well.

Yamamoto: By the way, the AEC says the Japanese may have the 31" chamber.

Kitagaki: Let me summarize. We are behind in this field. Topics we have heard discussed are those worked on by people in the forefront of physics, and may not be valid for the Japanese. It may not be wise to get into problems being done in the U.S. ...

Ballam: We've been talking about experiments for you to do!

Kitagaki: We might find a hole in the present program and work there (rather than redo U.S. experiments).

Takahashi: He means, I think, new inventions are needed. The Soviets concentrate on heavy liquid chambers, for example. What is your opinion on the reasons, and the usefulness of this?

Pless: The Russian physicists admit that, having invested heavily in the Xenon chamber, they have to use it. It would be the same in this country.

Takeda: May I make my final statement. In our discussions of future experiments, I find detailed differences, but not real qualitative change in physics at 10 GeV and, say, 500 GeV. So working at 8 - 12 GeV, doing reasonably accurate experiments, we will still be using the same techniques as the higher energy domain and can hope they may yield, event for event, almost as much understanding. If the high energy region is indeed very different, we will have to join in at NAL. But if so, our program will have produced experienced people to do this. Therefore we are not at all discouraged.

Derrick: Can we push on to other techniques, like the streamer chamber?

Pless: It's really the same instrument, and requires big data processing installations which are the real cost.

Derrick: But it is especially good for small cross section events and doesn't necessarily need all that backup.

Flatté: I've tried to compare bubble chamber experiments with counters. Here are some numbers. The bubble chamber has a factor 10 more useful hydrogen than the usual counter target, and a factor 100 in solid angle. Though the counter man may use a beam 10^4/sec stronger than can be put into a chamber you can see he is only a factor 10 up in yield. Besides he spends 70% of his time checking equipment, and so has not much net gain over the chamber and a lot more systematic uncertainties.

But the bubble chamber is doing maybe 100 experiments at once, so I say, just take pictures and you will beat the counter people every time.

Now I'd like to add that the job of a scheduling committee is to choose between experiments, and it must conclude that a completely new energy is better than one close by an old experiment. But any other means of decision is presumptuous! If the Japanese have their own chamber, they can schedule their own experiments and that is a big advantage. [A recently proposed large exposure was turned down at SLAC amid much controversy, which creeps in here — Ed.]

Ballam: Take the case that big exposures at 7 and 12 GeV are being analyzed and that an experimenter asks for 10 GeV, promising mainly quicker delivery of results. Would you give them the exposure? I'm just illustrating scheduling problems the Japanese too will face.

Flatté: I wouldn't have asked for them.

24-5

Harari: If I were asked to recommend a procedure, I'd set up two big experiments at 4 and 8 GeV/c and offer them to anyone who could do them.

Ballam: And if someone wanted 6 GeV/c you'd say no?

Harari: I'd wait till the 4 and 8 were finished.

Flatte: Physicists should decide what experiments they want to do. At NAL they received 100 proposals and chose a few most theoretically promising ones from these.

Peters: I'd suggest that the accelerator and bubble chamber take pictures continuously and these could be given out by experiment, e.g., A_2 production at all energies, which another group does the t^0, etc.

Ballam: Suppose there's an A_6 meson with a threshold at 4.7 GeV. So if I run at one energy I get many more events.

Pless: Imagination can't survive a huge bureaucracy. NAL will tend to develop this and in my view we must fight it. Let me ask Ballam a loaded question on how much a good idea is worth. Now anyone can carry out the work, so would you give somebody's new experimental idea to someone else because he can do the experiment faster?

Ballam: Most such requests [for new techniques in previously covered regions] have in fact been granted.

Yamamoto: Let's go on to special beams and new techniques.

Ballam: There's the track sensitive target surrounded by heavy liquid to detect π^0's ...

Kitagaki: Can anyone comment on the use of a perpendicular view in a chamber?

Derrick: It's generally too complicated to do for not much gain, and it is not a quantum step in technique that may be needed.